

**Part I: Synthesis of an Unsymmetrically Pentafunctionalized
Corannulene Derivative**

and

**Part II: Synthesis of Platinum and Ethynyl-Platinum
Corannulenes**

Dissertation zur Erlangung
der naturwissenschaftlichen Doktorwürde
Dr. sc. nat.

vorgelegt der
Mathematisch-naturwissenschaftlichen Fakultät
der Universität Zürich

von

Roman M. Maag
von Winkel ZH

Promotionskomitee:

Prof. Dr. Jay S. Siegel (Vorsitz)
Prof. Dr. Kim K. Baldrige
Prof. Dr. Cristina Nevado
Prof. Dr. Roger Alberto

Zürich, 2012

Abstract of the Dissertation

Part I:

Synthesis of an Unsymmetrically Pentafunctionalized Corannulene Derivative

and

Part II:

Synthesis of Platinum and Ethynyl-Platinum Corannulenes

by

Roman M. Maag

University of Zurich, 2012

Prof. Dr. Jay S. Siegel, Chair

Corannulene ($C_{20}H_{10}$) is a polycyclic aromatic hydrocarbon that can be considered as the smallest fragment of Buckminsterfullerene exhibiting a curved surface. Among the interesting properties of corannulene are rapid bowl inversion and esthetically appealing fivefold symmetry (C_{5v}), which is rare in chemistry. Whereas the first synthesis in 1968 only afforded milligram quantities, several improvements in the synthetic strategy finally culminated in the development of an efficient process which today furnishes corannulene in kilogram quantities. A key intermediate in the established synthetic route is a presubstituted fluoranthene, bearing the necessary carbon skeleton of the desired corannulene. With this strategy, mirror-symmetric, substituted derivatives are readily accessible.

Fivefold chlorination of corannulene provides *sym*-pentachlorocorannulene, an important starting material for further substitution towards C_5 symmetric structures. Various transition-metal catalyzed coupling reactions allow the introduction of sp , sp^2 , and sp^3 carbons and the chlorides also allow nucleophilic aromatic substitution with thiolates or alcoholates. Corannulene also undergoes electrophilic aromatic substitution, allowing for the preparation of brominated or nitrated derivatives which are the mostly utilized intermediates for monosubstituted C_1 -symmetric derivatives.

Despite the effective methods currently used to synthesize a variety of substituted corannulenes, the controlled synthesis of derivatives with five different groups has not been realized. In this thesis, the development of a strategy toward a corannulene derivative with five different functional groups at the 1,3,5,7,9-position is described. Due to lack of regioselectivity the task is not feasible by the stepwise substitution of *sym*-pentachlorocorannulene. Instead, a synthetic route through a presubstituted fluoranthene was chosen and a new

synthetic method for the construction of required highly substituted fluoranthene derivatives was developed to meet this goal. As a key step, the convergent synthesis comprises a [4+2] cycloaddition between a substituted acenaphthylene and thiophene-*S,S*-dioxide. In the course of the investigations described herein, electron withdrawing groups on the thiophene-*S,S*-dioxide derivatives turned out to be crucial for the cycloaddition to occur in the manner of an inverse electron demand Diels–Alder reaction.

The Diels–Alder reaction between the thiophene-*S,S*-dioxides and the acenaphthylenes produced two regioisomers of the fluoranthene derivatives, which were separated by normal phase HPLC. However, a derivative was found of which the regioisomers could be separated by standard gravity column chromatography. This finding significantly improved the practicality of the synthetic route. The respective isomers could be unambiguously identified by 2D NMR spectroscopy, which was confirmed by X-ray crystallography in one case.

Whereas the synthesis of the fluoranthene derivatives proceeded in good yields, the final ring closure of the fluoranthenes and further dehydrogenation proved to be challenging and gave the target pentasubstituted corannulene in rather low yield. The 1,3,5,7,9-pentafunctionalized derivative was analyzed by 2D NMR spectroscopy and its bowl inversion barrier was determined by variable temperature NMR spectroscopy to be 8.9 kcal/mol.

In the second part of the thesis, the synthesis of two directly core-platinated and three ethynyl-platinum corannulenes is described. The platinum corannulenes bear either 2, 4, or 5 planar platinum(II) centers. The direct platinum corannulenes were synthesized from the corresponding corannulene halide through oxidative addition of a Pt(0) complex. For the preparation of ethynyl-platinum corannulenes, a one-pot platina desilylation reaction was found giving the alkynyl platinum complexes in good to excellent yields. With this procedure, the isolation of terminal acetylenes could be avoided.

The compounds were intensively analyzed by NMR spectroscopy and, when feasible, by X-ray crystallography. In one case the dynamic behavior of the bowl inversion was assessed by VT NMR spectroscopy which supports a persistent bowl structure in solution. The geometries of these platinum-corannulenes render them as well-structured molecular tectons for the future assembly of coordination Platonic polyhedra. The fivefold symmetric supramolecular tectons bode especially well for the assembly of icosahedral structures.

Zusammenfassung der Dissertation

Teil I:

Synthese eines unsymmetrisch pentafunctionalisierten Corannulenderivates

und

Teil II:

Synthese von Platin- und Ethynylplatin Corannulenen

von

Roman M. Maag

Universität of Zürich, 2012

Prof. Dr. Jay S. Siegel, Vorsitz

Corannulen ($C_{20}H_{10}$) ist ein polyaromatischer Kohlenwasserstoff, welcher als kleinstes Fragment des Buckminsterfullerens (C_{60}) betrachtet werden kann das eine schalenförmige Struktur aufweist. Eine faszinierend Eigenschaft von Corannulen ist dessen Schaleninversion und die ansprechende fünffache Symmetrie (C_{5v}), die eher selten in der Chemie vorkommt. Wobei die erste Synthese von 1968 Corannulen nur in analytischen Mengen lieferte, führten mehrere synthetische Fortschritte zur Entwicklung eines effizienten Prozesses, der heute die Darstellung im Kilogramm Bereich ermöglicht. Das entscheidendes Zwischenprodukt ist ein entsprechend substituiertes Fluoranthenderivat, welches schon das Kohlenstoffgerüst von Corannulen besitzt. Diese Strategie ermöglichte auch die Synthese zahlreicher C_s -symmetrisch substituierter Corannulenderivate.

Die fünffache Chlorierung von Corannulen liefert *sym*-Pentachlorocorannulen, ein nütliches Ausgangsmaterial, welches Zugang zu einer Vielzahl C_5 -symmetrischer Verbindungen bietet. Übergangsmetall-katalysierte Kupplungsreaktionen ermöglichen die Einführung von sp -, sp^2 - und sp^3 -Kohlenstoffzentren, und die Chloride können durch nukleophile aromatische Substitution mit Thiolaten oder Alkoxiden ausgetauscht werden. Des Weiteren erlaubt elektrophile aromatische Substitution unter anderem die Herstellung bromierter und nitrierter Derivate von Corannulen, welche die meistgebrauchten Intermediate für die Herstellung einfach substituierter C_1 -symmetrischer Corannulenverbindungen darstellen.

Trotz der vielen effektiven Methoden, die die Synthese einer Vielzahl von Corannulenderivaten erlaubt, wurde die kontrollierte Synthese von Derivaten mit fünf verschiedenen Substituenten noch nicht realisiert. In dieser Arbeit wird die Entwicklung einer synthetischen Strategie beschrieben, die es erlaubt fünf verschiedene funktionelle Grup-

pen in den Positionen 1,3,5,7 und 9 des Corannulengerüstes einzuführen. Aufgrund der fehlenden Regioselektivität ist die Synthese über eine schrittweise Substitution der Chloride von *sym*-Pentachlorocorannulen kaum praktikabel. Stattdessen wurde der Weg über ein entsprechend vorsubstituiertes Fluoanthenderivat gewählt. Eine neuartige Methode für den Aufbau solcher dicht substituierter Fluoranthene wurde entwickelt um die Aufgabenstellung zu erfüllen. Der zentrale Schritt besteht aus einer [4+2]-Cycloaddition eines substituierten Acenaphthylenes mit einem Thiophene-*S,S*-dioxid. Im Laufe dieser Arbeit stellte sich dabei heraus, dass elektronenziehende Substituenten am Thiophene-*S,S*-dioxid entscheidend für den Ablauf dieser Diels–Alder Reaktion mit inversem Elektronenbedarf sind.

Die Diels–Alder Reaktion der hier beschriebenen Thiophene-*S,S*-dioxide mit Acenaphthylenen lieferte zwei regioisomere Fluoranthenderivate, welche durch präparative HPLC getrennt werden konnten. Im Zuge der Untersuchungen wurde jedoch ein Derivat gefunden, dessen Isomere über normale Säulenchromatographie getrennt werden konnten, was die Zweckmässigkeit des Syntheseweges entscheidend verbesserte. Die Isomere konnten über 2D NMR Spektroskopie eindeutig identifiziert werden, was in einem Fall durch Röntgenstrukturanalyse bestätigt wurde.

Während die Synthese der hier beschriebenen Fluoranthenderivate in guten Ausbeuten realisiert werden konnte, lieferten der darauf folgende Ringschluss und die Dehydrierung das erwünschte pentasubstituierte Corannulen in eher unbefriedigenden Ausbeuten. Das 1,3,5,7,9-pentasubstituierte Corannulenderivat wurde mittels der 2D NMR Spektroskopie analysiert. Auch wurde die Aktivierungsbarriere des Schaleninversionsprozesses der Zielverbindung mit VT-NMR-Experimenten auf 8.9 kcal/mol bestimmt.

Im zweiten Teil dieser Arbeit wird die Synthese von Platin- und Ethynylplatin-Komplexen des Corannulens beschrieben. Die synthetisierten Platin-Komplexe enthalten entweder 2, 4 oder 5 planare Platin(II)-Zentren. Kernsubstituierte Platin-Komplexe wurden ausgehend von den entsprechenden Halocorannulen durch oxidative Addition eines Pt(0)-Komplexes dargestellt. Für die Synthese der Ethynylplatin-Komplexe wurde eine Eintopf-Platinadesilylierung gefunden, die die Ethynylplatin-Komplexe ausgehend von den entsprechenden TMS-acetylenen in sehr guten Ausbeuten liefert. Mit dieser Methode kann die Isolierung der ansonsten benötigten terminalen Alkine umgangen werden.

Die Verbindungen wurden durch detaillierte NMR-Analysen und, wenn möglich, durch Röntgenstrukturanalyse charakterisiert. In einem Fall wurde die Dynamik der Schaleninversion mittels VT-NMR-Experimenten untersucht, welche die schalenförmige Struktur der Verbindungen in Lösung bestätigte. Die Geometrie der vorliegenden Komplexe ermöglicht den Aufbau neuartiger Koordinations-Polyeder, im Speziellen sind die fünffach symmetrischen Bausteine vielversprechend für die zukünftige Konstruktion ikosaedrischer Strukturen.

Acknowledgments

I would like to thank everyone who gave me the possibility to complete this thesis ...

PROF. JAY S. SIEGEL

for giving me the opportunity to work in his research group, his encouragement and for providing me with many insights into different aspects of chemistry.

PROF. KIM K. BALDRIDGE

for her calculations, and for helpful discussions.

PROF. OLIVER ZERBE, DR. THOMAS FOX, SIMON JURT, AND NADJA BROSS

for the acquisition of NMR spectra, and great support with VT experiments.

PD ANTHONY LINDEN AND SASCHA BLUMENTRITT

for the elucidation of crystal structures.

PD LAURENT BIGLER, URS STALDER AND JEAN-CHRISTOPHE PROST

for the measurement of mass spectra.

PETER ÜBELHART

for constant support and instructions with HPLC.

FITORE KASUMAJ, SIMON DUTTWYLER, SILVIA ROCHA, DERIK FRANTZ

for their friendship, support and encouragement, for a good working environment and for great moments in- and outside the lab.

ALL SIEGEL, FINNEY, AND BALDRIDGE GROUP MEMBERS

BIANCA CITRINI

for her love, constant support and her patience.

MY PARENTS EDITH AND MARTIN

for making it possible for me to study chemistry and for their constant support.

Contents

I	Synthesis of a Pentafunctionalized Corannulene Derivative with Orthogonal Reactivity	1
1	Corannulene	2
1.1	Introduction—A Portrait of Corannulene	2
1.2	The First Synthesis of Corannulene	4
1.2.1	Failed Synthetic Approaches	5
1.3	Improved Synthetic Approaches	6
1.3.1	Flash Vacuum Pyrolysis	6
1.3.2	Solution Phase Chemistry	8
2	Corannulene Derivatives and their Symmetry	11
2.1	Introduction	11
2.2	C_s -symmetrical Corannulene Derivatives	13
2.2.1	Disubstituted Corannulene Derivatives	14
2.2.1.1	1,2-Substitution	14
2.2.1.2	2,5- and 1,6-Substitution	15
2.2.1.3	2,3-Substitution	16
2.2.2	Tetrasubstituted Corannulenes	17
2.3	C_5 -symmetrical Corannulene Derivatives	19
2.3.1	<i>sym</i> -Pentasubstitution	19
2.3.2	Decasubstitution	23
2.4	C_1 -Symmetrical, Monosubstituted Corannulene Derivatives	24
3	Controlled Synthesis of Fivefold Substituted Corannulene	26
3.1	Introduction	26

3.2	Aim of the Current Work	27
3.2.1	Target Molecules	27
3.2.2	Stereochemical Considerations	28
3.2.3	Isomer Count and Substituent Permutation	29
3.2.4	Preliminary Retrosynthetic Analysis	30
4	Synthetic Strategies Towards Highly Substituted Fluoranthenes	32
4.1	Literature Approaches to the Preparation of Fluoranthenes	32
4.2	Synthetic Strategy I — Ketone Condensation	36
4.2.1	Retrosynthetic Analysis	36
4.2.2	Synthesis of Acenaphthenequinone	37
4.2.3	Synthetic Studies toward Hexasubstituted Fluoranthene 91	39
4.3	Synthetic Strategy II — [4+2]-Cycloadditions	44
4.3.1	Pyrone Cycloaddition	44
4.3.1.1	Retrosynthetic Analysis	44
4.3.1.2	Synthesis of Acenaphthenone	45
4.3.1.3	Synthesis of Pyrones	46
4.3.1.4	Attempted Cycloaddition Routes to Target Fluoranthenes	47
4.3.2	Thiophene Cycloaddition	48
4.3.2.1	Retrosynthetic Analysis	48
4.3.2.2	Synthesis of Substituted Acenaphthylenes	48
4.3.2.3	Synthesis of Thiophene- <i>S,S</i> -dioxides	50
4.3.2.4	Synthesis of Hexa- and Heptasubstituted Fluoranthenes 91 and 92	52
4.3.2.5	Separation of Fluoranthene Regioisomers 91 and 92 and Their Identification by NMR Spectroscopy	55
4.3.3	Computational Analysis of Cycloadditions	57
5	Synthesis of 1,3,5,7,9-Pentasubstituted Corannulene	61
5.1	Model Fluoranthenes and Initial Studies	61
5.1.1	Aims	61
5.1.2	Synthesis of Model Fluoranthene	62
5.1.3	Bromination and Initial Ring Closure of the Model Fluoranthene	62
5.2	Synthesis of the Target Corannulene	66

5.2.1	Bromination of Highly Substituted Fluoranthenes 91a and 92a . . .	66
5.2.2	Ring Closure of Brominated Target Fluoranthenes	68
5.2.3	Final Synthetic Strategy Involving Alternative Coupling Conditions	69
5.2.3.1	Initial Studies	70
5.2.3.2	Ad Hoc Modification of Heptasubstituted Fluoranthenes 92 Toward Pentasubstituted Corannulene	73
5.2.4	Conclusion	76
5.3	Outlook	77
6	Experimental Section	79
6.1	General Data	80
6.1.1	Abbreviations	80
6.1.2	Chromatography and Acquisition of Spectra	81
6.2	Experimental Details	82
6.2.1	General procedure for the preparation of Fluoranthenes	112
6.2.2	X-ray Crystallographic Structure Information	123
II	Synthesis of Platinum and Ethynyl-Platinum Corannulenes	128
7	Corannulene-based Supramolecular Tectons	129
7.1	Introduction	129
7.2	Synthesis	129
7.2.1	Core-platinated Corannulenes	130
7.2.2	Ethynyl-platinum Corannulenes	131
7.3	Characterization	133
7.3.1	Pentakis-Pt(PEt ₃) ₂ Cl corannulene 212	133
7.3.2	Bis-Pt(PEt ₃) ₂ MeCN hexabromocarboranate corannulene 214b . . .	134
7.3.3	Bisethynyl-platinum corannulene 220	136
7.3.4	Conclusion	136
8	Experimental Section	137
8.1	General Data	137
8.1.1	Abbreviations	137
8.1.2	Chromatography and Acquisition of Spectra	137

8.2	Experimental Details	139
8.2.1	X-ray Crystallographic Structure Information	146
	References	149
A	Curriculum Vitae	161

List of Figures

1.1	Polar resonance form of 1	2
1.2	a) Side view of the carbon framework of 1 , and definition of bowl-depth; b) the four different C-C bonds of 1	3
2.1	Di- and tetrasubstituted corannulenes with different substitution patterns. .	14
3.1	Selected pentameric structures. Pentapeptide 83 and crown ethers 84 count the same numbers of atoms at the rim as the corannulene core.	26
4.1	Molecular structure of acenaphthenequinone 123 in the crystal. Thermal ellipsoids shown at the 50 % probability level.	39
4.2	¹ H NMR of fluoranthenes 91 . a) isolated regioisomer 91a (column chromatography); b) mixture of all four isomers, enriched with 91a (preparative TLC).	40
4.3	¹ H NMR of fluoranthenes 137 . a) isolated regioisomer 137a (column chromatography); b) mixture of the two isomers 137a and 137b	42
4.4	Aromatic region of ¹ H NMR of 144	43
4.5	Molecular structure of bromoacenaphthenone 149 in the crystal. Thermal ellipsoids shown at the 50 % probability level.	45
4.6	Molecular structure of thiophene- <i>S,S</i> -dioxide 159 in the crystal (aliphatic H atoms omitted). Thermal ellipsoids shown at the 50 % probability level. .	51
4.7	Preparative HPLC of 91 and 92 . a) Separation of 91a from 91b ; b) Step-wise separation of 92a from 92b . Column: Waters Spherisorb® S5, Nitrile, 250×20mm Semi-Prep. Column.	55
4.8	Analytical HPLC of a mixture of 91a and 91b (black), separated 91a (blue) and 91b (red). Detection wave length = 267nm. Column: Waters Spherisorb® S5, Nitrile, 3.0μm, 100×4.6mm.	56

4.9	NOESY NMR spectra of a) 91a and b) 91b	56
4.10	NOESY NMR spectra of isolated fluoranthenes 92a and 186	57
4.11	Frontier orbitals of thiophene- <i>S,S</i> -dioxide 159 . a) HOMO b) LUMO.	60
4.12	Frontier orbitals of 2-pyrone 145 . a) HOMO b) LUMO.	60
5.1	Structural similarities of the target fluoranthenes 91 and 92 with 190	61
5.2	VT ^1H NMR of 193a in CDCl_3 with a coalescence temperature of 310K. .	63
5.3	Molecular structure of corannulene diester 195 in the crystal. a) ORTEP representation with thermal ellipsoids drawn at 50 % probability. b) Crystal packing of 195 viewed along the <i>a</i> axis and c) along the <i>c</i> axis.	65
5.4	High resolution mass spectrum (ESI) of 196 with observed and simulated isotopic pattern for $[\text{M}+\text{Na}]^+$ (asterisk).	67
5.5	High resolution mass spectrum (APCI) of 197 with observed (top) and simulated (bottom) isotopic patterns for $[\text{M}]^+$ (asterisk) and the fragments $[\text{M}-\text{nBr}]^+$	67
5.6	Top: GC of the product mixture of tetrahydrocorannulenes 198 (a), dihydrocorannulene 199 (c) and target corannulene 89 (e) in a ratio of 31:53:5. Unassigned peaks stem from polysiloxanes (stationary phase GC column). Bottom: GC of target corannulene after purification.	69
5.7	GC of the product mixture obtained from Mn/CuCl ₂ promoted ring closure. a) Corannulene (1), b) tetrahydrocorannulene 202 , c) bromocorannulene (77) in a ratio of 67:20:13, respectively.	71
5.8	GC of the product mixture obtained from Mn/CuCl ₂ promoted ring closure toward 2,5-dimethylcorannulene (40 .) a, c, e) two diastereomers of tetrahydrocorannulene 41 and/or elimination product ($m/z=282.2\text{u}$), b) elimination product ($m/z=284.2\text{u}$), d) dihydrocorannulene 204 ($m/z=280.2\text{u}$), f) 2,5-dimethylcorannulene (40) in a ratio of 46:11:13:30, respectively.	72
5.9	Molecular structure of 4-methoxyphenyl substituted fluoranthene derivative 186 in the crystal. Thermal ellipsoids drawn at the 50 % probability level. .	75
5.10	Aromatic region of the ^1H NMR of (500 MHz) 1,3,5,7,9-pentasubstituted corannulene 209 . Hydrogens b and e show 4J -coupling with the adjacent ethyl and methyl groups, respectively.	76
5.11	VT ^1H NMR of target corannulene 209 in CD_2Cl_2	77

5.12	Schematic representation of the extension of pentafunctionalized corannulene with tailored “codons”.	78
7.1	^1H (a) and $^1\text{H}\{^{31}\text{P}\}$ NMR (b) of pentakis-Pt(PEt ₃) ₂ Cl corannulene 212 . . .	133
7.2	Asymmetric unit of the X-ray structure of pentakis-Pt(PEt ₃) ₂ Cl corannulene 212 . Thermal ellipsoids drawn at the 50 % probability level. Hydrogens and ethyl substituents on the phosphines are omitted for clarity.	134
7.3	^{31}P NMR of 212 in CD ₂ Cl ₂ showing eight singlets for the <i>trans</i> -oriented and two doublets for the <i>cis</i> -oriented phosphines. with their respective $^1J_{\text{Pt}-\text{P}}$ -couplings.	135
7.4	X-ray crystal structure of [bis-Pt(PEt ₃) ₂ MeCN corannulene] ²⁺ drawn at the 50 % probability level. Hydrogens, ethyl substituents on the phosphines and the hexabromocarborane anions are omitted for clarity.	135
7.5	X-ray crystal structure of Bisethynyl-platinum corannulene 220 drawn at the 50 % probability level. Hydrogens and the ethyl substituents on the phosphines are omitted for clarity.	136

List of Schemes

1.1	Conceptual retrosynthetic disconnections of the carbon framework of 1 . . .	4
1.2	First synthesis of 1 by Barth and Lawton.	5
1.3	Failed syntheses of 1 by Craig and Davis.	5
1.4	Flash Vacuum Pyrolysis of 2-ethynylbiphenyl (11) to phenanthrene (12 . . .	6
1.5	Syntheses of corannulene (1) from fluoranthenes via flash vacuum pyrolysis	7
1.6	Alternative syntheses of corannulene (1) via flash vacuum pyrolysis.	8
1.7	Syntheses of corannulene via reductive low-valent metal coupling.	9
1.8	Base-mediated synthesis of the corannulene core by alternative ring closing conditions according to Sygula and Rabideau.	10
2.1	Retrosynthetic disconnection of the rim (a) or the flank (b) carbons of 1 . .	11
2.2	Syntheses of 7,10-disubstituted fluoranthenes.	12
2.3	Syntheses of 1,6,7,10-tetrasubstituted fluoranthenes.	12
2.4	General retrosynthetic disconnection of C_s -symmetrical corannulenes to cor- respondingly presubstituted fluoranthenes and further to acenaphthenequinones A, dialkylketones B and acetylene equivalent C.	13
2.5	1,2-disubstituted and 1,3,4,6-tetrasubstituted corannulene derivatives. . . .	15
2.6	1,2-disubstituted and 1,2,5,6-tetrasubstituted corannulene derivatives. . . .	16
2.7	Synthetic route to 3,8-dibromo-5,6-dichloroacenaphthenequinone 48	17
2.8	Synthetic route to 2,3-dichlorocorannulene 49	17
2.9	Tetrasubstituted corannulenes.	18
2.10	Synthesis of 1,2,5,6-tetrasubstituted corannulene derivatives.	19
2.11	General retrosynthetic disconnection of <i>sym</i> -pentasubstituted corannulenes.	20
2.12	Chlorination mechanism of 1 with ICl.	21
2.13	Synthesis of <i>sym</i> -pentasubstituted corannulene derivatives.	22
2.14	Synthetic route to decasubstituted corannulenes.	23

2.15	Corannulene (1) and bromocorannulene (77) as starting point for further substitution.	24
2.16	Generation of corannulyne 81 from bromocorannulene 77 or trimethylsilyl trifluoromethanesulfonate 82	25
3.1	Retrosynthetic disconnection of 88 to intermediate 89 or 90 and highly substituted fluoranthene derivative 91 or 92	30
4.1	Early synthetic route to fluoranthene derivatives by Allen and Van Allan. . .	32
4.2	Annulation of maleic anhydride and fluorene (97) according to Bergmann. . .	33
4.3	Cycloadditions of cyclic and open chain dienes to acenaphthylene 99	33
4.4	Cycloaddition of alkenes to dialkylidene acenaphthene by Campbell and Gow. .	34
4.5	Transition-metal catalyzed formations of fluoranthene (96) and 7-substituted fluoranthene 110	34
4.6	Rh-catalyzed formal $[(2 + 2) + 2]$ cycloaddition of diynes by Wu <i>et al.</i> . . .	35
4.7	Base mediated formal $[2 + 4]$ cycloaddition of acenaphthenone 116 to pyrones 117 and lewis acid promoted formal $[3 + 3]$ cyclization of diene 119 . .	35
4.8	Retrosynthetic disconnection of target fluoranthenes 91/92 to cyclopentadienones 121/122 and acenaphthenequinones 123/124	36
4.9	Retrosynthetic disconnection of the acenaphthenequinones 124	37
4.10	Synthetic route to 1,3,6-trisubstituted naphthalene 126	37
4.11	Unsuccessful route to ketoacetal 134	38
4.12	Double Friedel–Crafts acylation of 126 leading to required acenaphthenequinone 123	38
4.13	Double Knoevenagel condensation of 3-heptanone (125) to 123 and subsequent Diels–Alder addition of ethyl propiolate leading to four regioisomers of hexasubstituted fluoranthenes 91a–91d	40
4.14	Double Knoevenagel condensation of β -keto ester (138) to 123 and subsequent Diels–Alder addition of norbornadiene leading to two regioisomers of pentasubstituted fluoranthenes 137a and 137b	41
4.15	Synthetic route to dibromo trialkylcorannulene 144	43
4.16	Retrosynthetic disconnection of fluoranthenes 91 and 92 to enolates 146 or 147 and the trisubstituted 2-pyrone 145	44
4.17	Synthesis of bromo acenaphthenone 149	45

4.18	Fe-mediated synthesis of methyl 6-methylcoumalate (150) and methyl 3-bromo-6-methylcoumalate (153).	46
4.19	Fe-mediated synthesis of methyl 6-methyl-3-propylcoumalate (145).	46
4.20	Failed envisioned cycloaddition of dienophiles 156 and enolates derived from 149 to 2-pyrones 145 , 150 and 153 in a regioselective manner.	47
4.21	Retrosynthetic disconnection of fluoranthenes 91 or 92 to thiophene- <i>S,S</i> -dioxide 159 and acenaphthylenes 157 or 158	48
4.22	Two different synthetic routes to the trisubstituted acenaphthenequinone 123 and acenaphthenone 162	49
4.23	Synthetic route to acenaphthylenes 157 and 149	50
4.24	Synthetic route to thiophene- <i>S,S</i> -dioxides 173 and 159	50
4.25	Synthetic route to thiophene- <i>S,S</i> -dioxide 174	52
4.26	Synthetic route to fluoranthenes 91 and 92 via cycloaddition of acenaphthylenes 157 and 158 to thiophene- <i>S,S</i> -dioxide 159	52
4.27	Formation of fluoranthene 181 by two consecutive [1,5]-hydride shifts and subsequent elimination of HBr.	54
4.28	Cycloaddition of acenaphthylene 183 to thiophene- <i>S,S</i> -dioxide 182 . Absence of reactivity toward thiophene- <i>S,S</i> -dioxide 185 lacking the electron-withdrawing bromines in the 3- and 4-position.	54
4.29	Successful cycloaddition of acenaphthylenes 157 and 158 to thiophene- <i>S,S</i> -dioxides and unsuccessful cycloadditions of enol ether 156 to pyrones.	58
4.30	Failed test reactions of electron-withdrawing and electron-donating dienophiles 187–189 with 2-pyrone 145	58
5.1	Outline of synthetic route to model fluoranthene 190	62
5.2	Benzylic bromination of model fluoranthene 190 leading to a mixture of diastereomers 193a and 193b	63
5.3	Coupling of benzylic bromides in 193 with method C ($\text{VCl}_3/\text{LiAlH}_4$) and dehydrogenation leading to corannulene 195	64
5.4	Benzylic bromination of 194 and subsequent elimination of HBr as an alternative aromatization toward model corannulene 195	64
5.5	Benzylic bromination of fluoranthenes 91a and 92a leading to diastereomeric mixtures 196 and 197	66

5.6	Ring closure of brominated fluoranthenes 196 leading to a mixture of tetrahydrocorannulenes 198 , dihydrocorannulene 199 and traces of target corannulene 89	68
5.7	Wurtz-type homocoupling of alkyl bromides with manganese and catalytic copper(II)chloride in aqueous media developed by Chan and coworkers. . .	69
5.8	Ring closure of octabromofluoranthene 22 leading to a mixture of tetrahydrocorannulene 202 , corannulene 1 and bromocorannulene 77	70
5.9	Ring closure of hexabrominated fluoranthene 42 leading to a mixture of dimethyltetrahydrocorannulene 41 , dimethyldihydrocorannulene 204 and dimethylcorannulene 40	72
5.10	Mn/CuCl ₂ promoted ring closure of 196 and subsequent dehydrogenation leading to target corannulene 89	73
5.11	Failed ring closure of brominated fluoranthene 197	73
5.12	Synthesis of fluoranthene 186 via Suzuki cross coupling of the isomeric mixture of fluoranthenes 92 with 4-methoxyphenylboronic acid. The thus obtained mixture of regioisomers can be separated by gravity column chromatography.	74
5.13	Mn/CuCl ₂ promoted ring closure of 208 and dehydrogenation leading to target corannulene 209	74
5.14	Envisioned further functionalization of pentasubstituted corannulene 209 . .	78
7.1	Retrosynthetic strategy for the formation of pentakis patinum 212 and pentakis ethynyl-platinum 213 corannulene derivatives from <i>sym</i> -pentachloro-corannulene (62).	130
7.2	Isomeric mixture of diplatinated tetrabromocorannulenes reported by Sharp and Lee.	130
7.3	Synthetic procedure for the direct metallation of halocorannulenes 62 and 43	131
7.4	Conversion of halocorannulenes 62 , 23 , and 43 to the TMS-acetylenes 216 , 217 and 218 and subsequent <i>in situ</i> desilylation/platination leading to ethynyl-platinum corannulenes 213 , 219 and 220	132

List of Tables

1.1	Summarized conditions for ring closure of 22	10
4.1	Conditions for Aldol-additions to diketone 123 on route to fluoranthenes 91 and 137	42
4.2	HOMO-LUMO gaps between selected dieneophiles and dienes. Green entries depict calculated values for reaction partners leading to cycloaddition products; red entries depict calculated values for performed, but unsuccessful reactions.	59
6.1	Crystallographic data for acenaphthenequinone 123	123
6.2	Crystallographic data for bromoacenaphthenone 149	124
6.3	Crystallographic data for thiophene- <i>S,S</i> -dioxide 159	125
6.4	Crystallographic data for heptasubstituted fluoranthene 186	126
6.5	Crystallographic data for corannulene diester 195	127
8.1	Crystallographic data for 212	146
8.2	Crystallographic data for 214b	147
8.3	Crystallographic data for 220	148

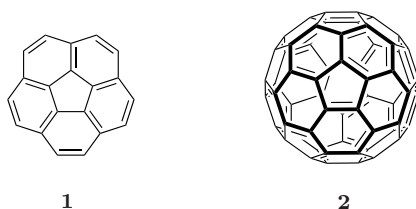
Part I

Synthesis of a Pentafunctionalized Corannulene Derivative with Orthogonal Reactivity

1 Corannulene

1.1 Introduction—A Portrait of Corannulene

Corannulene (**1**, $C_{20}H_{10}$), a [5]-circulene also known as dibenzo[*ghi,mno*]fluoranthene is the smallest member of the possible fragments of buckminsterfullerene (**2**, C_{60}) that exhibits a distinct curvature of its surface.



1 consists of five annulated benzene rings arranged about a central pentagon. As demonstrated by the mathematician Euler, a planar sheet of hexagons has to fold into a curved surface by the inclusion of pentagons. Eventually, the incorporation of 12 pentagons, without any of them adjacent to one another, leads to a closed icosahedral surface as seen for **2**, with their respective pentagons representing the vertices. The major deviation in **1** from sp^2 -bond angles of planar polyaromatic hydrocarbons (PAHs) forces the molecule to adopt a bowl-shaped geometry with an optimal compromise between strain and delocalization. In discussions on the major resonance contributor, a polar resonance form was proposed that contributes to the electronic structure of the molecule.¹

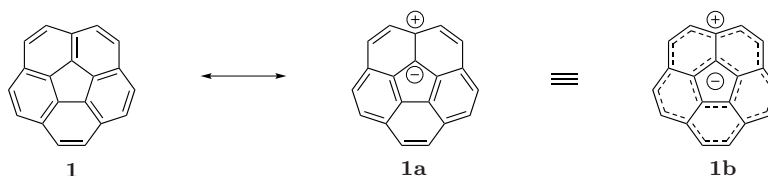


Figure 1.1: Polar resonance form of **1**.

This description highlights corannulene’s involuted electronic structure; it possesses an inner cyclopentadienyl anion (with 6 π electrons) and an outer cyclopentadecaheptenyl cation (with 20 π electrons), both of which follow Hückel’s $4n+2$ rule. The above approach also was the main inspiration for the latin-derived name “corannulene”; *cor* meaning heart or within, *annula* meaning ring. The name also references its association with the higher homologue, coronene.²

Early calculations³ showed that the non-planar structure of **1** retains over 90 % of the π -binding energy found in the planar structure, nonetheless it is difficult a-priori to predict whether a planar or a bowl-shaped geometry would predominate. The first X-ray analysis by Hanson and Nordman revealed corannulene’s curved surface with an ideal C_{5v} symmetry.⁴ The bowl-depth of **1** is defined by the distance between the planes given by the five carbon atoms in the central pentagon and the ten carbon atoms of the rim and in the present molecule measures 0.87 Å (Figure 1.2a).

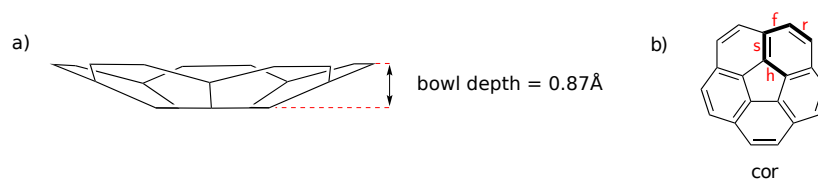


Figure 1.2: a) Side view of the carbon framework of **1**, and definition of bowl-depth; b) the four different C-C bonds of **1**.

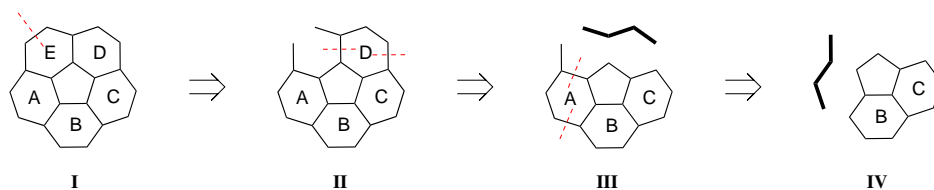
As suggested by Barth and Lawton, **1** undergoes bowl inversion through a planar transition state. The energy barriers of this transition for several mono- and disubstituted derivatives of **1** were accessed by variable temperature NMR.⁵ From these values the inversion barrier can be extrapolated for the parent structure **1**, and was estimated to be 11.5 kcal/mol.⁶

Due to its high symmetry, **1** is comprised of only four different C-C bonds (three chemically different C-atoms): hub (h), spoke (s), flank (f), and rim (r, Figure 1.2b).⁷ Bondlengths are alternating and shorter for the spoke and rim (1.38 and 1.39 Å, respectively) and longer for the hub and flank (1.42 and 1.44 Å, respectively).⁴ The ^1H NMR shows one single signal at $\delta = 7.81$ ppm confirming the magnetic isochrony of the ten hydrogen atoms around **1**. As expected, only three signals are recorded in the ^{13}C NMR: $\delta = 135.81, 130.84$ and 127.18 for hub, spoke and rim, respectively.⁸ Considering these

values, the resonance structure with the bonds localized toward a [5]-radialene is likely to be dominant. However, recent measurements of electron density from synchrotron data at 12 K reveal a slightly negative region within the central pentagon,⁹ as would be expected from the resonance structure depicted in Figure 1.1.

1.2 The First Synthesis of Corannulene

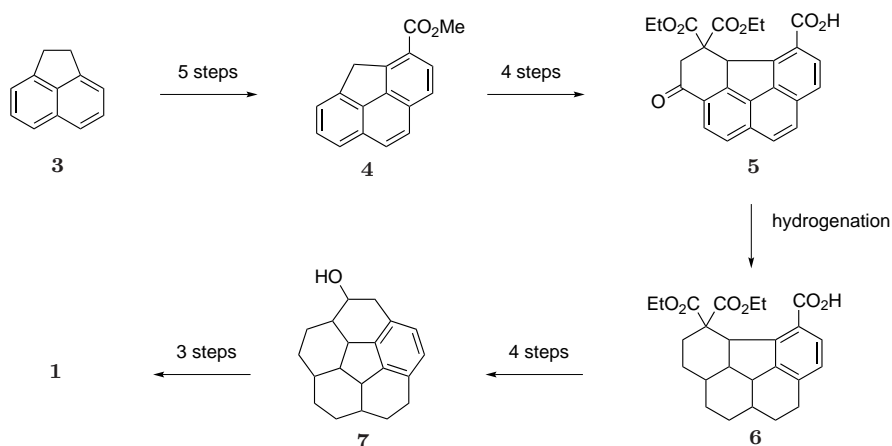
1 was first synthesized by Wayne E. Barth and Richard G. Lawton in 1966 by a laborious and circuitous route.¹ The general strategy for the construction of the carbon framework was to gradually annulate the carbon rings starting with an appropriate ring system. Disconnection of the rim bond of the last ring E in **I** leads to a simplified hydrocarbon fragment **II** possessing the central pentagon, ready for intramolecular cyclization (Scheme 1.1). Further cleavage of spoke and flank bonds of ring D in **II** delivers moiety **III** and a 4-carbon unit. This extends to the breakdown of ring A in **III** to deliver another 4-carbon unit and fragment **IV**.² The key intermediates of this approach to **1** are depicted in Scheme 1.2.



Scheme 1.1: Conceptual retrosynthetic disconnections of the carbon framework of **1**.

The synthesis starts with acenaphthene (**3**). Through alkylation with a 4-carbon unit (maleic anhydride), intramolecular acylation, and subsequent transformations the methylene phenanthrene **4** was obtained. Following this strategy, another 4-carbon unit was attached to the methylene position in **4** and cyclized to keto acid **5**, this comprises the carbon skeleton rings A–D. The authors claimed the subsequent hydrogenation occurred stereoselectively on one face of **5** to form benzoic acid **6**.^{1,2} The apparent cup-like structure bringing the carboxylic functions in close proximity for ring closure. Intramolecular acyloin condensation of **6** closed the last ring E and further conversions led to alcohol **7**. Aromatization of this initially synthesized saturated carbon framework, through dehydrogenation was crucial to the success of the strategy. In this way, any ring closure toward a strained structure has been bypassed. Clearly such a lengthy procedure prevented the

production of **1** in larger amounts, thus detailed studies on physical properties of **1** and its derivatization were not feasible.

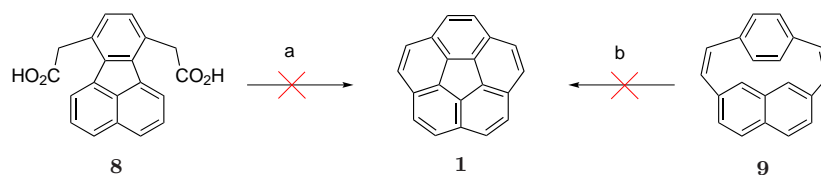


Scheme 1.2: First synthesis of **1** by Barth and Lawton.

1.2.1 Failed Synthetic Approaches

Subsequent to the work of Barth and Lawton, two different approaches to the solution phase synthesis of **1** were published by Craig and Robins (1968)¹⁰ and by Davy and Reiss (1979).^{11,12} Craig and Robins were the first to attempt the cyclization of fluoranthene derivatives to provide **1**. They envisioned the ring closure of diacetic acid **8** to a precursor of **1** under Friedel-Crafts conditions (path a, Scheme 1.3). Unfortunately all the employed conditions failed to give the desired ring closure.

The approach of Davy and Reiss was based on successful cyclizations of cyclophane dienes to coronene,¹³ pyrene¹⁴ and hexa[7]circulene.¹⁵ However, the oxidative cyclization of naphthalenocyclophanes **9** to **1** (path b, Scheme 1.3) failed as well.^{11,12}



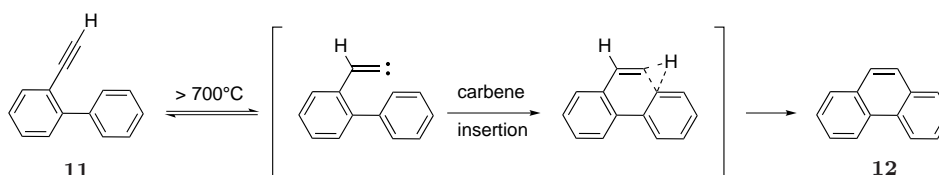
Scheme 1.3: Failed syntheses of **1** by Craig and Davis.

1.3 Improved Synthetic Approaches

1.3.1 Flash Vacuum Pyrolysis

After the first synthesis of corannulene in 1966 by Barth and Lawton,¹ the interest in this PAH waned for almost 20 years. Except for two failed attempts at its synthesis (see section 1.2.1), no other studies, synthetic or otherwise were published. The discovery of the fullerenes in 1985 by Kroto *et al.*¹⁶ though sparked new interest in various curved PAHs. The conception that PAHs were subunits of fullerenes spawned a whole new field of materials design and research.

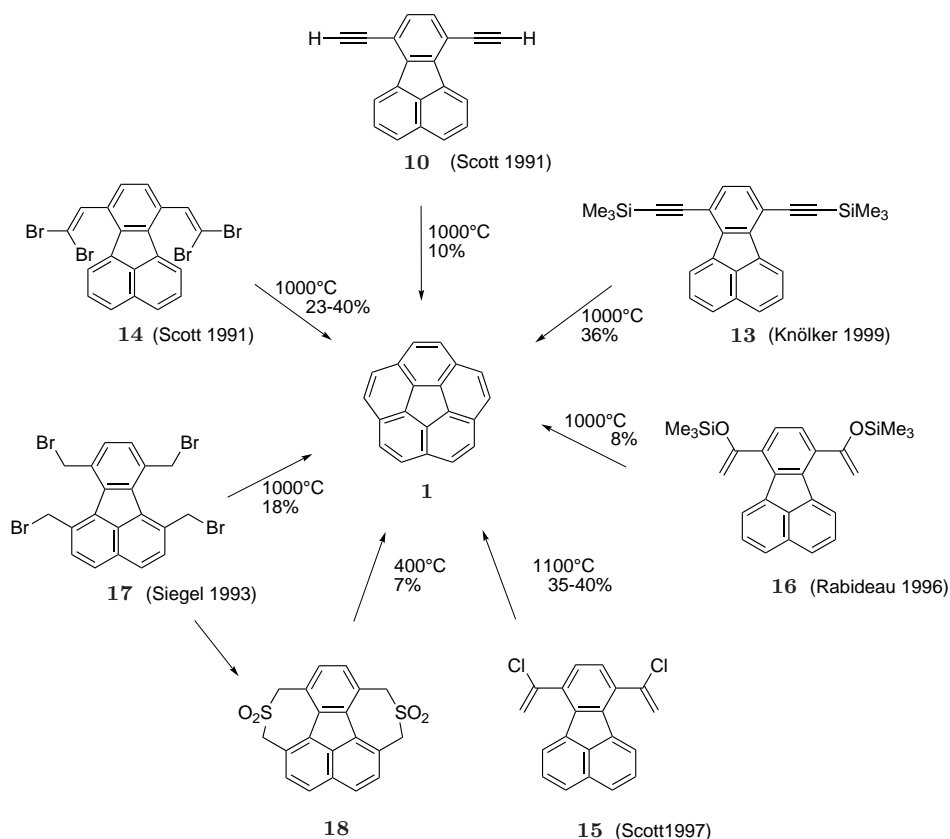
In 1991 L. T. Scott and coworkers reported a remarkably simple method for the preparation of **1**.⁸ The key step in this procedure is the formation of two six-membered rings during Flash Vacuum Pyrolysis (FVP) of diethynylfluoranthene **10** (Scheme 1.5). The cyclization of terminal acetylenes was inspired by the early work of R. F. C. Brown, who described the conversion of 1-ethynylanthracene to acenaphthylene¹⁷ and 2-ethynylbiphenyl (**11**) to phenanthrene (**12**, Scheme 1.4).¹⁸ Mechanistically it is believed that under the high reaction temperature the terminal acetylene allegedly rearranges to a vinylidene intermediate by a 1,2-hydride shift, this can then insert in nearby C-H bonds.



Scheme 1.4: Flash Vacuum Pyrolysis of 2-ethynylbiphenyl (**11**) to phenanthrene (**12**).

The success of FVP in the synthesis of curved and hence strained PAHs depends on one hand on the high temperatures applied, which allow planar precursors to bend into nonplanar geometries. The thermal energy therefore brings the reaction centers into close proximity. On the other hand, the reactions also take place in the gas phase, where intermolecular reactions that lead to polymerization are minimized. Indeed, the low volatility of fluoranthene **10** causes it to polymerize in the heated sublimation chamber of the FVP apparatus prior to vaporization. The cyclization itself is quantitative and the yield of 10 % reflects rather the amount of material that was sublimed into the pyrolysis tube. Knölker

et al. devised an alternative route to bis(trimethylsilyl)fluoranthene **13** in 1999, which upon FVP produced **1** in 36 % yield.¹⁹



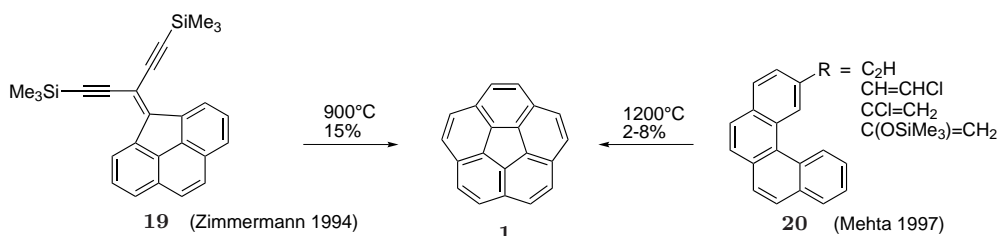
Scheme 1.5: Syntheses of corannulene (**1**) from fluoranthenes via flash vacuum pyrolysis

A precursor to **10**, bis(dibromovinyl)fluoranthene **14**, is less prone to polymerization under the applied temperatures, and **1** was obtained in up to 40 % yield. By varying the pyrolysis temperature, monobromo- and 1,6-dibromocorannulene could also be obtained from **14**.^{5,8} The promising use of divinyl fluoranthene **14** was optimized by the Scott group and culminated in the development of a 2-step procedure to bis(1-chlorovinyl)fluoranthene (**15**), which cyclizes to **1** in 35–40 % yield on a gram scale.²⁰ The authors postulate that the vinyl halides thermally eliminate HCl, to form the known precursor to **1**, diethynylfluoranthene **10** *insitu*. Rabideau *et al.* later showed, that silyl vinyl ethers **16** can also be deployed, however, with considerably less efficacy.²¹

Another route was presented by the Siegel group in 1992, in which the FVP was conducted with tetrabromide **17**,²² gave **1** in 18%.⁷ Conversion of **17** to the bissulfone **18** presented another attractive precursor: Extrusion of SO₂ under static vacuum at 400°C

affording **1** in 7% yield. Furthermore the tetrabromide **17** also ushered in a new era of solution phase chemistry that will be discussed in section 1.3.2.

Although tactically slightly different, the above precursors all have fluoranthene as common basic structure, and form two six-membered rings in the pyrolysis step. Zimmermann *et al.* in 1994, and Mehta and Panda in 1997, reported on different carbon skeletons as precursors to **1**. The enediyne motif on cyclopentaphenanthrene **19** forms two adjacent six-membered rings.²³ Whereas all the above FVP steps form two six-membered rings besides a preformed five-membered ring, Mehta and Panda describe a pyrolysis step in which one five-membered ring followed by a six-membered ring is formed.²⁴ The substituents on their benzophenanthrene precursors **20** are essentially the same "masked acetylenes" used for the ring closures of fluoranthenes.

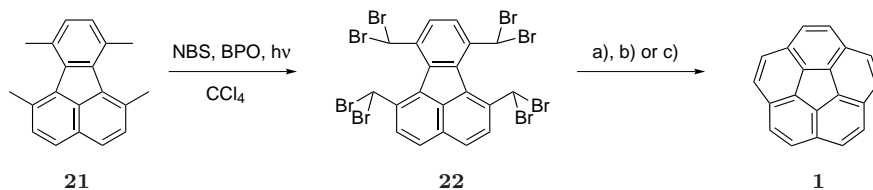


Scheme 1.6: Alternative syntheses of corannulene (**1**) via flash vacuum pyrolysis

Despite the success of FVP in the production of **1**, the method suffers from some disadvantages: The equipment used for FVP is restricted to several hundred milligrams from which only modest yields of **1** is obtained. Furthermore, the high temperatures applied do not tolerate additional functional groups, which limits the method for the synthesis of unsubstituted corannulene. Thus at this point, a scalable and efficient solution phase procedure for the synthesis of **1** was still lacking.

1.3.2 Solution Phase Chemistry

For solution phase synthesis, presubstituted fluoranthene derivatives (*e.g.* **8** or **17**) also seemed to be attractive precursors to **1**. The attempts to form the flanking bonds under intramolecular Friedel–Crafts conditions were unfortunately unsuccessful (see 1.2.1). This led to a retrosynthetic reconception where instead of disconnection of the flank, alternatively a rim bond cleavage would lead to 1,6,7,10-tetramethylfluoranthene (**21**, Scheme 1.7).²²



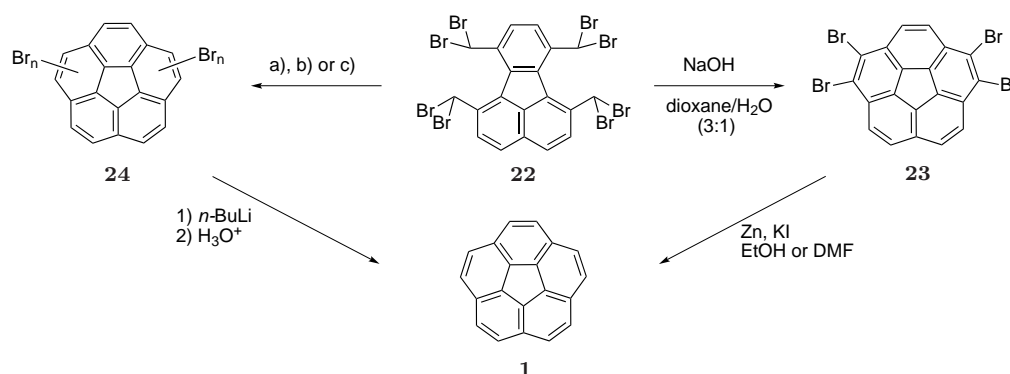
Scheme 1.7: Syntheses of corannulene via reductive low-valent metal coupling: a) $TiCl_3$ or $TiCl_4/LiAlH_4$; b) $TiCl_4/Zn-Cu$ couple; c) $VCl_3/LiAlH_4$.

Siegel *et al.* were the first to publish a solution phase protocol for the reductive coupling of benzylic bromides to form the rim bonds of a corannulene derivative (see Table 8.3).²⁵ A McMurry-type coupling was utilized employing Prakash and Olah's method,²⁶ in which a low-valent titanium reagent, obtained from treatment of $TiCl_3$ or $TiCl_4$ with $LiAlH_4$ is generated. While the coupling of the bromomethyl functions in **17** would lead to 1,2,5,6-tetrahydrocorannulene which must be further dehydrogenated, the dibromomethyl groups in **22** deliver **1** directly. Furthermore, the reactivity of dibromomethyl functions towards low-valent metal coupling is higher than for monobrominated benzylic positions.

Independently, the conditions for the reductive coupling were optimized by the Siegel and the Rabideau group. Changing the Ti-source from $TiCl_3$ to $TiCl_4$ and changing the reductant from $LiAlH_4$ to Zn-Cu couple increased the yield of **1** from 33 % to 80 %.⁶ Similarly, the change from $TiCl_3/TiCl_4$ to VCl_3 ²⁷ gave **1** in 70–75 % yield.²⁸ These methods share a common shortfall with FVP as the use of strong Lewis acidic compounds in combination with excess reductant is incompatible with the presence of several classes of functional groups.

An elegantly simple method for the ring closure of **22** was discovered by Sygula and Rabideau in the course of optimizing the chemistry of the ring closing step.^{29,30} The attempt to hydrolyze **22** into the corresponding tetraldehyde and apply the "original" McMurry conditions delivered not the aldehyde but 1,2,5,6-tetrabromocorannulene (**23**, Scheme 1.8) in excellent yields (>80 %). Reductive dehalogenation using Zn and KI leading then to **1**. The outcome of this base-mediated ring closure is solvent dependent: Whereas the reaction in dioxane/water cleanly delivers the tetrabromide **23**, the reaction in acetone/water produces a mixture of mono-, di- and tribromocorannulenes (**24**). Alternatively, this mixture of brominated corannulenes can also be obtained by heating octabromofluoranthene **22** with NaI or nickel powder in DMF over night.^{30–32} The two latter variants display milder methods for the pivotal ring closing step. Lithiation of the crude mixture of bromides **24**

with *n*-BuLi, followed by protolysis delivers parent compound **1**. A similar dehalogenation step with *n*-BuLi does not work for **23**, instead large amounts of butylated corannulenes were isolated. This base-mediated method for the ring closing not only facilitates the construction of the corannulene core, but also presents a versatile intermediate (**23**) for the synthesis of 1,2,5,6-tetrasubstituted corannulene derivatives.³³



Scheme 1.8: Base-mediated synthesis of the corannulene core by alternative ring closing conditions according to Sygula and Rabideau. a) NaOH in acetone/H₂O (3:1); b) Ni⁰-powder in DMF; c) NaI in DMF.

The optimized methods for the solution phase synthesis of parent **1** as well as the tetrabromo derivative **23** as a precursor enabled production of either compound on a multi gram scale. Recently a process for the kilogram production of corannulene by an analogous route was developed in our laboratories.⁷ The conditions for the ring closure of **22** are summarized in Table 1.1.

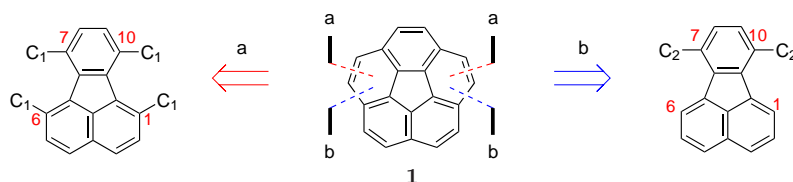
Table 1.1: Summarized conditions for ring closure of **22**.

entry	method	conditions	solvent	product	yield [%]	ref.
1	A	TiCl ₃ or TiCl ₄ /LiAlH ₄	DME or THF	1	33	6, 25
2	B	TiCl ₄ /Zn-Cu	DME	1	80	6
3	C	VCl ₃ /LiAlH ₄	DME	1	70–75	28
4	D	NaOH	dioxane/H ₂ O	23	83	29, 30, 33
5	E	NaOH	acetone/H ₂ O	24	>55	29, 30, 33
6	F	Ni ⁰ -powder	DMF	24	>75	30
7	G	NaI	DMF	24	>40	30

2 Corannulene Derivatives and their Symmetry

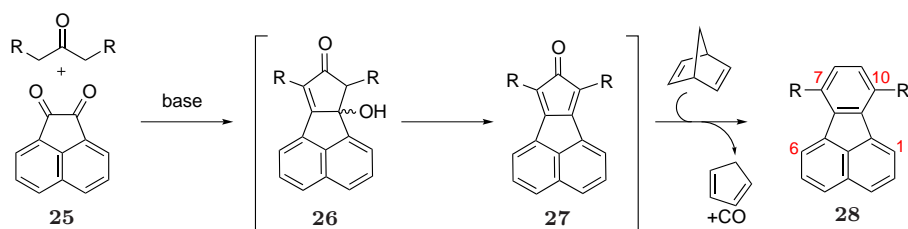
2.1 Introduction

As described in the previous chapter, synthetic approaches to **1** almost exclusively lead through fluoranthene derivatives. For the synthesis of **1** via FVP, 7,10-disubstituted fluoranthene derivatives, such as **15**, were employed. In contrast, 1,6,7,10-tetramethylfluoranthene (**21**) proved to be the precursor of choice for solution phase synthesis. Generally, flank disconnection of **1** leads to fluoranthenes bearing C₂ units in the 7 and 10 position, whereas the rim disconnection leads to fluoranthenes with 1,6,7,10-substitution pattern of C₁ units (Scheme 2.1)



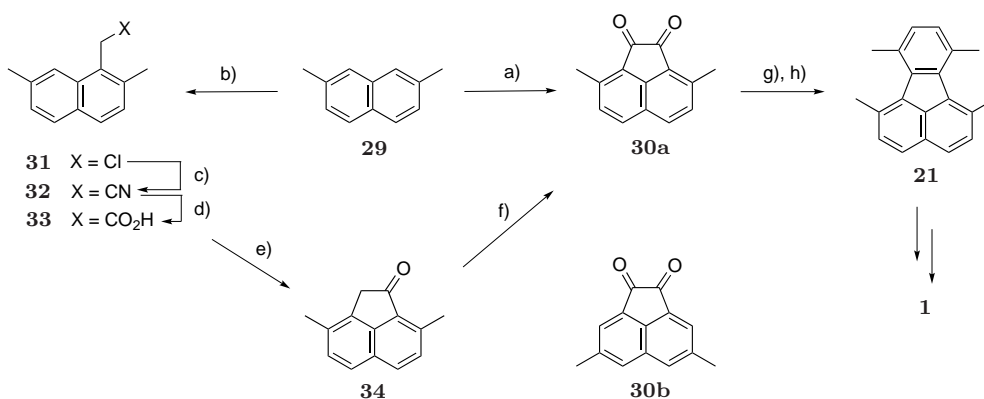
Scheme 2.1: Retrosynthetic disconnection of the rim (a) or the flank (b) carbons of **1**.

7,10-disubstituted fluoranthenes can be obtained from commercially available acenaphthenequinone **25**. As pioneered by Allen and VanAllan,^{34,35} the double Knoevenagel condensation of **25** with disubstituted ketones results in the formation of the corresponding carbinols **26**. Dehydration leads to cyclopentadienones **27** which readily undergo Diels–Alder reaction with acetylene equivalents (*e.g.* norbornadiene³⁶) to give 7,10-disubstituted fluoranthenes **28** (Scheme 2.2).



Scheme 2.2: Syntheses of 7,10-disubstituted fluoranthenes.

In the case of 1,6,7,10-tetramethylfluoranthene (**21**) the general strategy is analogous, but the substituents at C1 and C6 have to be introduced in an earlier stage of the synthesis. Generally, the scheme starts with 2,7-dimethyl naphthalene (**29**, Scheme 2.3), which is readily available via a synthesis devised by Leitch.³⁷ A double Friedel-Crafts acylation of **29** with oxalyl chloride delivers the 3,8-dimethylacenaphthenequinone (**30a**) together with its regioisomer **30b**. Separation of the regioisomers can be accomplished by either chromatography on Alumina,^{38,39} or fractionated crystallization.⁴⁰ A more elegant method for this separation was developed in our group,^{41,42} using Girard's reagent,^{43,44} which selectively forms the hydrazone salt with the undesired isomer. Similarly to the above synthesis, condensation of **30a** with 3-pentanone under basic conditions and subsequent cycloaddition with norbornadiene delivers the desired tetramethylfluoranthene **21**.



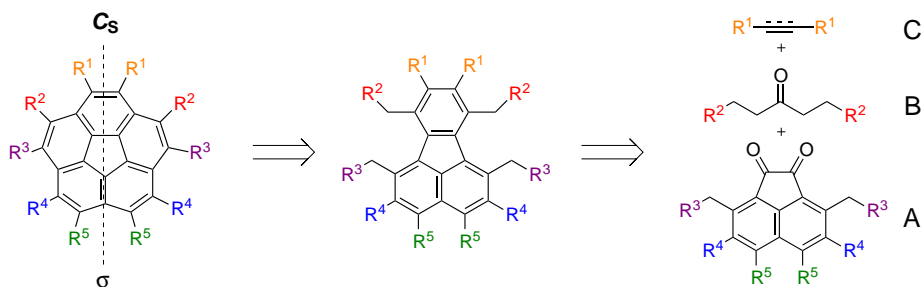
Scheme 2.3: Syntheses of 1,6,7,10-tetrasubstituted fluoranthenes. a) (COCl)₂, AlBr₃, CH₂Cl₂, –20°C to rt (35 %); b) (CHO)_x, 1M HCl in AcOH, 50°C (62 %); c) KCN, acetone/H₂O, reflux (99 %); d) H₂SO₄ in AcOH/H₂O, 90°C (90 %); e) 1. SOCl₂ CH₂Cl₂, reflux, 2. AlCl₃, reflux (82 %); f) SeO₂, doxane/H₂O, reflux (84 %); g) 3-pentanone, KOH in MeOH, rt; h) NBD, Ac₂O, reflux (63 %, 2 steps).

Alternatively, as applied earlier by Siegel and coworkers, **30a** can be obtained by a more involved, but higher yielding route:⁴⁵ Chloromethylation of **29** affords chloromethylnaphthalene **31**, and subsequent chloride displacement with cyanide gives acetonitrile **32**. Hydrolysis of **32** to the acid **33**, subsequent conversion to the acid chloride, and intramolecular Friedel-Crafts acylation yields acenaphthenone **34** which in turn can be oxidized to **30a**.⁶ The latter route avoids the tedious separation of the undesired isomer **30b**, increasing total synthetic throughput and minimizing waste streams.

Previously, only the synthesis of parent corannulene **1** and its precursors of type **28** or **21** were introduced. A more detailed discussion of different methods for the construction of fluoranthenes appears in chapter 4.1. In the following sections, a general view on the synthesis of substituted corannulenes will be discussed. Various strategies to access substituted corannulenes of different symmetry will also be presented. Benzo-fused,^{46–48} indenoannelated^{49–51} and other ring-extended systems,^{25,28,52,53} as well as metal complexes of corannulene will not be covered. As an overview, three different symmetries are possible for corannulene derivatives: C_s , C_5 and C_1 .

2.2 C_s -symmetrical Corannulene Derivatives

The route to 1,6,7,10-tetrasubstituted fluoranthenes (*e.g.* **21**) discussed above retains the bilateral symmetry of the initial 2,7-disubstituted naphthalene. Generally, the synthesis of fluoranthenes by this route is based on the disconnection in Scheme 2.4. In this case,



Scheme 2.4: General retrosynthetic disconnection of C_s -symmetrical corannulenes to correspondingly presubstituted fluoranthenes and further to acenaphthenequinones A, dialkylketones B and acetylene equivalent C.

the desired substituents of a final C_s -symmetric corannulene derivative must already be chosen at the level of the acenaphthenequinone A, dialkylketone B and the disubstituted dienophile C (Scheme 2.4). Depending on the particular location of the desired substituents

on the corannulene derivative, and their specific order of introduction, minor or significant changes in the synthetic strategy are required. To modulate the R^1 substituents, the nature of the dienophile **C** can be varied. Norbornadiene is commonly used for $R^1 = H$, although the reaction is not limited to this dienophile and substituted acetylenes are employed when alternative substitution was desired. To modify the substituents R^2 , a correspondingly substituted pentanone **B** has to be used to give benzylic positions on the resulting fluoranthene. Different substituents at positions 3 and 8 of the acenaphthene-quinone with methylene groups at the benzylic position have to be present to introduce substituents R^3 in the final corannulene. To date, no derivative of **A** with substituents R^4 has been used for the construction of substituted corannulenes. Introduction of R^5 groups will be explained below.

By following the strategy of preselecting the substituents needed, a number of di- and tetrasubstituted corannulene derivatives have been synthesized. The substitution patterns that have been achieved so far are depicted in Figure 2.1.

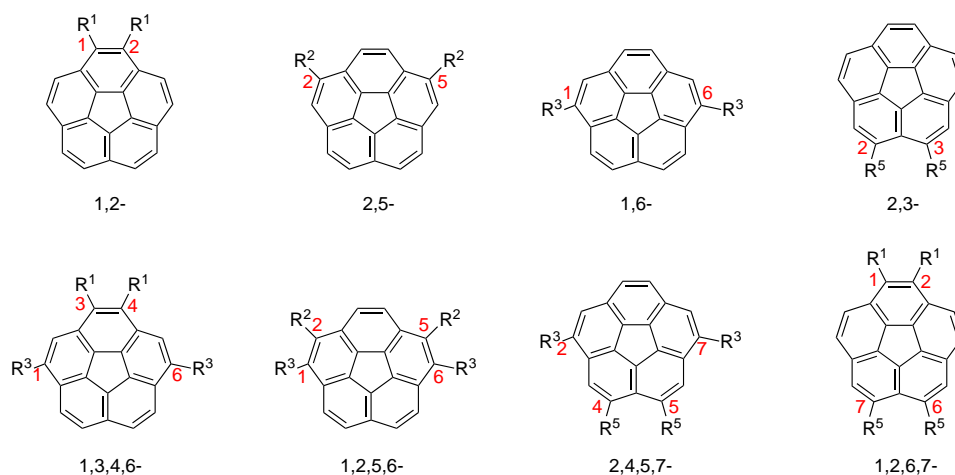


Figure 2.1: Di- and tetrasubstituted corannulenes with different substitution patterns.

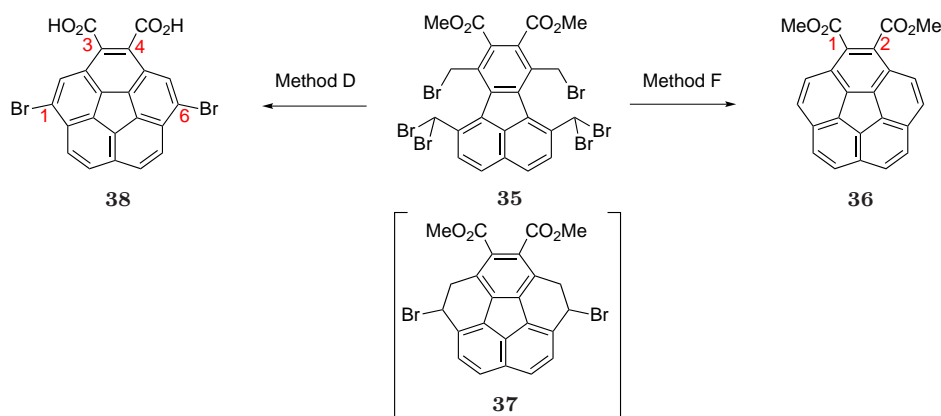
2.2.1 Disubstituted Corannulene Derivatives

2.2.1.1 1,2-Substitution

1,2-Disubstituted corannulene can be readily accessed as outlined by Rabideau and coworkers.⁵⁴ The Ni-mediated ring closing method F^{30–32} was applied to brominated fluoranthene diester **35** and the corannulene dicarboxylate **36** was obtained in good yield (60 %,

Scheme 2.5). Bromination of the methyl groups at C7 and C10 of the fluoranthene occurs only once because of the steric congestion between carbomethoxy and the methyl groups at C1 and C6.

The C–C bond formation occurs between a primary benzylic bromide and a primary benzyl dibromide (benzylidene bromide). In accordance with the postulated mechanism for the Ni-mediated ring closure (method F), the intermediate tetrahydrocorannulene **37** was suggested.⁵⁴ It has not been observed, however, probably due to the facile double elimination of HBr from **37**. Although accompanied by hydrolysis of the esters, the base mediated ring closing method D delivers the hydrolyzed 1,6-dibromo derivative **38** in about 20 % yield. The carboxylate and the bromine functions therefore also render the corannulene **38** as a starting point for the construction of 1,3,4,6-tetrasubstituted derivatives.



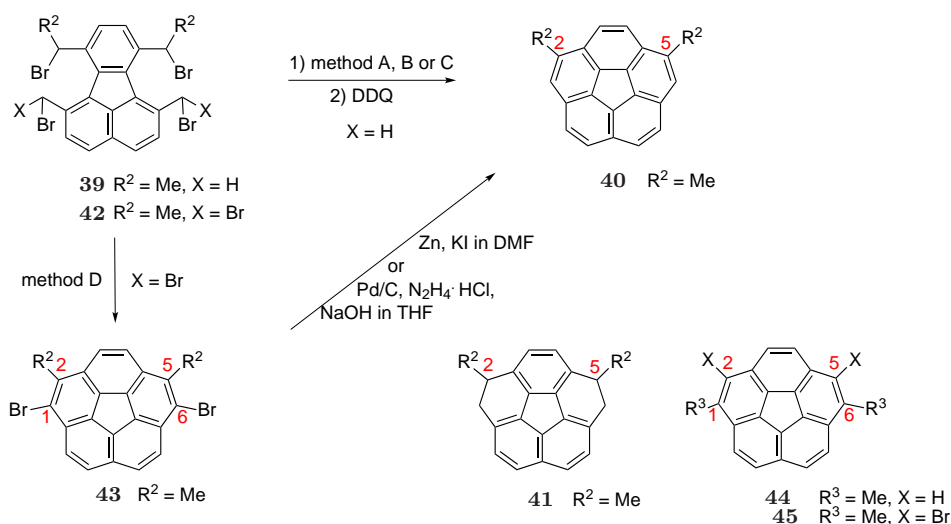
Scheme 2.5: 1,2-disubstituted and 1,3,4,6-tetrasubstituted corannulene derivatives.

2.2.1.2 2,5- and 1,6-Substitution

Siegel and coworkers were the first to publish the synthesis of alkyl substituted corannulenes, from adequately presubstituted fluoranthene derivatives.^{6,25} Originally, reductive coupling with low-valent metal (method A, B or C) was utilized to convert tetrabromide **39** to 2,5-disubstituted corannulene **40** in about 20 % yield (Scheme 2.6).²⁵ In comparison to **22**, the reductive coupling in **39** takes place between a secondary benzylic bromide and a primary benzylic bromide, which accounts for the lower yield due to the lower reactivity of halomethyl versus dihalomethyl groups. Another disadvantage of the coupling of monobrominated benzylic positions by methods A, B or C is the formation of tetrahydro-

corannulenes **41** as a mixture of diastereoisomers, which have to be dehydrogenated to the final corannulenes **40** in an additional step.

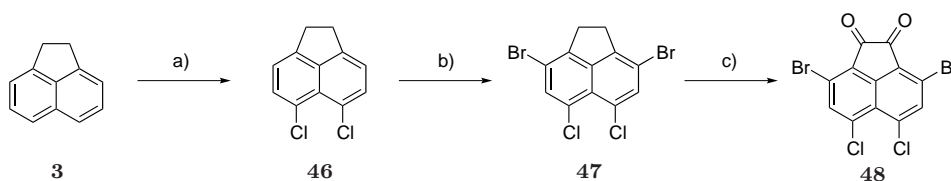
If the base mediated ring closing condition (method D) is applied to hexabromide **42**, in analogy to the formation of tetrabromocorannulene **23** from **22**, the dialkyl dibromocorannulene **43** is formed directly in over 60 % yield.^{40,55} **43** can then be hydrodehalogenated^{56,57} to disubstituted compounds **40**. Additionally, **43** serves as an ideal intermediate for further 1,6-substitution⁵⁵ allowing access to 1,2,5,6-tetrasubstituted corannulenes. The synthetic strategy summarized in Scheme 2.6 provides relatively easy access to disubstituted corannulenes such as **40**. For clarity, the example shown is the 2,5-disubstituted compounds **40** and the 1,6-dibrominated analog **43**, but in principle the same is true for 1,6-disubstituted corannulenes **44**⁶ and its 2,5-dibrominated analog **45**.



Scheme 2.6: 1,2-disubstituted and 1,2,5,6-tetrasubstituted corannulene derivatives.

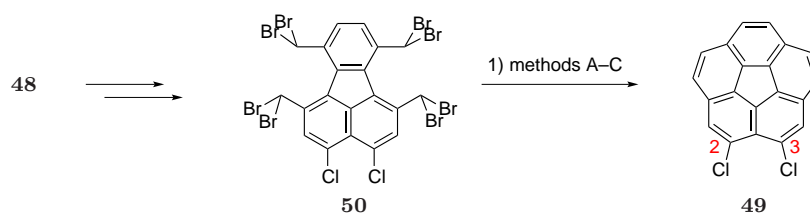
2.2.1.3 2,3-Substitution

For the introduction of R^5 substituents, the synthesis of the acenaphthenequinone moiety must be modified (Scheme 2.7); starting from acenaphthene (**3**), chlorination leads to peri-substituted 5,6-dichloroacenaphthene (**46**).⁵⁸ Further bromination selectively delivers 5,6-dichloro-3,8-dibromoacenaphthene (**47**),⁶ which can be oxidized to the acenaphthenequinone **48**. From **48**, the construction of the corresponding fluoranthene follows the path outlined in Scheme 2.2 or Scheme 2.3. The bromines can be converted to the alkyl chain necessary for the anticipated corannulene.



Scheme 2.7: Synthetic route to 3,8-dibromo-5,6-dichloroacenaphthenequinone **48**. a) SO_2Cl_2 , AlCl_3 , PhNO_2 (60 %); b) Br_2 , FeCl_3 , CH_2Cl_2 (90 %); c) CrO_3 , Ac_2O (90 %).

The prerequisite for the introduction of R^5 substituents is the construction of dichlorinated corannulenes of type **49**. After early installation of the chlorine atoms in dichlorofluoranthenes **50**, the construction of the corannulene core is analog to the cases explained above. The chlorides in **49** can be utilized in a variety of transformations: *e.g.* Kumada-, Negishi- or Sonogashira-type coupling, allowing the installation of sp^3 -, sp^2 -, and sp -carbon centers at R^5 . Furthermore, nucleophilic aromatic substitution with alcoholates or thiolates is also proved to be possible.⁵³ More details on the synthetic flexibility of chlorinated corannulenes is outlined below in section 2.3.1.



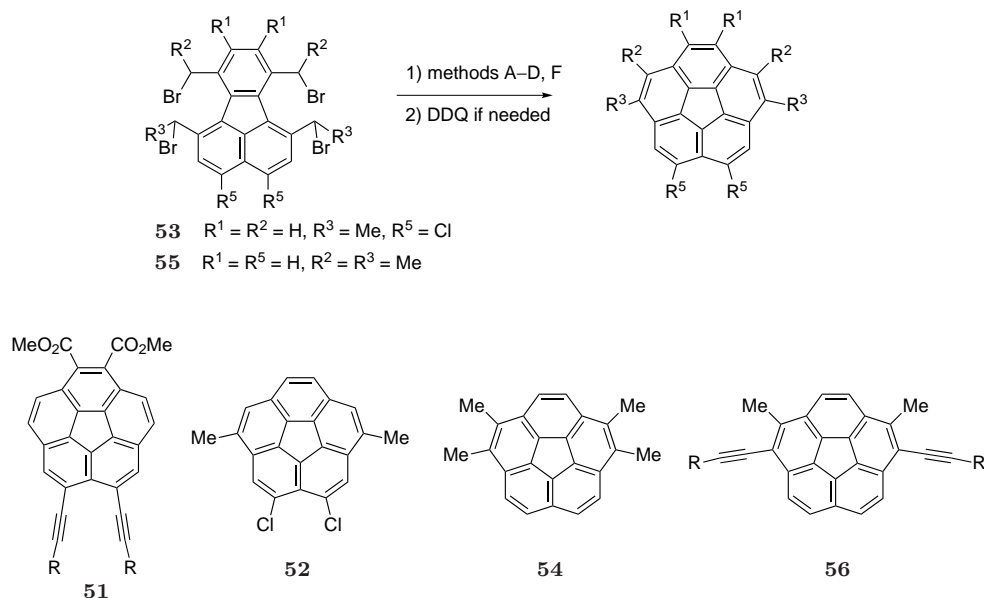
Scheme 2.8: Synthetic route to 2,3-dichlorocorannulene **49**.

2.2.2 Tetrasubstituted Corannulenes

Tetrasubstituted corannulene derivatives have almost all been synthesized by a combination of the methods described above. Again, depending on the functional groups present, or the type of benzylic bromide involved in coupling, one of the ring closing methods A–C, D or F was chosen.

1,2- or 2,3-disubstitution and as combination 1,2,6,7-tetrasubstitution (*e.g.* **51**) is well accessible, because the preinstalled substituents do not significantly perturb the final ring closing step. In the case of 2,5- and/or 1,6-substitution the yield of the corannulene obtained after dehydrogenation is highly dependent on the exact nature of the substituents:

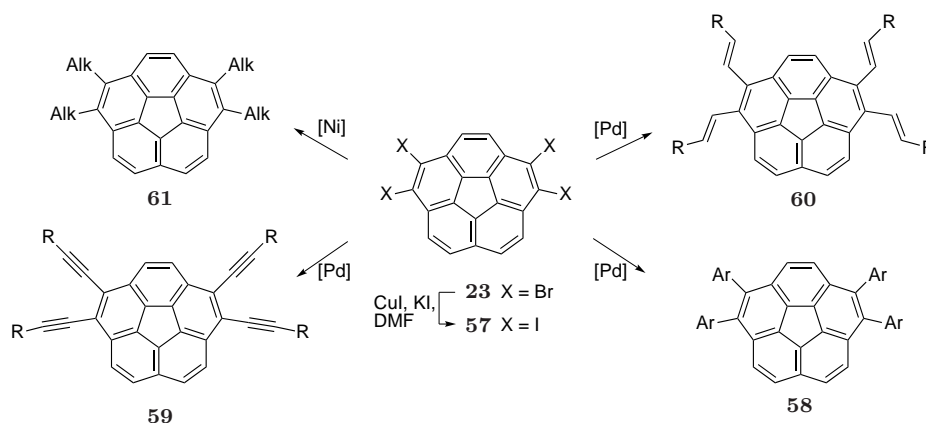
In a series of coupling between 1) primary benzylic dibromides (*e.g.* **49** from **50**), 2) primary benzylic bromide and secondary benzylic bromide (*e.g.* **52** from **53**) or 3) secondary benzylic bromides (*e.g.* **54** from **55**, Scheme 2.9) the yields decrease from about 80 % to below 50 % and further to below 10 %, respectively.⁶



Scheme 2.9: Tetrasubstituted corannulenes.

Therefore, for **54** or, as outline above, the construction of mixed tetrasubstituted corannulene derivatives of type **56**,⁵⁵ the dialkyl dibromocorannulenes such as **45** and **43** (Scheme 2.6) are better suited intermediates.

The most accessible C_s -symmetrical derivatives of **1** from a synthetic point of view are obtained from 1,2,5,6-tetrabromocorannulene (**23**).²⁹ The aryl bromide functionalities offer many ways of substitution with transition metal catalyzed coupling reactions. For better results in certain coupling conditions, the bromine atoms can be converted to iodides to give the tetraiodocorannulene **57**. By this route, tetraaryl- tetraethynyl-, tetraethenyl-, and tetralkylcorannulenes **58**, **59**, **60**, and **61**, respectively, could be accessed (Scheme 2.10).^{29,30,33}



Scheme 2.10: Synthesis of 1,2,5,6-tetrasubstituted corannulene derivatives.

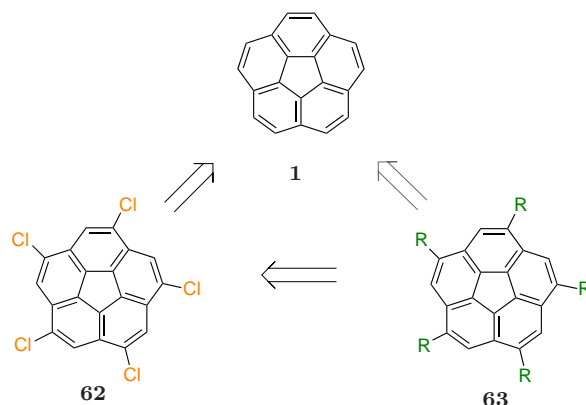
2.3 C_5 -symmetrical Corannulene Derivatives

2.3.1 *sym*-Pentasubstitution

The synthesis of C_s -symmetrical corannulenes is generally accomplished by starting from the corresponding fluoranthene precursors that already possesses the desired carbon skeleton for the final, corannulene derivative. In contrast, one strategy exists for the construction of 1,3,5,7,9-pentasubstituted (or *sym*-pentasubstituted*) The controlled pentachlorination of parent **1** that leads to *sym*-pentachlorocorannulene (**62**).^{59,60} This can be converted to other *sym*-pentasubstituted corannulene derivatives **63**, by either nucleophilic aromatic substitution of the five chlorine atoms, or by several transition metal catalyzed coupling reactions detailed below.

Fivefold symmetric direct electrophilic aromatic substitution under Friedel–Crafts conditions is limited to the installation of bulky groups.^{59,61} Reaction of **1** in *tert*-butyl chloride with AlCl_3 gives penta(*tert*-butyl)corannulene. Reactions with sterically less demanding alkyl- or acyl groups, as well as bromination, gives multiple isomers with different degrees of substitution.

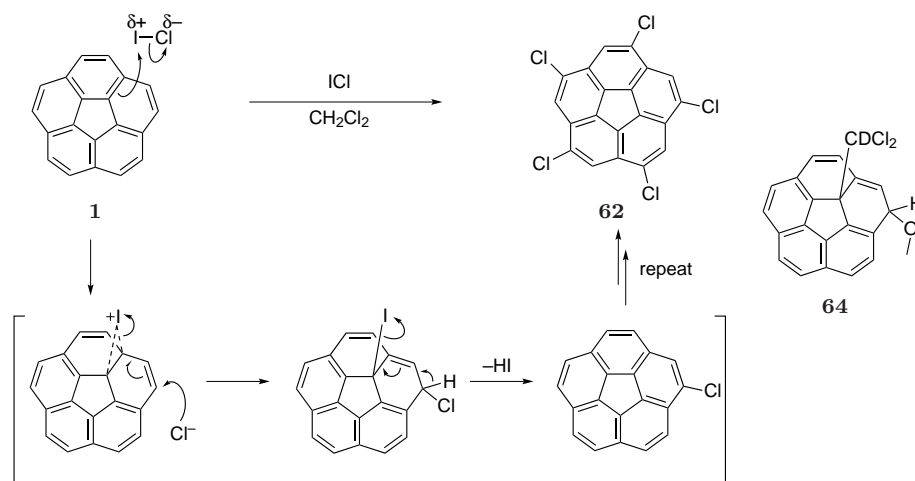
*The prefix *sym* is used to imply the C_5 -symmetrical 1,3,5,7,9-pentasubstitution of corannulene.



Scheme 2.11: General retrosynthetic disconnection of *sym*-pentasubstituted corannulenes.

In light of this, the high selectivity of the reaction of **1** with iodine monochloride to yield symmetrical **62** is surprising. Furthermore, due to the polarization of the I-Cl bond towards the more electronegative chlorine atom, iodination instead of chlorination would be expected if ICl was attacked by the rim atoms of **1**. Instead, the addition of iodine to the hub bond of **1** is proposed, followed by the attack of chloride to the rim. Subsequent elimination of HI rearomatizes the corannulene system and completes the 1,4-addition of ICl to one of the benzene rings. Repetition of these steps eventually leads to *sym*-pentachlorocorannulene (**62**, Scheme 2.13) in about 50% yield along with small amounts of under- and over-chlorinated corannulenes as side products.^{60,62} The proposed reaction mechanism is strongly supported by the addition of the dichlorocarbenium ion CDCl_2^+ to one of the hub carbon atoms of **1**. The thus formed carbocation was quenched with methanol to give methyl ether **64**.⁶³

In search of better reactivity towards metal catalyzed couplings, **62** has been converted to *sym*-pentakis[(pinacolato)boryl]corannulene in the Scott group.⁶⁴ Recently, Scott and coworkers discovered a direct Ir-catalyzed direct borylation of **1**. This borylation is being optimized, and coupling conditions for the novel *sym*-pentakis[(pinacolato)boryl]corannulene are currently examined. Pentaborylated corannulenes are promising new intermediates for the symmetrical fivefold extension of the corannulene core.



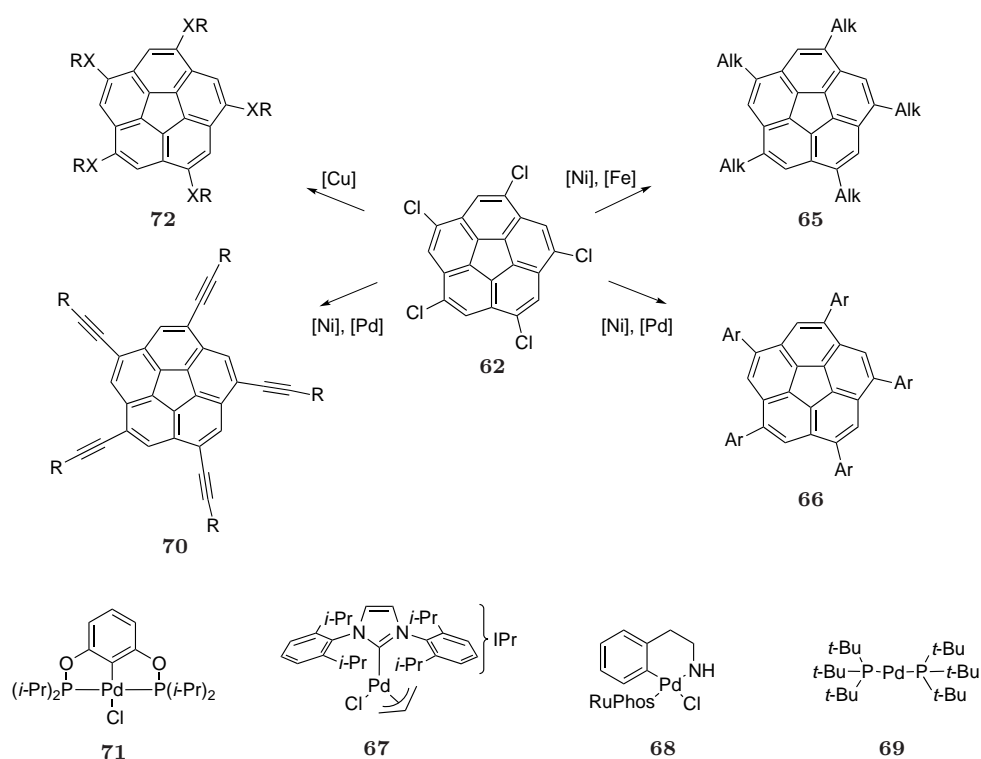
Scheme 2.12: Chlorination mechanism of **1** with ICl.

Hitherto, pentachlorocorannulene **62** played a central role in the fivefold derivatization of the corannulene nucleus, but it is far from an ideal synthetic intermediate. The material is sparingly soluble in common organic solvents, even at elevated temperatures, making it difficult to manipulate at reasonable concentrations. However, as the coupling advances, the solubilities of the respective intermediates gradually increases, accelerating further coupling. Generally, aryl chlorides are less reactive in transition-metal catalyzed cross-coupling reactions than aryl bromides or iodides. Furthermore, the catalytic cycle has to be completed five times per molecule, demanding a high reaction yield per site. Due to the difficulties in the purification of **62**, the under-chlorinated corannulenes present lead to a mixture of isomers of tetrasubstituted byproducts.⁶⁰ In consideration of the above difficulties, not observed with known bromocorannulenes, the coupling conditions for **62** deserve further explanation.

Pentaalkylcorannulenes **65** have been obtained by 1,3-bis(diphenylphosphino) nickel(II) chloride ($\text{NiCl}_2(\text{dppp})$)-catalyzed alkylation of **62** with trialkylaluminums (*i.e.* $\text{Al}(\text{CH}_3)_3$, $\text{Al}(\text{C}_2\text{H}_5)_3$, $\text{Al}(\text{C}_8\text{H}_{17})_3$) in between 30 and 50 % yield.^{6,65} Recently, $\text{Fe}(\text{acac})_3$ catalyzed alkylations using alkyl-magnesium halides were utilized in the Siegel group.⁶⁶

In the synthesis of pentaarylated corannulenes **66**, Zn-based Negishi-type coupling conditions were employed using $\text{NiCl}_2(\text{dppp})$.⁶⁷ The catalyst system with $\text{Pd}(\text{OAc})_2$ or $\text{Pd}_2(\text{dba})_3$ and Nolan's N-heterocyclic carbene (NHC) ligand 1,3-bis-(2,6-diisopropylphenyl)imidazoliumchloride ($\text{IPr}\cdot\text{HCl}$),^{51,68} or alternatively $(\text{IPr})\text{Pd}(\text{allyl})$ -complex **67** could be used as well.⁶⁹ The thermally more stable NHC ligands proved successful in the cou-

pling of sterically hindered aryl zincates (*i.e.* manisyl), and yields could be improved from 7 to 18–35 %. The yields for unhindered coupling partners range from about 30–50 %. Buchwald's system for the coupling of amines to aryl chlorides, RuPhos palladium(II) phenethylamine chloride **68**,⁷⁰ was recently used by Scott and coworkers to give pentakis(2,6-dichlorophenyl)corannulene in more than 50 % yield.⁷¹ Suzuki-type chemistry was also successful using Nolan's NHC ligand.⁵⁰ Improved conditions with the Pd-catalyst **69**, bearing Fu's bulky phosphine ligand tri(*tert*-butyl)phosphine,^{72,73} which tolerates boronic acids with a variety of functional groups were claimed by Keinan and coworkers to deliver the pentaarylated corannulenes in 59–83 % yield.⁷⁴



Scheme 2.13: Synthesis of *sym*-pentasubstituted corannulene derivatives.

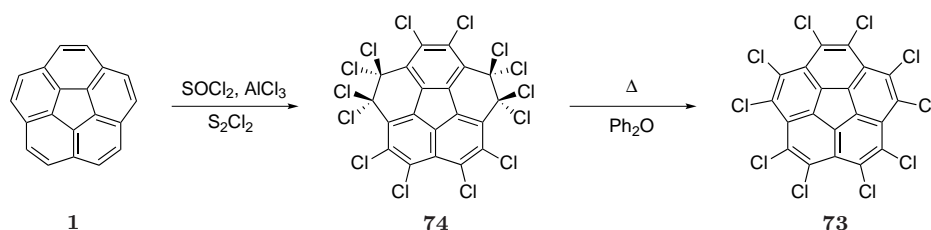
The introduction of five *sp* carbons to form pentaethynyl corannulenes **70** has been solved in several different approaches. Scott and coworkers reported a Kumada-type coupling with trimethylsilylethynyl magnesium bromide catalyzed by Ni(acac)₂, although no yield was provided.⁵⁹ Independently, the Siegel group also reported a protocol developed by Eberhard *et al.*,⁷⁵ in which the trimethylsilyl acetylene is used in large excess with the pincer catalyst **71** and ZnCl₂ to give *sym*-pentakis(trimethylsilylacetylene)corannulene in

53 % yield.⁶⁷ The most recent improvement in introduction of five acetylenes was reported by Wu *et al.* utilizing Stille-type coupling. Stannanes of the corresponding acetylenes were employed with Nolan’s NHC ligand, and yields between 70–95 % could be reached for a variety of acetylenes.⁵⁵

Finally, the chlorine atoms allow nucleophilic aromatic substitution with strong nucleophiles. Aromatic and aliphatic thiolates have been introduced into corannulene by the Scott^{60,62} and Siegel⁶⁷ group, and gave the corresponding corannulene thioethers **72** (X = S) in 35–55 % yield. Displacement of the chlorines by thiolates occurred at ambient temperature or at 120°C in the polar solvent 1,3-dimethylimidazolin-2-one (DMEU), whereas the alcoholates required more elevated temperatures of 180°C. Alternatively, Keinan and coworkers describe a copper-catalyzed Ullmann condensation with a variety of phenols.⁷⁶ Yields for the coupling of sterically unhindered and electron rich phenols range from 75–85 %, whereas hindered and electron deficient substrates gave between 17–50 % of the corannulene ethers **72** (X = O).

2.3.2 Decasubstitution

The only known synthetic intermediate for the production of decasubstituted corannulenes is decachlorocorannulene (**73**).^{59,62,77} **1** can be perchlorinated under Ballester⁷⁸ conditions, which delivers an overhalogenated tetradecachloro intermediate **74**. Refluxing in high boiling ether, such as (i-Pr)₂O or (Ph)₂O, extrudes four chlorines to give decachlorocorannulene (**73**) as a sparingly soluble solid.



Scheme 2.14: Synthetic route to decasubstituted corannulenes.

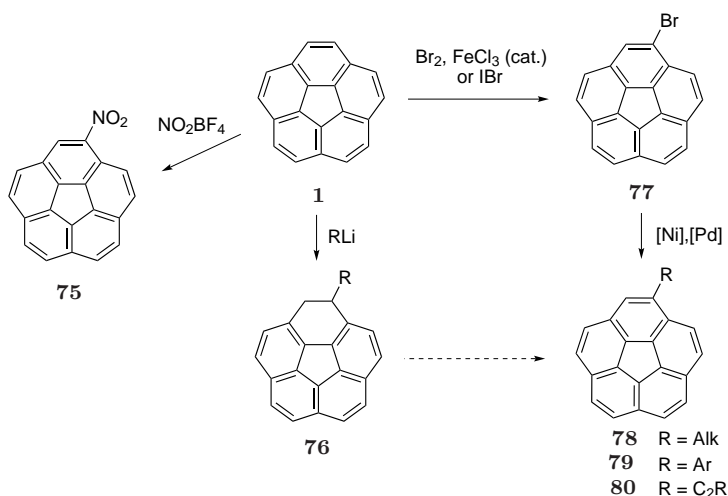
Much of the chemistry utilized for the conversion of pentachlorocorannulene **62** is transferable to decachlorocorannulene (**73**). Thus, the Pd-catalyzed reaction of **73** with a stannylalkyne and the NHC ligand IPr·HCl delivered decaethynylated corannulenes in about 10 % yield, corresponding to a coupling of 80 % per site.⁷⁹ Furthermore tenfold methyl-

tion⁶ has also been achieved, and the addition of a variety of thioethers^{59,62,67,77,80} have been reported as well. Tenfold arylation of **73** has not yet been accomplished.

2.4 C_1 -Symmetrical, Monosubstituted Corannulene Derivatives

As seen in the pentachlorination and the Friedel–Crafts alkylation, **1** undergoes electrophilic aromatic substitutions with several electrophiles. Although formylation, bromination, acylation, and nitration have been previously reported,^{59,81} experimental details are only available for the bromination^{6,82} and nitration. Nitrocorannulene (**75**) has recently been reported, and could be synthesized by the nitration of **1** with nitronium tetrafluoroborate in excellent yield (>95 %).⁸³

Interestingly, when **1** was treated with alkylolithium bases, the 1-alkyl-1,2-dihydrocorannulene **76** is directly formed.⁸⁴ The hydroalkylation proceeds smoothly and in excellent yield for bulky substituents like *tert*-butyl and isopropyl, whereas the additions of *n*-butyllithium and trimethylsilylmethylolithium are more sluggish. The reaction with methylolithium fails completely.



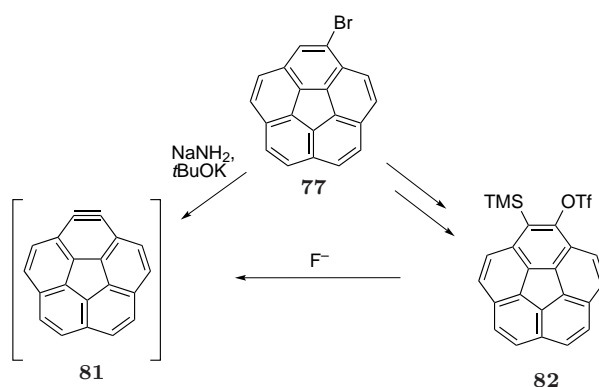
Scheme 2.15: Corannulene (**1**) and bromocorannulene (**77**) as starting point for further substitution.

Except for products derived from Friedel–Crafts-type chemistry, monobromocorannulene (**77**) is the pivotal starting molecule for the synthesis of monosubstituted corannulenes. **77** can be prepared by treatment of **1** with bromine and FeCl_3 .⁶ An issue with these reaction conditions is the formation of an isomeric mixture of dibromo- and tribromocorannulenes as side products. However, switching to IBr as the bromine source gave **77** in

2.4 C_1 -Symmetrical, Monosubstituted Corannulene Derivatives

90 % yield.⁸² Similar to the chemistry discussed above, different metal-catalyzed coupling reactions of bromocorannulene afford alkyl-, aryl- and ethynyl derivatives, **78**, **79** and **80**.

Furthermore, 1,2-didehydrocorannulene (or corannulyne) **81** can be generated from **77** by treatment with strong bases, which in turn can be used as nucleophiles.⁸⁵ In six steps, **77** can also be transformed to the trimethylsilyl trifluoromethanesulfonate **82** as corannulyne source. Trimethylsilyl trifluoromethanesulfonates are attractive aryne precursors because elimination of the TMS and OTf groups can be effected under mild conditions by treatment with a fluoride source (Scheme 2.16).⁸⁶



Scheme 2.16: Generation of corannulyne **81** from bromocorannulene **77** or trimethylsilyl trifluoromethanesulfonate **82**.

In conclusion, a versatile toolbox for the construction of various corannulene derivatives of C_s -, C_5 - and C_1 -symmetry is available. For the synthesis of C_s -symmetrical corannulenes, the choice of the preceding fluoranthene derivative, combined with the conditions of the ring closure determines the substitution of the corresponding corannulene. C_5 -symmetric corannulenes are, with very few exceptions, derived from metal catalyzed coupling of *sym*-pentachlorocorannulene (**62**) and or nucleophilic aromatic substitutions. For the monosubstituted C_1 -symmetric derivatives, the routes through bromocorannulene (**77**) mark a common starting point.

3 Controlled Synthesis of Fivefold Substituted Corannulene

3.1 Introduction

Fivefold symmetry is quite abundant in flowers, fruits and molecules, although somewhat less frequent than *e.g.* sixfold symmetry.⁸⁷ At the molecular scale, fivefold symmetry is common in metal complexes^{88–91} and biomolecules such as proteins^{92–95} and DNA nanostructures.^{96–98} However, C_5 -symmetrical organic molecules can be considered as relatively rare. Only a few pentameric examples allow substitution of the periphery, and most of them consist of conformationally flexible macrocycles, such as pentapeptides **83**,⁹⁹ crown ethers, and aza-crown ethers **84**.^{100,101} Structurally more persistent or rigid examples are calix[5]arenes **85**,^{102–105} calix[5]furans and -pyrroles¹⁰⁶ or cucurbit[5]urils (Figure 3.1).¹⁰⁷ Interestingly, the recently reported pentaamide **86**^{108,109} folds into an almost planar disk arrangement with nearly C_5 -symmetry due to an interior H-bonded network.

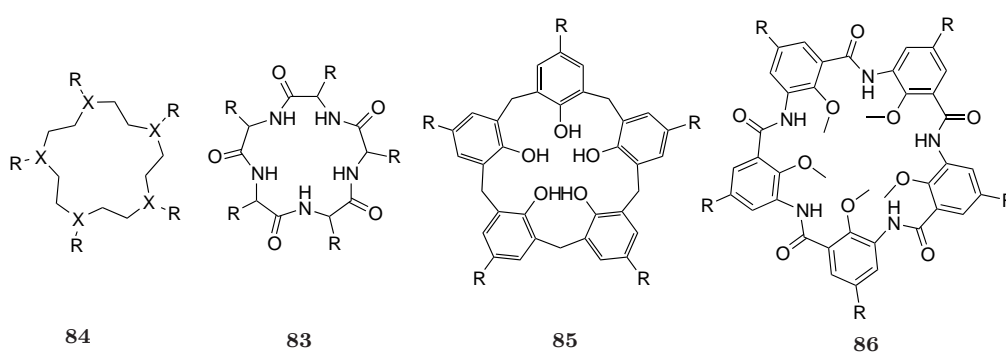


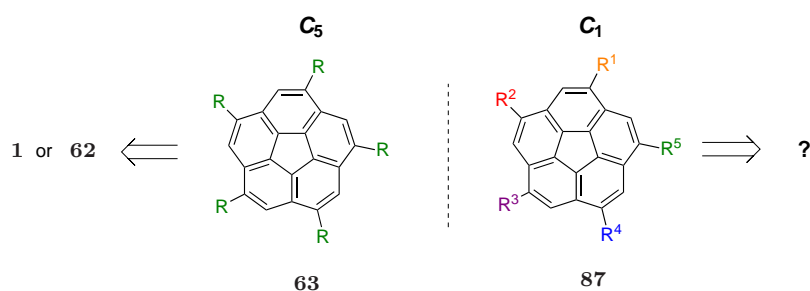
Figure 3.1: Selected pentameric structures. Pentapeptide **83** and crown ethers **84** count the same numbers of atoms at the rim as the corannulene core.

More generally, fivefold symmetrical molecules can serve as scaffolds for extended supra-molecular structures. Such a designed molecule could act both, as target ligand for *e.g.*

a corresponding C_5 -symmetric protein or as a synthetic receptor for various substrates of interest itself. Pentakis(arylthio)corannulenes **72** were reported by the Scott group to embrace buckminsterfullerene (**2**) with its electron-rich substituents and form donor–acceptor complexes.⁶⁰ T. Hayama designed and synthesized a corannulene-based C_5 -symmetric antagonist bearing fitted linker substituents with galactose tips. The fivefold ligand was anticipated to bind to a pentameric subunit of cholera toxin.⁶⁹

3.2 Aim of the Current Work

Few known pentameric structures allow the possibility of having substituents pointing at the corners of a regular pentagon, that is if substitution is even possible at all. In this context, corannulene (**1**) ideally serves as scaffold for derivatives with C_5 -symmetric substitution. As seen in the previous chapter, different methods have been developed to symmetrically substitute the core starting from *sym*-pentachlorocorannulene (**62**) or **1**. Despite the variety of C_5 -symmetric derivatives **63** thus accessible, the controlled synthesis of C_1 symmetric corannulenes with five different groups at the 1,3,5,7,9-positions remained unsolved. The purpose of this thesis is to synthesize a corannulene derivative of type **87**, with five distinct substituents of arbitrary choice, and the development of a feasible synthetic route to the target.



3.2.1 Target Molecules

The target molecule and its synthesis should meet the following criteria:

- five different substituents in the positions 1,3,5,7 and 9 of the corannulene core
- orthogonal reactivity of the five substituents
- synthetic control over the location of the substituent of choice

- control over isomer-count of possible corannulene derivatives

The prototype **88** was chosen as it contains several functional groups; a carbonyl moiety, a benzylic bromide, a *tert*-butyl group, an aromatic bromide and an ethene. This initial choice of substituents fulfills the condition of orthogonality and allows each site to be selectively addressed by choosing the appropriate reaction conditions.

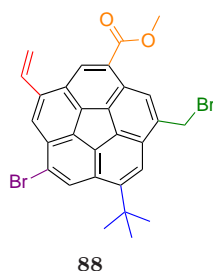


Figure 3.2: Target compound **88** with five orthogonal substituents.

Five functionalities are thus generated, displaying both, maximal diversity of function and a maximal symmetry of spatial distribution (with corannulene as fivefold template). Open to the chemist’s imagination, each of the envisioned functional groups in the target compound allows for several chemical transformations or extensions.

3.2.2 Stereochemical Considerations

Unsubstituted corannulene is an achiral molecule. If at least one substituent is introduced, and no mirror plane is present with higher substitution, the corresponding corannulene derivative becomes chiral due to bowl inversion. The two minima in the bowl inversion process are representing the enantiomers, the transition state being achiral. *Sym*-pentasubstituted corannulenes, as well as corannulenes with five different substituents therefore exist as enantiomeric couples that interconvert rapidly at room temperature. D. Bandera *et al.* was able to dynamically resolve the two equilibrating enantiomers of *sym*-pentasubstituted corannulenes by complexation with an enantiomerically pure metal–norbornadiene complex which lead to the formation of a single diastereomer.^{110,111}

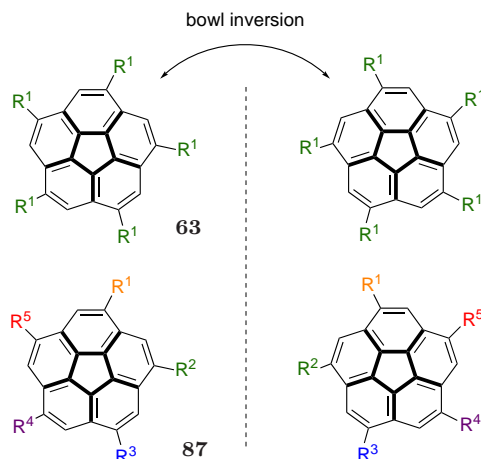


Figure 3.3: *sym*-Pentasubstituted and differently pentasubstituted corannulenes with their enantiomeric couple (*P*- and *M*-isomers).

3.2.3 Isomer Count and Substituent Permutation

The methods of *sym*-pentasubstituting corannulene starting from **62** overcome the sluggish reactivity of the chlorides towards Pd-catalyzed coupling reactions by judicious choice of the Pd-ligand, combined with an excess of the coupling partner and prolonged reaction time. Assuming that monosubstitution of **62** occurs cleanly, one could imagine a subsequent introduction of new substituents to reach derivatives of type **87**. Neglecting any possible regioselectivity for subsequent couplings, one faces a stochastic problem: The number of possible isomers after five single coupling steps with five different coupling partners would amount to a total of 24 isomers. As seen above, each isomer consists of an enantiomeric couple due to the bowl-shape of the corannulene core. At room temperature the inversion is rapid and the isomers are operationally achiral. However, if enantiomeric relations are distinguished or the bowl inversion is locked due to the nature of the substituents, the number of non-superimposable structures of type **87** results in a total number of 48 stereoisomers!*

*The circular substitution pattern of corannulene has a direction, the number of isomers P is given by $P = (n - 1)!$, where n is the number of substituents.

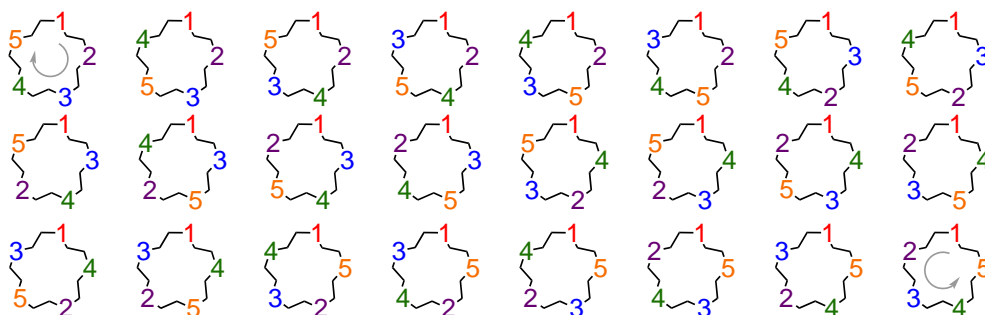


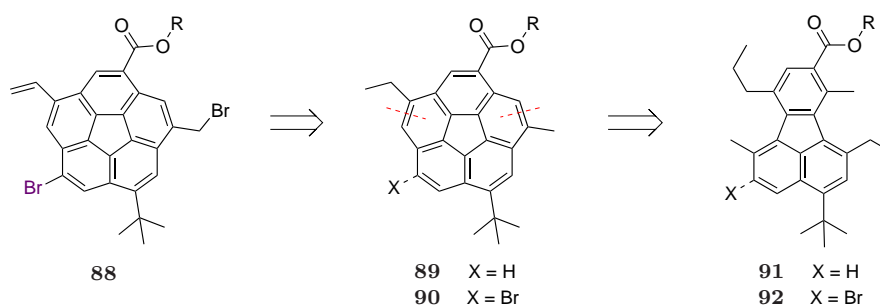
Figure 3.4: Depiction of the 24 unique regioisomers of the general structure **87**. Enantiomers that arise from bowl inversion of corannulene are not illustrated.

The above considerations concerning the idealized stepwise extension of **62** or **1** clearly show the vast number of isomers generated. Envisioning corannulene as a platform for diversity with the idea of exploiting this diversity, motivated us to develop a controlled synthesis of a corannulene derivative with five different substituents.

3.2.4 Preliminary Retrosynthetic Analysis

To control the possible isomer count and the location of a particular substituent, a strategy is needed in which the desired substituents are introduced in early steps of the synthesis. Given the successful synthesis of various substituted corannulenes from correspondingly presubstituted fluoranthenes (see section 2.2), it seemed promising to follow an analogous strategy.

On route to target compound **88**, the less functionalized compounds **89** and **90** were seen as key intermediates. Disconnection of the rim bonds indicated (Scheme 3.1) leads to the densely substituted fluoranthene derivatives **91** or **92**.



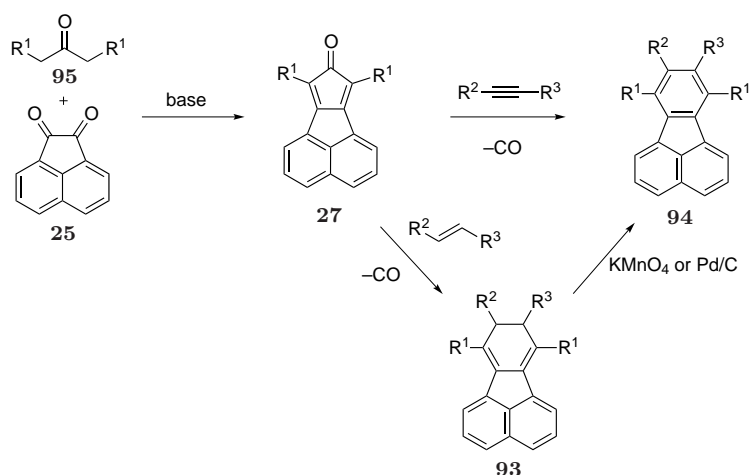
Scheme 3.1: Retrosynthetic disconnection of **88** to intermediate **89** or **90** and highly substituted fluoranthene derivative **91** or **92**.

One possibility for the introduction of the aromatic bromide present in **88** was planned after the corannulene core is synthesized, and could occur at the sterically least hindered position of **89**. In another conceivable route, the bromide function is already present in the fluoranthene derivative **92**, and will be carried through the ring closing and subsequent steps towards **88**. Strategies to accomplish the synthesis of fluoranthene derivatives **91** or **92** will be presented in the following chapter.

4 Synthetic Strategies Towards Highly Substituted Fluoranthenes

4.1 Literature Approaches to the Preparation of Fluoranthenes

In 1940 Allen and Van Allan reported the cycloaddition of vinyl phenyl ketone to cyclopentadienones of type **27** (Scheme 2.2) with subsequent elimination of CO to give an asymmetric dihydrofluoranthene **93**.³⁴ Substituting alkenes with acetylenes, or acetylene equivalents like norbornadiene (NBD),³⁶ directly delivers substituted fluoranthenes **94** (Scheme 4.1). As shown earlier, cyclopentadienones are readily obtained by the double Knoevenagel condensation of diketones (*e.g.* **25**) with acetone derivatives **95**. The subsequent cycloaddition of acetylenes, or alkenes has been the most widely used method to access fluoranthene derivatives en route to corannulenes.

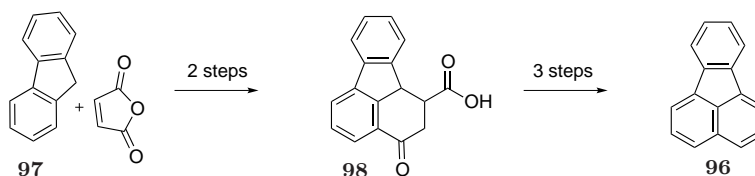


Scheme 4.1: Early synthetic route to fluoranthene derivatives by Allen and Van Allan.

Another early method to prepare fluoranthene (**96**) was devised by Bergmann and Ochrin, and is conceptually the same as Barth and Lawton used to construct the corannu-

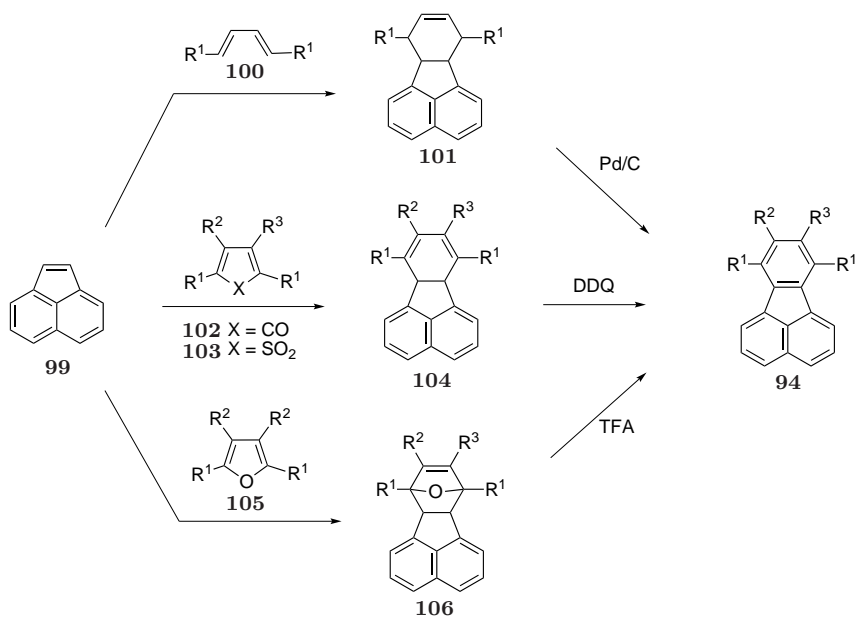
4.1 Literature Approaches to the Preparation of Fluoranthenes

lene core (see Scheme 1.2). Addition of maleic anhydride to fluorene **97**, and subsequent cyclization, leads to keto acid **98**. Reduction of the ketone, aromatization, followed by decarboxylation yielded **96** (Scheme 4.2).¹¹² Bergmann was also the first to report the



Scheme 4.2: Annulation of maleic anhydride to fluorene (**97**) according to Bergmann.

cycloaddition of acenaphthylene (**99**) to butadiene derivatives **100** which leads to tetrahydrofluoranthenes of type **101** (Scheme 4.3).¹¹³ The latter method was used by other researchers in the controlled synthesis of hydro- and hydroxyfluoranthenes,¹¹⁴ as well as corannulenes.¹¹⁵

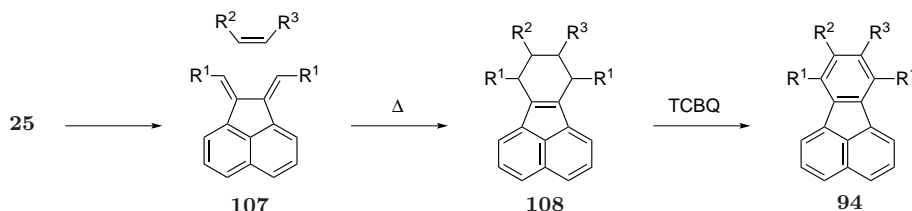


Scheme 4.3: Cycloadditions of cyclic and open chain dienes to acenaphthylene **99**.

Other pericyclic reactions with **99** involve cyclic dienes like cyclopentadienones **102**^{116–118} and tetrachlorothiophene-*S,S*-dioxides **103**,¹¹⁹ which, after extrusion of CO or SO₂, deliver substituted dihydrofluoranthenes **104**. Furans **105** were employed as well, and the intermediate Diels–Alder adduct **106** can be deoxygenated/aromatized to the corresponding fluoranthene **94** via dehydration with trifluoroacetic acid (TFA).¹²⁰

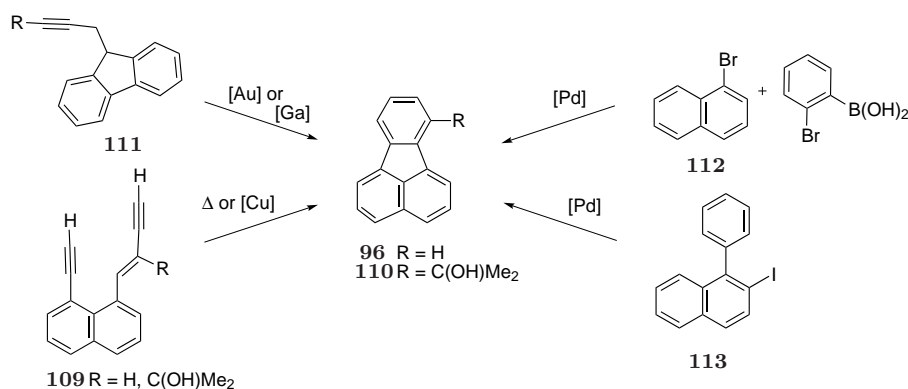
4.1 Literature Approaches to the Preparation of Fluoranthenes

Campbell and Gow converted the diketone **25** into a dimethyl glycol, from which the dimethylidene acenaphthene **107** was generated *in situ*, and condensed with a dienophile to deliver tetrahydrofluoranthenes **108**.^{121,122} Dehydrogenation to the fluoranthenes **94** was effected with tetrachlorobenzoquinone (TCBQ).



Scheme 4.4: Cycloaddition of alkenes to dialkylidene acenaphthene by Campbell and Gow.

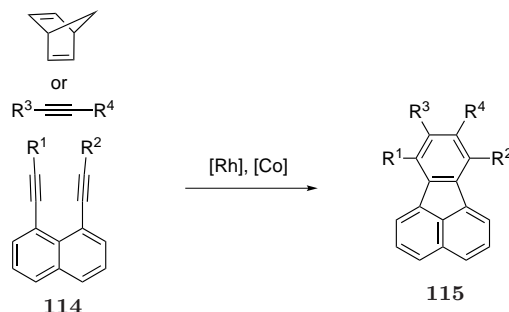
An interesting approach was presented by Enchavarren and coworkers, in which the alkyne and the enyne of naphthalene derivatives **109** are intramolecularly cyclized to parent fluoranthene (**96**) or 7-substituted fluoranthene **110** when heated.¹²³ The reaction also proceeds at room temperature in the presence of catalytic amounts of Cu(I). Very recently, alkyne substituted fluorene derivatives **111** were cyclized to 3-substituted fluoranthenes with Au(I)- or GaCl₃ catalysts.¹²⁴ Another transition-metal catalyzed indenoannulation was reported by de Meijere *et al.* in which bromonaphthalene **112** and 2-bromophenyl boronic acid undergo a one-pot Suzuki–Heck-type coupling cascade to form **96**.¹²⁵ Larock *et al.* reported a 1,4-palladium migration after insertion to 2-iodo-1-phenylnaphthalene **113**, again followed by a Heck-type annulation. The above methods are restricted to the formation of unsubstituted fluoranthene (**96**).



Scheme 4.5: Transition-metal catalyzed formations of fluoranthene (**96**) and 7-substituted fluoranthene **110**.

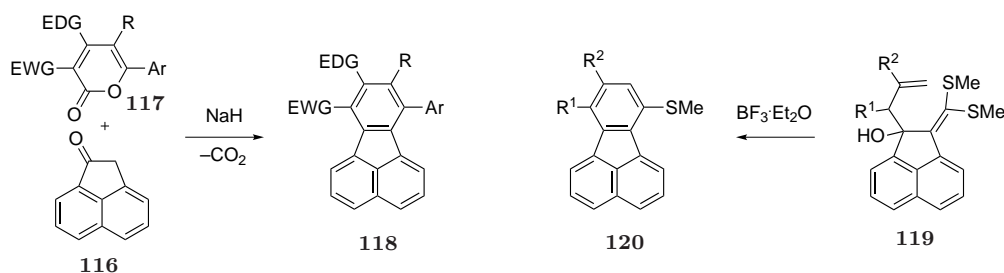
4.1 Literature Approaches to the Preparation of Fluoranthenes

A Rh-catalyzed formal [(2+2)+2] cycloaddition of diynes **114** to acetylenes or norbornadiene was published by Wu *et al.* (Scheme 4.6).^{49,126} The procedure allows the construction of symmetric and asymmetric 7,8,9,10-substituted fluoranthenes **115**.



Scheme 4.6: Rh-catalyzed formal [(2+2)+2] cycloaddition of diynes by Wu *et al.*

Two novel paths to fluoranthene derivatives are shown in Scheme 4.7. The method devised by Goel *et al.* starts from acenaphthenone **116**.¹²⁷ Enolate formation with NaH and Michael-type addition to the pyrone **117** gives **118** via intramolecular cyclization followed by elimination of water and carbon dioxide. Also starting from **116**, Panda *et al.* demonstrated that α -oxoketene dithioacetal formation followed by Grignard addition delivers the carbinol **119**.¹²⁸ A formal [3+3] cyclization reaction induced by BF₃·Et₂O then yield the fluoranthene **120**.



Scheme 4.7: Base mediated formal [2+4] cycloaddition of acenaphthenone **116** to pyrones **117** and lewis acid promoted formal [3+3] cyclization of diene **119**.

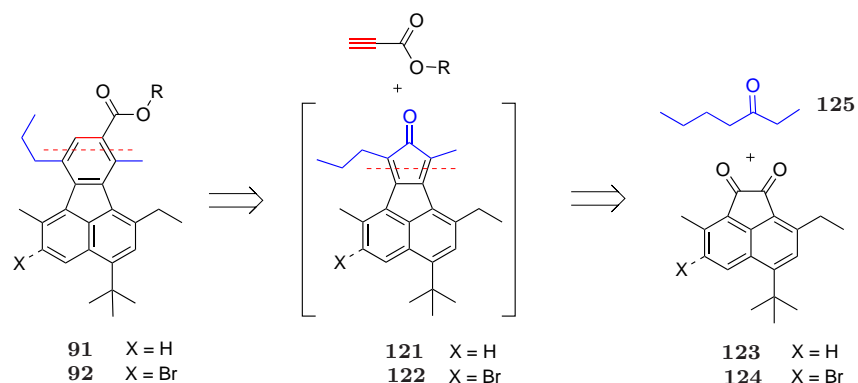
In conclusion, various methods for the construction of fluoranthene, as well as different types of substituted fluoranthenes, are available. Obviously, as shown above, the nature of the syntheses dictate the type and/or location of the substituents. Therefore, only few of the presented syntheses are suitable for the construction of the desired target fluoranthenes **92**, with its seven substituents at defined locations. In the following sections, different

synthetic strategies towards the synthesis of the target fluoranthene **92** (see Scheme 4.8) will be presented.

4.2 Synthetic Strategy I — Ketone Condensation

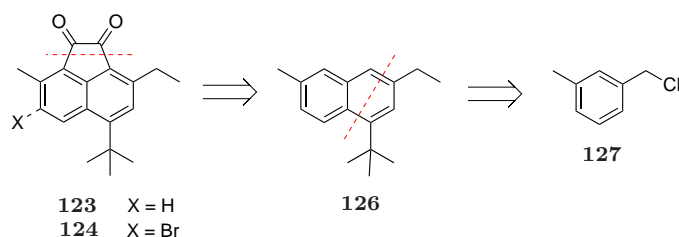
4.2.1 Retrosynthetic Analysis

According to the majority of synthetic procedures for substituted fluoranthene derivatives en route to corannulenes, the initial retrosynthetic disconnection of the target fluoranthenes **91** or **92** follows the “traditional” path to the cyclopentadienones **121** or **122** and an acetylene, namely an alkylpropiolate (Scheme 4.8). Further breakdown would lead to substituted acenaphthenequinones **123** or **124** and the asymmetric ketone 3-heptanone (**125**). As mentioned before, at which stage the introduction of the bromine should take place was not clear in preliminary synthetic plans.



Scheme 4.8: Retrosynthetic disconnection of target fluoranthenes **91/92** to cyclopentadienones **121/122** and acenaphthenequinones **123/124**.

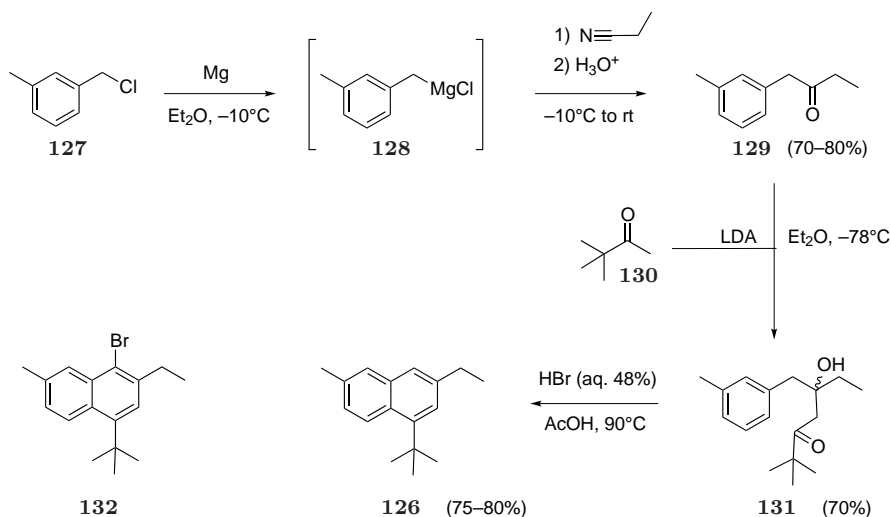
The acenaphthenequinone building blocks **123** and **124** were envisioned to come from the corresponding naphthalene precursor **126** (Scheme 4.9), in analogy to the synthesis of 3,8-dimethylacenaphthenequinone (**30a**, see Scheme 2.3). Also in analogy to the synthesis of 2,7-dimethylnaphthalene developed by Leitch *et al.*,³⁷ the trialkylnaphthalene **126** should be derived from 3-methyl benzylchloride (**127**).



Scheme 4.9: Retrosynthetic disconnection of the acenaphthenequinones **124**.

4.2.2 Synthesis of Acenaphthenequinone

The trisubstituted naphthalene **126** was the first intermediate targeted, its synthesis was conducted as follows (Scheme 4.10). From benzylchloride **127** the corresponding Grignard reagent **128** was formed, and quenched with propionitrile.¹²⁹ The intermediate imine salt underwent subsequent acidic hydrolysis at low temperature, leading to ketone **129** in about 70–80 %.



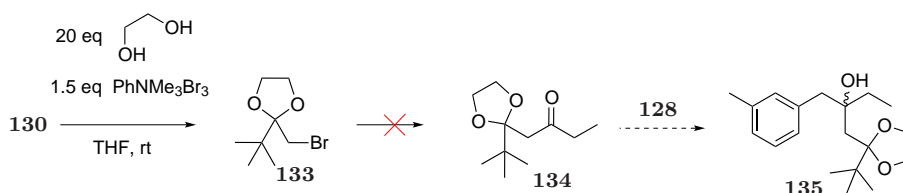
Scheme 4.10: Synthetic route to 1,3,6-trisubstituted naphthalene **126**.

The reaction could be run on >20g scale, and the crude product was purified by vacuum distillation. Attempts to generate **129** by means of deactivated dialkylcadmium reagents^{130,131} and propionic acid chloride failed and led to the Wurtz coupling dimer instead. Aldoladdition of 3,3-dimethylbutanone (pinacolone, **130**) to **129** with lithium diisopropylamide (LDA) delivered the hydroxyketone **131** in about 70 % yield, ready for cyclization. The reaction mixture had to be hydrolyzed with saturated NH_4Cl solution at -78°C , otherwise the adduct would undergo retro-Aldol reaction to regenerate the

starting materials. Typically the crude Aldol adduct was directly employed in the cyclodehydration step, which was effected by Bradsher's reagent (generally refluxing mineral acid–acetic acid mixtures).^{132,133} The thus obtained apolar naphthalene **126** could be easily separated from polar residues by column chromatography on silica and was obtained in 75–80 % yield.

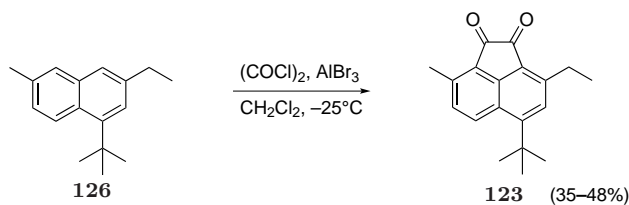
As anticipated, treatment of **126** with Br₂ or CuBr₂·Al₂O₃¹³⁴ only led to bromination at the *peri* positions with the bromonaphthalene **132** as main product. This result confirmed that bromine had to be introduced at a later point, as well as the highest reactivity of the 4-position toward electrophiles.

The above synthetic route has proven effective for the synthesis of target naphthalene **126** and was chosen because the initial strategy was not successful (Scheme 4.11): Pinacone **130** was converted in one step to the bromoacetal **133**.¹³⁵ Formation of the Grignard reagent of the latter, also at low temperatures, always ended in dimerization and the ketoacetal **134**, that would have led to hydroxyacetal **135**, could not be obtained.



Scheme 4.11: Unsuccessful route to ketoacetal **134**.

With the required naphthalene derivative **126** in hand, the double Friedel–Crafts acylation with oxalyl chloride delivered the expected acenaphthenequinone **123** (Scheme 4.12) in moderate yields, although the educt only offers one *peri* position (4,5) for attack. At



Scheme 4.12: Double Friedel–Crafts acylation of **126** leading to required acenaphthenequinone **123**.

temperatures above -15°C increasingly retro-Friedel–Crafts dealkylation occurred due to the strong lewis acid AlBr₃ and the de-*tert*-butylated acenaphthenequinone was obtained as a major side product. Hence it was crucial to hydrolyze the reaction mixture at low

temperatures. The diketone **123** was obtained as a bright yellow solid. Crystals suitable for X-ray diffraction were obtained by slow evaporation of a mixture of $\text{CH}_2\text{Cl}_2/n$ -hexane (Figure 4.1). The fused ringsystem is perfectly planar. The C–C bond between the two carbonyl functions measures $1.565(2)\text{\AA}$, which is quite long compared to acenaphthenequinone (1.533\AA).¹³⁶

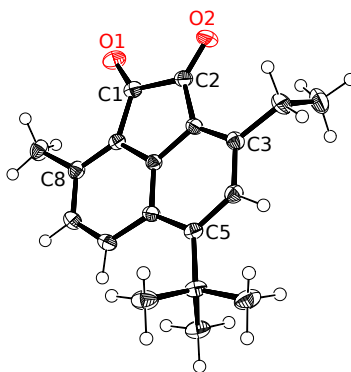


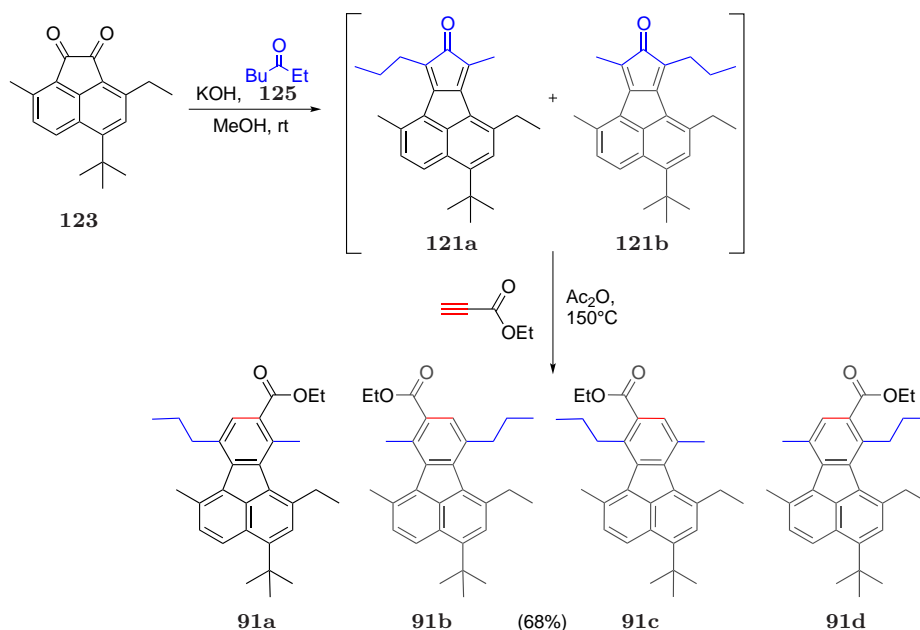
Figure 4.1: Molecular structure of acenaphthenequinone **123** in the crystal. Thermal ellipsoids shown at the 50 % probability level.

4.2.3 Synthetic Studies toward Hexasubstituted Fluoranthene **91**

An underlying impetus for our synthetic plan is outlined in Scheme 4.8 was to investigate possible regioselectivities in the individual steps. Could the Knoevenagel condensation of ketone **125** to acenaphthenequinone **123** could show selectivity due to steric clashes of the alkyl groups and slight electronic differences of the carbonyl functions in **123**? Also, could the cycloaddition of the alkyl propiolate to the intermediate cyclopentadienone **121** also be made selective towards the desired regioisomer?

Initially, identical conditions as the preparation of tetramethylfluoranthene were used. Addition/condensation of 3-heptanone (**125**) to the trisubstituted acenaphthenequinone **124** in methanolic potassium hydroxide at room temperature gave a crude mixture of carbinols, along with already dehydrated cyclopentadienones **121**. Depending on the drying agent in the workup, either the carbinols (for Na_2SO_4) or the cyclopentadienone (for MgSO_4) were obtained. The above crude, reddish mixture cyclopentadienones was then refluxed with ethyl propiolate in acetic anhydride. The dark mixture started to show intense bright blue fluorescence when irradiated with a UV-lamp ($\lambda=366\text{nm}$), indicative of the formation of fluoranthenes. The mixture thus obtained was analyzed by ^1H NMR. All the four possible isomers **91a–91d** were present, with essentially no exploitable selectivity

toward the desired isomer (Scheme 4.13). After careful column chromatography on silica



Scheme 4.13: Double Knoevenagel condensation of 3-heptanone (**125**) to **123** and subsequent Diels–Alder addition of ethyl propiolate leading to four regioisomers of hexasubstituted fluoranthenes **91a–91d**.

and preparative TLC it was possible to isolate the desired derivative **91a** in analytical quantity (Figure 4.2a). Figure 4.2b shows the aromatic region of a ^1H NMR of a sample containing all four isomers, enriched with the desired isomer **91a**.

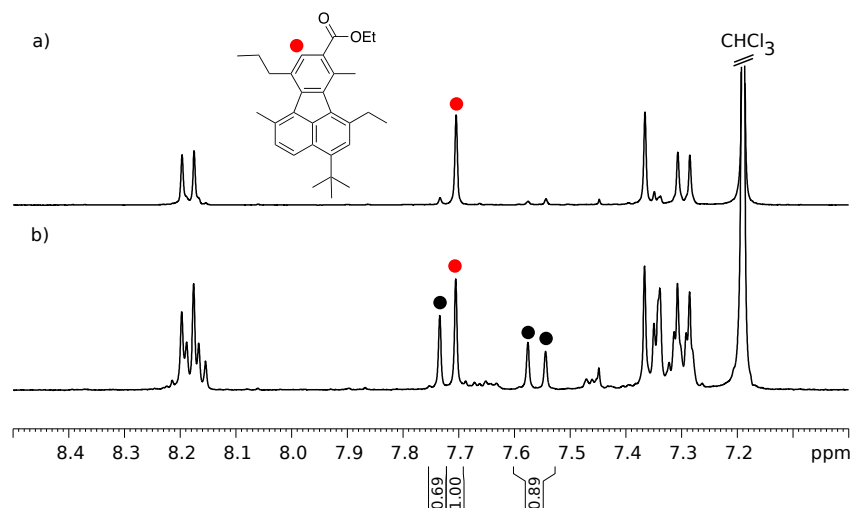
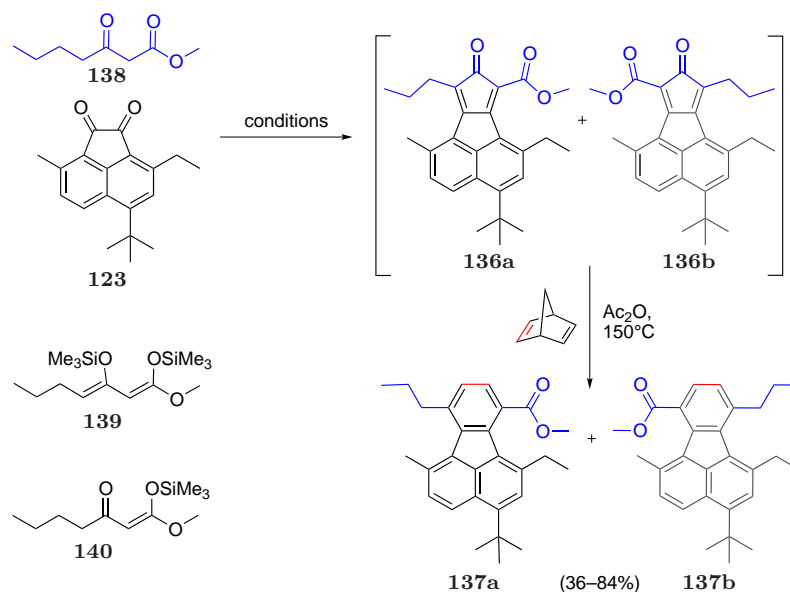


Figure 4.2: ^1H NMR of fluoranthenes **91**. a) isolated regioisomer **91a** (column chromatography); b) mixture of all four isomers, enriched with **91a** (preparative TLC).

Because no practical selectivity in the two successional reactions were found, the strategy was slightly modified. Instead of the asymmetric, simple ketone, a β -ketoester was chosen. As opposed to dialkyl ketones with pK_a -values at the α -positions of *ca.* 20, the pK_a of the methylene group between the keto functions of a β -ketoester is *ca.* 11.¹³⁷ Treatment of β -ketoesters with base first generates the anion/enolate at the CH-acidic position, and second at the more basic γ -position. The dicarbanion is an ambident nucleophile, however, attack of electrophiles occurs exclusively by the more basic carbon. Furthermore, the selectivity of attack can often be controlled by varying the base and reaction temperatures.



Scheme 4.14: Double Knoevenagel condensation of β -keto ester (**138**) to **123** and subsequent Diels–Alder addition of norbornadiene leading to two regioisomers of pentasubstituted fluoranthenes **137a** and **137b**.

Treatment of β -keto ester **138** with two equivalents of LDA at low temperatures and addition of the diketone **123** led to crude mixture of aldol addition and -condensation products, *i.e.* **136a** and **136b**. For simplicity of analysis the adducts were submitted to Diels–Alder reaction with norbornadiene (Scheme 4.14), leading to the two regiomeric fluoranthene methyl esters **137a** and **137b** in about 80 % yield. Cycloaddition reactions with the β -ketoester derived Aldol-adducts **136** were only conducted with NBD. Even with the Aldol-conditions at low temperatures, virtually no selectivity between the two isomers could be detected, as evidenced by ^1H NMR (Figure 4.3b). Switching to thermodynamic control of the reaction by employing sodium methoxide in methanol at room temperature delivered similar results after cycloaddition with norbornadiene.

The β -ketoester could also be converted to the corresponding 1,3-bis(trimethylsiloxy)-1,3-diene **139**, which was achieved in two steps:

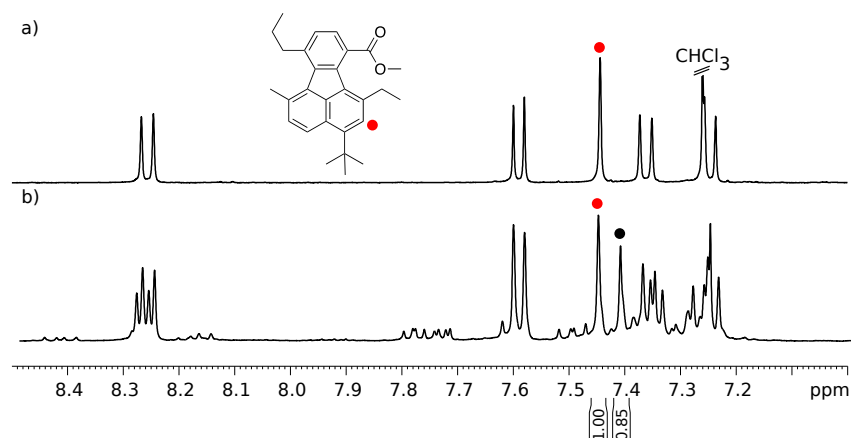


Figure 4.3: ^1H NMR of fluoranthenes **137**. a) isolated regioisomer **137a** (column chromatography); b) mixture of the two isomers **137a** and **137b**.

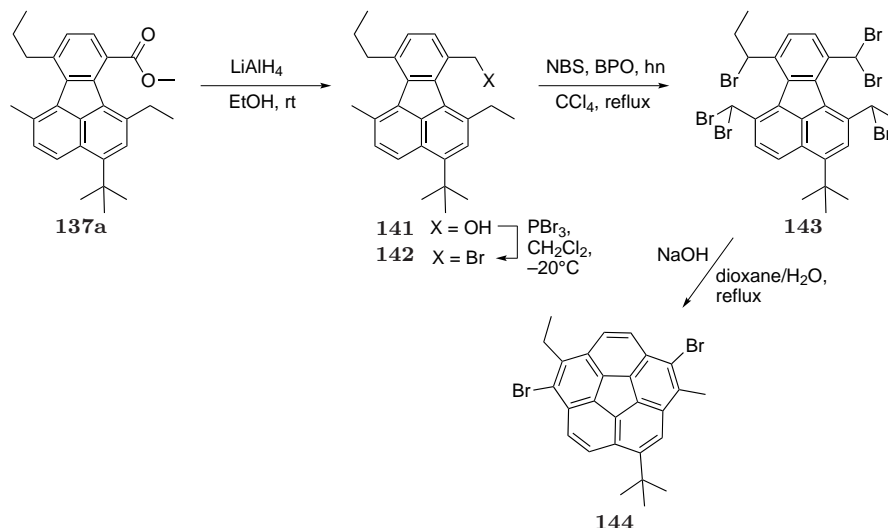
Silylation to enol ether **140** was achieved with Et_3N and SiMe_3Cl , the second with LDA and SiMe_3Cl .¹³⁸ A domino Mukaiyama-Aldol^{139,140} cyclization of **139** and **123** promoted by TiCl_4 was successful, although subsequent reaction with NBD again showed formation of the regioisomers in a ratio of 1:1 (84 % yield).

The silyl enol ether **140** was used under mixed conditions, with one equivalent TiCl_4 and one equivalent LDA, but yields were unsatisfactory in this case (<40 %). Again, analytical amounts of the isomer **137a** could be isolated after careful chromatography on silica (Figure 4.3a). None of the the applied reaction conditions (Table 4.1) lead to any considerable selectivity in favor of any of the isomers.

Table 4.1: Conditions for Aldol-additions to diketone **123** on route to fluoranthenes **91** and **137**.

entry	nucleophile	Aldol conditions	dienophile	product	yield [%]
1	125	KOH/MeOH, rt	ethyl propiolate	91	76
2	138	LDA/THF, −78°C to rt	norbornadiene	137	81
3	138	NaOMe/MeOH, rt	norbornadiene	137	78
4	139	TiCl_4 /THF, −78°C to rt	norbornadiene	137	84
5	140	TiCl_4 /LDA/THF, −78°C to rt	norbornadiene	137	36

The small amount of **137a** isolated was subjected to further transformation to test the practicality in the synthesis of the desired corannulene derivatives. Reduction of the ester functionality with LiAlH_4 delivered the corresponding benzylic alcohol **141**. Already



Scheme 4.15: Synthetic route to dibromo trialkylcorannulene **144**.

being functionalized at one of the benzylic positions, **141** was treated with PBr_3 to afford the benzylic bromide **142**. Further light induced benzylic bromination of **142** with N-bromo succinimide (NBS) and benzoyl peroxide (BPO) in carbon tetrachloride (CCl_4) gave the hexabromofluoranthene **143**. In analogy to symmetrically substituted fluoranthene derivatives (Scheme 2.6), the ring closure of **143** was achieved by treatment with NaOH in dioxane/water and delivered the dibromo trialkylcorannulene **144**. The crude material was purified by preparative TLC (silica). The aromatic region of the ^1H NMR is shown in Figure 4.4, an AB spin system with a strong roof effect (7.95–7.85ppm), typical for corannulene systems, is clearly evident.

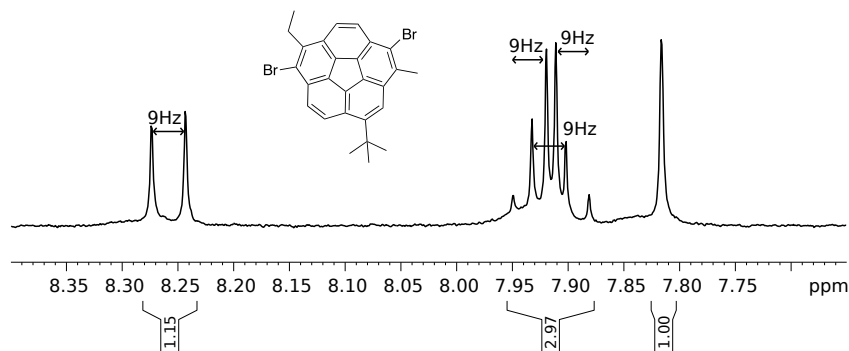


Figure 4.4: Aromatic region of ^1H NMR of **144**.

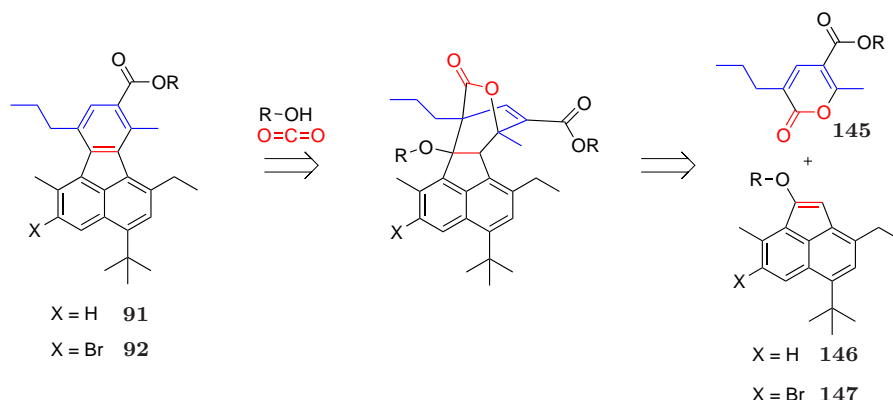
However, the above routes to fluoranthenes **91** and **137**, and corannulene derivatives of type **144**, were discarded due to several reasons. The base-mediated ring closure has only restricted compatibility with functional groups, and the resulting brominated derivatives need a further hydrodebrominating step. This condition is unsuitable in the presence of an aromatic bromide function in the final product. Finally, the four isomers generated in the sequence, Aldol addition–cycloaddition, need separation on a preparative scale, whereas three of the four isomers obtained will not lead to the desired substitution pattern in the final corannulene derivative and have to be discarded.

4.3 Synthetic Strategy II — [4+2]-Cycloadditions

4.3.1 Pyrone Cycloaddition

4.3.1.1 Retrosynthetic Analysis

In the above section it was demonstrated that the reaction sequence, Aldol-addition Diels–Alder reaction did not result in the expected selectivity, but delivered a mixture of four physically similar fluoranthene derivatives. The search for selectivity, or even better specificity, in favor of the desired fluoranthene isomer **91a** or **92a** led to the investigation of a cycloaddition reaction between a substituted pyrone **145** (Scheme 4.16) and an enolate of acenaphthenone **146** or **147**. Enolates taken into consideration were base generated Na-, or Li-enolates, as well as silyl enol ethers and alkyl enol ethers. The carbanion and the



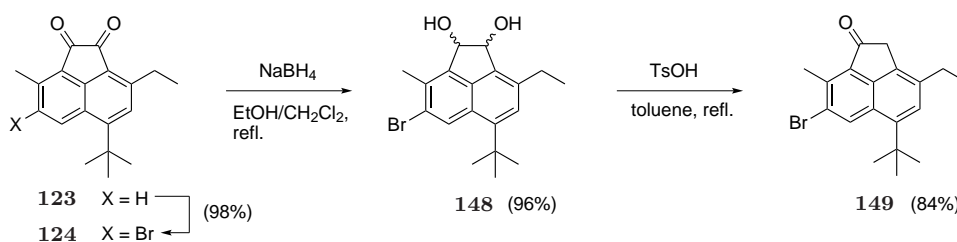
Scheme 4.16: Retrosynthetic disconnection of fluoranthenes **91** and **92** to enolates **146** or **147** and the trisubstituted 2-pyrone **145**.

increased electron density thus generated on the β -carbon of the enolate was expected to direct the attack on the pyrone moiety to the desired orientation, as shown in Scheme 4.16.

The bridged lactone cycloadduct should extrude CO₂ and an alcohol or water upon elevating of temperature and deliver the desired fluoranthene scaffold.

4.3.1.2 Synthesis of Acenaphthenone

It was found that acenaphthenequinone **123** could be selectively brominated at the ortho-position under forcing conditions. Refluxing of **123** in an excess of bromine delivered the bromoacenaphthenequinone **124** exclusively.



Scheme 4.17: Synthesis of bromo acenaphthenone **149**.

Reduction of the quinone **124** with NaBH₄¹⁴¹ delivered a mixture of *cis*- and *trans*-diols **148**, with the latter being the major isomer (ratio of ~1:5, as determined by ¹H NMR). Subsequent elimination of H₂O from the diol mixture **148**, promoted by catalytic amounts of *p*-toluenesulfonic acid, yielded the acenaphthenone **149**. The elimination reaction was conducted under high dilution conditions in toluene to avoid polymerization reactions of the starting material.

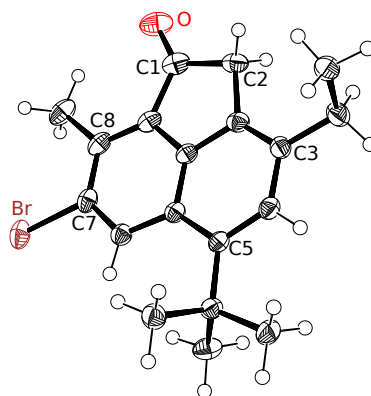


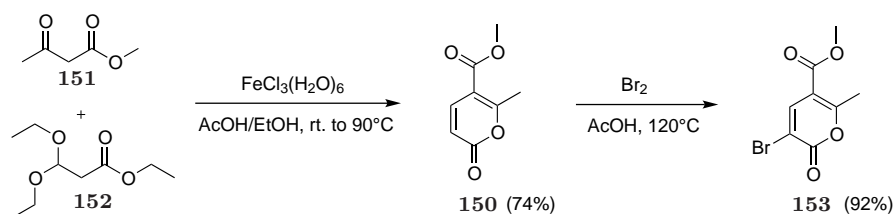
Figure 4.5: Molecular structure of bromoacenaphthenone **149** in the crystal. Thermal ellipsoids shown at the 50 % probability level.

Noteworthy, the elimination reaction occurs regiospecifically, exclusively delivering the isomer **149** as confirmed by 2D NMR spectroscopy and X-ray analysis (Figure 4.5). A

plausible explanation is the combined effect of the electron donating *tert*-butyl group at the 6-position and the withdrawing aromatic bromide at the 4-position which favor the stabilization of the carbocation at the 1-position of the acenaphthene diol **148**. This interpretation is supported by the Hammett σ -values of -0.15 and 0.37 for a *para tert*-butyl and a *meta* bromo substituent, respectively.¹⁴²

4.3.1.3 Synthesis of Pyrones

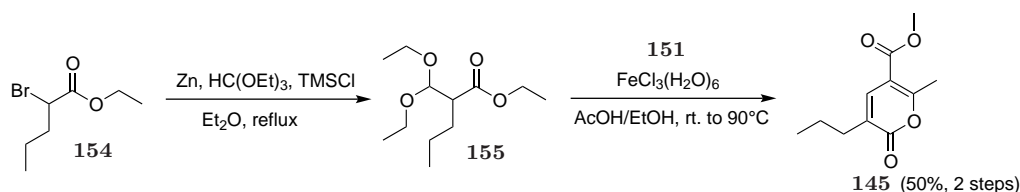
According to the procedure of Ishii¹⁴³ and coworkers, the pyrone ester **150** was synthesized by a cyclodimerization reaction of methylacetoacetate (**151**) and ethyl 3,3-diethoxypropionate (**152**) in good yield (74%). The reaction is catalyzed by $\text{FeCl}_3 \cdot 6\text{H}_2\text{O}$, and occurs smoothly in the mixed solvent system acetic acid/methanol. Bromination of **150**



Scheme 4.18: Fe-mediated synthesis of methyl 6-methylcoumalate (**150**) and methyl 3-bromo-6-methylcoumalate (**153**).

with bromine or NBS in acetic acid delivered the 3-brominated pyrone derivative **153** in over 90% yield.^{144, 145}

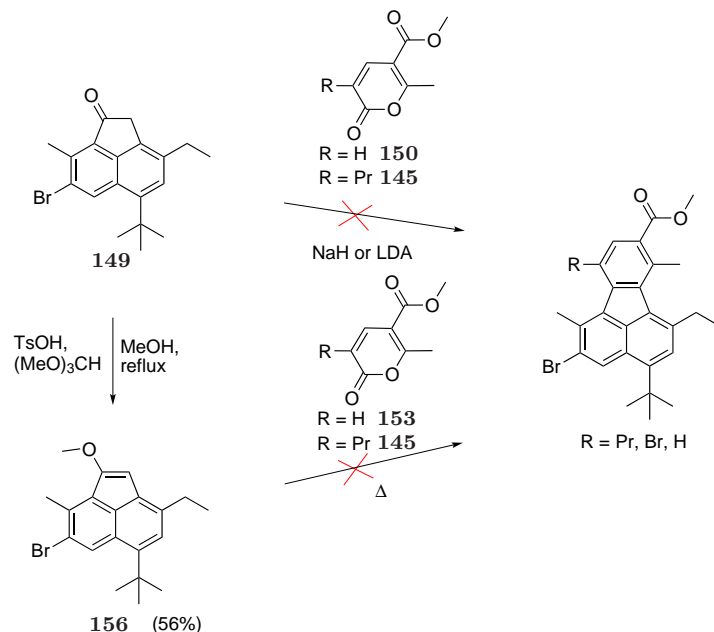
Attempts to alkylate the latter under Suzuki-type¹⁴⁶ or Friedel–Crafts conditions to afford the 3,6-dialkylpyrone **145** failed. Instead, a modified Reformatsky-type reaction of ethyl 2-bromopentanoate (**154**) with triethyl orthoformate¹⁴⁷ delivered the alkylated precursor **155** for the reaction described above.^{148, 149} The acetal **155** could not be purified by distillation or column chromatography, due to fragile EtOH-elimination generating the vinyl ether. Therefore, the crude **155** was cyclodimerized with **151** and delivered the desired 3,6-dialkylpyrone (**145**), however, in considerably lower yield (~50%) than **150**.



Scheme 4.19: Fe-mediated synthesis of methyl 6-methyl-3-propylcoumalate (**145**).

4.3.1.4 Attempted Cycloaddition Routes to Target Fluoranthenes

With the three pyrone derivatives **145**, **150** and **153** in hand, a limited set of experiments was conducted to examine their reactivity towards the dienophiles of choice. Inspired



Scheme 4.20: Failed envisioned cycloaddition of dienophiles **156** and enolates derived from **149** to 2-pyrones **145**, **150** and **153** in a regioselective manner.

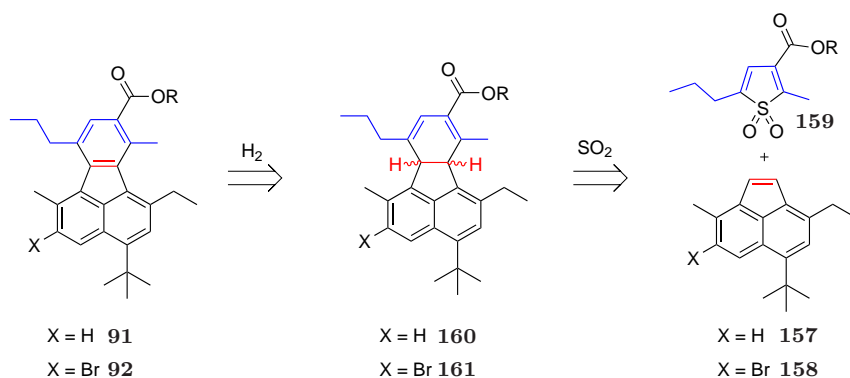
by the work of Goel *et al.*¹²⁷ (Scheme 4.7), analogous conditions were chosen for the cycloaddition. Treatment of ketone **149** with NaH or LDA in THF gave deep-purple solutions of the corresponding Na- and Li-enolates. Unfortunately, the pyrones **145** or **150** were not reactive towards the enolates generated, even at elevated temperatures and only starting materials could be detected after hydrolysis (Scheme 4.20).

To exclude the lack of reactivity of the pyrones **145** or **150** towards the polar (Michael-type) addition of a base generated enolate, **149** was converted to the methyl enol ether **156** by treatment with trimethyl orthoformate and catalytic TsOH.¹⁴⁷ Again, attempted cycloadditions of **156** and pyrone **150**, or even to the more electron withdrawing **153**, were not successful.

4.3.2 Thiophene Cycloaddition

4.3.2.1 Retrosynthetic Analysis

Another conceivable disconnection of the target fluoranthenes **91** or **92** leads to substituted acenaphthylenes **157** or **158**, and to a thiophene-*S,S*-dioxide **159**. Due to the oxidation of the sulfur atom, thiophene-*S,S*-dioxides are no longer aromatic thiophenes, but masked dienes that can undergo cycloaddition reactions to dienophiles. After cycloaddition, the intermediate, SO₂-bridged adduct extrudes SO₂, and thus generates the intermediate dihydrofluoranthenes **160** or **161**. Dehydrogenation of the latter would deliver the fluoranthene targets **91** or **92**.



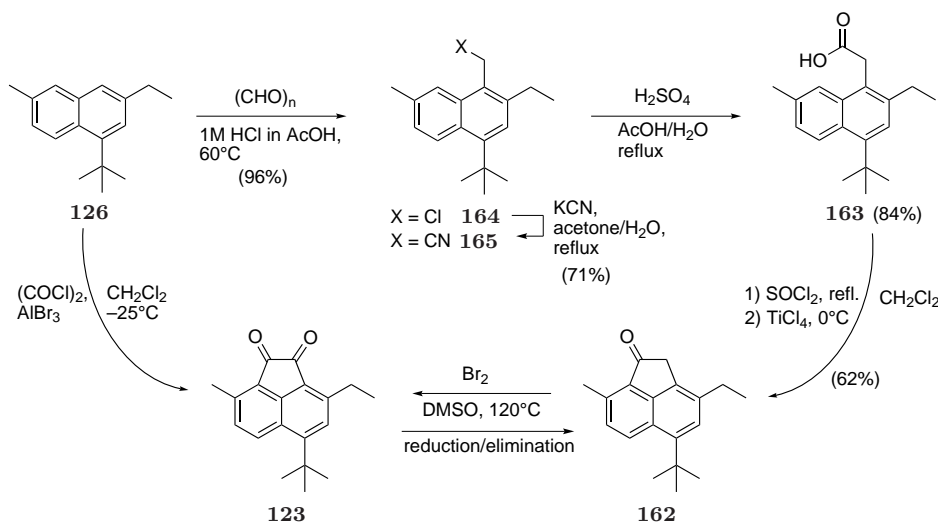
Scheme 4.21: Retrosynthetic disconnection of fluoranthenes **91** or **92** to thiophene-*S,S*-dioxide **159** and acenaphthylenes **157** or **158**.

4.3.2.2 Synthesis of Substituted Acenaphthylenes

For the synthesis of the brominated acenaphthenone **147**, the detour through diketone **123** has to be taken (see Scheme 4.17). The unbrominated acenaphthenone **162** is accessible by two routes. In analogy to the synthesis of **147**, a reduction/elimination sequence starting from diketone **123** delivers the acenaphthenone **162**. Unlike the diol **148**, the diol derived from **123** does not eliminate H₂O in a stereospecific manner. Therefore a mixture of isomers is obtained (ratio of ~1:4, as determined by GC/MS), where the compound **162** shown in Scheme 4.22 is the major isomer.

As shown earlier (Scheme 2.3), **162** can also be obtained in regioisomerically pure form by a more elaborate route. Chloromethylation of naphthalene **126**, subsequent chloride displacement with cyanide, and acidic hydrolysis gave rise to naphthylacetic acid **163**. The latter, as well as the intermediate chloromethyl and cyanomethyl naphthalenes **164** and

165 are isolated as regioisomeric mixtures (ratio of ~1:3.5, as determined by ^1H NMR and GC/MS); the structures shown in Scheme 4.22 depicting the major isomers. Acid **163** was chlorinated with SOCl_2 in CH_2Cl_2 , and the crude acid chloride was employed in an intramolecular Friedel–Crafts cyclization affording ketone **162**. AlCl_3 or AlBr_3



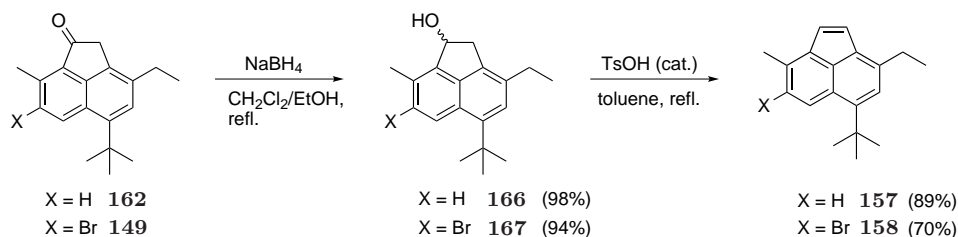
Scheme 4.22: Two different synthetic routes to the trisubstituted acenaphthenequinone **123** and acenaphthenone **162**.

proved to be too Lewis acidic for the cyclization step. At the temperature needed for the reaction to take place, mainly de-*tert*-butylated products were found. Switching to less Lewis acidic TiCl_4 at 0°C avoided de-*tert*-butylated products, and gave mainly the desired acenaphthenone **162**. The major isomer can be isolated by recrystallizing the mixture from *n*-hexane, but generally the mixture of regioisomers was used for further conversion.

Diketone **123** can also be obtained by oxidation of acenaphthenone **162** with SeO_2 . Kornblum oxidation with Br_2 in DMSO was a convenient alternative^{150, 151}. However, compared to 3,8-diethylacenaphthenone, the poor solubility of **162** in DMSO made it necessary to conduct the initial α -bromination of the ketone in CHCl_3 , followed by heating of the thus obtained crude product in DMSO.

Similarly to the chemistry discussed earlier, reduction of the acenaphthenequinones **162** or **149** with NaBH_4 delivers the benzylic alcohols **166** or **167**. Elimination of H_2O , promoted by catalytic amounts of TsOH in toluene (high dilution) led to the bright yellow acenaphthylenes **157** and **158**. **157** with its low melting point of 43°C was first obtained as an oil, which solidifies to a waxy material upon prolonged standing. As an oil, **157** is prone to polymerization and must be stored under refrigeration and solvent free.

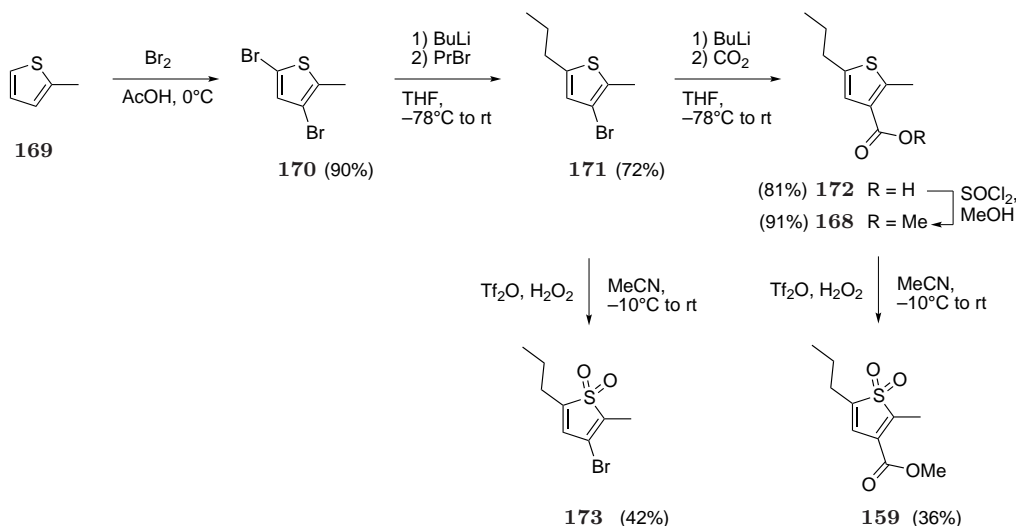
4.3 Synthetic Strategy II — [4+2]-Cycloadditions



Scheme 4.23: Synthetic route to acenaphthylenes **157** and **149**.

4.3.2.3 Synthesis of Thiophene-*S,S*-dioxides

Although the desired thiophene derivative **168** could be obtained by alternative routes, the reaction sequence shown in Scheme 4.24 was the most suitable in terms of scale, ease and minimization of side products. Starting with 2-methylthiophene (**169**), bromination in acetic acid selectively delivered the 3,5-dibrominated compound **170**.^{152,153} Bromine–lithium exchange occurs exclusively at the α -position of **170** and subsequent quenching with an excess of 1-bromopropane furnished the dialkylated bromothiophene **171**. The latter two compounds could conveniently be purified by bulb-to-bulb distillation on multi-gram scale. The remaining bromine in **171** was converted to the carboxylate by a second halogen-metal exchange followed by quenching with CO_2 and the thus obtained thenoic acid **172** was smoothly esterified to the methyl ester **168** with SOCl_2 in methanol.



Scheme 4.24: Synthetic route to thiophene-*S,S*-dioxides **173** and **159**.

Oxidation of the rather electron poor thiophenes proved to be challenging. Usually, thiophenes are oxidized by peracids such as peracetic acid (H_2O_2 in acetic acid), the most com-

monly used being *m*-chloroperbenzoic acid (*m*-CPBA). The electron withdrawing bromine atom and the carbonyl function in **171** and **168**, render the thiophene sulfur atoms considerably less nucleophilic and therefore less prone to oxidation. Thiophenes bearing electron withdrawing groups have been converted to the *S,S*-dioxides by using strong oxidants such as $\text{HOF} \cdot \text{CH}_3\text{CN}$ ^{154–156} or dimethyldioxirane,¹⁵⁷ as well as anhydrous trifluoroperacetic acid prepared from 100 % H_2O_2 and trifluoroacetic anhydride.^{158,159} H_2O_2 with ZrCl_4 as lewis acid activator¹⁶⁰ or with P_2O_5 to form peroxyphosphoric¹⁶¹ acid have also been applied.

As expected, initial prolonged stirring of **171** and **168** with *m*-CPBA in CH_2Cl_2 only returned unconverted starting material, even under reflux for two days. Employing 35 % H_2O_2 in TFA also gave unsatisfactory yields. Gratifyingly, a slightly modified procedure from Nenajdenko *et al.*,¹⁵⁸ in which trifluoroperacetic anhydride was oxidized to the trifluoroperacetic acid by using 35 % instead of anhydrous H_2O_2 , delivered the desired thiophene-*S,S*-dioxide **159** in a moderate but acceptable yield of ~40 %. The same oxidizing conditions were applied to the brominated intermediate **171**, thus delivering the 3-bromo substituted thiophene dioxide **173**.

Chromatography of the crude oil on silica gave X-ray quality crystals after slow evaporation of the solvent (*n*-hexane/ CH_2Cl_2). Two molecules with almost identical conformations are displayed in the asymmetric unit (Figure 4.6). The bond alternations of the thiophene carbon atoms clearly show the diene character of **159**.

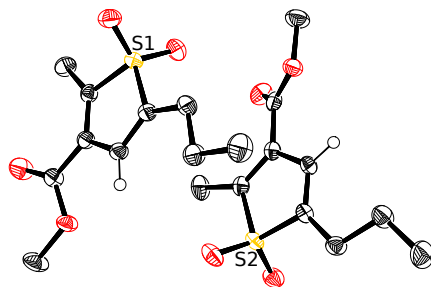
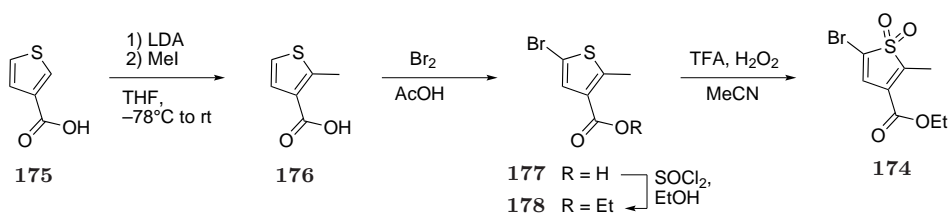


Figure 4.6: Molecular structure of thiophene-*S,S*-dioxide **159** in the crystal (aliphatic H atoms omitted). Thermal ellipsoids shown at the 50 % probability level.

The electronically altered, brominated thiophene-*S,S*-dioxide **174**, capable of delivering a fluoranthene derivative that would also be relevant for the construction of the desired fluoranthenes **91** or **92** was prepared as well (Scheme 4.25). Selective *ortho*-lithiation of 3-thenoic acid (**175**) with LDA, and methylation with iodomethane, gave methyl thenoic acid **176**. Bromination led to the bromo thenoic acid **177** and esterification furnished thenoic ester **178**. As opposed to **168**, oxidation of the latter thiophene was possible with

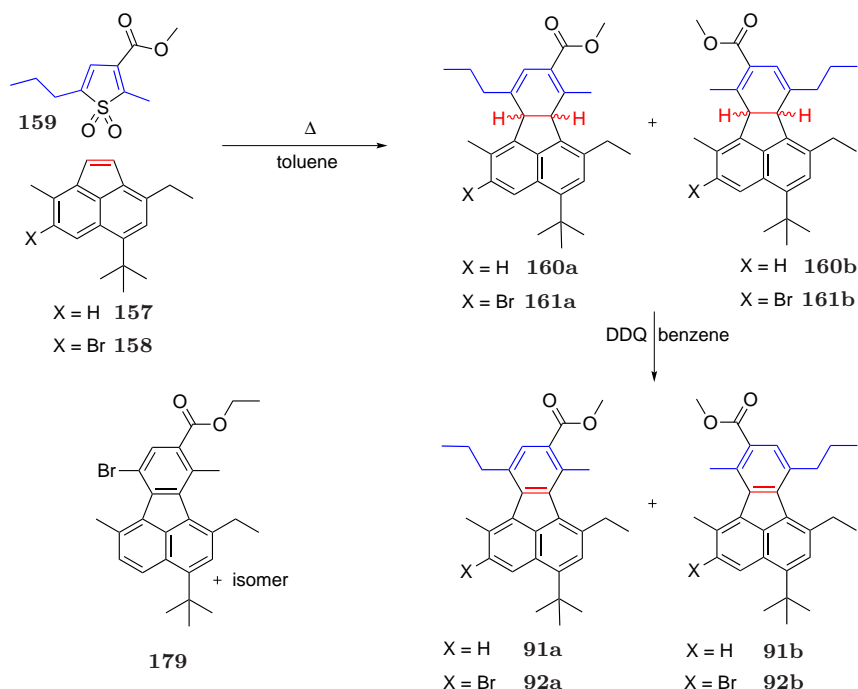
trifluoroperacetic acid generated from TFA and 35 % H_2O_2 , the *S,S*-dioxide **174** being obtained in over 80 % yield.



Scheme 4.25: Synthetic route to thiophene-*S,S*-dioxide **174**.

4.3.2.4 Synthesis of Hexa- and Heptasubstituted Fluoranthenes **91** and **92**

Cycloaddition of the acenaphthylenes **157** or **158** and thiophene-*S,S*-dioxide **159** in refluxing toluene cleanly delivered a regioisomeric mixture of dihydrofluoranthenes **160** and **161** in over 80 % yield (Scheme 4.26). Alternatively, the reaction could also be carried out by heating the educts under solvent-free conditions. The SO_2 -bridged cycloadduct could not be detected. Typically, the thiophene component was applied in ~ 1.3 -fold excess to ensure complete consumption of the more precious dienophile. The course of the cycloaddition reactions could conveniently be monitored by GC/MS analysis.



Scheme 4.26: Synthetic route to fluoranthenes **91** and **92** via cycloaddition of acenaphthylenes **157** and **158** to thiophene-*S,S*-dioxide **159**.

Differential scan calorimetry was carried out with **157** and **158**, because melting point determination was somewhat difficult with the waxy compounds. An exothermic process, starting at roughly 130°C for **157** and 112°C for **158**, indicates degradation of the dienophiles at these temperatures. Therefore, refluxing in solvents higher boiling than toluene were avoided.

Either the crude dihydrofluoranthenes, or material purified by flash column chromatography on silica, was submitted to dehydrogenation with DDQ in benzene. After filtration through cellite, the crude material was initially purified by column chromatography on deactivated Alox or Silica, and the hexa- and heptasubstituted fluoranthenes **91** and **92** were obtained as mixture of regioisomers in ~70 % yield. Using the same reaction sequence, an isomeric mixture of brominated fluoranthene derivatives **179** was also obtained. The latter was considered as a feasible starting material to deliver fluoranthenes of type **91** after propylation, but further examination was not continued.

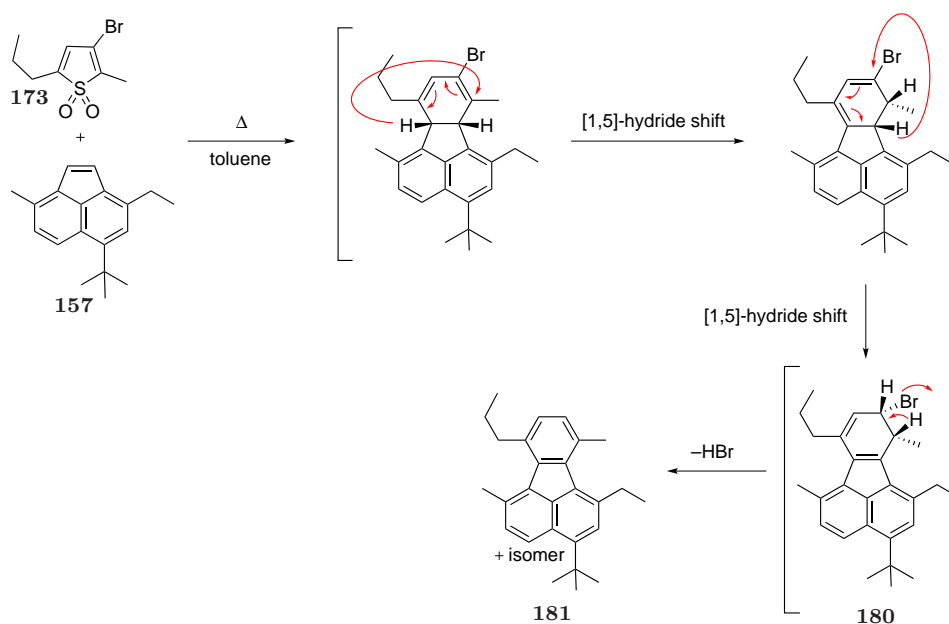
Compared to the initial synthetic strategy (Scheme 4.16), the Diels–Alder approach to fluoranthene derivatives **91**, **92** and **179** delivers two regioisomers instead of four. Attempts of separating the physically similar regioisomers by standard column chromatography were not successful in our hands.

Additionally, cycloaddition was performed with thiophene-*S,S*-dioxide **173** and trisubstituted acenaphthylene **157** en route to target fluoranthene **91**. The reaction readily occurs, but under the conditions applied a putative sequence of two [1,5]-hydride shifts * lead to an isomeric dihydrofluoranthene **180** in which an elimination of HBr directly delivers the pentaalkylated fluoranthene **181**. The elimination of HBr in the above manner might be desirable for the synthesis of substituted fluoranthenes, but lacking functionality at the 9-position makes this synthetic route unfeasible for our needs.

For the preparation of hitherto not described 7,8-dibrominated fluoranthene derivatives and for gaining a limited overview over the scope of the cycloaddition of thiophene-*S,S*-dioxides to acenaphthylenes, the symmetrical 3,4-dibromo-2,5-dimethylthiophene and its *S,S*-dioxide **182** were prepared as well. The elimination of HBr during the reaction was not observed in the dihydrofluoranthene intermediate obtained from the cycloaddition of **182** and dimethylacenaphthylene **183**. However, while attempting to purify the dihydrofluoranthene by column chromatography on silica, the aromatized elimination product was

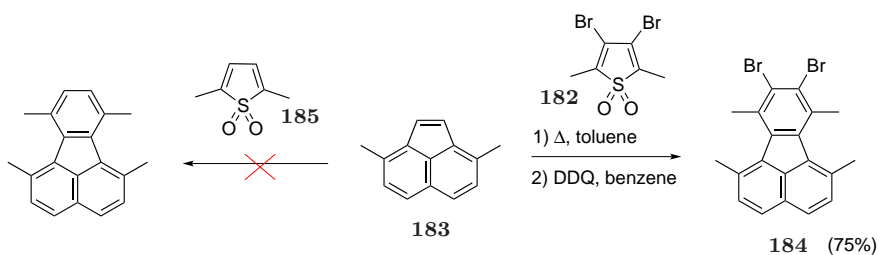
*A single [1,3]-hydride shift would also form a dihydrofluoranthene properly situated for a 1,4 elimination of HBr. However, the [1,3]-shift would have to occur antarafacially and is therefore geometrically impossible.

4.3 Synthetic Strategy II — [4+2]-Cycloadditions



Scheme 4.27: Formation of fluoranthene **181** by a two consecutive [1,5]-hydride shifts and subsequent elimination of HBr.

generated. To avoid the elimination of HBr, the crude material was subjected to DDQ oxidation immediately and the dibrominated fluoranthene **184** was isolated in good yield (75%). Control experiments with dimethylthiophene-*S,S*-dioxide (**185**) were performed as well, but even under prolonged heating for several days in high boiling solvents such as *p*-xylene, no cycloadduct could be detected by GC/MS. The latter finding emphasizes the importance of an electron withdrawing groups at the 3-position of the thiophene-*S,S*-dioxides which promote *inverse* electron demand Diels–Alder cycloaddition.



Scheme 4.28: Cycloaddition of acenaphthylene **183** to thiophene-*S,S*-dioxide **182**. Absence of reactivity toward thiophene-*S,S*-dioxide **185** lacking the electron-withdrawing bromines in the 3- and 4-position.

4.3.2.5 Separation of Fluoranthene Regioisomers **91** and **92** and Their Identification by NMR Spectroscopy

Suitable conditions for preparative HPLC were elaborated with the corresponding analytical column (Normal Phase, Waters Spherisorb® S5, Nitrile, 3.0 μ m, 100 \times 4.6mm). The eluent that suited best was *n*-hexane/EtOAc (200:1), advantageous as well as it could be recycled. Retention times for both isomer mixtures **91** and **92** were very close, therefore only small amounts of material, typically 10–20 mg, could be injected. Furthermore, the compounds showed a strong tailing effect, causing long elution times.

As can be seen in Figure 4.8a, the preparative chromatogram of an isomeric mixture of **91** almost shows baseline separation. The desired isomer elutes first and with careful fractionation can therefore be separated in one run. The same method was applied to the isomeric mixture of **92**. Compared to **91**, retention times of the isomers were closer and baseline separation could not be achieved. The mixture had to be enriched continuously, typically three runs were sufficient for the separation of the desired isomer, which elutes first as well (Figure 4.8b). In both cases, sequential injection of the samples further increased the efficiency of the separation.

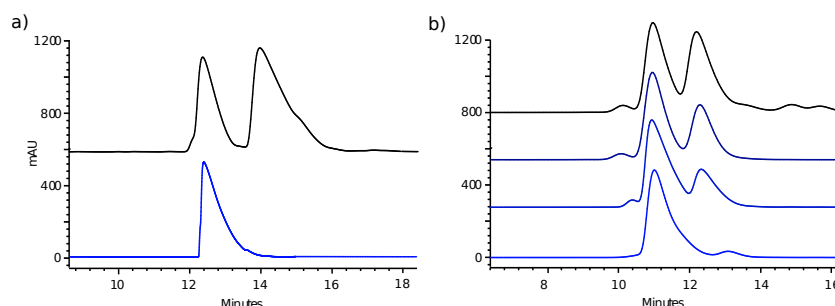


Figure 4.7: Preparative HPLC of **91** and **92**. a) Separation of **91a** from **91b**; b) Stepwise separation of **92a** from **92b**. Column: Waters Spherisorb® S5, Nitrile, 250 \times 20mm Semi-Prep. Column.

The isolated isomers were analyzed by 2D NMR spectroscopy (NOESY). There are two possible through space interactions for the compounds **91** and **92**, namely the coupling of methylene protons (red) to methyl protons (blue) for the desired isomer **91a** (Figure 4.9a), or the coupling of methyl protons or methylene protons with each other in the undesired isomer **91b** (Figure 4.9b). We were therefore able to identify the desired isomers in each fluoranthene derivative pair, as shown in Figure 4.10. Additionally, the isomeric mixture of fluoranthenes **92** was further converted to the methoxyphenyl substituted derivative

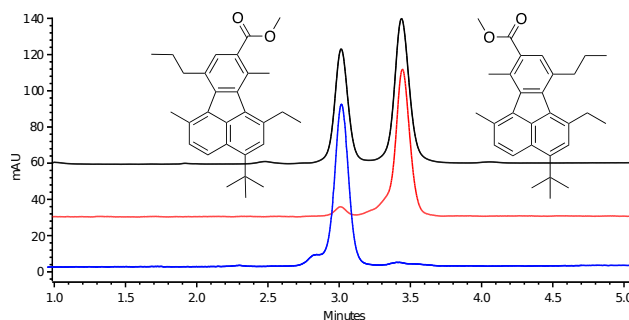


Figure 4.8: Analytical HPLC of a mixture of **91a** and **91b** (black), separated **91a** (blue) and **91b** (red). Detection wave length = 267nm. Column: Waters Spherisorb® S5, Nitrile, 3.0 μ m, 100 \times 4.6mm.

186 under Suzuki cross coupling conditions (Figure 4.10b). These were generated as key intermediates later in our work and the NOESY spectra showed the same general trends as those observed in the separated **91** and **92**. Intriguingly, the isomeric mixture of **186** was separable by careful column chromatography on silica. Although the two isomers still run very close, this finding significantly increased the feasibility of preparative isomeric separation. Therefore, the difficulty in obtaining the desired isomer through preparative HPLC in significant amounts was reduced to a standard chromatographic issue. The desired isomer could be identified by NOESY NMR spectroscopy. In all examples, the desired isomers always elute first under the conditions utilized for HPLC.

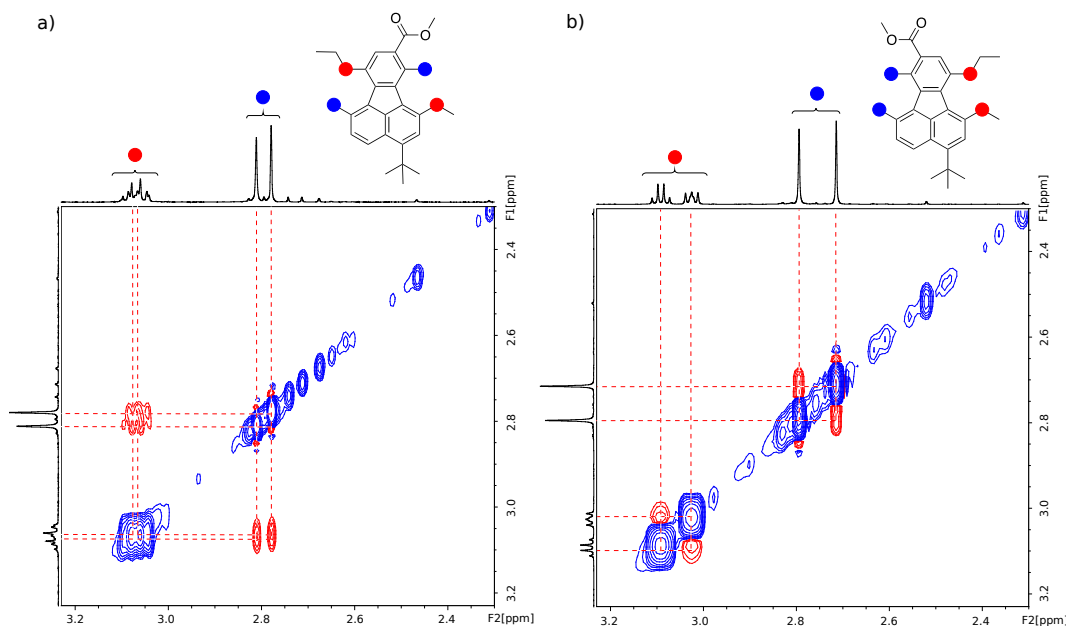


Figure 4.9: NOESY NMR spectra of a) **91a** and b) **91b**.

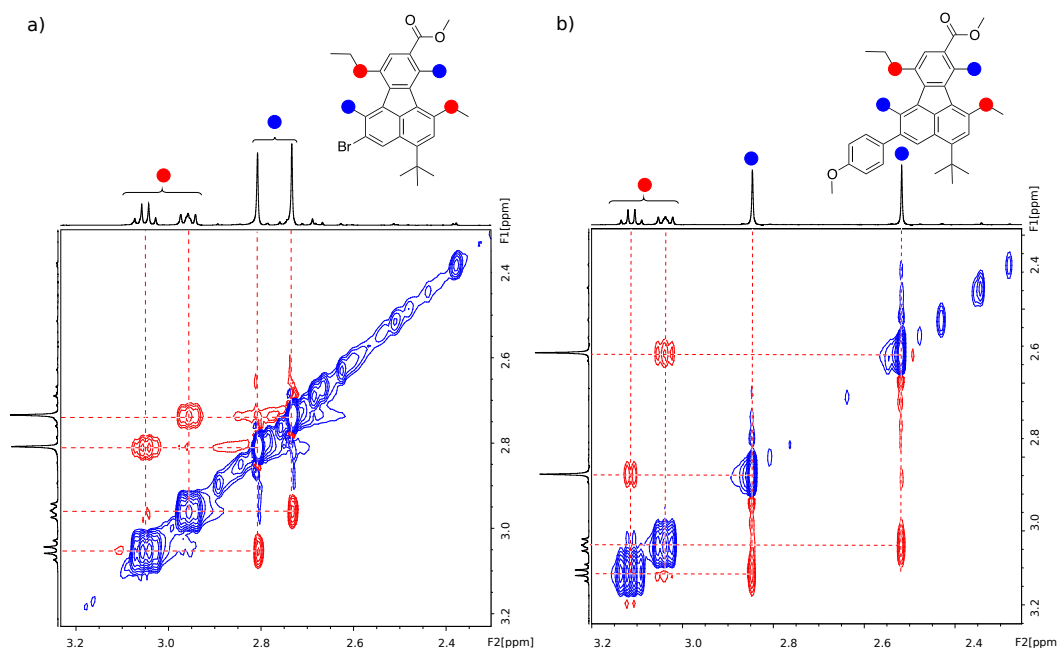


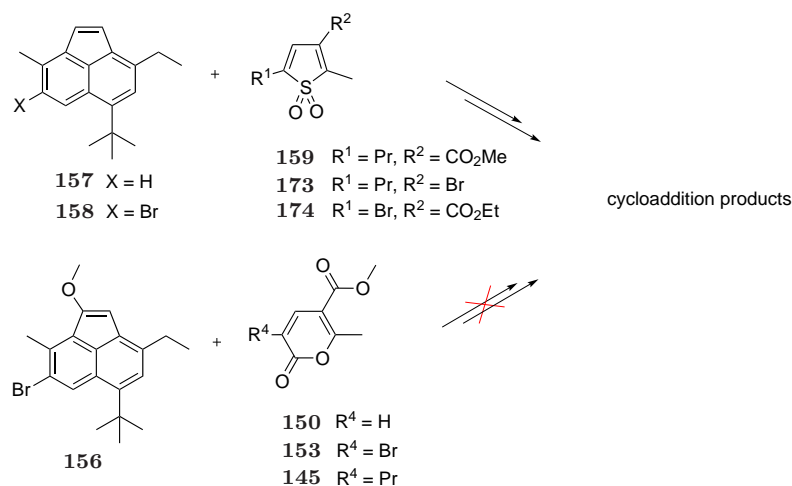
Figure 4.10: NOESY NMR spectra of isolated fluoranthenes **92a** and **186**.

4.3.3 Computational Analysis of Cycloadditions

As illustrated in the previous section, cycloadditions of acenaphthylenes **157** and **158** to various substituted thiophenes **159**, **173** and **174** have been successful, provided electron withdrawing substituents are on the thiophenes, resulting in favored *inverse* electron demand Diels–Alder reactions. The complete lack of reactivity of the analogously substituted pyrone derivatives, **145**, **150** and **153**, was unexpected. Even the increase of electron density at the dienophile by employing enol ether **156** or enolates generated from **162** did not lead to the desired addition products. Although a plethora of different substituted 2-pyrones is known to undergo both, *normal* and *inverse* electron demand Diels–Alder reactions,^{162–166} specific substitutions at the 3- and 6-positions are reported to hinder, or completely inhibit the addition of dienophiles.¹⁶⁵

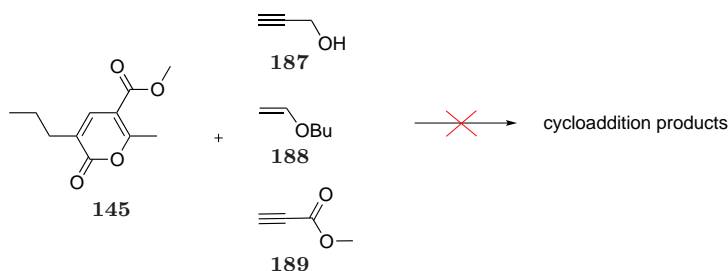
These results were furthermore unsatisfactory, since a variety of dienophiles bearing electron withdrawing or electron donating substituents are known to undergo the desired cycloaddition to substituted 2-pyrones.¹⁶⁷ Hence, a limited set of control experiments were performed with the pyrone **145** of interest as well as the sterically non-demanding, electron donating propargylic alcohol **187**, butyl vinyl ether **188**, and the electron accepting ethyl propiolate **189** (Scheme 4.30). The dienophiles were employed in large excess with, in these cases, no additional solvent. However, heating of the components in a pressure tube

4.3 Synthetic Strategy II — [4+2]-Cycloadditions



Scheme 4.29: Successful cycloaddition of acenaphthylenes **157** and **158** to thiophene-*S,S*-dioxides and unsuccessful cycloadditions of enol ether **156** to pyrones.

above the boiling points of the respective dienophiles for two days did not afford any cycloaddition products. These experiments suggested that steric and electronic demand of the employed dienophiles **187–189** do not account for the lack of reactivity.



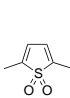
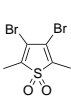
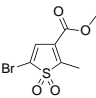
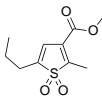
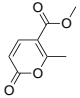
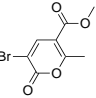
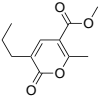
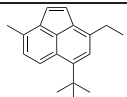
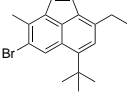
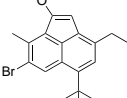
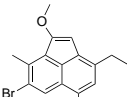
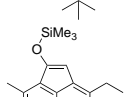
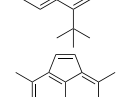
Scheme 4.30: Failed test reactions of electron-withdrawing and electron-donating dienophiles **187–189** with 2-pyrone **145**.

To gain better insight into the failed attempts of the cycloaddition of pyrones to the acenaphthylene dienophiles, an array of representative systems were analyzed computationally, using B97-D/TZVP DFT methodology. The highest occupied molecular orbital (HOMO) of a series of dienophiles and the lowest unoccupied molecular orbital (LUMO) of the dienes of interest were analyzed, and the HOMO/LUMO gaps compared. Although, from the perspective of synthetic utility, some of the combinations of the dienophiles and the dienes are not of immediate interest, the analysis of all the possible combinations of dienes with dienophiles provides additional information concerning the reactivity of this set of compounds (Table 4.2). The green entries depict values for the HOMO/LUMO gaps (eV)

of the cycloaddition reaction partners for which the reactions were successful, whereas the red entries show the experiments that did not lead successfully to a cycloaddition product.

Regarding the reactions between thiophene-*S,S*-dioxides were in general experimentally successful. In these cases the calculated HOMO/LUMO values range from ~ 1.4 to ~ 1.9 eV. Remarkably, comparison of calculated values of the thiophenes with those of the experimentally unsuccessful pyrones, one finds that the lowest energy gap in the latter set is ~ 1.8 eV, also in the range of the former set. This suggests that factors other than the electronic properties may be responsible for lack of reactivity in the pyrones. In particular, steric factors in the 3,6-disubstituted pyrones **153** and **145** are difficult to assess, since the cycloaddition of 2,5-disubstituted thiophenes **159** and **174** readily occurs. However, a combination of steric clashing of both partners is reasonable, as supported by the failed experiment of the more electron donating trimethylsilyl enol ether with the thiophene **159**. The latter combination exhibits the smallest HOMO/LUMO gap of the experimentally examined combinations (~ 1.2 eV). In addition, none of the tested dienophiles substituted with electron donating substituents underwent cycloaddition to 2-pyrones.

Table 4.2: HOMO-LUMO gaps between selected dieneophiles and dienes. Green entries depict calculated values for reaction partners leading to cycloaddition products; red entries depict calculated values for performed, but unsuccessful reactions.

							
	2.204	1.825	1.398	1.738	2.272	2.051	2.467
	2.409	2.030	1.602	1.943	2.476	2.255	2.671
	1.975	1.596	1.168	1.509	2.042	1.822	2.238
	1.930	1.550	1.123	1.464	1.997	1.776	2.192
	1.671	1.292	0.864	1.205	1.738	1.518	1.933
	2.320	1.941	1.513	1.854	2.387	2.167	2.582

Comparison of the frontier orbitals of thiophene-*S,S*-dioxide **159** (Figure 4.11) and 2-pyrone **145** (Figure 4.12), reveals further insight into the reactivity. In the case of **159**, the LUMO is mostly localized across the 1,4-diene system (Figure 4.11b), with the highest coefficients for the orbital lobes at the carbon atoms involved in the cycloaddition reaction. The situation is different for **145**. The carbonyl functionality in the 2-pyrone is in conjugation with the 1,4-diene as well. This situation brings about a competing Michael-type system to the conjugation of the diene. As illustrated in Figure 4.12, the frontier orbitals of the pyrone show additional density located at the carbonyl-C atom. Furthermore the LUMO lobe with the largest coefficient is localized at C4. As such, an approaching dienophile might likewise interact across this moiety besides the area located across the 1,4-diene system.

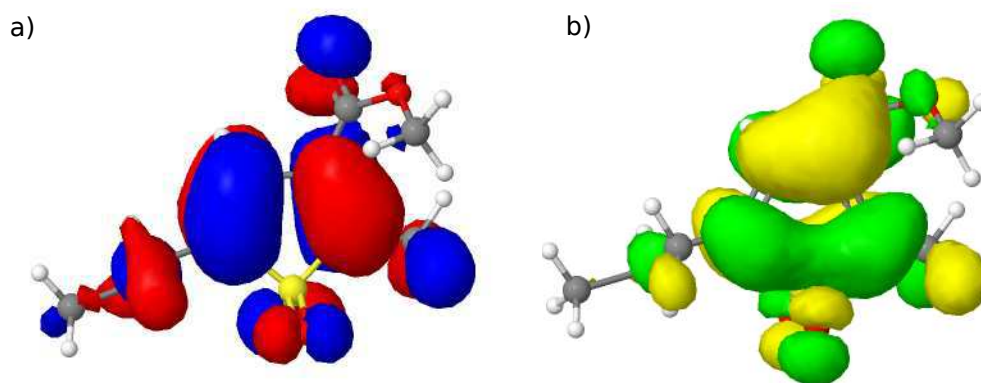


Figure 4.11: Frontier orbitals of thiophene-*S,S*-dioxide **159**. a) HOMO b) LUMO.

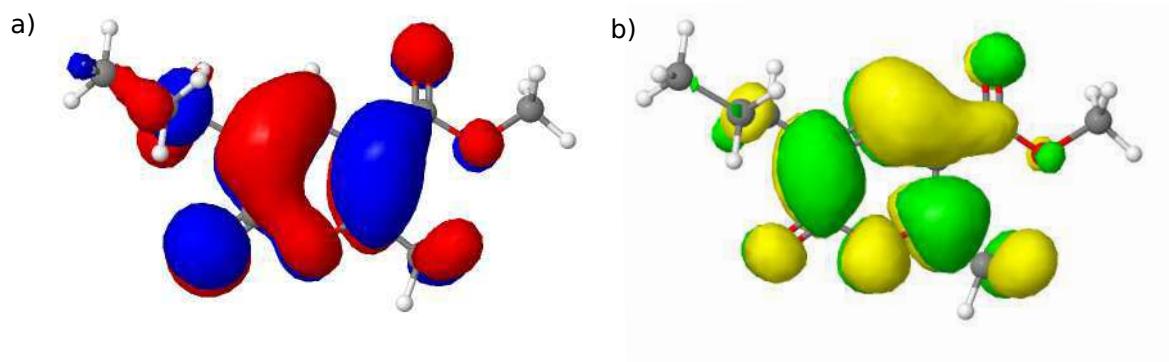


Figure 4.12: Frontier orbitals of 2-pyrone **145**. a) HOMO b) LUMO.

5 Synthesis of 1,3,5,7,9-Pentasubstituted Corannulene

5.1 Model Fluoranthenes and Initial Studies

5.1.1 Aims

The fluoranthenes already synthesized all have the substituents of the target corannulene in place and are only lacking the final coupling of the benzylic positions. With the tediously separated fluoranthenes **91a** and **92a** in hand, a model compound for probing the final bromination and ring closing step was desired. A C_s symmetrical fluoranthene derivative was chosen, in which the chemical environment of the benzylic functions is similar to the target fluoranthenes **91** and **92**. The readily prepared diethyl dimethylfluoranthene diester **190** was chosen. The highlighted part of the molecule in Figure 5.1 shows a similar carbon framework as the target fluoranthene. An ester function is close to the methyl group, which is opposite the benzylic position of an ethyl group that will undergo ring closure to the corresponding corannulene. A comparable situation as in the left portion of the target fluoranthenes is already known from previous literature work on corannulene syntheses.

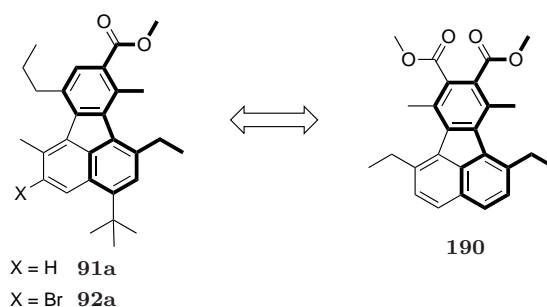
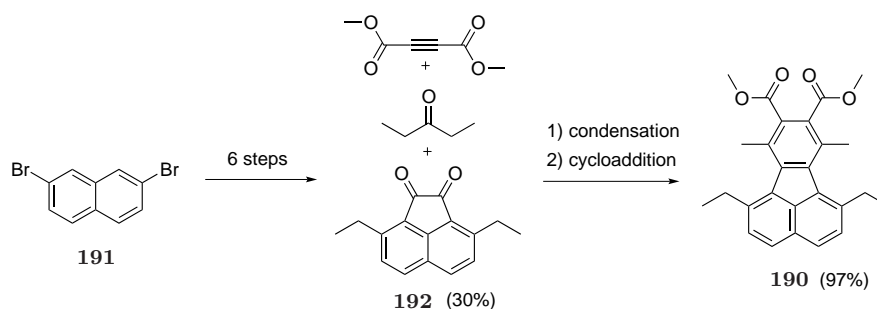


Figure 5.1: Structural similarities of the target fluoranthenes **91** and **92** with **190**.

5.1.2 Synthesis of Model Fluoranthene

Starting with 2,7-dibromonaphthalene **191**, Ni-catalyzed ethylation with ethyl magnesium bromide gave 2,7-diethylnaphthalene in good yields.⁶ The five-step ring annulation synthesis, as described earlier (Scheme 2.3), was followed, giving the diethyl quinone **192** in about 30% overall yield. The longer route was chosen to avoid the regioisomeric issue observed with the double Friedel–Crafts acylation with oxalyl chloride. Condensation of **192** with 3-pentanone and subsequent cycloaddition with dimethyl acetylene dicarboxylate gave fluoranthene **190** in high yields (Scheme 5.1).



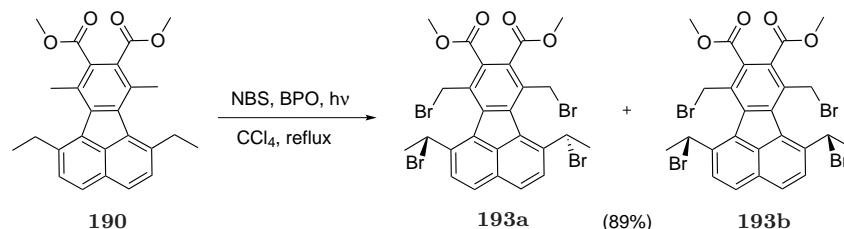
Scheme 5.1: Outline of synthetic route to model fluoranthene **190**.

5.1.3 Bromination and Initial Ring Closure of the Model Fluoranthene

Bromination of fluoranthene **190** with NBS, promoted by irradiation with an incandescent lamp (commercial Osram tungsten bulbs between 100–375W were used throughout the work) afforded a diastereomeric mixture of tetrabromofluoranthenes **193** (Scheme 5.2). The reaction was carried out in CCl_4 , and its course could therefore conveniently be followed by ^1H NMR. As observed in earlier work by Rabideau and coworkers, the radical bromination of the methyl groups *ortho* to the ester functions only led to monobromination, even with a large excess of NBS.

The diastereomeric couple obtained after bromination consists of a chiral tetrabromofluoranthene **193a** and an achiral *meso*-tetrabromofluoranthene **193b** in a ratio of $\sim 2:3$, as determined by ^1H NMR spectroscopy. Stereochemical relations render the methylene protons of the chiral **193a** as diastereotopic, whereas the methylene protons of **193b** are enantiotopic. The latter stereochemical feature makes these two compounds easily distinguishable by ^1H NMR spectroscopy. Therefore, for analytical purposes the first eluting diastereomer was separated by fast flash column chromatography on silica. Since the

brominated fluoranthenes are non-fluorescent, the reappearance of blue fluorescing bands ($\lambda=366\text{nm}$) on silica indicate debromination/hydrolysis or irreversible absorption of bromofluoranthenes on silica.



Scheme 5.2: Benzylic bromination of model fluoranthene **190** leading to a mixture of diastereomers **193a** and **193b**.

Due to the two signals obtained for the methylene protons in the ^1H NMR, the first eluting compound was identified as the chiral **193a** (Figure 5.2). At room temperature the methylene protons of **193a** gave rise to one doublet ($^2J = 11.3\text{Hz}$) and one broad signal. Upon heating the sample in CDCl_3 , the broad signal decoalesces at 310K, and appears as clear doublet ($^2J = 11.3\text{Hz}$) above 320K. The quartet observed for the benzylic position of the bromoethyl groups also experiences a sharpening of the signal. The findings from VT-NMR indicate a hindered, interdependent rotation of the bromomethyl and bromoethyl groups. Using the Gutowsky–Holm approximation,^{168–170} the energy barrier of the rotation was determined to be $16.2 \pm 0.5 \text{ kcal/mol}$.

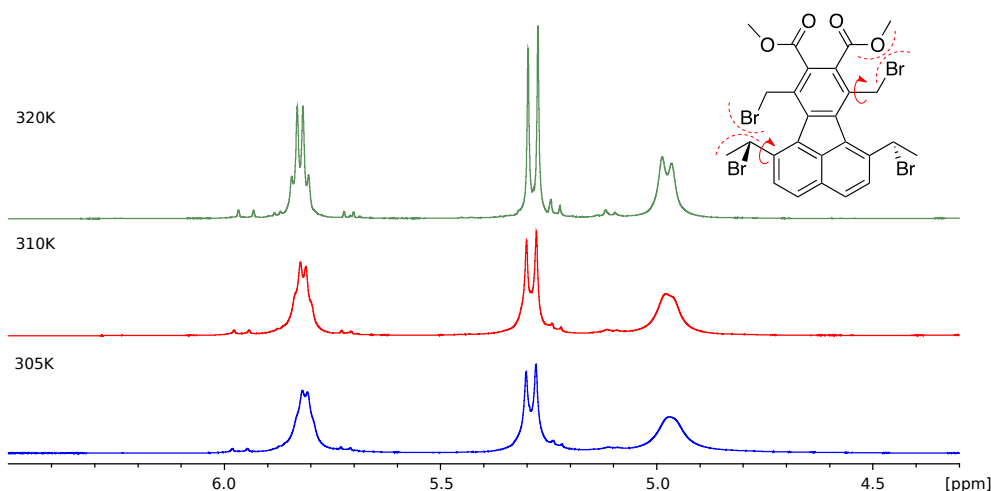
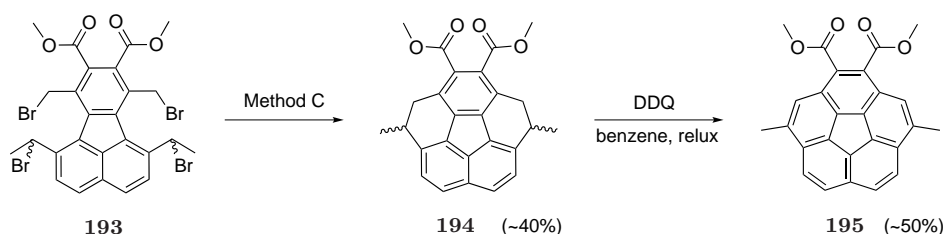


Figure 5.2: VT ^1H NMR of **193a** in CDCl_3 with a coalescence temperature of 310K.

Given the success of Ni-mediated (method F, see Scheme 2.5) ring closures of bromofluoranthenes bearing carbonyl functions at positions 8 and 9, these ring closing conditions

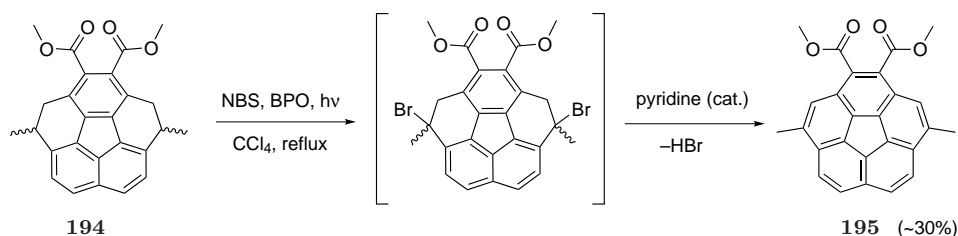
were initially chosen for the coupling of the benzylic positions of bromofluoranthenes **193**. Regarding the intended coupling of a primary benzylic bromide with a secondary benzylic bromide, the expected product was the tetrahydrocorannulene **194** (Scheme 5.3). While heating **193** in DMF with Ni-powder consumed all starting material, neither the desired product nor the parent fluoranthene (from hydrodehalogenation) could be detected.

Method B ($\text{TiCl}_4/\text{ZnCu}$) was chosen next, because it is known to couple benzylic mono-bromides (primary or secondary). However, the slow syringe pump addition of tetrabromide **193** to a slurry of TiCl_4 and ZnCu-couple over two days produced a complex mixture, as evidenced by TLC. The oxophilicity of low valent titanium reagents might also lead to unexpected reaction products due to couplings with the ester function.^{171, 172}



Scheme 5.3: Coupling of benzylic bromides in **193** with method C ($\text{VCl}_3/\text{LiAlH}_4$) and dehydrogenation leading to corannulene **195**.

Finally, the slow syringe pump addition of tetrabromide **193** to a slurry of $\text{VCl}_3/\text{LiAlH}_4$ (Method C) delivered the desired tetrahydrocorannulene **194** in a modest 40 % yield. The product was obtained as a mixture of diastereomers, as determined by GC/MS and ^1H NMR. TLC analysis of the reaction mixtures also showed considerable amounts of byproducts, judged from a wide variety of luminescent material below the desired compound fraction.



Scheme 5.4: Benzylic bromination of **194** and subsequent elimination of HBr as an alternative aromatization toward model corannulene **195**.

The dehydrogenation of tetrahydrocorannulene **194** was effected by DDQ in refluxing benzene, and delivered the dimethyl dimethylcorannulene dicarboxylate **195** in approxi-

mately 50 % yield. The overall yield of the sequence, bromination, ring closure, dehydrogenation was approximately 20 %. Alternatively, the secondary benzylic position in **194** could be selectively brominated under light induced radical conditions. Treatment with catalytic amounts of pyridine promoted HBr elimination and afforded the same product **195**, however, in a lower ~10 % yield over the two steps.

The different, characteristic luminescences ($\lambda=366\text{nm}$) of the three compounds, fluoranthene **190**, tetrahydrocorannulene **194** and corannulene **195** could be exploited for their detection while following the course of the reactions by TLC. As would be expected, the fluoranthene **190** exhibits a strong, bright blue emission, whereas the ring closed tetrahydrocorannulene **194** shows a somewhat less intense, darker blue emission and the final model corannulene **195** has a considerably less intense, greenish luminescence.

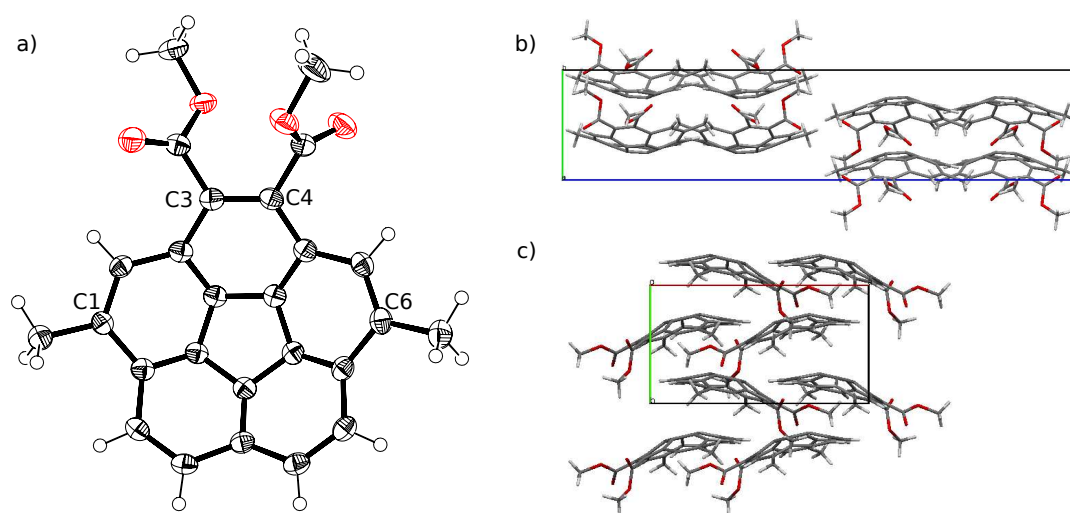


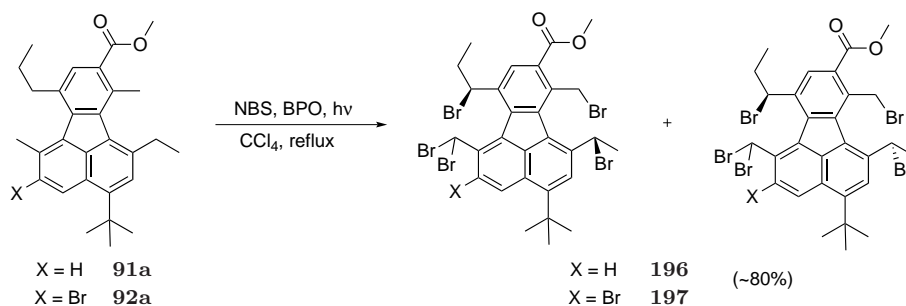
Figure 5.3: Molecular structure of corannulene diester **195** in the crystal. a) ORTEP representation with thermal ellipsoids drawn at 50 % probability. b) Crystal packing of **195** viewed along the *a* axis and c) along the *c* axis.

Crystals of **195**, suitable for X-ray analysis were obtained by slow evaporation of a solution in $\text{CHCl}_3/n\text{-hexane}$. The measured bowl depth of 0.871\AA is essentially the same as for parent corannulene **1**. Also the average bond lengths of the different bond types, hub, spoke, flank and rim do not deviate substantially from **1**, although the rim bonds bearing substituents are slightly longer ($1.387(3)\text{\AA}$ for C1–C2/C5–C6 and $1.397(3)\text{\AA}$ for C3–C4) than the unsubstituted ones ($1.374(3)\text{\AA}$). As seen for other substituted corannulene⁵⁵ derivatives, the molecules are packed in antiparallel columnar stacks (Figure 5.3b) in a zigzag-like fashion (Figure 5.3c).

5.2 Synthesis of the Target Corannulene

5.2.1 Bromination of Highly Substituted Fluoranthenes **91a** and **92a**

The same radical bromination conditions for the benzylic bromination of fluoranthene diester **190** were applied to the separated isomers **91a** and **92a**. As expected, analysis of the crude bromination products by ^1H NMR showed the formation of pentabromides **196**, and hexabromides **197**, as a diastereomeric mixture in a ratio of 2:1 (Scheme 5.5). A similar signal broadening of one of the methylene protons of **196** and **197** was observed, as it had been for the chiral fluoranthene **193a** described above. The crude reaction mixture was cooled and the precipitated succinimide and excess NBS were filtered off, and further removed by aqueous washes of the product solution. Filtration, or chromatography, on silica was avoided due to decomposition observed on TLC (reappearance of fluorescent material).



Scheme 5.5: Benzylic bromination of fluoranthenes **91a** and **92a** leading to diastereomeric mixtures **196** and **197**.

In addition to ^1H NMR measurements of the crude mixtures, mass spectrometry (MS) was an important tool for the clear identification of the brominated fluoranthenes. Due to the high level of bromination and molecular weight, electron impact (EI) was not an option as ionization method. MS using electron spray ionization (ESI) of the pentabrominated species showed some overbromination as well as strong fragmentation by the loss of Br_2 or HBr . Therefore the most intense peak in the MS does not indicate the main bromination product, but the most stable molecular ion that forms in the ionization process (Figure 5.4). The isotopic pattern of the sodium adduct $[\text{M}+\text{Na}]^+$ of **196** perfectly fits the simulated pattern of a pentabrominated compound.

[1, 5]

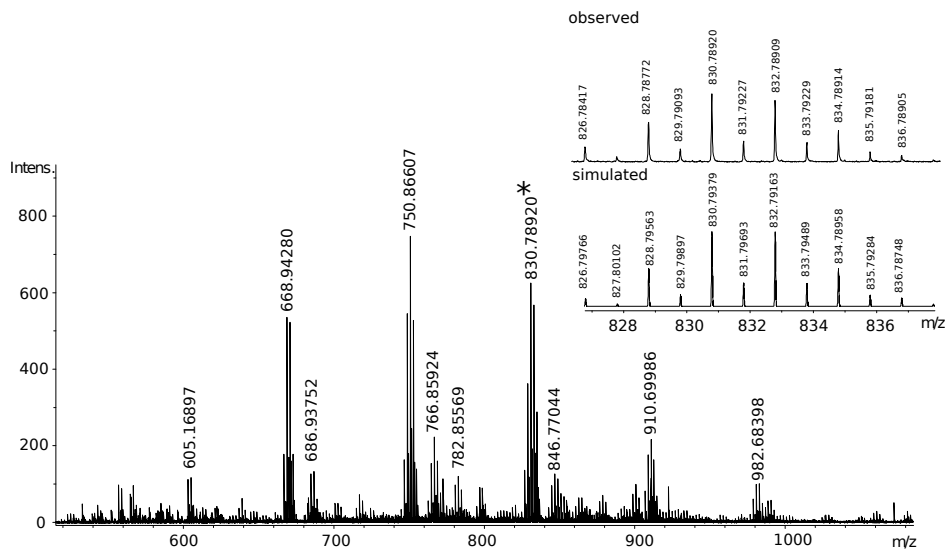


Figure 5.4: High resolution mass spectrum (ESI) of **196** with observed and simulated isotopic pattern for $[M+Na]^+$ (asterisk).

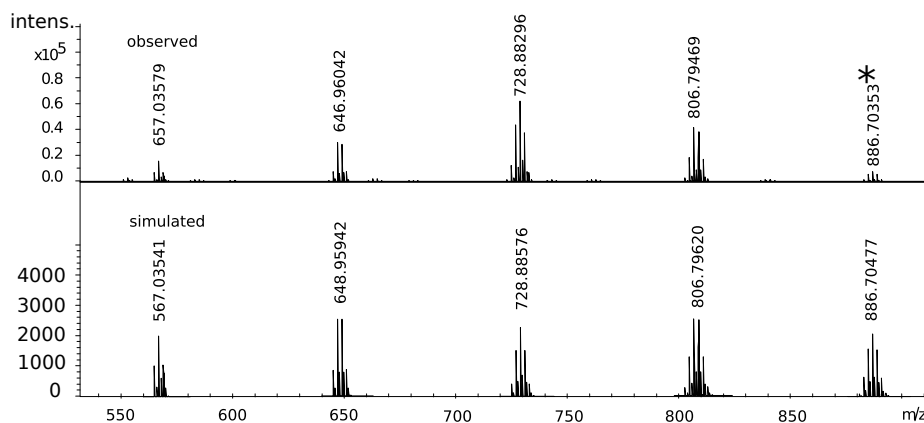
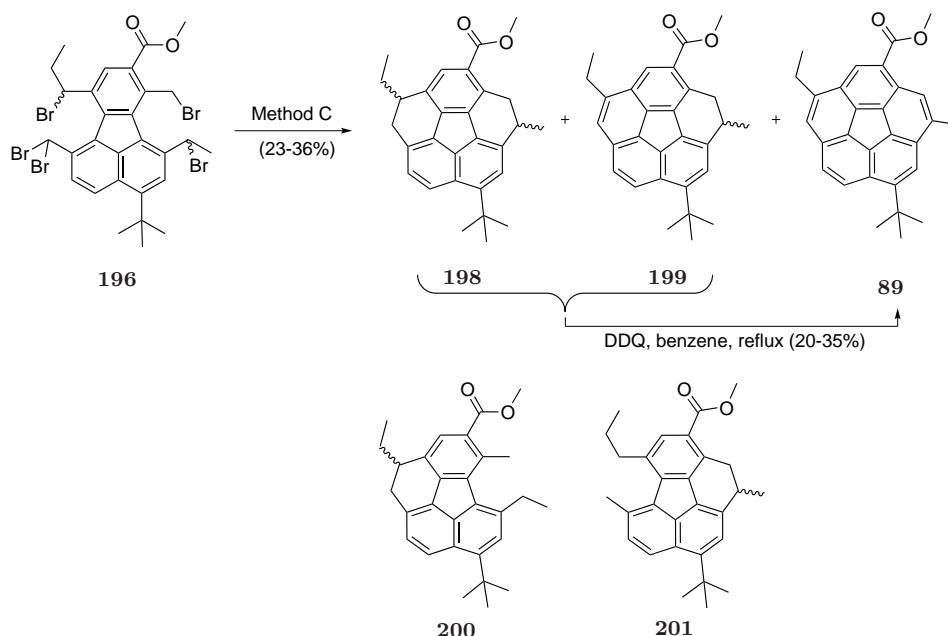


Figure 5.5: High resolution mass spectrum (APCI) of **197** with observed (top) and simulated (bottom) isotopic patterns for $[M]^+$ (asterisk) and the fragments $[M-nBr]^+$.

Due to difficulties in obtaining reliable mass spectra of the benzylic and core brominated compound **197** using ESI, the following spectra were recorded under atmospheric pressure chemical ionization (APCI). The method was found to be superior to ESI, especially for high molecular weight brominated fluoranthenes. As seen in Figure 5.5, the spectrum clearly shows the molecular ion, and its fragments, and has a much lower signal to noise ratio. Again, the fragment containing a total of 4 bromine atoms seems to be the most stable one in the ionization method.

5.2.2 Ring Closure of Brominated Target Fluoranthenes

The previously successful conditions of method C for the reductive coupling of the bromides in **193** were also applied to the brominated target fluoranthene **196**. In contrast to the modelcompound **193**, ring closure of **196** yielded a mixture of tetrahydrocorannulenes **198**, dihydrocorannulene **199** and traces of the desired corannulene **89** (Scheme 5.6). The ratio of **198**(a):**199**(c):**89**(e) was determined to be 25:53:5 by GC (Figure 5.6). The peak at $t_R=20.63$ min (b) shows a mass of $m/z=412.2u$, which corresponds to products (**200** and **201**) where at least one reductive coupling of benzylic bromides did not occur, but hydrodehalogenation of the benzylic bromides took place. The mass of $m/z=410.2u$ for peak d at $t_R=21.17$ min either shows a diastereomer of tetrahydrocorannulene **198** a partially ring closed fluoranthene.



Scheme 5.6: Ring closure of brominated fluoranthenes **196** leading to a mixture of tetrahydrocorannulenes **198**, dihydrocorannulene **199** and traces of target corannulene **89**.

After purification, the product fractions were subjected to dehydrogenation, again with DDQ in benzene, to oxidize the intermediates **198** and **199** to the desired corannulene **89**. After removal of DDQH₂ by filtration, the crude product was purified by column chromatography on silica. The overall yield for the three steps, bromination, ring closure and dehydrogenation was an unsatisfactory 5-10 %.

Method C was utilized to cyclize hexabromide **197**, which would lead to the target pentasubstituted corannulene **90**. Traces of a similar distribution of ring closed products

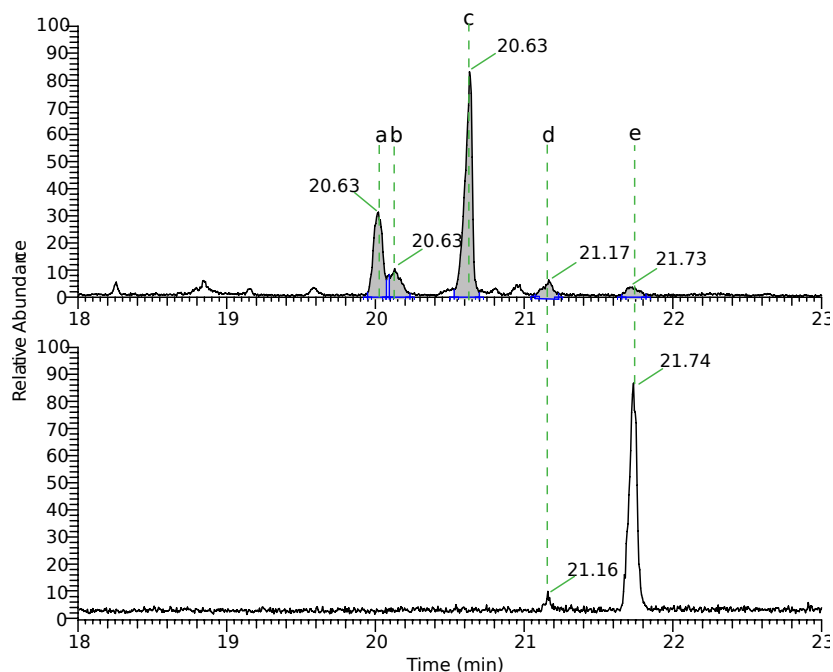
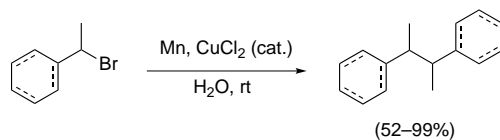


Figure 5.6: Top: GC of the product mixture of tetrahydrocorannulenes **198** (a), dihydrocorannulene **199** (c) and target corannulene **89** (e) in a ratio of 31:53:5. Unassigned peaks stem from polysiloxanes (stationary phase GC column). Bottom: GC of target corannulene after purification.

as for the latter case could only be detected by mass spectrometry and no significant amount of target corannulene **90** could be isolated after treatment with DDQ.

5.2.3 Final Synthetic Strategy Involving Alternative Coupling Conditions

The unsatisfactory results obtained with method C in the synthesis of **89**, and the vain endeavor in obtaining the pentasubstituted corannulene **90** by the same route, motivated the search for a more efficient set of conditions for the reductive coupling of benzylic bromides. Clearly, the coupling of a secondary benzylic bromide with the primary monobromide *ortho* to the ester function, and the therefore necessary final dehydrogenation step, makes the final ring closure toward the target compounds challenging.



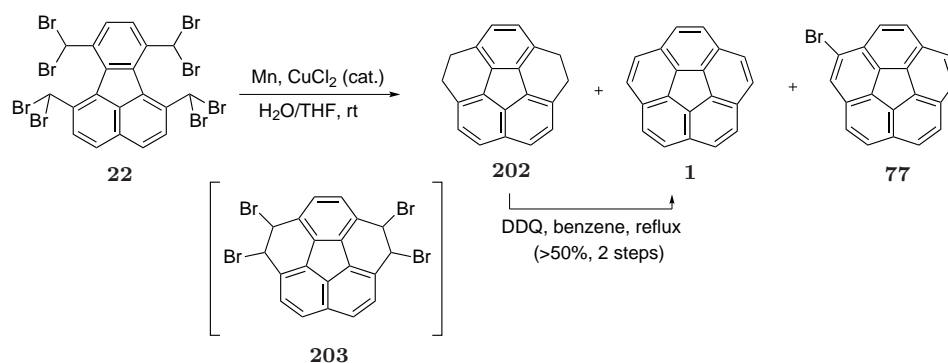
Scheme 5.7: Wurtz-type homocoupling of alkyl bromides with manganese and catalytic copper(II)chloride in aqueous media developed by Chan and coworkers.

5.2 Synthesis of the Target Corannulene

A Wurtz-type coupling, reported by Chan and coworkers,¹⁷³ involving manganese powder and catalytic copper(II)chloride seemed to be a promising alternative to the known methods for the coupling of benzylic bromides to yield corannulene derivatives. The method is described to efficiently couple allylic and benzylic, as well as alkyl bromides and iodides in oxygen-free aqueous media (Scheme 5.7). The high yielding coupling of secondary benzylic bromides reported and the tolerance toward carboxylic acid derivatives made the procedure attractive for the ring closure of brominated fluoranthenes. The reported absence of elimination products in the case of primary and secondary alkyl halides constitutes a further advantage of these conditions.

5.2.3.1 Initial Studies

To probe the feasibility of the above coupling conditions for the synthesis of corannulene derivatives, the ring closure was first tried with **22** to obtain the parent corannulene **1** (Scheme 5.8). The reaction conditions had to be slightly modified for the intramolecular coupling of the bromides in **22**. To increase solubility, a mixture of H₂O/THF was used, and the concentration was kept very low (~0.006mM) to minimize intermolecular couplings leading to polymeric products. The reaction was followed by GC/MS, and the products identified were the desired corannulene **1** (a), tetrahydrocorannulene **202** (b) and bromocorannulene **77** (c) in a ratio of 67:20:13 (Figure 5.7).



Scheme 5.8: Ring closure of octabromofluoranthene **22** leading to a mixture of tetrahydrocorannulene **202**, corannulene **1** and bromocorannulene **77**.

The reaction probably leads through the tetrabromo tetrahydrocorannulene **203**, which could not be detected. As can be seen from the GC/MS trace, no hydrodehalogenation products from **22**, or partially ring closed fluoranthenes could be identified (Figure 5.7). The GC/MS analysis shows that the coupling of primary benzylic monobromides with pri-

mary dibromides either affords the fully dehydrogenated corannulene (coupling, hydrodehalogenation and elimination of residual HBr), or the tetrahydrocorannulene (coupling, followed by hydrodehalogenation). Thus, the tetrahydrocorannulene does not form due to underbrominated fluoranthenes in the starting material. The 13 % of bromocorannulene formed most likely comes from the competing processes of dehalogenation and elimination of HBr in the intermediate **203**.

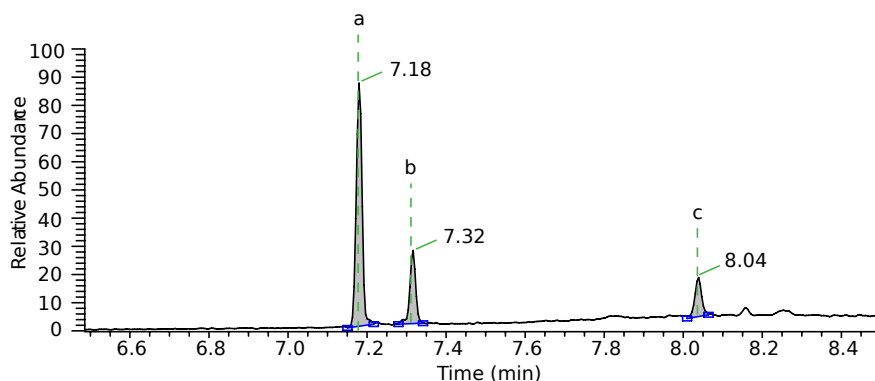


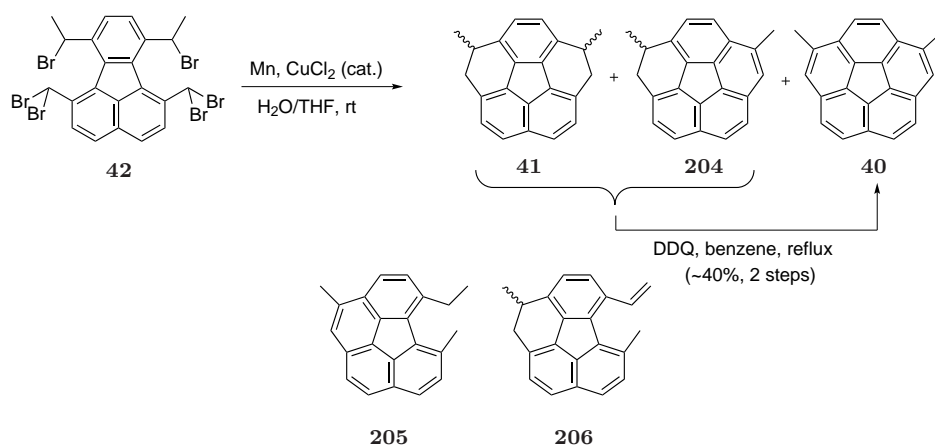
Figure 5.7: GC of the product mixture obtained from Mn/CuCl₂ promoted ring closure. a) Corannulene (**1**), b) tetrahydrocorannulene **202**, c) bromocorannulene (**77**) in a ratio of 67:20:13, respectively.

As tetrahydrocorannulene **202** is formed in the reaction, a further dehydrogenation step was necessary. The crude reaction mixture was treated with DDQ in benzene, and **1** could be obtained in over 50 % yield after column chromatography.

These promising new conditions were then used with brominated diethyl dimethylfluoranthene **42** (Scheme 5.9). Similar to the ring closure discussed in 5.2.2 (Scheme 5.6), the main products formed were the dimethyltetrahydrocorannulene **41**, and the desired 2,5-dimethylcorannulene **40**, but also a substantial amount of hydrodehalogenated and/or partially ring closed fluoranthenes, as well as dihydro dimethylcorannulene **204**, were formed. With alkyl chains longer than methyl, the additional possibility of HBr elimination arises. Combined with the more hampered coupling of the primary benzylic dibromides with secondary benzylic monobromide, this accounts for the more complex reaction mixture, presumably involving compounds like **205** and **206**.

The reaction conditions could well be applied to the ring closure of brominated model fluoranthene **193** as well as for target fluoranthene **196**. As described above for the more simple test substrates leading to **1**, and dimethylcorannulene **40**, the crude reaction mixtures comprise of more elimination products and partially ring closed fluoranthenes.

5.2 Synthesis of the Target Corannulene



Scheme 5.9: Ring closure of hexabrominated fluoranthene **42** leading to a mixture of dimethyltetrahydrocorannulene **41**, dimethyldihydrocorannulene **204** and dimethylcorannulene **40**.

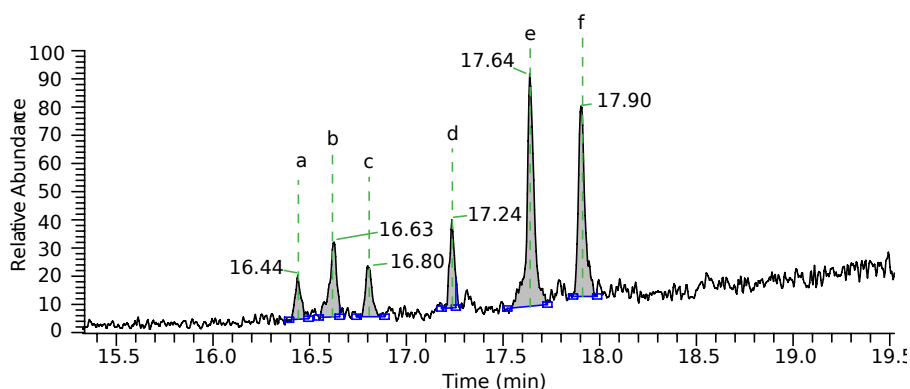
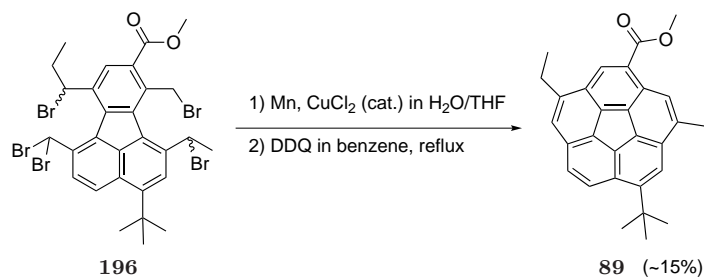


Figure 5.8: GC of the product mixture obtained from Mn/CuCl_2 promoted ring closure toward 2,5-dimethylcorannulene (**40**.) a, c, e) two diastereomers of tetrahydrocorannulene **41** and/or elimination product ($m/z=282.2u$), b) elimination product ($m/z=284.2u$), d) dihydrocorannulene **204** ($m/z=280.2u$), f) 2,5-dimethylcorannulene (**40**) in a ratio of 46:11:13:30, respectively.

Nonetheless, although the yields of the Mn/CuCl_2 method were lower than that way with **1** and **40**, the isolated yield of model corannulene **195** (~20 %) and target corannulene **89** (~15 %) were slightly higher after the dehydrogenation step, starting from the corresponding fluoranthene (Scheme 5.10).

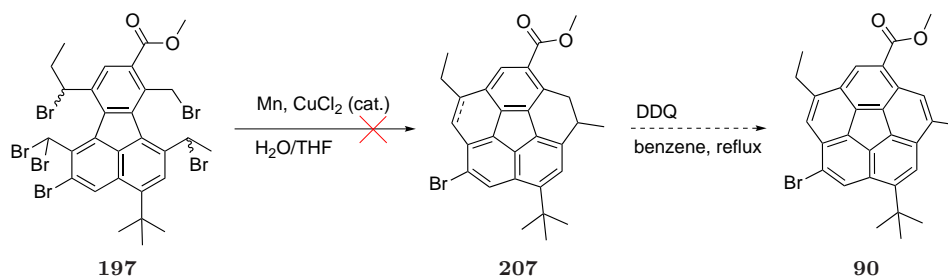
Given the comparable yields of the ring closing methods used so far toward the target corannulene **89** the benefits of these reaction conditions are the shorter reaction times, the aqueous solvent mixture, and the convenient reaction setup. Furthermore the reaction conditions generates less polymeric byproducts, and the purification of the desired corannulene **89** was therefore not as troublesome.



Scheme 5.10: Mn/CuCl₂ promoted ring closure of **196** and subsequent dehydrogenation leading to target corannulene **89**.

5.2.3.2 Ad Hoc Modification of Heptasubstituted Fluoranthenes **92** Toward Pentasubstituted Corannulene

As described above, ring closure method C was successfully applied to the synthesis of target corannulene **89**, however it could not be transferred to the ring closure of **197** to pentasubstituted **90** (Scheme 5.11). Similarly, the conditions using Mn/CuCl₂ did not

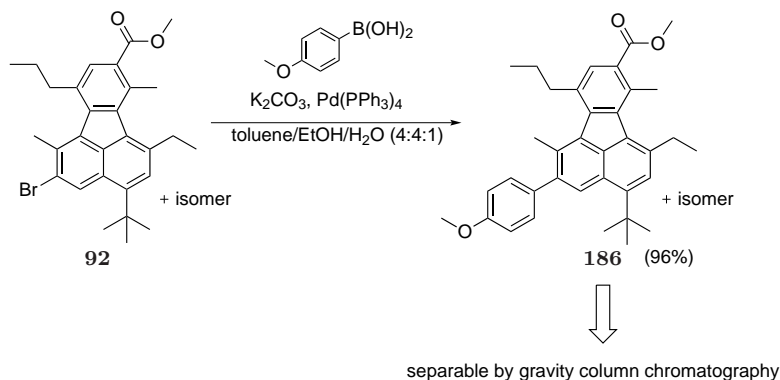


Scheme 5.11: Failed ring closure of brominated fluoranthene **197**.

give the expected ring closed product mixture **207**, as judged by mass spectrometry. The above finding was rationalized by the formation of active Cu⁰, which is formed in the catalytic cycle. The capacity of Cu⁰ to oxidatively insert into C–Br bonds and promote Ullmann-type transformations, or hydrodehalogenations, may account for the absence of desired ring closed products.

The problem could be solved by converting the aromatic bromide to a 4-methoxyphenyl substituent. The 4-methoxy substitution was chosen to fulfill the requirement of having a fifth, orthogonal substituent for future functionalization. Furthermore, different protecting groups for phenols are feasible such as the triisopropylsilyl group. The 4-methoxy substituted fluoranthenes **186** were obtained in excellent yield by Suzuki cross coupling¹⁷⁴ of the isomeric mixture of fluoranthenes **92** and 4-methoxyphenylboronic acid (Scheme 5.12).

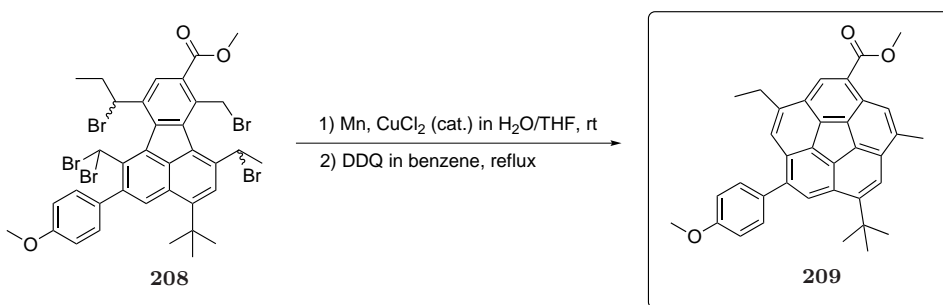
5.2 Synthesis of the Target Corannulene



Scheme 5.12: Synthesis of fluoranthene **186** via Suzuki cross coupling of the isomeric mixture of fluoranthenes **92** with 4-methoxyphenylboronic acid. The thus obtained mixture of regioisomers can be separated by gravity column chromatography.

As mentioned earlier, the isomeric mixture of **186** could be separated by standard gravity column chromatography.

Compared to the resin-like fluoranthene derivatives mentioned above, which slowly solidify upon prolonged standing and only if isomerically pure, **186** is a crystalline solid. X-ray quality crystals of the desired isomer were grown from *n*-hexane (Figure 5.9). The measured dihedral angle between the two mean planes defined through atoms C2/C3/C4/C5 and atoms C7/C8/C9/C10 in **186** amounts 26.6°. In comparison to 1,6,7,10-tetramethylfluoranthene (**21**, ~16°), and a series of 1,6,7,10-substituted diazafluoranthenes¹⁷⁵ (~13–21°), the fluoranthene derivative **186** exhibits a large twist. The distances between the benzylic positions is 3.17 Å (methyl–ethyl) and 3.22 Å (methyl–propyl), which are only marginally larger than for tetramethylfluoranthene **21**.



Scheme 5.13: Mn/CuCl₂ promoted ring closure of **208** and dehydrogenation leading to target corannulene **209**.

Benzylic bromination of **186** was achieved by standard radical bromination protocol using NBS, BPO, and incandescent light. The pentabromide **208** was subjected to

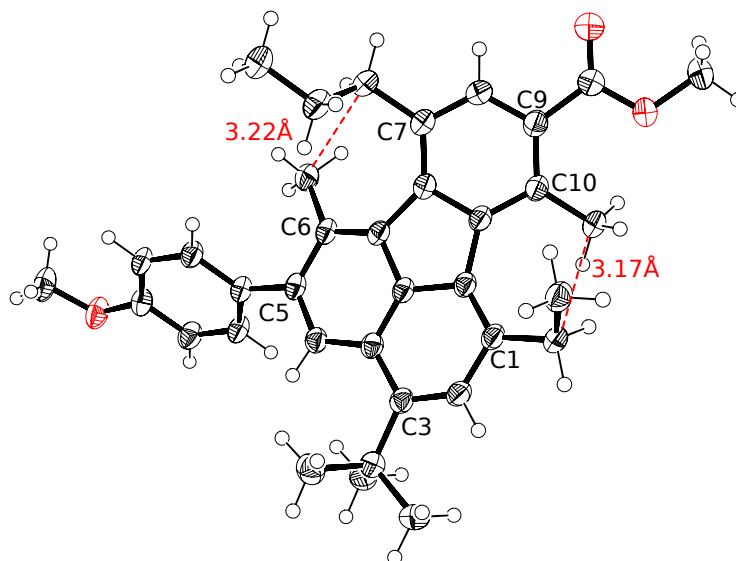


Figure 5.9: Molecular structure of 4-methoxyphenyl substituted fluoranthene derivative **186** in the crystal. Thermal ellipsoids drawn at the 50 % probability level.

Mn/CuCl₂ reductive coupling. Subsequent dehydrogenation with DDQ of the product fraction delivered the desired 1,3,5,7,9-pentasubstituted corannulene **209**, bearing five different substituents with different reactivity (Scheme 5.13). Purification of the compound mixture was achieved by column chromatography on silica and the product was obtained in about 10 % yield over the three steps.

¹H NMR spectroscopy of the pentasubstituted corannulene **209** reveals five resonances for the five different aromatic hydrogen atoms (Figure 5.10). The assignment of the individual hydrogens atoms was accomplished by NOESY NMR spectroscopy. As highlighted, the signals for hydrogens b and e exhibit a quartet-like (⁴*J*=1.1 Hz) and a triplet-like (⁴*J*=0.9 Hz) shape due to ⁴*J*-coupling with the adjacent ethyl and methyl groups, respectively.

Due to the bowl inversion of the corannulene core, the target compound **209** exists as a rapidly interconverting enantiomeric couple. The chirality of the pentasubstituted corannulenes like **209** renders the methylene protons of the ethyl group as diastereotopic. A VT-NMR experiment in CD₂Cl₂ revealed a coalescence temperature (*T_c*) of 193K, which, according to the Gutowsky–Holm approximation,^{168–170} corresponds to an inversion barrier of 8.9 ± 0.5 kcal/mol (Figure 5.11).

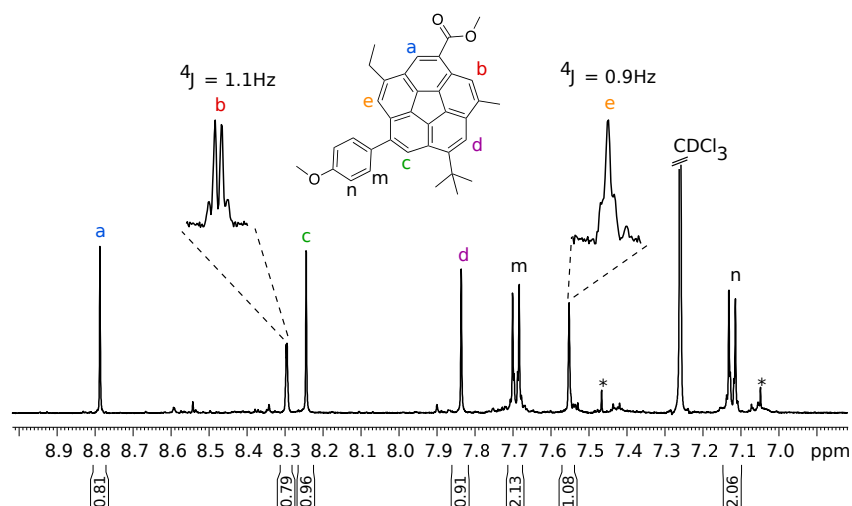


Figure 5.10: Aromatic region of the ^1H NMR of (500 MHz) 1,3,5,7,9-pentasubstituted corannulene **209**. Hydrogens b and e show 4J -coupling with the adjacent ethyl and methyl groups, respectively.

5.2.4 Conclusion

In conclusion a 1,3,5,7,9-pentasubstituted corannulene has been synthesized, bearing a unique substituent at every position. To meet the goal, the initial target had to be slightly modified. Furthermore alternative conditions for the reductive coupling of benzylic bromides were successfully applied for the final ring closure toward corannulene **209**.

The synthesis of pentasubstituted corannulenes like **209** involved the development of a new route to the suitably 1,3,5,6,7,9,10-heptasubstituted fluoranthenes such as **92** or **186**. The synthetic strategy toward fluoranthenes described in this work delivers two regioisomers of which the desired species were isolated prior to taking further synthetic steps.

Although only milligram quantities of the target compounds could be isolated, the development and the accomplishment of the above synthesis constitutes the first example of a convergent approach to synthesize pentasubstituted corannulenes and demonstrates its feasibility. The efficient synthesis of fluoranthene precursors, via Diels–Alder reactions of correspondingly presubstituted acenaphthylenes and thiophene-*S,S*-dioxides, stands in contrast to the low-yielding sequence of ring-closure and final dehydrogenation to give the targets **89** and **209**. However, compared to the first, lengthy synthesis of parent corannulene **1** by Barth and Lawton, this work should stimulate organic chemists to develop and find more efficient synthetic strategies toward a pentasubstituted corannulene with preselected substituents for particular needs.

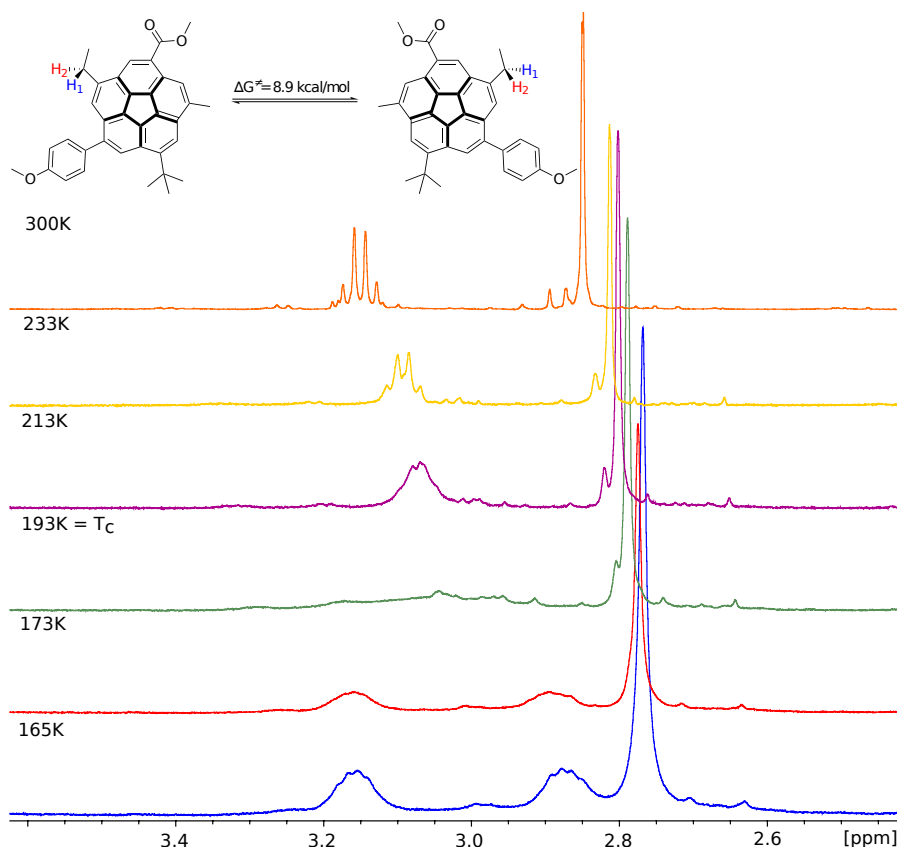
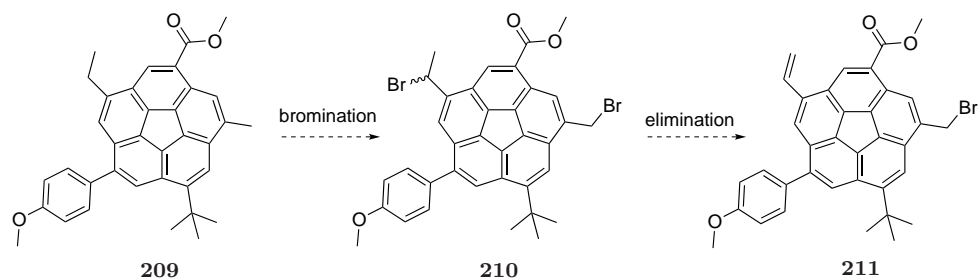


Figure 5.11: VT ^1H NMR of target corannulene **209** in CD_2Cl_2 .

5.3 Outlook

After demonstrating the feasibility of synthesizing pentasubstituted corannulene like **209** through a fluoranthene precursor, the obvious future goal would be to improve the ring closing and the dehydrogenation step. Having reasonable amounts of pentasubstituted corannulenes in hand, should facilitate further investigations.

Although the differential reactivity of the secondary benzylic position on the ethyl group, compared to those on the methyl group can be exploited (*i.e.* radical bromination), it would be desirable to further convert the two alkyl chains into distinct functional groups. A conceivable approach to fulfill the latter requirement is outlined in Scheme 5.14. Benzylic bromination of **209** is envisioned to deliver the dibromide **210**. Elimination with bulky bases should then promote elimination of HBr without affecting the bromomethyl group with undesired substitution and lead to the orthogonally pentafunctionalized corannulene **211**.



Scheme 5.14: Envisioned further functionalization of pentasubstituted corannulene **209**.

Having the corannulene core decorated with five distinct functional groups, sets a “first sphere” of previously chosen substituents, that meet our individual, designed requirements. In the schematic representation it becomes clear, why the “first sphere” could be arbitrarily chosen: now, every site A, B, C, D, and E (Figure 5.12) that displays orthogonal reactivity can be individually addressed with predesigned moieties. These complementary pieces create the “second sphere” with the previously chosen termini. Only at this point the chemist is in full control over all the permutational possibilities by choosing the nature of the complementary piece that generates the second sphere. With such a combinatorial system, one is in principal both, in control of the order and the nature of the relative substituent.

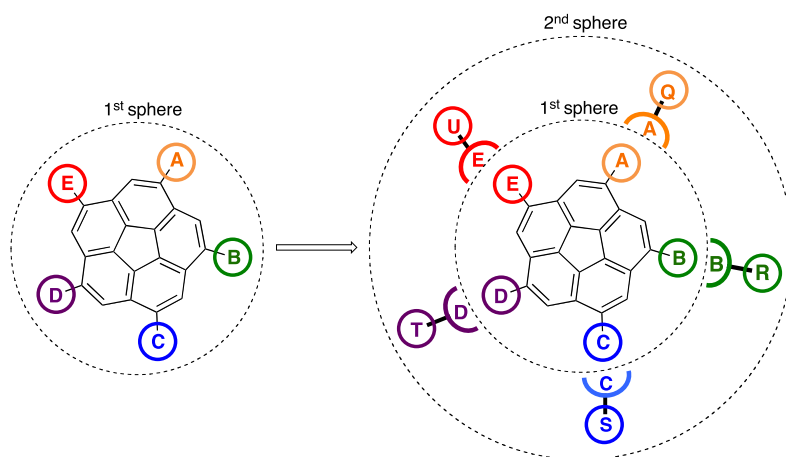


Figure 5.12: Schematic representation of the extension of pentafunctionalized corannulene with tailored “codons”.

6 Experimental Section

6.1 General Data

6.1.1 Abbreviations

Ac ₂ O	acetic anhydride
AcOH	acetic acid
aq.	aqueous
BPO	Dibenzoylperoxide
deact.	deactivated
DMF	<i>N,N</i> -dimethylformamide
DMSO	dimethyl sulfoxide
Et ₂ O	diethyl ether
EtOAc	ethyl acetate
EtOH	ethanol
equiv.	equivalent
hrs.	hours
MeOH	methanol
m.p.	melting point
MtBE	methyl <i>tert</i> -butyl ether
NBS	<i>N</i> -bromosuccinimide
org.	organic
prep.	preparative
<i>R_f</i>	retention factor
rt	room temperature
TFA	trifluoroacetic acid
TFAA	trifluoroacetic acid anhydride
THF	tetrahydrofuran
TLC	thin-layer chromatography
TsOH	<i>p</i> -toluenesulfonic acid

6.1.2 Chromatography and Acquisition of Spectra

Thin-layer chromatography was performed on plastic-backed 0.2 mm UV₂₅₄ silica gel plates from Macherey-Nagel. **Preparative thin-layer chromatography** was performed on glass-supported 1 mm UV₂₅₄ silica gel plates from Merck. Visualization with 254 nm UV light.

Melting points were determined using a heating microscope from Christoffel Labor- and Betriebstechnik and are uncorrected.

Infrared spectra were recorded on a JASCO FT/IR-4100 spectrometer. Absorption bands are given in wave numbers (cm^{-1}), and the intensities are characterized as follows: *s* = strong (0–33 % transmission), *m* = medium (34–66 % transmission), *w* = weak (67–100 % transmission).

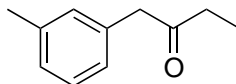
NMR spectra were recorded on Bruker AV-500 (^1H , ^{13}C), and Bruker AV-400 (^1H , ^{13}C). Chemical shifts are given relative to tetramethylsilane ($\delta(\text{Si}(\text{CH}_3)_4) \equiv 0$ ppm for ^1H and ^{13}C unless otherwise indicated. Data are reported as follows: chemical shift in ppm, multiplicity (*s* = singlet, *d* = doublet, *t* = triplet, *q* = quadruplet, *m* = multiplet, *dd* = doublet of doublet, *dt* = doublet of triplet, etc.), coupling constant nJ in Hz, integration, and interpretation. Multiplicities in ^{13}C NMR spectra were determined using DEPT (Distortionless Enhancement by Polarization Transfer) experiments.

Mass spectra were recorded on a HP 5890 GC–MS instrument (EI, 70 eV) or performed by the MS Laboratory of the Organisch-chemisches Institut of the University of Zurich (ESI, EI and high-resolution mass spectra). Data are reported as follows: *m/z*, % relative intensity and possible fragment.

X-ray structure analyses were carried out by the Laboratorium für Computerchemie und Röntgenstrukturanalyse of the Organisch-chemisches Institut of the University of Zurich. A Nonius KappaCCD diffractometer with $\text{MoK}\alpha$ radiation ($\lambda = 0.71037 \text{ \AA}$) was used.

6.2 Experimental Details

(3-Methylphenyl)butan-2-one (**129**)



C₁₁H₁₄O
Mol. Wt.: 162.23

To a 3-necked 500 mL round-bottom flask, equipped with stir bar and N₂ inlet, magnesium turnings (5.19 g, 213.4 mmol) were added and covered with dry Et₂O (60 mL). The suspension was cooled to an internal temperature between -15°C and -10°C with an acetone/ice/NH₄Cl bath. A solution of 3-methylbenzylchloride (30 g, 28.2 mL, 213.4 mmol) in Et₂O (80 mL) was added via addition funnel to the vigorously stirred suspension over a period of 2 hrs. such that the temperature did not exceed -5°C . Upon complete addition the greenish-grey mixture was stirred another hour at -10°C . At this temperature a solution of propionitrile (19.22 g, 15.1 mL, 214.1 mmol) in Et₂O was added over a period of 30 min. with an addition funnel. The resulting greyish suspension was stirred another 48 hrs. and allowed to warm to rt. The mixture was then poured into an erlenmeyer flask containing ice, conc. HCl (50 mL) and H₂O (200 mL) where the grignard adduct hydrolyzes to the desired ketone. The mixture was saturated with NaCl and extracted with Et₂O (4×100 mL). The org. layer was dried over MgSO₄, filtered and evaporated, to give the crude product as a yellow liquid. Vacuum distillation (5 mbar, 85°C) gave the pure product **129** as a colorless liquid (28.91 g, 84%).

$R_f = 0.3$ (silica, *n*-hexane/acetone 20:1)

IR (film): 3019 w , 2978 w , 2939 w , 1710 s , 1607 w , 1590 w , 1489 w , 1458 w , 1411 w , 1378 w , 1348 w , 1199 w , 1109 m , 1039 w , 990 w , 775 m , 698 s , 436 m .

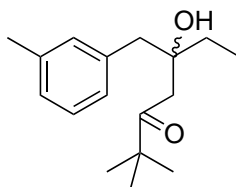
¹H NMR (500 MHz, CDCl₃): 7.21 (t , $^3J = 7.5$, 1 H); 7.07 (d , $^3J = 7.5$, 1 H); 7.04-6.97 (m , 2 H); 3.64 (s , 2 H); 2.47 (q , $^3J = 7.5$); 2.33 (s , 3 H); 1.02 (t , $^3J = 7.5$).

¹³C{¹H} NMR (125 MHz, CDCl₃): 209.21; 138.36; 134.38; 130.12; 128.59; 127.71; 126.39; 49.81; 21.35; 7.78.

MS (EI): 162 (14, M^+), 105 (73, $[M - C_3H_5O]^+$), 91 (10, $[C_7H_7]^+$), 77 (56, $[C_6H_5]^+$), 57 (100, $[C_3H_5O]^+$).

HRMS (EI): $[M^+]$ calculated for $C_{11}H_{14}O$: 162.10447; found 162.10456.

2,2-dimethyl-5-hydroxy-5-[(3-methylphenyl)methyl]heptan-3-one (131)



$C_{17}H_{26}O_2$
Mol. Wt.: 262.39

In an oven-dried 2-necked 500 mL round bottom flask, equipped with stir bar, septum and N_2 inlet, a solution of *i*-Pr₂NH (11.92 g, 16.56 mL, 73.95 mmol) in dry Et₂O (200 mL) was cooled to 0 °C in an ice bath. A solution of *n*-BuLi (29.6 mL, 2.5 M in *n*-hexane, 74 mmol) was added slowly and the resulting mixture was stirred for 30 min. at 0 °C. The ice bath was exchanged with a dry ice/acetone bath and at −78 °C 3,3-dimethylbutan-2-one (6.8 g, 8.5 mL, 67.9 mmol) was added dropwise via syringe. The resulting solution was stirred another 1.5 hrs. at −78 °C, followed by the slow addition of **129** (10g, 61.64 mmol) via syringe. The reaction mixture was stirred another 8 hrs. and was then hydrolyzed with sat. aq. NH_4Cl (150 mL) at −78 °C and allowed to warm to rt. After two clear phases separated, the org. phase was collected and the aq. phase was acidified with 10 % aq. HCl, followed by extraction with Et₂O (3 × 100 mL). The combined org. layers were dried over $MgSO_4$, filtered and evaporated to yield a yellow oil. Column chromatography on silica gel with CH_2Cl_2/n -pentane (2:1) as eluant gave the desired product **131** as a colorless oil (16.2 g, 73 %).

R_f = 0.27 (silica, CH_2Cl_2/n -pentane (2:1))

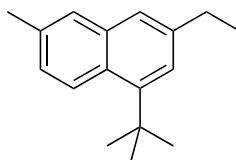
IR (film): 3489 w (broad), 3026 w , 2967 s , 2936 m , 2879 w , 1688 s , 1607 w , 1589 w , 1478 m , 1463 m , 1395 s , 1366 m , 1066 s , 1004 m , 987 m , 971 m , 735 m , 700 s , 559 m .

^1H NMR (500 MHz, CDCl_3): 7.17 (*t*, $^3J = 7.5$, 1 H); 7.03 (*d*, $^3J = 7.5$, 1 H); 7.00 (*s*, 1 H); 6.99 (*d*, $^3J = 7.5$, 1 H); 2.80 (*s*, 2 H); 2.64 (*d*, $^2J = 17.5$, 1 H); 2.53 (*d*, $^2J = 17.5$, 1 H); 2.32 (*s*, 3 H); 1.53 (*q*, $^3J = 7.5$); 1.11 (*s*, 9 H); (*t*, $^3J = 7.5$).

$^{13}\text{C}\{^1\text{H}\}$ NMR (125 MHz, CDCl_3): 219.05; 137.54; 137.51; 131.32; 127.92; 127.46; 127.11; 74.13; 44.94; 44.71; 42.60; 31.68; 26.35; 21.42; 8.08.

HRMS (ESI): $[\text{M}+\text{Na}]^+$ calculated for $\text{C}_{17}\text{H}_{26}\text{O}_2$: 285.18250; found 185.18276. $[\text{M}+\text{H}]^+$ calculated for $\text{C}_{17}\text{H}_{26}\text{O}_2$: 263.20056; found 263.20034.

1-*t*-butyl-3-ethyl-6-methylnaphthalene (**126**)



$\text{C}_{17}\text{H}_{22}$
Mol. Wt.: 226.36

In a 50 mL round-bottom flask, equipped with stir bar and reflux condenser, the hydroxyketone **131** (2.11 g, 8.04 mmol) was dissolved in AcOH (25 mL) and 48 % aq. HBr (30 mL) was added. The color changes to orange immediately and the reaction mixture was stirred and heated to 90 °C for 4 hrs. After cooling to rt. the now dark mixture was neutralized with sat. aq. NaHCO_3 and extracted with CH_2Cl_2 (3×50 mL). The combined org. layers were dried over MgSO_4 , filtered and evaporated to give a brownish oil. Column chromatography on silica gel with *n*-pentane as eluant gave the desired product **126** as a colorless oil that solidifies upon standing (2.02g, 77 %).

$R_f = 0.68$ (silica, *n*-pentane)

M.p.: 39–41 °C

IR (film): 2991*w*, 2961*m*, 2930*w*, 2871*w*, 1629*w*, 1615*w*, 1507*w*, 1459*m*, 1396*m*, 1364*w*, 989*w*, 899*m*, 882*s*, 817*s*, 472*m*.

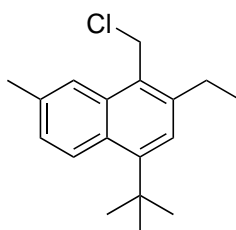
^1H NMR (500 MHz, CDCl_3): 8.28 (*d*, $^3J = 8.9$, 1 H); 7.57 (*s*, 1 H); 7.40 (*s*, 1 H); 7.27 (*d*, $^4J = 1.9$, 1H); 7.24 (*dd*, $^3J = 8.9$, $^4J = 4$); 2.77 (*q*, $^3J = 7.6$, 2 H); 2.47 (*s*, 3 H); 1.61 (*s*, 9 H); 1.31 (*t*, $^3J = 7.6$, 3 H).

$^{13}\text{C}\{^1\text{H}\}$ NMR (100 MHz, CDCl_3): 145.96; 140.90; 135.95; 134.23; 128.37; 128.28; 126.80; 126.13; 124.47; 124.08; 36.13; 32.03; 29.38; 21.44; 15.53.

MS (EI): 226 (41, M^+), 211 (100, $[\text{M} - \text{CH}_3]^+$), 197 (20, $[\text{M} - \text{C}_2\text{H}_5]^+$), 183 (36, $[\text{C}_{14}\text{H}_{15}]^+$), 165 (53), 152 (38), 141 (24), 128 (24), 115 (16).

HRMS (EI): $[\text{M}^+]$ calculated for $\text{C}_{17}\text{H}_{21}\text{O}$: 226.17215; found 226.17228.

**4-*t*-butyl-1-(chloromethyl)-2-ethyl-7-methylacenaphthalene
and 5-*t*-butyl-1-(chloromethyl)-7-ethyl-2-methylacenaphthalene (164)**



$\text{C}_{18}\text{H}_{23}\text{Cl}$
Mol. Wt.: 274.83

The naphthalene **126** (6.26 g, 27.66 mmol) and paraformaldehyde (996 mg, 33.17 mmol) were added to a sealable 100 mL bottle, equipped with stir bar, and a solution of HCl in AcOH (~ 1 M, 56 mL) was added. The sealed bottle was placed in an oil bath, preheated to 55 °C, and stirred for 25 hrs. After cooling to rt., the olive-colored solution was carefully poured into cooled sat. aq. NaHCO_3 (1L) and extracted with CH_2Cl_2 (4×60 mL). The combined org. layers were dried over MgSO_4 , filtered and evaporated to give the crude product **164** (mixture of regioisomers) as a brownish resin (7.58 g, 91 % by GC/MS). An analytically pure sample (colorless resin, mixture of regioisomers) was obtained by flash column chromatography on silica using *n*-hexane as the eluant. Usually the crude product was used in the next step due to partial decomposition on silica and Al_2O_3 .

$R_f = 0.24$ (silica, *n*-hexane)

MS (EI): (mixture of isomers) 274 (58, M^+), 259 (42, $[\text{M} - \text{CH}_3]^+$), 239 (100, $[\text{M} - \text{Cl}]^+$), 223 (28), 209 (11), 195 (23), 179 (18), 165 (21).

4-*t*-butyl-1-(chloromethyl)-2-ethyl-7-methylacenaphthalene:

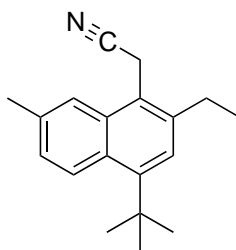
^1H NMR (500 MHz, CDCl_3): 8.35 (*d*, $^3J = 8.9$, 1H); 7.93 (*s*, 1H); 7.29 (*dd*, $^3J = 8.9$, $^4J = 1.6$, 1H); 7.27 (*s*, 1H); 5.08 (*s*, 2H); 2.89 (*q*, $^3J = 7.6$, 2H); 2.55 (*s*, 3H); 1.60 (*s*, 9H); 1.32 (*t*, $^3J = 7.6$, 3H).

$^{13}\text{C}\{^1\text{H}\}$ NMR (125 MHz, CDCl_3): 147.67; 141.02; 135.35; 133.65; 128.96; 127.48; 127.25; 126.15; 124.75; 123.87; 40.32; 36.21; 32.13; 27.45; 22.09; 16.32.

5-*t*-butyl-1-(chloromethyl)-7-ethyl-2-methylnaphthalene:

^1H NMR (500 MHz, CDCl_3): 8.34 (*d*, $^3J = 8.9$, 1H); 7.80 (*s*, 1H); 7.35 (*d*, $^4J = 1.3$, 1H); 7.24 (*d*, $^3J = 8.9$, 1H); 5.08 (*s*, 2H); 2.84 (*q*, $^3J = 7.6$, 2H); 2.57 (*s*, 3H); 1.60 (*s*, 9H); 1.35 (*t*, $^3J = 7.6$, 3H).

**2-(1-*t*-butyl-3-ethyl-6-methylnaphthalen-4-yl)acetonitrile
and 2-(1-*t*-butyl-3-ethyl-6-methylnaphthalen-5-yl)acetonitrile (**165**)**



$\text{C}_{19}\text{H}_{23}\text{N}$
Mol. Wt.: 265.39

In a 50 mL round-bottom flask, equipped with stir bar and reflux condenser, the crude (chloromethyl)naphthalene **164** (3.43 g, 12.48 mmol) was dissolved in acetone/ H_2O (10:1) and KCN (2.6 g, 39.24 mmol) was added. The suspension was refluxed for 20 hrs. and allowed to cool to rt. The suspension was decanted and the remaining solids were washed with Et_2O . H_2O and sat. aq NaHCO_3 was added to the supernatant and the mixture was extracted with Et_2O (3×60 mL). The combined organic layers were washed with H_2O (3×100 mL), dried over MgSO_4 , filtered and evaporated to give the crude product (mixture of regioisomers) as a brown resin. Column chromatography on silica with *n*-hexane/ EtOAc (3:1) gave the desired product **165** (mixture of regioisomers) as a colorless resin (2.88 g, typically 87 % for 2 steps).

$R_f = 0.17$ (silica, *n*-hexane/ EtOAc (3:1))

MS (EI): 265 (50, M^+), 250 (100, $[M - CH_3]^+$), 223 (28), 209 (31), 195 (36), 179 (38), 165 (85), 152 (36).

2-(1-*t*-butyl-3-ethyl-6-methylnaphthalen-4-yl)acetonitrile:

1H NMR (500 MHz, $CDCl_3$): 8.39 (*d*, $^3J = 8.8$, 1H); 7.77 (*s*, 1H); 7.35 (*dd*, $^3J = 8.8$, $^4J = 1.2$, 1H); 7.30 (*s*, 1H); 4.06 (*s*, 2H); 2.86 (*q*, $^3J = 7.7$, 2H); 2.58 (*s*, 3H); 1.62 (*s*, 9H); 1.33 (*t*, $^3J = 7.7$).

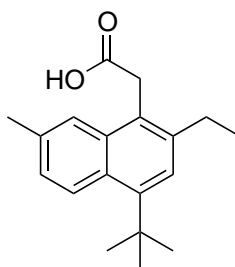
$^{13}C\{^1H\}$ NMR (125 MHz, $CDCl_3$): 147.21; 140.10; 135.80; 133.53; 128.97; 127.68; 126.37; 124.71; 123.28; 120.68; 118.48; 36.14; 32.12; 28.06; 22.06; 16.83; 15.86.

2-(1-*t*-butyl-3-ethyl-6-methylnaphthalen-5-yl)acetonitrile:

1H NMR (500 MHz, $CDCl_3$): 8.38 (*d*, $^3J =$, 1H); 7.64 (*s*, 1H); 7.40 (*s*, 1H); 7.29 (*d*, $^3J = 8.8$, 1H); 4.08 (*s*, 2H); 2.86 (*q*, $^3J = 7.7$, 2H); 2.57 (*s*, 3H); 1.63 (*s*, 9H); 1.37 (*t*, $^3J = 7.7$).

$^{13}C\{^1H\}$ NMR (125 MHz, $CDCl_3$): 147.20; 142.43; 133.64; 133.61; 129.25; 127.63; 126.77; 124.43; 124.02; 119.38; 118.01; 36.24; 32.25; 29.99; 20.47; 17.78; 15.83.

**2-(1-*t*-butyl-3-ethyl-6-methylnaphthalen-4-yl)acetic acid
and 2-(1-*t*-butyl-3-ethyl-6-methylnaphthalen-5-yl)acetic acid (163)**



$C_{19}H_{24}O_2$
Mol. Wt.: 284.39

In a 250 mL round-bottom flask, equipped with stir bar and reflux condenser, the naphthylacetonitrile **165** (4.09 g, 15.4 mmol) was dissolved in AcOH (50 mL) and H_2O (15 mL) was added. The solution was cooled to 0 °C in an ice bath and conc. H_2SO_4 (6 mL) was added slowly with vigorous stirring. The now dark reaction mixture was heated to reflux for 18 hrs. After cooling in an ice bath, H_2O was added and the emulsion was

extracted with CH_2Cl_2 (3×80 mL). The combined org. layers were dried over MgSO_4 , filtered and evaporated to give a dark resin. Column chromatography on silica with *n*-hexane/EtOAc (4:1) gave the desired product (mixture of regioisomers) as a tan resin which solidified upon standing. Trituration with *n*-hexane delivers **163** as colorless solid (3.54 g, 81 %).

$R_f = 0.2$ (silica, *n*-hexane/EtOAc (4:1))

HRMS (ESI): $[\text{M}-\text{H}]^-$ calculated for $\text{C}_{19}\text{H}_{24}\text{O}_2$: 283.17035; found 283.17055.

2-(1-*t*-butyl-3-ethyl-6-methylnaphthalen-4-yl)acetic acid:

^1H NMR (500 MHz, acetone- d_6): 8.52 (*d*, $^3J = 8.9$, 1H); 8.05 (*s*, 1H); 7.50 (*s*, 1H), 7.46 (*dd*, $^3J = 8.9$, $^4J = 1.8$, 1H); 4.26 (*s*, 2H); 3.03 (*q*, $^3J = 7.6$); 2.64 (*s*, 3H); 1.76 (*s*, 9H); 1.41 (*t*, $^3J = 7.6$).

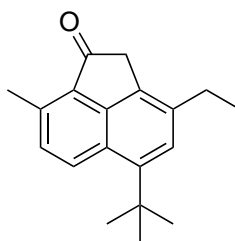
$^{13}\text{C}\{^1\text{H}\}$ NMR (125 MHz, CDCl_3): 177.75; 145.66; 140.06; 134.77; 134.32; 128.57; 127.21; 125.64; 124.51; 124.05; 123.85; 35.83; 33.81; 31.93; 27.61; 21.82; 15.61.

2-(1-*t*-butyl-3-ethyl-6-methylnaphthalen-5-yl)acetic acid:

^1H NMR (500 MHz, acetone- d_6): 8.46 (*d*, $^3J = 8.9$, 1H); 7.97 (*s*, 1H); 7.52 (*d*, $^4J = 1.4$, 1H), 7.47 (*d*, $^3J = 8.9$, 1H); 4.28 (*s*, 2H); 2.95 (*q*, $^3J = 7.6$); 2.68 (*s*, 3H); 1.76 (*s*, 9H); 1.45 (*t*, $^3J = 7.6$).

$^{13}\text{C}\{^1\text{H}\}$ NMR (125 MHz, CDCl_3): 177.50; 146.48; 141.36; 134.31; 133.78; 128.85; 127.60; 126.63; 126.49; 123.77; 119.98; 35.99; 34.91; 32.05; 29.70; 20.49; 15.52.

**5-(*t*-butyl)-3-ethyl-8-methylacenaphthen-1-one
and 6-(*t*-butyl)-8-ethyl-3-methylacenaphthen-1-one (162)**



$\text{C}_{19}\text{H}_{22}\text{O}$
Mol. Wt.: 266.38

In an oven-dried 2-necked 100 mL round-bottom flask, equipped with stir bar, reflux condenser with N₂ inlet and septum, the naphthylacetic acid (1.11g, 3.9 mmol) was dissolved in dry CH₂Cl₂ (45 mL). SOCl₂ (982 mg, 0.6 mL, 7.77 mmol) was added dropwise via syringe and the solution gets darker. The reaction mixture was refluxed for 20 hours, and the solvent and remaining volatiles were removed under reduced pressure. The dark residue was dissolved in dry CH₂Cl₂ and cooled to -5 °C with an ice/acetone bath. TiCl₄ (3.9 mL, 1M in CH₂Cl₂) was added dropwise and the deep purple solution was stirred another 40 min. at -5 °C. H₂O was added and the org. layer was separated. The aq. phase was neutralized with sat. aq. NaHCO₃ and extracted with CH₂Cl₂ (3 × 70 mL). The combined org. layers were washed with sat. aq. NaHCO₃ (3 × 100 mL) and brine (3 × 100 mL) and dried over MgSO₄. Filtration and evaporation to dryness yielded the crude product as a brown solid. Column chromatography on silica with *n*-hexane/EtOAc (20:1) as the eluant gave the pure product **162** (mixture of regioisomers) as an off-white solid (593 mg, 57 %).

Through recrystallization from *n*-hexane the pure 5-(*t*-butyl)-3-ethyl-8-methylacenaphthen-1-one (major isomer) could be separated as colorless needles.

5-(*t*-butyl)-3-ethyl-8-methylacenaphthen-1-one:

R_f = 0.4 (silica, *n*-hexane/EtOAc (20:1))

M.p.: 143–144.5 °C

IR (film): 2965 m , 2953 m , 2914 w , 2878 w , 1702 s , 1617 w , 1590 m , 1466 w , 1376 w , 1365 w , 1331 w , 1268 w , 1195 m , 887 w , 836 w , 628 w .

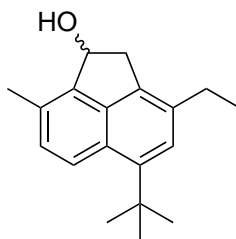
¹H NMR (500 MHz, CDCl₃): 8.40 (*d*, ³*J* = 8.6, 1H); 7.38 (*d*, ³*J* = 8.6, 1H); 7.33 (*s*, 1H); 3.66 (*s*, 2H); 2.81 (*s*, 3H); 2.77 (*q*, ³*J* = 7.6, 2H); 1.61 (*s*, 9H); 1.30 (*t*, ³*J* = 7.6, 3H).

¹³C{¹H} NMR (125 MHz, CDCl₃): 204.88; 145.50; 144.84; 136.56; 136.30; 132.08; 131.42; 129.36; 129.31; 126.61; 125.19; 40.65; 36.21; 31.86; 27.12; 17.87; 15.27.

MS (EI): 266 (44, M⁺), 251 (100, [M - CH₃]⁺), 207 (20), 223 (28, [CH₁₆H₁₅O]⁺), 193 (34), 179 (30), 165 (23), 152 (10).

HRMS (EI): [M⁺] calculated for C₁₉H₂₂O: 266.16706; found 266.16686.

**5-(*t*-butyl)-3-ethyl-8-methylacenaphthen-1-ol
and 6-(*t*-butyl)-8-ethyl-3-methylacenaphthen-1-ol (**166**)**



C₁₉H₂₄O
Mol. Wt.: 268.39

To a 100 mL round-bottom flask, equipped with stir bar and reflux condenser with N₂ inlet, the acenaphthenone **162** (1.05 g, 3.94 mmol), MeOH (25 mL), and CH₂Cl₂ (25 mL) were added. NaBH₄ (686 mg, 18.13 mmol) was added in portions to the mixture and stirring was continued at ambient temperature until evolution of H₂ ceased. The mixture was heated to reflux for 3 hrs. after which a clear solution formed. The solvents were removed by rotary evaporation and the residue was taken up in CH₂Cl₂. H₂O and 10 % aq. HCl were added, the org. layer was separated and washed with 10 % aq. HCl and brine. The org. phase was dried over MgSO₄, filtered and evaporated to give the crude alcohol **166** (mixture of regioisomers) as a colorless resin (1.04 g).

5-(*t*-butyl)-3-ethyl-8-methylacenaphthen-1-ol:

R_f = 0.18 (silica, *n*-hexane/EtOAc (10:1))

IR (film): 3276 m (broad), 2959 s , 2928 m , 2871 m , 1727 w , 1619 w , 1497 w , 1480 w , 1461 m , 1417 m , 1392 m , 1363 m , 1255 m , 1181 w , 1162 w , 1131 w , 1057 m , 1034 m , 907 m , 884 m , 818 s , 792 m , 733 s .

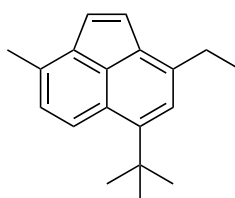
¹H NMR (400 MHz, C₆D₆): 8.13 (d , ³ J = 8.6, 1H); 7.33, (s , 1H); 7.17 (d , ³ J = 8.6, 1H); 5.35 (t , ³ J = 7.4, 1H), 3.26 (dd , ² J = 17.5, ³ J = 7.4, 1H); 2.83 (dd , ² J = 17.5, ³ J = 2.05, 1H); 2.59 (q , ³ J = 7.6, 2H); 2.45 (s , 3H); 1.59 (s , 9H); 1.21 (t , ³ J = 7.6, 3H).

¹H NMR (400 MHz, CDCl₃): 8.15 (d , ³ J = 8.6, 1H); 7.30, (d , ³ J = 8.6, 1H); 7.28 (s , 1H); 5.70 (dd , ³ J = 7.0, ³ J = 1.5, 1H), 3.64 (dd , ² J = 17.5, ³ J = 7.2, 1H); 3.13 (dd , ² J = 17.5, ³ J = 1.5, 1H); 2.75 (q , ³ J = 7.5, 2H); 2.59 (s , 3H); 1.87 (s , 1H); 1.62 (s , 9H); 1.30 (t , ³ J = 7.5, 3H).

$^{13}\text{C}\{^1\text{H}\}$ NMR (100 MHz, CDCl_3): 143.61; 143.01; 139.03; 136.17; 135.21; 130.75; 128.78; 126.64; 125.90; 125.11; 73.93; 40.04; 36.04; 31.70; 26.78; 17.78; 15.12.

HRMS (ESI): $[\text{M}+\text{Na}]^+$ calculated for $\text{C}_{19}\text{H}_{24}\text{NaO}$: 291.17194 ; found 291.17184.

5-(*t*-butyl)-3-ethyl-8-methylenacenaphthylene (**157**)



$\text{C}_{19}\text{H}_{22}$
Mol. Wt.: 250.38

In an oven-dried 1L round-bottom flask, equipped with stir bar and reflux condenser with N_2 inlet, a solution of the acenaphthenol **166** (1.12 g, 4.18 mmol) in dry toluene (500 mL) was prepared. $\text{TsOH} \cdot \text{H}_2\text{O}$ (40 mg, 0.21 mmol) was added and the solution was heated to reflux for 2 hrs. The now yellow solution was then cooled in an ice bath, basic Al_2O_3 (~13 g) was added and the suspension was stirred for 5 min. The suspension was filtered and the filter cake was rinsed with *n*-hexane. The filtrate was evaporated to give the crude product as a yellow-brownish oil. Column chromatography on silica with *n*-hexane as the eluant afforded the pure acenaphthylene **157** as a yellow oil which solidified upon standing (938 mg, 89%).

$R_f = 0.3$ (silica, *n*-hexane)

M.p.: 43 °C (determined by DSC)

IR (film): 3087 w , 2963 m , 2931 w , 2871 w , 1621 m , 1493 w , 1480 m , 1430 m , 1363 m , 1264 w , 1180 m , 1115 w , 1089 m , 880 m , 826 s , 796 w , 732 s , 697 w , 674 m , 514 w .

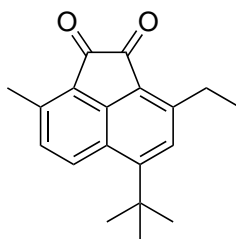
^1H NMR (400 MHz, CDCl_3): 8.19 (d , $^3J = 8.6$, 1H); 7.25; (d , $^3J = 8.6$, 1H); 7.24 (d , $^3J = 8.6$, 1H); 7.10 (d , $^3J = 5.4$, 1H); 7.09 (d , $^3J = 5.4$, 1H); 2.96 (q , $^3J = 7.6$, 2H); 2.64 (s , 1H); 1.63 (s , 9H); 1.37 (t , $^3J = 7.6$, 3H).

$^{13}\text{C}\{^1\text{H}\}$ NMR (100 MHz, CDCl_3): 149.37; 141.44; 138.55; 135.45; 134.06; 129.80; 128.18; 127.31; 126.10; 125.77; 124.89; 124.61; 36.69; 33.44; 27.15; 18.73; 16.83.

MS (EI): 250 (38, M^+), 235 (100, $[M - CH_3]^+$), 221 (22, $[M - C_2H_5]^+$), 207 (32 $[C_{16}H_{15}]^+$), 189 (53), 179 (28 $[C_{14}H_{11}]^+$), 165 (38), 152 (22).

HRMS (EI): $[M^+]$ calculated for $C_{19}H_{22}$: 250.17215; found 250.17178.

5-*t*-butyl-3-ethyl-8-methylacenaphthenequinone (**123**)



$C_{19}H_{20}O_2$
Mol. Wt.: 280.36

Procedure A (from 1-*t*-butyl-3-ethyl-6-methylnaphthalene): CH_2Cl_2 (120 mL) was added to a N_2 -flushed, oven-dried 500 mL 3-necked round-bottom flask, equipped with stir bar and N_2 inlet. After degassing for 15 min. with N_2 , the solvent was cooled to an internal temperature between $-25\text{ }^\circ\text{C}$ and $-30\text{ }^\circ\text{C}$ with an acetone/dry ice bath and $AlBr_3$ (9.9 g, 37.1 mmol) was added quickly. Then, a solution of the naphthalene (3 g, 13.25 mmol) and oxalylchloride (2.86 g, 1.91 mL, 22.53 mmol) in CH_2Cl_2 (50 mL) was added dropwise over 30 min. with an addition funnel. Evolving HBr was vented through 2 washing bottles containing aqueous NaOH. During the addition, the dark reaction mixture was allowed to warm to a temperature between $-10\text{ }^\circ\text{C}$ and $-15\text{ }^\circ\text{C}$ and stirred another 8 hrs. The mixture was hydrolyzed with chilled H_2O (200 mL), transferred to a 6 L separation funnel and washed extensively with H_2O ($5 \times 200\text{ mL}$). The org. layer was dried over $MgSO_4$, filtered and evaporated, to give the crude product as a brownish solid. Column chromatography on silica gel with *n*-hexane/EtOAc (10:1) as the eluant yielded pure product **123** as a bright yellow solid (1.42 g, 38%). The retro Friedel–Crafts (de-*t*-butylated) product was isolated as well (397 mg).

Procedure B (from 5-(*t*-butyl)-3-ethyl-8-methylacenaphthen-1-one): To a 10 mL round-bottom flask, equipped with stir bar and septum with N_2 inlet, was added the acenaphthenone (100 mg, 0.396 mmol) and $CHCl_3$ (2 mL). In a vial, a solution of Br_2 (110 μL , 2.148 mmol) in $CHCl_3$ (5 mL) was prepared, of which 1 mL (0.43 mmol Br_2) is added via syringe to the solution of the acenaphthenone. The mixture was stirred for 3 hrs. at rt. and was

quenched with sat. aq. NaHCO_3 and 10 % aq. $\text{Na}_2\text{S}_2\text{O}_3$. The mixture was extracted with CH_2Cl_2 and evaporated to dryness. The crude residue was dissolved in DMSO (3 mL) and heated to 100 °C for 20 hrs. DMSO was removed at 80 °C under reduced pressure and the crude product was obtained as a brown solid. Column chromatography on silica gel with *n*-hexane/EtOAc (10:1) as the eluant yielded pure product **123** as a bright yellow solid (89 mg, 85 %).

R_f = 0.18 (silica, *n*-hexane/EtOAc (20:1))

M.p.: 158–160 °C

IR (film): 3418 w , 2965 m , 2935 w , 2874 w , 1715 s , 1642 w , 1613 w , 1583 s , 1495 w , 1479 w , 1461 m , 1366 m , 1323 w , 1267 m , 1243 w , 1195 m , 1184 m , 1116 w , 1040 m , 1017 w , 904 m , 889 w , 841 w , 795 w , 745 w , 623 w , 428 w .

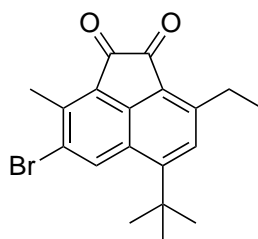
^1H NMR (500 MHz, CDCl_3): 8.52 (d , $^3J = 8.8$, 1H); 7.51 (s , 1H); 7.47 (d , $^3J = 8.8$, 1H); 3.27 (q , $^3J = 7.6$, 2H); 2.86 (s , 3H); 1.65 (s , 9H); 1.34 (t , $^3J = 7.6$, 3H).

$^{13}\text{C}\{^1\text{H}\}$ NMR (125 MHz, CDCl_3): 190.05; 188.55; 153.84; 149.08; 143.99; 136.63; 132.06; 129.31; 126.24; 126.13; 125.83; 122.95; 36.98; 31.13; 25.57; 17.90; 15.37.

MS (EI): 280 (72, M^+), 265 (12, $[\text{M} - \text{CH}_3]^+$), 252 (22, $[\text{M} - 2 \times \text{CH}_3]^+$), 237 (26 $[\text{C}_{16}\text{H}_{13}\text{O}_2]^+$), 224 (76), 209 (28), 193 (25), 178 (62), 165 (100), 152 (66) 139 (21), 128 (14), 115 (18).

HRMS (EI): $[\text{M}^+]$ calculated for $\text{C}_{19}\text{H}_{20}\text{O}_2$: 280.14633; found 280.14604.

6-*t*-butyl-4-bromo-8-ethyl-3-methylacenaphthenequinone (**124**)



$\text{C}_{19}\text{H}_{19}\text{BrO}_2$
Mol. Wt.: 359.26

In a 10 mL round-bottom flask, equipped with stir bar and reflux condenser with N₂ inlet, the diketone **123** (1.1 g, 3.93 mmol) and CHCl₃ (2mL) were added. To the solution was added Br₂ (3.75 g, 1.2 mL, 23.5 mmol) and the mixture was heated to 60 °C for 1 hr. After cooling to rt., the mixture was diluted with H₂O and basified with sat. aq. Na₂CO₃. 10 % aq. Na₂S₂O₃ was added and the mixture was extracted with CH₂Cl₂. The org. layer was washed with brine and 10 % aq. Na₂S₂O₃ again, dried over MgSO₄, filtered and evaporated to give a yellow solid. Column chromatography on silica with *n*-hexane/EtOAc (20:1) as eluant afforded the pure product **124** as a yellow solid (1.38 g, 98 %).

R_f = 0.27 (silica, *n*-hexane/EtOAc (20:1))

M.p.: 243–245 °C

IR (film): 3428*w*, 2973*w*, 2960*w*, 2935*w*, 2875*w*, 1737*m*, 1718*s*, 1577*m*, 1470*m*, 1307*w*, 1269*w*, 1188*w*, 1151*m*, 1138*w*, 1043*w*, 1019*w*, 978*w*, 949*w*, 906*m*, 745*w*, 732*w*, 418*w*.

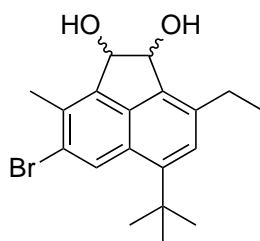
¹H NMR (400 MHz, CDCl₃): 8.85 (*s*, 1H); 7.54 (*s*, 1H); 3.25 (*q*, ³*J* = 7.6); 2.92 (*s*, 2H); 1.64 (*s*, 3H); 1.34 (*t*, ³*J* = 7.6).

¹³C{¹H} NMR (100 MHz, CDCl₃): 189.03; 187.25; 153.12; 147.87; 144.36; 136.84; 135.10; 127.40; 127.27; 126.81; 125.65; 122.80; 36.98; 31.18; 25.63; 17.68; 15.21.

MS (EI): 360 (90, M⁺), 345 (27, [M – CH₃]⁺), 304 (76), 251 (18), 223 (38), 208 (32), 192 (54), 179 (60), 165 (100), 152 (73).

HRMS (EI): [M⁺] calculated for C₁₉H₁₉BrO₂: 358.05684; found 358.05633.

3-methyl-4-bromo-6-(*t*-butyl)-8-ethylacenaphthenediol (**148**)



C₁₉H₂₃BrO₂
Mol. Wt.: 363.29

To a 100 mL round-bottom flask, equipped with stir bar and reflux condenser with N₂ inlet, was added the bromodiketone **124** (554 mg, 1.54 mmol), CH₂Cl₂ (55 mL), and EtOH (12 mL). To the vigorously stirred solution was added NaBH₄ (341 mg, 9 mmol) in portions. Stirring was continued until the evolution of H₂ ceased and the mixture was heated to reflux for 2 hrs. The solvents were removed by rotary evaporation and the residue was taken up in CH₂Cl₂. H₂O and 10 % aq. HCl was added, the org. layer was separated and washed with 10 % aq. HCl and brine. The org. phase was dried over MgSO₄, filtered and evaporated to give the crude product (mixture of *cis*- and *trans*-isomers) as a yellowish resin (536 mg, 96 %). For analytical purposes the isomers were separated by preparative TLC (silica *n*-hexane/EtOAc (3:1)). The major *trans*-isomer was obtained as a colorless solid, the minor *trans*-isomer was obtained as an off-white solid.

***trans*-3-methyl-4-bromo-6-(*t*-butyl)-8-ethylacenaphthenediol:**

R_f = 0.2 (silica, *n*-hexane/EtOAc (2:1))

M.p.: 185–187 °C

IR (film): 3241*m* (broad), 3146*m* (broad), 2966*m*, 2934*m*, 2874*m*, 1711*w*, 1602*w*, 1477*m*, 1462*m*, 1392*m*, 1365*m*, 1345*m*, 1266*m*, 1224*m*, 1142*m*, 1109*s*, 1063*m*, 1047*m*, 1028*m*, 997*s*, 958*m*, 889*s*, 735*m*, 420*s*.

¹H NMR (500 MHz, C₆D₆): 8.72 (*s*, 1H); 7.32 (*s*, 1H); 5.08 (*d*, ³*J* = 6); 4.97 (*d*, ³*J* = 6); 2.82 (*dq*, ²*J* = 13.6, ³*J* = 7.5, 1H); 2.72 (*dq*, ²*J* = 13.6, ³*J* = 7.5, 1H); 2.51 (*s*, 3H); 1.46 (*s*, 9H); 1.25 (*t*, ³*J* = 7.5, 3H).

¹³C{¹H} NMR (125 MHz, CDCl₃): 145.59; 140.81; 138.58; 137.51; 135.96; 131.70; 129.50; 127.20; 126.56; 124.71; 82.94; 81.54; 36.06; 31.45; 25.69; 18.61; 15.74.

MS (EI): 364 (33, M⁺), 343 (39, [M – CH₃]⁺), 331 (15), 251 (24), 221 (45), 207 (100), 191 (46), 179 (40), 165 (60), 34 (152), 73 (72).

HRMS (ESI): [M+Na]⁺ calculated for C₁₉H₂₃BrO₂: 385.07736; found 385.07617.

***cis*-3-methyl-4-bromo-6-(*t*-butyl)-8-ethylacenaphthenediol:**

M.p.: 154.5–156.5 °C

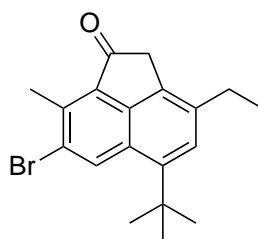
R_f = 0.28 (silica, *n*-hexane/EtOAc (2:1))

IR (film): 3276 m (broad), 2962 m , 2930 m , 2872 m , 1717 w , 1604 w , 1477 m , 1460 m , 1390 m , 1365 m , 1264 m , 1101 s , 1069 m , 1030 w , 997 w , 957 m , 891 w , 859 w , 734 w .

^1H NMR (400 MHz, C_6D_6): 8.67 (s , 1H); 7.30 (s , 1H); 4.94 (t , $^3J = 6.5$); 4.83 (t , $^3J = 6.5$); 2.88 (dq , $^2J = 13.6$, $^3J = 7.5$, 1H); 2.79 (dq , $^2J = 13.6$, $^3J = 7.5$, 1H); 2.59 (s , 3H); 1.45 (s , 9H); 1.28 (t , $^3J = 7.5$, 3H).

$^{13}\text{C}\{^1\text{H}\}$ NMR (125 MHz, CDCl_3): 145.08; 141.26; 138.38; 136.96; 136.24; 131.58; 128.98; 127.15; 126.50; 124.79; 73.36; 71.96; 36.00; 31.38; 25.67; 18.47; 15.73.

5-t-butyl-7-bromo-3-ethyl-8-methylacenaphthen-1-one (149)



$\text{C}_{19}\text{H}_{21}\text{BrO}$
Mol. Wt.: 345.27

To a 500 mL round-bottom flask, equipped with stir bar and reflux condenser with N_2 inlet, a solution of the bromidiol **167** (554 mg, 1.53 mmol) in dry toluene (200 mL) was prepared. $\text{TsOH} \cdot \text{H}_2\text{O}$ (54 mg, 0.28 mmol) was added and the solution was heated to reflux for 3 hrs. The solution was then cooled in an ice bath, basic Al_2O_3 (~ 4 g) was added and the suspension was stirred for 5 min. The suspension was filtered and the filter cake was rinsed with toluene. The filtrate was evaporated and the yellowish residue was recrystallized from *n*-hexane to give **149** as tan needles. (433 mg, 84 %).

$R_f = 0.31$ (silica, *n*-hexane/EtOAc (20:1))

M.p.: 189–191 $^\circ\text{C}$

IR (film): 2989 w , 2962 m , 2931 m , 2872 w , 1714 s , 1620 w , 1584 w , 1478 m , 1460 m , 1405 m , 1392 m , 1374 m , 1363 m , 1265 m , 1173 m , 1051 m , 1018 w , 1007 m , 9957 m , 926 w , 892 m , 740 m , 613 m .

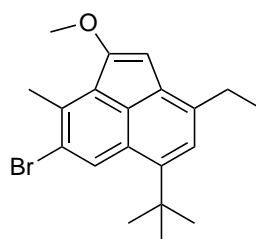
^1H NMR (500 MHz, CDCl_3): 8.73 (*s*, 1H); 7.34 (*s*, 1H); 3.67 (*s*, 2H); 2.87 (*s*, 3H); 2.75 (*q*, $^3J = 7.5$); 1.6 (*s*, 9H); 1.29 (*t*, $^3J = 7.5$).

$^{13}\text{C}\{^1\text{H}\}$ NMR (125 MHz, CDCl_3): 203.50; 144.24; 143.87; 136.46; 136.31; 134.36; 132.91; 128.53; 127.18; 126.06; 125.38; 40.33; 35.97; 31.66; 26.94; 17.04; 14.98.

MS (EI): 344 (40, M^+), 329 (83, $[\text{M} - \text{CH}_3]^+$), 315 (14), 250 (43), 222 (38), 207 (65), 193 (88), 178 (69), 165 (100), 152 (51), 139 (18), 73 (19).

HRMS (EI): $[\text{M}^+]$ calculated for $\text{C}_{19}\text{H}_{21}\text{BrO}$: 344.07758; found 344.07715.

5-t-butyl-7-bromo-3-ethyl-1-methoxy-8-methylacenaphthylene (**156**)



$\text{C}_{20}\text{H}_{23}\text{BrO}$
Mol. Wt.: 359.30

To a 50 mL round-bottom flask, equipped with stir bar and reflux condenser with N_2 inlet, was added bromoacenaphthenone **149** (256 mg, 0.74 mmol) and suspended in MeOH (24 mL). Trimethoxymethane (786 mg, 810 μL , 7.4 mmol) and $\text{TsOH} \cdot \text{H}_2\text{O}$ (11 mg, 0.058 mmol) were added and the mixture was heated to reflux, at which point a clear solution formed. Stirring and heating was continued for 24 hours and the mixture was allowed to cool to rt. where an orange precipitate formed. The suspension was further cooled in an ice bath and subsequently filtered to give **156** as a yellow-orange solid (150 mg, 56 %). The filtrate was treated with 2M aq. NaOH and extracted with Et_2O . The org. layers were dried over Na_2SO_4 , filtered and evaporated to give another portion that was purified by column chromatography on Al_2O_3 using *n*-hexane as the eluant.

$R_f = 0.17$ (Al_2O_3 , *n*-hexane)

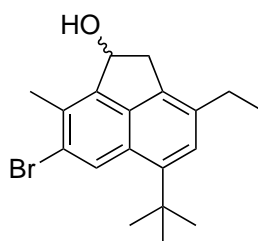
IR (film): 2962*m*, 2930*w*, 2871*w*, 2825*w*, 1732*w*, 1714*w*, 1622*w*, 1596*w*, 1547*s*, 1472*m*, 1461*m*, 1449*m*, 1407*m*, 1378*w*, 1364*w*, 1319*m*, 1307*w*, 1271*m*, 1254*w*, 1209*m*, 1186*m*, 1172*m*, 1089*w*, 993*m*, 957*w*, 884*w*, 761*w*, 748*w*.

^1H NMR (400 MHz, CDCl_3): 8.52 (*s*, 1H); 7.12 (*s*, 1H); 5.95 (*s*, 1H); 3.98 (*s*, 3H); 2.81 (*q*, $^3J = 7.6$); 2.76 (*s*, 3H); 1.58 (*s*, 9H); 1.32 (*t*, $^3J = 7.6$, 3H).

$^{13}\text{C}\{^1\text{H}\}$ NMR (100 MHz, CDCl_3): 162.82; 145.23; 137.44; 134.25; 132.95; 132.39; 131.25; 127.10; 125.88; 125.13; 124.45; 95.87; 57.70; 36.36; 33.23; 26.90; 18.57; 16.27.

MS (EI): 358 (50, M^+), 343 (86, $[\text{M} - \text{CH}_3]^+$), 302 (15), 287 (17), 264 (48), 249 (47), 233 (25), 219 (48), 205 (56), 189 (79), 178 (64), 165 (67), 152 (36).

5-*t*-butyl-7-bromo-3-ethyl-8-methylacenaphthenol (**167**)



$\text{C}_{19}\text{H}_{23}\text{BrO}$
Mol. Wt.: 347.29

To a 50 mL round-bottom flask, equipped with stir bar and reflux condenser with with N_2 inlet, the bromoacenaphthenone **149** (433 g, 1.26 mmol), EtOH (9 mL), and CH_2Cl_2 (15 mL) were added. NaBH_4 (214 mg, 5.66 mmol) was added in portions to the mixture and stirring was continued at ambient temperature until evolution of H_2 ceased. The mixture was heated to reflux for 2 hrs. after which a clear solution formed. The solvents were removed by rotary evaporation and the residue was taken up in CH_2Cl_2 . H_2O and 10 % aq. HCl were added, the org. layer was separated and washed with 10 % aq. HCl and brine. The org. phase was dried over MgSO_4 , filtered and evaporated to give the crude product as a yellowish solid (410 mg). Column chromatography on silica with *n*-hexane/EtOAc (10:1) as the eluant afforded the pure product **167** as a colorless solid (1.38 g, 98 %).

$R_f = 0.13$ (silica, *n*-hexane/EtOAc (10:1))

M.p.: 139–140 °C

IR (film): 3257*w* (broad), 2962*m*, 2931*w*, 2871*w*, 1604*w*, 1477*w*, 1460*m*, 1418*w*, 1405*w*, 1389*m*, 1364*m*, 1252*w*, 1168*w*, 1130*w*, 1057*m*, 1035*m*, 997*w*, 954*m*, 906*m*, 889*m*, 732*s*.

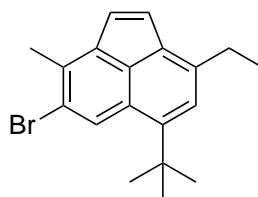
^1H NMR (500 MHz, CDCl_3): 8.46 (*s*, 1H); 7.26 (*s*, 1H); 5.66 (*d*, $^3J = 6.7$, 1H); 3.62 (*dd*, $^2J = 17.6$, $^3J = 7.6$, 1H); 3.11 (*dd*, $^2J = 17.6$, $^3J = 1.5$, 1H); 2.70 (*q*, $^3J = 7.6$, 2H); 2.60 (*s*, 3H); 1.92 (*s*, 1H); 1.56 (*s*, 9H); 1.26 (*t*, $^3J = 7.6$, 3H).

$^{13}\text{C}\{^1\text{H}\}$ NMR (125 MHz, CDCl_3): 144.39; 142.52; 137.70; 135.84; 135.45; 130.79; 129.06; 127.13; 125.86; 124.35; 39.73; 35.75; 31.41; 26.52; 18.49; 14.88.

MS (EI): 346 (29, M^+), 331 (64, $[\text{M} - \text{CH}_3]^+$), 313 (22, $[\text{M} - \text{CH}_3 - \text{H}_2\text{O}]^+$), 281 (18), 267 (10, $[\text{M} - \text{Br}]^+$), 252 (23, $[\text{M} - \text{CH}_3 - \text{Br}]^+$), 234 (17), 207 (48), 189 (41), 179 (38), 165 (49), 152 (38), 73 (100).

HRMS (ESI): $[\text{M} + \text{Na}]^+$ calculated for $\text{C}_{19}\text{H}_{23}\text{BrO}$: 369.08245; found 369.08250.

3-methyl-4-bromo-6-(*t*-butyl)-8-ethylacenaphthylene (**158**)



$\text{C}_{19}\text{H}_{21}\text{Br}$
Mol. Wt.: 329.27

In an oven-dried 100 mL round-bottom flask, equipped with stir bar and reflux condenser with N_2 inlet, a solution of the bromoacenaphthenol **167** (125 mg, 0.36 mmol) in dry toluene (50 mL) was prepared. $\text{TsOH} \cdot \text{H}_2\text{O}$ (22 mg, 0.116 mmol) was added and the solution was heated to reflux for 2 hrs. The now yellow solution was then cooled in an ice bath, basic Al_2O_3 (~2 g) was added and the suspension was stirred for 5 min. The suspension was filtered and the filter cake was rinsed with *n*-hexane. The filtrate was evaporated to give the crude product as a yellow-brownish oil. Column chromatography on silica with *n*-hexane as the eluent afforded pure **158** as a yellow solid (77 mg, 70%).

$R_f = 0.3$ (silica, *n*-hexane/EtOAc (10:1))

M.p.: 101 °C (determined by DSC)

IR (film): 2967*w*, 2927*w*, 2870*w*, 1617*w*, 1480*w*, 1466*m*, 1453*m*, 1404*w*, 1364*m*, 1263*m*, 1181*m*, 1090*m*, 955*m*, 882*m*, 814*m*, 839*s*, 729*s*, 706*m*, 677*m*.

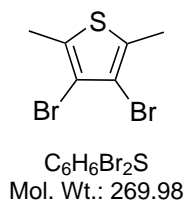
^1H NMR (500 MHz, CDCl_3): 8.51 (*s*, 1H); 7.22 (*s*, 1H); 7.09 (*d*, $^3J = 5.5$, 1H); 7.04 (*d*, $^3J = 5.5$, 1H); 2.93 (*q*, $^3J = 7.6$, 2H); 2.67 (*s*, 3H); 1.61 (*s*, 9H); 1.35 (*s*, 3H).

$^{13}\text{C}\{^1\text{H}\}$ NMR (125 MHz, CDCl_3): 148.71; 141.87; 139.83; 135.15; 133.66; 130.09; 128.58; 126.77; 126.35; 125.52; 125.20; 123.63; 36.43; 33.16; 26.92; 19.56; 16.49.

MS (EI): 328 (42, $[\text{M}]^+$), 313 (72, $[\text{M} - \text{CH}_3]^+$), 299 (12), 234 (78), 219 (36), 203(68), 189 (100), 178 (23), 165 (23), 152 (14).

HRMS (EI): $[\text{M}]^+$ calculated for $\text{C}_{19}\text{H}_{21}\text{Br}$: 328.08266; found 328.08279.

3,4-dibromo-2,5-dimethylthiophene



To a 500 mL round-bottom flask, equipped with stir bar and N_2 inlet, 2,5-dimethylthiophene (3 g, 26.74 mmol) was added and dissolved in CHCl_3 (150 mL). To the solution was added NBS (12 g, 67.42 mmol) in two portions and the suspension was stirred for 2.5 hrs. The now orange solution was diluted with Et_2O (300 mL) and the mixture was washed with H_2O (3×400 mL) and 10 % aq. $\text{Na}_2\text{S}_2\text{O}_3$. The org. layer was dried over MgSO_4 , filtered and evaporated to give the crude product as a brown oil. Column chromatography on silica using *n*-hexane as the eluant gave the pure product as a colorless solid (4.04 g, 56 %) along with mix fractions containing thiophenes over-brominated at the benzylic position. The compound should be stored in a cold, dark place.

$R_f = 0.5$ (silica, *n*-hexane)

M.p.: 39–40°C °C

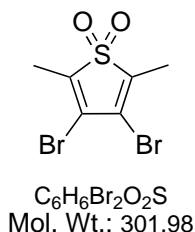
IR (film): 2918*w*, 2851*w*, 1536*w*, 1437*w*, 1377*w*, 1292*m*, 1263*w*, 1146*m*, 1028*m*, 996*w*, 828*s*, 740*s*, 705*w*, 504*m*.

^1H NMR (400 MHz, CDCl_3): 2.39 (*s*).

$^{13}\text{C}\{^1\text{H}\}$ NMR (100 MHz, CDCl_3): 131.49; 111.71; 15.77.

MS (EI): 268 (87, $[M]^+$), 189 (100, $[M - Br]^+$), 110 (66, $[M - 2 \times Br]^+$), 93 (43).

3,4-dibromo-2,5-dimethylthiophene-1,1-dioxide (182)



To a 100 mL round-bottom flask, equipped with stir bar, was added 3,4-dibromo-2,5-dimethylthiophene (1 g, 3.7 mmol) and CH_2Cl_2 (25 mL) and the solution was cooled to 0°C in an ice bath. To the cooled solution was added via addition funnel a solution of *m*-CPBA (~70 %, 3.45 g, ~14 mmol) in CH_2Cl_2 (25 mL). The ice bath was removed and stirring was continued for 20 hrs. The mixture was extensively washed with sat. aq. $NaHCO_3$. The org. phase was dried over $MgSO_4$, filtered and evaporated to give the crude material as almost colorless solid. Column chromatography on silica with *n*-hexane/ CH_2Cl_2 (3:2) as eluant gave the pure product **182** as colorless solid (876 mg, 78 %).

$R_f = 0.34$ (silica, *n*-hexane/ CH_2Cl_2 (3:2))

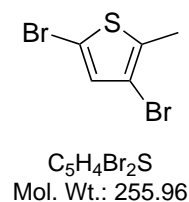
IR (film): 2915 w , 2843 w , 1699 w , 1620 w , 1605 w , 1574 w , 1433 w , 1376 w , 1299 s , 1181 s , 1156 s , 1110 s , 1084 w , 1029 w , 998 m , 788 w , 741 w , 709 w , 558 m , 541 m , 526 m , 458 m .

1H NMR (400 MHz, $CDCl_3$): 2.19 (*s*).

$^{13}C\{^1H\}$ NMR (100 MHz, $CDCl_3$): 137.70; 123.84; 10.41.

MS (EI): 300 (11, $[M]^+$), 252 (46, $[M - SO]^+$), 173 (13, $[M - SO - Br]^+$), 78 (100).

3,5-dibromo-2-methylthiophene (170)



To a 2-necked 100 mL round-bottom flask, equipped with stir bar, addition funnel, and N₂ inlet was added 2-methylthiophene (5 g, 4.85 mL, 50.93 mmol) and acetic acid (20 mL). The solution was cooled in an ice bath and a solution of Br₂ (16.3 g, 5.24 mL, 102 mmol) in acetic acid (10 mL) was added dropwise. The orange solution was stirred over night and allowed to warm to rt. The mixture was then poured onto cooled sat. aq. Na₂CO₃ and extracted with Et₂O. The combined org. layers were washed with 10 % aq. Na₂S₂O₃ and H₂O and dried over MgSO₄. Filtering and evaporation of the solvent gave the crude product as a brownish liquid. Bulb-to-bulb distillation (10 mbar, 130–140 °C) gave the pure product **170** as yellowish liquid (11.65 g, 90 %).

$R_f = 0.51$ (silica, *n*-hexane)

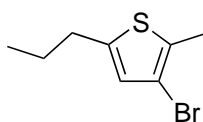
IR (film): 3096 w , 2918 w , 1533 m , 1448 m , 1304 m , 1143 w , 1022 m , 951 m , 815 s , 783 s , 691 m , 625 m , 600 m , 472 s .

¹H NMR (500 MHz, CDCl₃): 6.86 (*s*, 1H); 2.33 (*s*, 3H).

¹³C{¹H} NMR (125 MHz, CDCl₃): 136.01; 131.91; 108.65; 108.45; 14.83.

MS (EI): 254 (45, [M]⁺), 175 (86, [M – Br]⁺), 96 (100, [M – 2 × Br]⁺), 69 (57).

3-bromo-2-methyl-5-propylthiophene (**171**)



C₈H₁₁BrS
Mol. Wt.: 219.14

In a 2-necked 100 mL round-bottom flask, equipped with septum and N₂ inlet a solution of **170** (5 g, 19.53 mmol) in dry THF (25 mL) was cooled to –78 °C in a dry ice/acetone bath. A solution of *n*-BuLi (7.81 mL, 2.5 M in *n*-hexane, 19.53 mmol) was added by syringe and the deep green mixture was stirred for 45 min. at –78 °C, followed by the quick addition of *n*-propyliodide. The mixture was stirred another 10 min. and was then allowed to warm to –15 °C (ice/acetone bath), at which temperature it turned brown. After one hour, cooling was removed and the solution was allowed to warm to rt. The mixture was quenched with H₂O and 25 % aq. NH₃ (quenching of *n*-propyliodide). After

acidifying with 10 % aq. HCl, the mixture was extracted with *n*-hexane (3×60 mL) and the combined org. layers were dried over MgSO_4 , filtered and evaporated to give the crude product as a brown oil. Bulb-to-bulb distillation (10 mbar, 140–150 °C) gave the product **171** as yellowish liquid (3.1 g, 72 %).

$R_f = 0.55$ (silica, *n*-hexane)

IR (film): 2959*m*, 2929*m*, 2871*w*, 1547*m*, 1456*m*, 1437*m*, 1379*m*, 1337*m*, 1323*w*, 1174*w*, 1156*m*, 1135*w*, 1031*w*, 992*m*, 818*s*, 795*s*, 781*m*, 596*m*, 500*m*, 486*m*.

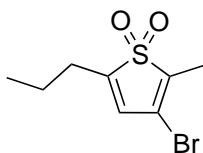
^1H NMR (300 MHz, CDCl_3): 6.57 (*s*, 1H); 2.67 (*t*, $^3J = 7.4$, 2H); 2.33 (*s*, 3H); 1.64 (*sext.*, $^3J = 7.4$, 2H); 0.95 (*t*, $^3J = 7.4$, 3H).

$^{13}\text{C}\{^1\text{H}\}$ NMR (100 MHz, CDCl_3): 142.83; 131.55; 126.81; 108.14; 32.28; 24.74; 14.78; 13.76.

MS (EI): 218 (21, $[\text{M}]^+$), 189 (100, $[\text{M} - \text{C}_2\text{H}_5]^+$) 110 (26, $[\text{M} - \text{C}_2\text{H}_5 - \text{Br}]^+$)

HRMS (ESI): $[\text{M}]^+$ calculated for $\text{C}_8\text{H}_{11}\text{BrS}$: 217.97648; found 217.97650.

1,1-dioxo-3-bromo-2-methyl-5-propylthiophene (**173**)



$\text{C}_8\text{H}_{11}\text{BrO}_2\text{S}$
Mol. Wt.: 251.14

To a 2-necked 100 mL round-bottom flask, equipped with stir bar, addition funnel and thermometer, was added H_2O_2 (35 % in H_2O , 3.3 mL, ~110 mmol) and cooled in a ice/acetone/ NH_4Cl bath. Via dropping funnel TFAA (43.13 g, 28.54 mL, 205.35 mmol) was added while the speed of the addition was chosen so that the temperature did not exceed 0 °C (very exothermic). After complete addition the mixture was stirred another 10 min. at 0 °C, followed by the addition of a solution of the **171** (3 g, 13.69 mmol) in MeCN (30 mL). The addition speed was chosen so that the temperature of the mixture did not exceed 30 °C. After complete addition, the mixture was stirred another 3 hrs. at rt. and was then added portion wise to sat. aq. NaHCO_3 . The neutral mixture was extracted

with CH₂Cl₂ (3 × 100 mL), the combined org. layers were dried over MgSO₄, filtered and evaporated to give the crude product as a brown, wax. Column chromatography on silica with *n*-hexane/CH₂Cl₂ (10:1 to 2:1) gave the pure product **173** as a colorless solid (1.44 g, 42 %).

R_f = (silica, *n*-hexane)

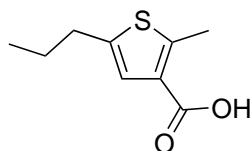
M.p.: 72–73 °C

¹H NMR (400 MHz, CDCl₃): 6.30 (*tm*, ⁴*J* = 1.9, 1H); 2.50 (*tm*, ³*J* = 7.4, 2H); 2.08 (*s*, 3H); 1.71 (*sext.*, ³*J* = 7.4, 2H); 1.02 (*t*, ³*J* = 7.4).

¹³C{¹H} NMR (100 MHz, CDCl₃): 145.30; 136.35; 126.11; 120.16; 26.26; 20.22; 13.78; 9.44.

MS (EI): 250 (31, [M]⁺), 202 (22), 173 (100), 105 (29), 91 (66), 77 (27).

2-methyl-5-propylthiophene-3-carboxylic acid (**172**)



C₉H₁₂O₂S
Mol. Wt.: 184.26

In a 2-necked 100 mL round-bottom flask, equipped with septum and N₂ inlet a solution of **171** (5 g, 22.82 mmol) in dry THF (50 mL) was cooled to −78 °C in a dry ice/acetone bath. A solution of *n*-BuLi (10.1 mL, 2.5 M in *n*-hexane, 25.1 mmol) was added by syringe and the brownish solution was stirred for 30 min. at −78 °C. CO₂ (sublimed from dry ice, dried by passing through a column of CaCl₂ and a column of silica) was then bubbled through the solution via cannula at −78 °C for 10 min. The cooling bath was removed and CO₂ was bubbled another 20 min. The mixture was then treated with H₂O and 10 % aq. HCl and extracted with CH₂Cl₂. The org. phase was extracted with sat. aq. NaHCO₃ and acidified with conc. aq. HCl. The precipitate was filtered and dried to give the acid **172** as an almost colorless solid (1.57 g, 37 %). The org. phases were dried over

MgSO₄, filtered and evaporated to give a brown residue that was subjected to column chromatography on silica using *n*-hexane/EtOAc (5:1) as eluent. Another portion of **172** was obtained as tan solid (1.84 g, 44 %).

$R_f = 0.3$ (silica, *n*-hexane/EtOAc (5:1))

M.p.: 71–73 °C

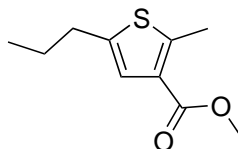
IR (film): 2960*m*, 2929*m*, 2871*w*, 2606*w* (broad), 1672*s*, 1555*m*, 1497*m*, 1443*m*, 1379*w*, 1267*m*, 1232*w*, 1185*w*, 1141*w*, 1024*w*, 933*w*, 842*w*, 782*w*, 724*m*, 517*w*.

¹H NMR (400 MHz, CDCl₃): 7.10 (*s*, 1H); 2.70 (*s*, 3H); 2.69 (*t*, ³*J* = 7.4, 2H); 1.67 (*sext.*, ³*J* = 7.4, 2H); 0.97 (*t*, ³*J* = 7.4, 3H).

¹³C{¹H} NMR (100 MHz, CDCl₃): 169.12; 149.57; 141.00; 126.90; 126.02; 31.72; 24.51; 15.65; 13.56.

HRMS (EI): [M]⁺ calculated for C₉H₁₂SO₂: 184.05580; found 184.05562.

methyl 2-methyl-5-propylthiophene-3-carboxylate (**168**)



C₁₀H₁₄O₂S
Mol. Wt.: 198.28

To a 2-necked 250 mL round-bottom flask, equipped with stir bar, reflux condenser with N₂ inlet, and septum was added **172** (4.55g, 24.67 mmol) and dissolved in MeOH (70 mL). At ambient temperature SOCl₂ (5.89 g, 3.6 mL, 49.51 mmol) was added dropwise via syringe. The yellow solution turned darker and was refluxed for 20 hrs. After cooling to rt., the mixture was diluted with H₂O and basified with sat. aq. NaHCO₃. The mixture was extracted with CH₂Cl₂ (3 × 80 mL) and the combined org. phases were dried over MgSO₄. Filtration and evaporation of the solvent gave the crude ester as a brown oil. Bulb-to-bulb distillation (6 mbar, 140–150 °C) gave the pure product **168** as slightly yellowish oil (4.46 g, 91 %).

$R_f = 0.38$ (silica, *n*-hexane/EtOAc (20:1))

IR (film): 2957 w , 2930 w , 2872 w , 1710 s , 1556 w , 1496 m , 1436 m , 1379 m , 1368 m , 1253 s , 1215 s , 1192 m , 1172 m , 1142 m , 1059 m , 962 w , 911 w , 853 w , 843 w , 778 s , 757 m , 733 m .

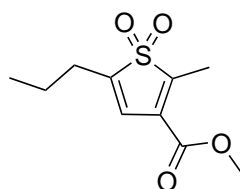
^1H NMR (400 MHz, CDCl_3): 7.04 (s , 1H); 3.82 (s , 3H); 2.67 (s , 3H); 2.67 (t , $^3J = 7.4$, 2H); 1.66 ($sext.$, $^3J = 7.4$, 2H); 0.96 (t , $^3J = 7.4$, 3H).

$^{13}\text{C}\{^1\text{H}\}$ NMR (100 MHz, CDCl_3): 164.26; 147.37; 140.81; 127.41; 125.64; 51.26; 31.75; 24.56; 15.40; 13.57.

MS (EI): 198 (42, $[\text{M}]^+$), 169 (81), 137 (100), 109 (25).

HRMS (EI): $[\text{M}]^+$ calculated for $\text{C}_{10}\text{H}_{14}\text{SO}_2$: 198.07145; found 198.07131.

methyl 1,1-dioxo-2-methyl-5-propylthiophene-3-carboxylate (**159**)



$\text{C}_{10}\text{H}_{14}\text{O}_4\text{S}$
Mol. Wt.: 230.28

To a 2-necked 25 mL round-bottom flask, equipped with stir bar, addition funnel and thermometer, was added H_2O_2 (35% in H_2O , 2 mL, ~ 27 mmol) and cooled in a ice/acetone/ NH_4Cl bath. Via syringe TFAA (9.06 g, 6 mL, 43.12 mmol) was added drop-wise while the speed of the addition was chosen so that the temperature did not exceed 0 $^\circ\text{C}$ (very exothermic). After complete addition the mixture was stirred another 10 min. at 0 $^\circ\text{C}$, followed by the addition of a solution of the methyl **168** (570 mg, 2.88 mmol) in MeCN (4 mL). The addition speed was chosen so that the temperature of the mixture did not exceed 30 $^\circ\text{C}$. After complete addition, the mixture was stirred another 3 hrs. at rt. and was then added to sat. aq. NaHCO_3 . The neutral mixture was extracted with EtOAc (3×40 mL) and the combined org. layers were dried over MgSO_4 , filtered and evaporated. The residue was taken up in toluene and filtered through a small plug of celite. Column chromatography on silica with n -hexane/ CH_2Cl_2 (4:1) gave the pure product **159** as an almost colorless resin (235 mg, 36%).

$R_f = 0.27$ (silica, n -hexane/EtOAc (8:1))

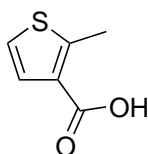
IR (film): 2961 w , 2934 w , 2876 w , 1722 s , 1437 m , 1341 m , 1300 s , 1242 m , 1219 m , 1196 m , 1155 s , 1111 m , 1047 m , 943 w , 888 w , 836 w , 777 m , 723 w , 641 w , 549 m .

^1H NMR (500 MHz, CDCl_3): 6.72 (t , $^4J = 1.9$, 1H); 3.90 (s , 3H); 2.50 (tm , $^3J = 7.4$, 2H); 2.43 (s , 3H); 1.73 ($sext.$, $^3J = 7.4$, 2H); 1.02 (t , $^3J = 7.4$).

$^{13}\text{C}\{^1\text{H}\}$ NMR (125 MHz, CDCl_3): 163.14; 147.15; 143.00; 124.22; 122.06; 52.77; 26.32; 20.06; 13.60; 9.26.

MS (EI): 230 (35, $[\text{M}]^+$), 198 (20), 153 (100), 137 (15), 121 (41), 105 (24), 91 (58), 77 (54).

2-methylthiophene-3-carboxylic acid (176)



$\text{C}_6\text{H}_6\text{O}_2\text{S}$
Mol. Wt.: 142.18

To an oven-dried 2-necked 500 mL round-bottom flask, equipped with stir bar, septum and N_2 inlet was added dry THF (80 mL) and $i\text{-Pr}_2\text{NH}$ (11.07 g, 15.46 mL, 68.66 mmol) and the solution was cooled to 0 °C in an ice bath. A solution of $n\text{-BuLi}$ (44.86 mL, 1.6 M in $n\text{-hexane}$, 71.78 mmol) was added via syringe and stirring was continued for 15 min. The LDA-solution was transferred via cannula to a solution of thiophene-3-carboxylic acid (4 g, 31.21mmol) in THF (80 mL), precooled to -78 °C in a dry ice/acetone bath. Addition took 20 min. and a colorless precipitate formed. Stirring was continued for 30 min., followed by the addition of methyl iodide. The cooling bath was removed and a clear solution formed. At ambient temperature the mixture was quenched with H_2O and 10 % aq. HCl and extracted with Et_2O (3×100 mL). The combined org. layers were washed with brine, dried over MgSO_4 , filtered and evaporated to give the crude product **176** as a tan solid, pure enough for the next step. An analytically pure sample was obtained from $\text{H}_2\text{O}/\text{MeOH}$.

$R_f = 0.3$ (silica, $n\text{-hexane}/\text{EtOAc}$ (10:1))

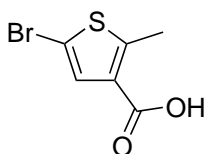
M.p.: 101–102 °C

^1H NMR (400 MHz, CDCl_3): 7.45 (*d*, $^3J =$, 1H); 7.01 (*d*, $^3J =$, 1H); 2.77 (*s*, 3H).

$^{13}\text{C}\{^1\text{H}\}$ NMR (100 MHz, CDCl_3): 168.99; 152.04; 130.17; 127.95; 121.71; 16.14.

MS (EI): .

5-bromo-2-methylthiophene-3-carboxylic acid (**177**)



$\text{C}_6\text{H}_5\text{BrO}_2\text{S}$
Mol. Wt.: 221.07

To a 2-necked 50 mL round-bottom flask, equipped with stir bar, septum and N_2 inlet, was added **176** acid (2 g, 14.07 mmol) and AcOH (30 mL). Via syringe Br_2 (2.48 g, 0.8 mL, 15.52 mmol) was added dropwise at rt. and the solution was stirred another 3 hrs. The mixture was cooled in an ice bath and poured into chilled H_2O . The yellowish precipitate was collected by filtration and washed with 10 % aq. HCl and H_2O . After drying, **177** was obtained as a tan solid (2.87 g, 92 %).

$R_f = 0.3$ (silica, *n*-hexane/EtOAc (10:1))

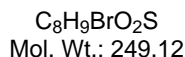
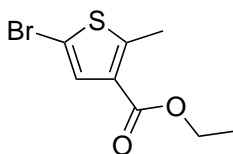
M.p.: 139–141 °C

IR (KBr): 2923*m*, 2872*m*, 2652*m*, 2581*m*, 1971*w*, 1686*s*, 1539*s*, 1462*s*, 1447*s*, 1379*w*, 1345*m*, 1268*s*, 1174*w*, 1066*w*, 1008*w*, 962*w*, 918*m*, 841*w*, 778*m*, 728*m*, 648*w*, 520*w*, 482*w*.

^1H NMR (400 MHz, CDCl_3): 7.39 (*s*, 1H); 2.70 (*s*, 3H).

$^{13}\text{C}\{^1\text{H}\}$ NMR (100 MHz, CDCl_3): 167.92; 153.49; 132.29; 128.42; 108.05; 16.10.

MS (EI): 220 (100, $[\text{M}]^+$), 202 (68), 176 (52), 141 (48), 95 (92), 85 (32), 69 (62), 53.

ethyl 5-bromo-2-methylthiophene-3-carboxylate (178)

To a 2-necked 50 mL round-bottom flask, equipped with stir bar, reflux condenser with N_2 inlet, and septum was added **177** (1 g, 4.52 mmol) and dissolved in EtOH (25 mL). Via syringe SOCl_2 (1.08 g, 660 μL , 9.08 mmol) was added at rt. and the darkened solution was heated to 70°C for 20 hrs. After cooling to rt., the mixture was diluted with H_2O and basified with sat. aq. NaHCO_3 . The mixture was extracted with CH_2Cl_2 (3×50 mL) and the combined org. phases were dried over MgSO_4 . Filtration and evaporation of the solvent gave the crude ester as a brownish oil. Column chromatography on silica with *n*-hexane/EtOAc (100:1) as eluant gave the pure product **178** as slightly yellowish oil (999 mg, 89%).

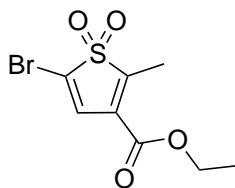
R_f = (silica, *n*-hexane/EtOAc (10:1))

M.p.: $95\text{--}98^\circ\text{C}$

^1H NMR (400 MHz, CDCl_3): 7.33 (*s*, 1H); 4.29 (*q*, $^3J =$, 2H); 2.67 (*s*, 3H); 1.35 (*t*, $^3J =$, 3H).

$^{13}\text{C}\{^1\text{H}\}$ NMR (100 MHz, CDCl_3): 162.48; 150.55; 131.51; 128.93; 107.12; 60.50; 15.34; 14.32.

MS (EI): 248 (76, $[\text{M}]^+$), 219 (100, $[\text{M} - \text{C}_2\text{H}_5]^+$), 203 (60), 174 (15), 141 (12), 96 (52).

ethyl 5-bromo-2-methyl-1,1-dioxothiophene-3-carboxylate (174)

$\text{C}_8\text{H}_9\text{BrO}_4\text{S}$
Mol. Wt.: 281.12

In a 50 mL round-bottom flask, equipped with stir bar and addition funnel was added **178** (771 mg, 3.1 mmol) and TFA (3 mL) and the solution was cooled in an ice bath. A solution of peroxytrifluoroacetic acid (~ 4 M) was prepared by adding TFA (20 mL) to cooled H_2O_2 (10 mL, 35 % in H_2O). Via addition funnel, the peroxytrifluoroacetic acid solution was added dropwise to the thiophene during 10 min. and the reaction mixture was stirred another 10 min. at 0 °C. The ice bath was removed and stirring continued for 40 hrs. The solution was then poured into sat. aq. NaHCO_3 and extracted with CH_2Cl_2 . The combined org. layers were dried over MgSO_4 , filtered and evaporated to give an almost colorless solid. Column chromatography on silica with *n*-hexane/ CH_2Cl_2 (4:1) gave the pure product **174** as an almost colorless solid (684 mg, 79 %).

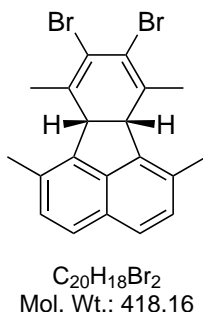
$R_f = 0.3$ (silica, *n*-hexane/EtOAc (10:1))

M.p.: 95–97 °C

^1H NMR (400 MHz, CDCl_3): 7.22 (*s*, 1H); 4.37 (*q*, $^3J =$, 2H); 2.48 (*s*, 3H); 1.38 (*t*, $^3J =$, 3H).

$^{13}\text{C}\{^1\text{H}\}$ NMR (100 MHz, CDCl_3): 161.57; 147.98; 127.64; 125.60; 118.48; 62.52; 14.13; 10.20.

MS (EI): 280 (33, $[\text{M}]^+$), 252 (24), 234 (34), 203 (44); 173 (22), 155 (16), 137 (26), 109 (56), 63 (86); 43 (100).

8,9-dibromo-6b,10a-dihydro-1,6,7,10-tetramethylfluoranthene

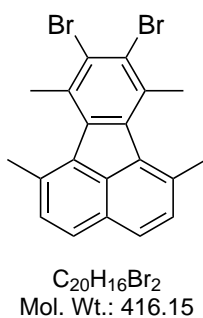
To a 10 mL round-bottom flask, equipped with stir bar and reflux condenser with N₂ inlet, 3,8-dimethylacenaphthylene (120 mg, 0.67 mmol) and 3,4-dibromo-2,5-dimethylthiophene-1,1-dioxide (201 mg, 0.67 mmol) were added and dissolved in dry toluene (2 mL). The mixture was degassed three times by pulling vacuum and heated to reflux for 48 hrs. After cooling to rt., the mixture was diluted with CH₂Cl₂ and washed with H₂O. The org. phase was dried over MgSO₄, filtered and evaporated to give a reddish-brown solid.

$R_f = 0.2$ (silica, *n*-hexane)

¹H NMR (500 MHz, CDCl₃): 7.52 (*d*, ³*J* =, 1H); 7.21 (*d*, ³*J* =, 1H); 4.21 (*s*, 1H); 2.47 (*s*, 3H); 2.05 (*s*, 3H).

¹³C{¹H} NMR (100 MHz, CDCl₃): 139.77; 137.51; 134.98; 130.41; 130.03; 127.83; 123.60; 118.85; 51.03; 24.91; 19.74.

MS (EI): 418 (24, [M]⁺), 403 (20, [M – CH₃]⁺), 339 (22), 324 (18); 258 (100), 243 (52), 228 (34).

8,9-dibromo-1,6,7,10-tetramethylfluoranthene (184)

In a 10 mL round bottom flask equipped with stir bar and N₂ inlet was added the dihydrofluoranthene (256 mg, 0.61mmol) and dissolved in dry toluene (4 mL). DDQ (209 mg, 0.92 mmol) was added and the dark suspension was stirred at rt. for 20 hrs. The reaction mixture was filtered through a plug of silica and rinsed with CH₂Cl₂. The filtrate was evaporated and adsorbed on silica and purified by column chromatography using *n*-hexane as the eluant. The pure product was obtained as a yellowish solid (190 mg, 75 %).

R_f = 0.3 (silica, *n*-hexane/EtOAc (10:1))

M.p.: 202–204 °C

IR (film): 3038 w , 3008 w , 2953 w , 2915 w , 1610 m , 1502 m , 1443 s , 1406 s , 1376 m , 1318 m , 1192 m , 1048 m , 1038 m , 1029 m , 979 s , 936 s , 923 s , 791 m , 766 m .

¹H NMR (500 MHz, CDCl₃): 7.23 (d , ³ J =, 1H); 7.39 (d , ³ J =, 1H); 2.80 (s , 3H); 2.74 (s , 3H).

¹³C{¹H} NMR (125 MHz, CDCl₃): 140.38; 133.95; 133.57; 132.88; 132.00; 131.53; 128.32; 126.98; 126.64; 26.89; 24.73.

MS (EI): 416 (80, [M]⁺), 401 (20, [M – CH₃]⁺), 337 (12), 256 (24); 239 (100), 226 (59), 208 (32).

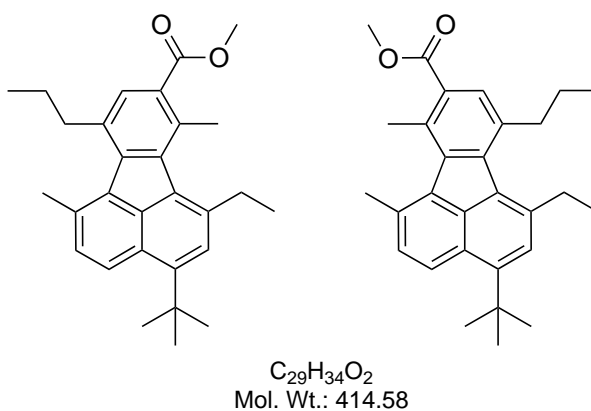
6.2.1 General procedure for the preparation of Fluoranthenes

To an oven dried 50 mL round-bottom flask, equipped with stir bar and reflux condenser with N₂ inlet, was added the acenaphthylene (2 mmol), thiophene-1,1-dioxide (2.6 mmol) and dry toluene (10 mL). The yellow solution was degassed three times by pulling vacuum and heated to reflux for 24 hrs. After cooling to rt., the solvent was removed by rotary evaporation and the crude product was obtained as brown resin. Column chromatography on silica using *n*-hexane/EtOAc (50:1) as eluent gave the dihydrofluoranthenes (mixture of regioisomers as yellow resin (typically ~80 %).

In an oven dried 100 mL round-bottom flask, equipped with stir bar and reflux condenser with N₂ inlet, the dihydrofluoranthene (1 mmol) was dissolved in dry benzene (35 mL). DDQ (2 mmol) was added in one step and the dark suspension was heated to reflux for 4 hrs. After cooling to rt., the mixture was filtered through a plug of silica and thoroughly rinsed with CH₂Cl₂. The filtrate was evaporated giving a dark residue which was sonicated with

n-hexane. The resulting suspension was filtered through celite giving a yellow solution. The solution was washed with sat. aq. NaHCO₃ and the org. phase was dried over MgSO₄ and filtered. The solvent was evaporated and the crude product was subjected to column chromatography on silica using *n*-hexane/EtOAc (50:1). The fluoranthenes (mixture of regioisomers) were obtained as yellow resins.

methyl 4-*tert*-butyl-6-ethyl-1,7-dimethyl-10-propylfluoranthene-8-carboxylate (91a) and methyl 3-*tert*-butyl-1-ethyl-6,7-dimethyl-10-propylfluoranthene-8-carboxylate (91b)



The separation of the two isomers (70 %) was achieved by HPLC (Waters Spherisorb® S5, Nitrile, 250×20mm) with *n*-hexane/EtOAc (200:1). The solvent mixture was recycled through rotary evaporation.

$R_f = 0.3$ (silica, *n*-hexane/EtOAc (10:1))

methyl 4-*tert*-butyl-6-ethyl-1,7-dimethyl-10-propylfluoranthene-8-carboxylate (91a):

IR (film): 2956 m , 2932 w , 2871 w , 1715 s , 1600 w , 1583 w , 1453 m , 1433 m , 1363 w , 1278 m , 1257 m , 1207 s , 1173 m , 1055 m , 906 m , 789 m , 731 s .

¹H NMR (500 MHz, CDCl₃): 8.26 (d , ³ $J = 8.6$, 1H); 7.80 (s , 1H); 7.44 (s , 1H); 7.37 (d , ³ $J = 8.6$, 1H); 3.94 (s , 3H); 3.13–3.03 (m , 4H); 2.81 (s , 3H); 2.78 (s , 3H); 1.70 ($sext.$, ³ $J = 7.5$, 2H); 1.66 (s , 9H); 1.35 (t , ³ $J = 7.5$, 3H); (t , ³ $J = 7.5$, 3H).

$^{13}\text{C}\{^1\text{H}\}$ NMR (125 MHz, CDCl_3): 169.00; 147.20; 142.79; 141.92; 138.72; 135.72; 135.12; 134.38; 132.54; 132.28; 131.39; 131.25; 130.60; 129.47; 126.87; 126.49; 125.36; 52.08; 37.95; 36.40; 32.73; 29.40; 24.60; 24.47; 22.36; 15.38; 14.26.

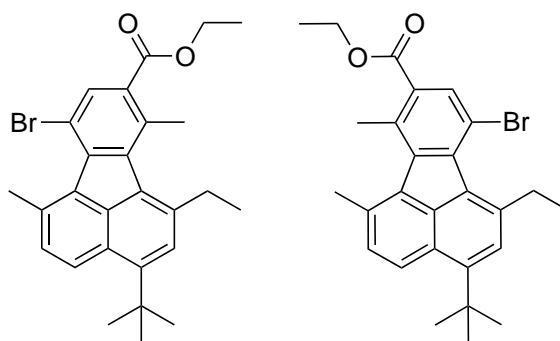
methyl 3-*tert*-butyl-1-ethyl-6,7-dimethyl-10-propylfluoranthene-8-carboxylate (91b):

^1H NMR (400 MHz, CDCl_3): 8.26 (*d*, $^3J = 8.6$, 1H); 7.85 (*s*, 1H); 7.43 (*s*, 1H); 7.39 (*d*, $^3J = 8.6$, 1H); 3.96 (*s*, 3H); 3.11 (*q*, $^3J = 7.5$, 2H); 3.08–3.02 (*m*, 2H); 2.82 (*s*, 3H); 2.73 (*s*, 3H); 1.73 (*sext.*, $^3J = 7.5$, 2H); 1.68 (*s*, 9H); 1.37 (*t*, $^3J = 7.5$, 3H); 0.97 (*t*, $^3J = 7.5$, 3H).

$^{13}\text{C}\{^1\text{H}\}$ NMR (100 MHz, CDCl_3): 168.97; 147.90; 142.33; 142.29; 139.76; 135.86; 135.81; 134.36; 131.82; 131.61; 131.58; 131.36; 130.43; 129.32; 127.15; 126.27; 125.39; 52.02; 37.78; 36.41; 32.72; 29.77; 24.65; 24.44; 22.60; 16.09; 14.26.

HRMS (EI): $[\text{M}]^+$ calculated for $\text{C}_{29}\text{H}_{34}\text{NaO}_2$: 437.24510; found 437.24484.

ethyl 10-bromo-4-*tert*-butyl-6-ethyl-1,7-dimethylfluoranthene-8-carboxylate and ethyl 10-bromo-3-*tert*-butyl-1-ethyl-6,7-dimethylfluoranthene-8-carboxylate (179)



$\text{C}_{27}\text{H}_{29}\text{BrO}_2$
Mol. Wt.: 465.42

The separation of the two isomers (91 %) was achieved by HPLC (Waters Spherisorb® S5, Nitrile, 250×20mm) with *n*-hexane/EtOAc (200:1). The solvent mixture was recycled through rotary evaporation.

$R_f = 0.3$ (silica, *n*-hexane/EtOAc (10:1))

ethyl 10-bromo-4-*tert*-butyl-6-ethyl-1,7-dimethylfluoranthene-8-carboxylate:

^1H NMR (400 MHz, CDCl_3): 8.33 (*d*, $^3J =$, 1H); 8.12 (*s*, 1H); 7.46 (*s*, 1H); 7.39 (*d*, $^3J =$, 1H); 4.42 (*q*, $^3J =$, 2H); 3.08 (*q*, $^3J =$, 2H); 3.03 (*s*, 3H); 2.82 (*s*, 3H); 1.67 (*s*, 9H); 1.45 (*t*, $^3J =$, 3H); 1.35 (*t*, $^3J =$, 3H).

$^{13}\text{C}\{^1\text{H}\}$ NMR (100 MHz, CDCl_3): 167.12; 148.21; 144.15; 143.21; 139.80; 135.69; 134.64; 134.22; 133.26; 132.85; 131.40; 131.16; 131.08; 127.79; 126.64; 125.34; 112.63; 61.27; 36.47; 32.76; 29.60; 27.07; 22.41; 15.38; 14.63.

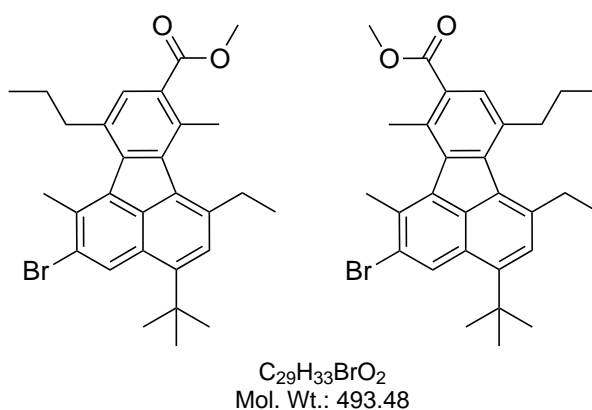
ethyl 10-bromo-3-*tert*-butyl-1-ethyl-6,7-dimethylfluoranthene-8-carboxylate:

^1H NMR (400 MHz, CDCl_3): 8.30 (*d*, $^3J =$, 1H); 8.16 (*s*, 1H); 7.45 (*s*, 1H); 7.40 (*d*, $^3J =$, 1H); 4.42 (*q*, $^3J =$, 2H); 3.49 (*q*, $^3J =$, 2H); 2.81 (*s*, 3H); 2.72 (*s*, 3H); 1.67 (*s*, 9H); 1.46 (*t*, $^3J =$, 3H); 1.37 (*t*, $^3J =$, 3H).

$^{13}\text{C}\{^1\text{H}\}$ NMR (100 MHz, CDCl_3): 167.06; 149.01; 144.58; 142.86; 142.03; 135.73; 135.06; 134.64; 132.79; 132.54; 130.68; 130.47; 129.97; 128.05; 126.96; 125.36; 113.05; 61.25; 36.50; 32.70; 31.41; 24.53; 22.67; 16.57; 14.62.

HRMS (EI): $[\text{M}]^+$ calculated for $\text{C}_{29}\text{H}_{34}\text{NaO}_2$: ; found .

methyl 4-*tert*-butyl-2-bromo-6-ethyl-1,7-dimethyl-10-propylfluoranthene-8-carboxylate (92a) and methyl 3-*tert*-butyl-5-bromo-1-ethyl-6,7-dimethyl-10-propylfluoranthene-8-carboxylate (92b)



The separation of the two isomers (64 %) was achieved by HPLC (Waters Spherisorb® S5, Nitrile, 250×20mm) with *n*-hexane/EtOAc (200:1). The solvent mixture was recycled through rotary evaporation.

methyl 4-*tert*-butyl-2-bromo-6-ethyl-1,7-dimethyl-10-propylfluoranthene-8-carboxylate (92a):

$R_f = 0.3$ (silica, *n*-hexane/EtOAc (10:1))

IR (film): 2958 w , 2932 w , 2872 w , 1717 s , 1585 w , 1458 m , 1433 m , 1378 w , 1364 w , 1277 m , 1255 m , 1200 s , 1168 m , 1054 m , 995 w , 957 w , 906 m , 731 s .

^1H NMR (500 MHz, CDCl_3): 8.61 (s , 1H); 7.81 (s , 1H); 7.42 (s , 1H); 3.95 (s , 3H); 3.05 (q , $^3J = 7.5$, 2H); 2.96 (t -like, $^3J = 7.5$, 2H); 2.81 (s , 3H); 2.73 (s , 3H); 1.69 ($sext.$, $^3J = 7.5$, 2H); 1.64 (s , 9H); 1.35 (t , $^3J = 7.5$, 3H); 0.90 (t , $^3J = 7.5$, 3H).

$^{13}\text{C}\{^1\text{H}\}$ NMR (125 MHz, CDCl_3): 168.67; 146.31; 142.11; 141.64; 138.96; 136.95; 134.38; 132.05; 131.40; 131.07; 130.81; 130.07; 130.06; 127.25; 125.86; 125.49; 51.95; 37.32; 36.12; 32.45; 32.43; 29.22; 24.54; 24.35; 21.96; 15.15; 14.16.

methyl 3-*tert*-butyl-5-bromo-1-ethyl-6,7-dimethyl-10-propylfluoranthene-8-carboxylate (92b):

$R_f = 0.3$ (silica, *n*-hexane/EtOAc (10:1))

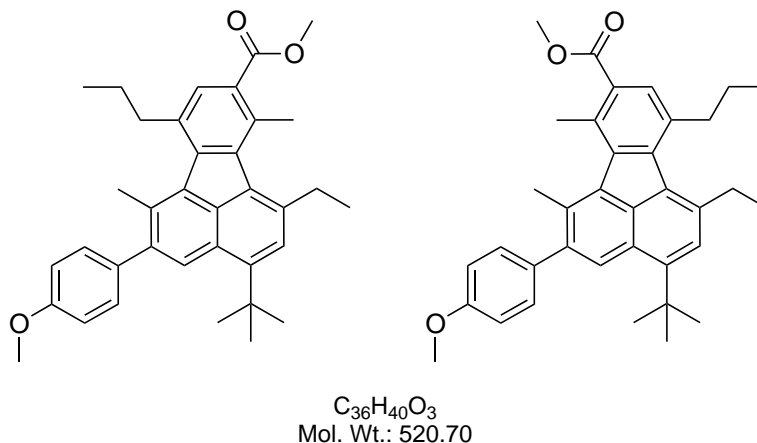
IR (film):

^1H NMR (500 MHz, CDCl_3): 8.60 (s , 1H); 7.85 (s , 1H); 7.40 (s , 1H); 3.95 (s , 3H); 3.13–2.98 (m , 4H); 2.74 (s , 3H); 2.69 (s , 3H); 1.71 ($sext.$, $^3J = 7.5$, 2H); 1.65 (s , 9H); 1.34 (t , $^3J = 7.5$, 3H); 0.96 (t , $^3J = 7.5$, 3H).

$^{13}\text{C}\{^1\text{H}\}$ NMR (125 MHz, CDCl_3): 168.67; 147.17; 142.42; 141.83; 140.21; 137.89; 134.77; 134.59; 132.38; 131.79; 131.58; 131.06; 129.70; 129.54; 128.08; 126.13; 125.86; 52.13; 37.73; 36.34; 32.65; 31.96; 29.80; 25.15; 24.73; 22.59; 16.10; 14.21.

HRMS (EI): $[\text{M}+\text{Na}]^+$ calculated for $\text{C}_{29}\text{H}_{33}\text{BrO}_2$: 515.15616; found 515.15511.

methyl 4-tert-butyl-2-(4-methoxyphenyl)-6-ethyl-1,7-dimethyl-10-propylfluoranthene-8-carboxylate and methyl 3-tert-butyl-5-(4-methoxyphenyl)-1-ethyl-6,7-dimethyl-10-propylfluoranthene-8-carboxylate (186)



The isomeric mixture of bromofluoranthenes **92** (378 mg, 0.766 mmol), 4-methoxyphenylboronic acid (151.5 mg, 0.996 mmol) and K₂CO₃ were dissolved in a thoroughly degassed solvent mixture of toluene (13 mL), EtOH (13 mL) and H₂O (3.3 mL). To the mixture was added Pd(PPh₃)₄ and the solution was heated to reflux for 5 hrs. After cooling to rt, the mixture was washed with 10 % aq. HCl (3×50 mL) and brine (3×50 mL) and the org. phase was dried over MgSO₄. Filtering and evaporating the solvent gave the crude product as a yellow solid, which was purified by column chromatography on silica with *n*-hexane/EtOAc (100:1 to 50:1). The two isomers can be separated by normal gravity column chromatography, mixed fractions are resubmitted.

methyl 4-tert-butyl-2-(4-methoxyphenyl)-6-ethyl-1,7-dimethyl-10-propylfluoranthene-8-carboxylate:

$R_f = 0.3$ (silica, *n*-hexane/EtOAc (10:1))

IR (film): 2955 m , 2932 w , 2871 w , 2835 w , 1714 s , 1608 m , 1513 m , 1462 m , 1433 m , 1390 m , 1364 m , 1281 m , 1264 s , 1245 s , 1200 s , 1174 s , 1160 m , 1055 m , 1036 m , 994 w , 958 w , 894 m , 835 m , 737 s , 705 m , 580 m .

¹H NMR (500 MHz, CDCl₃): 8.25 (*s*, 1H); 7.83 (*s*, 1H); 7.46 (*s*, 1H); 7.43 (*d*, ³*J* = 8.5, 2H); 7.04 (*d*, ³*J* = 2H); 3.96 (*s*, 3H); 3.91 (*s*, 3H); 3.11 (*q*, ³*J* = 7.5, 2H); 3.04 (*t*-like,

$^3J = 7.5$, 2H); 2.85 (*s*, 3H); 2.52 (*s*, 3H); 1.74 (*sext.*, $^3J = 7.5$, 2H); 1.66 (*s*, 9H); 1.37 (*t*, $^3J = 7.5$, 3H); 0.94 (*t*, $^3J = 7.5$, 3H).

$^{13}\text{C}\{^1\text{H}\}$ NMR (125 MHz, CDCl_3): 169.07; 159.06; 147.23; 143.00; 142.24; 142.16; 138.67; 136.76; 135.54; 135.16; 134.43; 132.15; 131.31; 131.25; 131.16; 130.99; 129.80; 128.09; 126.95; 125.12; 113.98; 55.58; 52.06; 37.81; 36.44; 32.73; 29.52; 24.39; 23.27; 22.26; 15.53; 14.44.

HRMS (EI): $[\text{M}]^+$ calculated for $\text{C}_{36}\text{H}_{40}\text{NaO}_3$: 543.28697; found 543.28700.

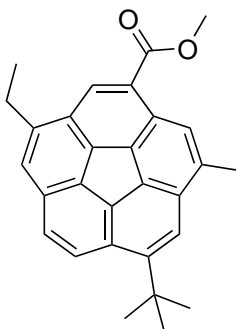
methyl 3-*tert*-butyl-5-(4-methoxyphenyl)-1-ethyl-6,7-dimethyl-10-propylfluoranthene-8-carboxylate:

$R_f = 0.3$ (silica, *n*-hexane/EtOAc (10:1))

IR (film): 2959*m*, 2873*w*, 1718*m*, 1608*w*, 1513*m*, 1461*m*, 1437*m*, 1391*w*, 1378*w*, 1365*w*, 1319*s*, 1219*m*, 1175*m*, 1108*w*, 1088*w*, 1058*w*, 1034*m*, 908*m*, 836*m*, 729*m*.

^1H NMR (500 MHz, CDCl_3): 8.23 (*s*, 1H); 7.85 (*s*, 1H); 7.44 (*d*, $^3J = 8.5$, 2H); 7.04 (*d*, $^3J = 8.5$, 2H); 3.95 (*s*, 3H); 3.90 (*s*, 3H); 3.14 (*q*, $^3J = 7.5$, 2H); 3.05 (*t*-like, $^3J = 7.5$, 2H); 2.80 (*s*, 3H); 2.46 (*s*, 3H), 1.73 (*sext.*, $^3J = 7.5$, 2H), 1.66 (*s*, 9H); 1.35 (*t*, $^3J = 7.5$, 3H); 0.96 (*t*, $^3J = 7.5$, 3H).

$^{13}\text{C}\{^1\text{H}\}$ NMR (125 MHz, CDCl_3): 168.80; 159.07; 147.92; 142.68; 142.40; 142.38; 139.75; 137.50; 135.46; 135.28; 134.44; 131.94; 131.64; 131.44; 131.20; 130.73; 129.30; 127.62; 127.45; 125.20; 113.97; 55.58; 52.04; 37.88; 36.45; 32.70; 29.90; 24.71; 23.72; 22.68; 16.27; 14.22.

methyl 1-tert-butyl-7-ethyl-3-methylcorannulene-5-carboxylate (89)

$C_{29}H_{26}O_2$
Mol. Wt.: 406.52

Bromination: The desired isomer **91a** (74.7 mg, 0.18 mmol), NBS (170 mg, 0.955 mmol) and BPO (1.2 mg) were suspended in CCl_4 (10 mL). The mixture was degassed and heated to reflux while irradiating with an incandescent light bulb (Osram, 100 W). After 6 hrs., the mixture was cooled in an ice bath and the succinimide was filtered with a fritte. The filtrate was evaporated (recycling of CCl_4) and dissolved in CH_2Cl_2 . The CH_2Cl_2 solution was thoroughly washed with H_2O , dried over $MgSO_4$, filtered and evaporated to deliver the crude bromide as a mixture of diastereomers (~145 mg).

Ring closure, procedure A: To an oven-dried 2-necked 50 mL round bottom flask, equipped with stir bar, septum and reflux condenser, was added VCl_3 (382 mg, 2.43 mmol) and $LiAlH_4$ (35 mg, 0.926 mmol) and the solids were covered with DME (8 mL) while cooling in an ice bath. The mixture was then refluxed for 1 hour, prior to the syringe pump-addition (0.01mm/min., 3 days) of the brominated fluoranthene (93.5 mg, 0.116 mmol) in DME (12 mL). After cooling, the suspension was diluted with CH_2Cl_2 , filtered through celite and washed with brine (3×30 mL) and 10 % aq. HCl (3×30 mL). The org. layer was dried over $MgSO_4$, filtered and evaporated to give the crude product (mixture of tetra- and dihydrofluoranthenes) as yellow-brownish residue (~48 mg).

Ring closure, procedure B: To an oven-dried 2-necked 25 mL round bottom flask, equipped with stir bar was added the crude bromofluoranthene (91 mg, 0.112 mmol) in THF (10 mL) and H_2O (6.5 mL) was added. The solution was thoroughly degassed and $CuCl_2$ was added and the solution turned from yellow to greenish immediately. The mixture was stirred at rt for 5 min., prior to the addition of Mn-powder in one step. The reaction mixture was stirred at rt for 18 hrs. and was then quenched with 5 % aq. HCl

and extracted with MtBE (3×60 mL). The org. phase was washed with brine (3×50 mL), dried over MgSO_4 , filtered and evaporated to give the crude product as a brownish resin (~ 45 mg).

Dehydrogenation: The crude product (43 mg) was dissolved in dry benzene (3 mL) and DDQ (48 mg, 0.211 mmol) was added. The dark mixture was refluxed for 3 hrs. and was diluted with *n*-hexane after cooling to rt. The suspension was filtered through a plug of Al_2O_3 , which was thoroughly rinsed with *n*-hexane/EtOAc (20:1). The filtrate was washed with sat. aq. NaHCO_3 , dried over MgSO_4 , filtered and evaporated to give the crude corannulene **89** as a yellow-brownish resin. Preparative TLC with *n*-hexane/EtOAc (50:1) afforded the pure product as a yellowish resin (7 mg, 10–16 %, 3 steps).

$R_f = 0.3$ (silica, *n*-hexane/EtOAc (10:1))

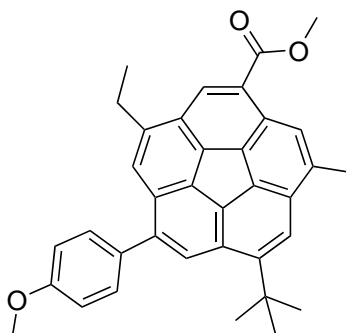
IR (film): 2953 m , 2930 m , 2871 w , 1712 s , 1621 w , 1457 m , 1436 m , 1397 w , 1364 w , 1317 w , 1260 s , 1247 s , 1210 m , 1190 m , 1160 m , 1093 m , 1065 w , 1030 m , 876 m , 811 w , 779 m , 737 m .

^1H NMR (500 MHz, CDCl_3): 8.80 (*s*, 1H); 8.30 (*q*, $^4J =$, 1H); 8.24 (*d*, $^3J =$, 1H); 7.81 (*s*, 1H); 7.72 (*d*, $^3J =$, 1H); 7.56 (*t*, $^4J =$); 4.09 (*s*, 3H); 3.23 (*dq*, $^3J =$, $^4J =$, 2H); 2.84 (*d*, $^4J =$, 3H); 1.71 (*s*, 9H); 1.52 (*t*, $^3J =$).

$^{13}\text{C}\{^1\text{H}\}$ NMR (125 MHz, CDCl_3): 168.07; 150.90; 144.03; 138.33; 138.16; 136.59; 134.20; 134.17; 133.96; 131.44; 130.70; 130.65; 129.15; 128.78; 128.68; 127.96; 127.60; 126.51; 125.97; 124.07; 119.73; 52.45; 37.42; 32.83; 26.35; 19.24; 16.72.

MS (EI): 406 (54, $[\text{M}]^+$), 391 (100, $[\text{M} - \text{CH}_3]^+$), 359 (17), 331 (7), 317 (11), 303 (7).

HRMS (EI): $[\text{M}]^+$ calculated for $\text{C}_{29}\text{H}_{26}\text{O}_2$: 406.19328; found 406.19360.

methyl 1-tert-butyl-7-ethyl-9-(4-methoxyphenyl)-3-methylcorannulene-5-carboxylate (209)

$C_{36}H_{32}O_3$
Mol. Wt.: 512.64

Bromination: The desired isomer of the fluoranthenes **186** (112 mg, 0.215 mmol) was dissolved in CCl_4 (5 mL) and NBS (199 mg, 1.12 mmol) and BPO (2 mg) were added. The mixture was heated to reflux by irradiating with an incandescent light bulb (Osram, 100 W). After 7 hrs. the suspension was cooled in an ice bath and the succinimide was filtered with a fritte. The filtrate was evaporated (recycling of CCl_4) and dissolved in CH_2Cl_2 . The CH_2Cl_2 solution was thoroughly washed with H_2O , dried over $MgSO_4$, filtered and evaporated to deliver the crude bromide as a mixture of diastereomers (185 mg).

Ring closure: To an oven-dried 2-necked 50 mL round bottom flask, equipped with stir bar was added the crude bromofluoranthene (185 mg) in THF (16 mL) and H_2O (10 mL) was added. The solution was thoroughly degassed and $CuCl_2$ was added and the now yellow-greenish mixture was stirred at rt for 3 min., prior to the addition of Mn-powder in one step. The reaction mixture was stirred at rt for 24 hrs. and was then quenched with 10 % aq. HCl and extracted with MtBE (3×60 mL). The org. phase was washed with brine (3×50 mL), dried over $MgSO_4$, filtered and evaporated to give the crude product as an orange-brownish resin (83 mg).

Dehydrogenation: The crude product (42 mg) was dissolved in dry benzene (4 mL) and DDQ (55.6 mg, 0.245 mmol) was added. The dark mixture was refluxed for 5 hrs. and was diluted with *n*-hexane after cooling to rt. The suspension was filtered through a plug of Al_2O_3 , which was thoroughly rinsed with *n*-hexane/EtOAc (20:1). The filtrate was washed with sat. aq. $NaHCO_3$, dried over $MgSO_4$, filtered and evaporated to give the crude corannulene **209** as a yellow-brownish resin (18 mg). Preparative TLC with

n-hexane/EtOAc (50:1) followed by *n*-hexane/EtOAc/toluene (50:1:1) afforded the pure product as a yellowish resin (5.2 mg, 11 %, 3 steps).

$R_f = 0.3$ (silica, *n*-hexane/EtOAc (10:1))

IR (film): 2955 w , 2930 w , 2871 w , 1715 m , 1607 w , 1514 m , 1463 m , 1438 w , 1394 w , 1365 w , 1247 s , 1207 w , 1175 m , 1137 w , 1121 w , 1094 w , 1069 w , 1035 w , 988 w , 882 w , 835 w .

^1H NMR (500 MHz, CDCl_3): 8.79 (s , 1H); 8.30 (q , $^4J = 1.1$, 1H); 8.25 (s , 1H); 7.84 (s , 1H); 7.69 (d , $^3J = 8.7$); 7.55 (t , $^4J = 0.9$); 7.12 (d , $^3J = 8.7$); 4.09 (s , 3H); 3.93 (s , 3 H); 3.15 (dq , $^3J = 7.5$, $^4J = 0.9$, 2H); 2.85 (d , $^4J = 1.1$, 3H); 1.74 (s , 9H); 1.46 (t , $^3J = 7.5$).

$^{13}\text{C}\{^1\text{H}\}$ NMR (125 MHz, CDCl_3): 167.83; 159.44; 150.54; 144.25; 140.07; 138.26; 137.99; 135.70; 134.36; 134.32; 133.54; 132.57; 131.00; 130.35; 130.32; 130.21; 128.60; 128.57; 127.70; 127.63; 127.56; 126.19; 123.98; 119.74; 114.28; 55.44; 22.24; 37.29; 32.61; 26.43; 19.03; 16.90.

HRMS (EI): $[\text{M}]^+$ calculated for $\text{C}_{36}\text{H}_{32}\text{NaO}_3$: 535.22491; found 535.22409.

6.2.2 X-ray Crystallographic Structure Information

Table 6.1: Crystallographic data for acenaphthenequinone **123**.

Crystallized from	<i>n</i> -hexane/CH ₂ Cl ₂
Empirical formula	C ₁₉ H ₂₀ O ₂
Formula weight [g mol ⁻¹]	280.36
Crystal color, habit	yellow, prism
Crystal dimensions [mm ³]	0.25 × 0.30 × 0.35
Temperature [K]	160(1)
Crystal system	monoclinic
Space group	<i>C</i> 2/ <i>c</i> (#15)
<i>Z</i>	8
Reflections for cell determination	4447
2 θ range for cell determination [°]	4–60
Unit cell parameters	
<i>a</i> [Å]	13.8478(2)
<i>b</i> [Å]	14.8558(3)
<i>c</i> [Å]	14.7147(3)
α [°]	90
β [°]	100.473
γ [°]	90
<i>V</i> [Å ³]	2976.68(10)
<i>F</i> (000)	1200
<i>D_x</i> [g cm ⁻³]	1.251
μ (Mo <i>K</i> α) [mm ⁻¹]	0.074
Scan type	ϕ and ω
2 θ_{\max} [°]	60
Total reflections measured	36888
Symmetry-independent reflections	4343
<i>R</i> _{int}	0.063
Reflections with <i>I</i> > 2 σ (<i>I</i>)	3496
Reflections used in refinement	4342
Parameters refined	196
Final <i>R</i> (<i>F</i>) [<i>I</i> > 2 σ (<i>I</i>) reflections]	0.0540
<i>wR</i> (<i>F</i> ²) (all data)	0.1535
Weights:	$w = [\sigma^2(F_0^2) + (0.12P)^2 + 134.3579P]^{-1}$ where $P = (F_0^2 + 2F_c^2)/3$
Goodness of fit	1.091
Secondary extinction coefficient	0.010(2)
Final Δ_{\max}/σ	0.001
$\Delta\rho$ (max; min) [e Å ⁻³]	0.40; -0.38
$\sigma(d_{C-C})$ [Å]	0.002

Table 6.2: Crystallographic data for bromoacenaphthenone **149**.

Crystallized from	<i>n</i> -hexane
Empirical formula	C ₁₉ H ₂₁ BrO
Formula weight [g mol ⁻¹]	345.28
Crystal color, habit	colorless, plate
Crystal dimensions [mm ³]	0.05 × 0.25 × 0.40
Temperature [K]	160(1)
Crystal system	triclinic
Space group	<i>P</i> $\bar{1}$ (#2)
<i>Z</i>	2
Reflections for cell determination	35473
2 θ range for cell determination [°]	4–60
Unit cell parameters	
<i>a</i> [Å]	7.4203
<i>b</i> [Å]	9.6723(1)
<i>c</i> [Å]	11.6966(2)
α [°]	89.188(1)
β [°]	86.5533(9)
γ [°]	70.8867(8)
<i>V</i> [Å ³]	791.76(2)
<i>F</i> (000)	356
<i>D_x</i> [g cm ⁻³]	1.448
μ (Mo <i>K</i> α) [mm ⁻¹]	2.600
Scan type	ϕ and ω
2 θ_{\max} [°]	60
Transmission factors (min; max)	0.627; 0.887
Total reflections measured	22650
Symmetry-independent reflections	4624
<i>R</i> _{int}	0.051
Reflections with <i>I</i> > 2σ(<i>I</i>)	4128
Reflections used in refinement	4624
Parameters refined	195
Final <i>R</i> (<i>F</i>) [<i>I</i> > 2σ(<i>I</i>) reflections]	0.0331
<i>wR</i> (<i>F</i> ²) (all data)	0.0893
Weights:	$w = [\sigma^2(F_0^2) + (0.12P)^2 + 134.3579P]^{-1}$ where $P = (F_0^2 + 2F_c^2)/3$
Goodness of fit	1.037
Final Δ_{\max}/σ	0.002
$\Delta\rho$ (max; min) [e Å ⁻³]	0.72; -0.79
$\sigma(d_{C-C})$ [Å]	0.002–0.003

Table 6.3: Crystallographic data for thiophene-*S,S*-dioxide **159**.

Crystallized from	<i>n</i> -hexane/CH ₂ Cl ₂
Empirical formula	C ₁₀ H ₁₄ O ₄ S
Formula weight [g mol ⁻¹]	230.28
Crystal color, habit	colorless, prism
Crystal dimensions [mm ³]	0.18 × 0.20 × 0.33
Temperature [K]	160(1)
Crystal system	triclinic
Space group	<i>P</i> $\bar{1}$ (#2)
<i>Z</i>	4
Reflections for cell determination	4999
2 θ range for cell determination [°]	4–59
Unit cell parameters	
<i>a</i> [Å]	9.8117(4)
<i>b</i> [Å]	9.9207(5)
<i>c</i> [Å]	14.1862(6)
α [°]	77.719(4)
β [°]	70.829(4)
γ [°]	60.824(5)
<i>V</i> [Å ³]	1136.49(9)
<i>F</i> (000)	488
<i>D_x</i> [g cm ⁻³]	1.346
μ (Mo <i>K</i> α) [mm ⁻¹]	0.277
Scan type	ω
2 θ_{\max} [°]	58.5
Transmission factors (min; max)	0.940; 1.000
Total reflections measured	13248
Symmetry-independent reflections	5359
<i>R</i> _{int}	0.028
Reflections with <i>I</i> > 2 σ (<i>I</i>)	3993
Reflections used in refinement	5359
Parameters refined	277
Final <i>R</i> (<i>F</i>) [<i>I</i> > 2 σ (<i>I</i>) reflections]	0.0451
<i>wR</i> (<i>F</i> ²) (all data)	0.1225
Weights:	$w = [\sigma^2(F_0^2) + (0.12P)^2 + 134.3579P]^{-1}$ where $P = (F_0^2 + 2F_c^2)/3$
Goodness of fit	1.098
Final Δ_{\max}/σ	0.001
$\Delta\rho$ (max; min) [e Å ⁻³]	0.35; -0.44
$\sigma(d_{C-C})$ [Å]	0.003

Table 6.4: Crystallographic data for heptasubstituted fluoranthene **186**.

Crystallized from	<i>n</i> -hexane
Empirical formula	C ₃₆ H ₄₀ O ₃
Formula weight [g mol ⁻¹]	520.71
Crystal color, habit	yellow, prism
Crystal dimensions [mm ³]	0.08 × 0.16 × 0.20
Temperature [K]	160(1)
Crystal system	triclinic
Space group	<i>P</i> $\bar{1}$ (#2)
<i>Z</i>	2
Reflections for cell determination	9060
2 θ range for cell determination [°]	6–149
Unit cell parameters	
<i>a</i> [Å]	9.5808(10)
<i>b</i> [Å]	11.1917(6)
<i>c</i> [Å]	13.8585(9)
α [°]	77.607(5)
β [°]	76.473(7)
γ [°]	87.490(6)
<i>V</i> [Å ³]	1411.07(19)
<i>F</i> (000)	560
<i>D_x</i> [g cm ⁻³]	1.225
μ (Cu <i>K</i> α) [mm ⁻¹]	0.593
Scan type	ω
2 θ_{\max} [°]	148.8
Transmission factors (min; max)	0.083; 1.000
Total reflections measured	22258
Symmetry-independent reflections	5587
<i>R</i> _{int}	0.067
Reflections with <i>I</i> > 2 σ (<i>I</i>)	4516
Reflections used in refinement	5587
Parameters refined	361
Final <i>R</i> (<i>F</i>) [<i>I</i> > 2 σ (<i>I</i>) reflections]	0.0566
<i>wR</i> (<i>F</i> ²) (all data)	0.1675
Weights:	$w = [\sigma^2(F_0^2) + (0.12P)^2 + 134.3579P]^{-1}$ where $P = (F_0^2 + 2F_c^2)/3$
Goodness of fit	1.056
Final Δ_{\max}/σ	0.001
$\Delta\rho$ (max; min) [e Å ⁻³]	0.44; -0.38
$\sigma(d_{C-C})$ [Å]	0.002–0.003

Table 6.5: Crystallographic data for corannulene diester **195**.

Crystallized from	<i>n</i> -hexane/CHCl ₃
Empirical formula	C ₂₆ H ₁₈ O ₄
Formula weight [g mol ⁻¹]	394.42
Crystal color, habit	pale yellow, plate
Crystal dimensions [mm ³]	0.05 × 0.15 × 0.30
Temperature [K]	160(1)
Crystal system	orthorhombic
Space group	<i>Pbca</i> (#61)
<i>Z</i>	8
Reflections for cell determination	3763
2 θ range for cell determination [°]	4–50
Unit cell parameters	
<i>a</i> [Å]	14.0086(3)
<i>b</i> [Å]	7.5540(1)
<i>c</i> [Å]	35.5825(6)
α [°]	90
β [°]	90
γ [°]	90
<i>V</i> [Å ³]	3765.4(2)
<i>F</i> (000)	1648
<i>D_x</i> [g cm ⁻³]	1.391
μ (Mo <i>K</i> α) [mm ⁻¹]	0.0934
Scan type	ϕ and ω
2 θ_{\max} [°]	50
Total reflections measured	34014
Symmetry-independent reflections	3309
<i>R</i> _{int}	0.061
Reflections with <i>I</i> > 2 σ (<i>I</i>)	2495
Reflections used in refinement	3309
Parameters refined	276
Final <i>R</i> (<i>F</i>) [<i>I</i> > 2 σ (<i>I</i>) reflections]	0.0552
<i>wR</i> (<i>F</i> ²) (all data)	0.1537
Weights:	$w = [\sigma^2(F_0^2) + (0.12P)^2 + 134.3579P]^{-1}$ where $P = (F_0^2 + 2F_c^2)/3$
Goodness of fit	1.173
Secondary extinction coefficient	0.026(2)
Final Δ_{\max}/σ	0.001
$\Delta\rho$ (max; min) [e Å ⁻³]	0.67; -0.58
$\sigma(d_{C-C})$ [Å]	0.003

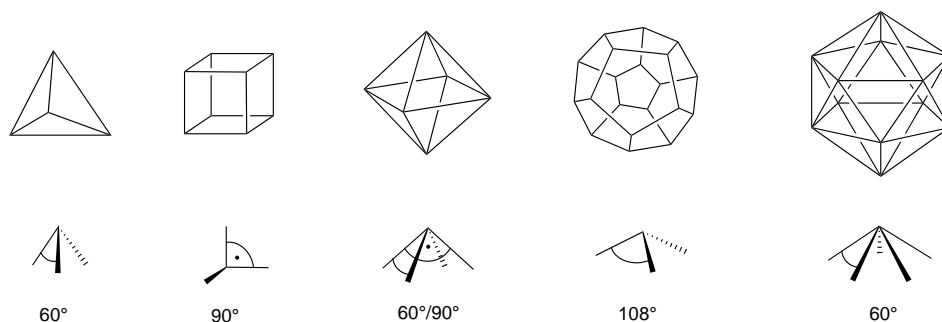
Part II

Synthesis of Platinum and Ethynyl-Platinum Corannulenes

7 Corannulene-based Supramolecular Tectons

7.1 Introduction

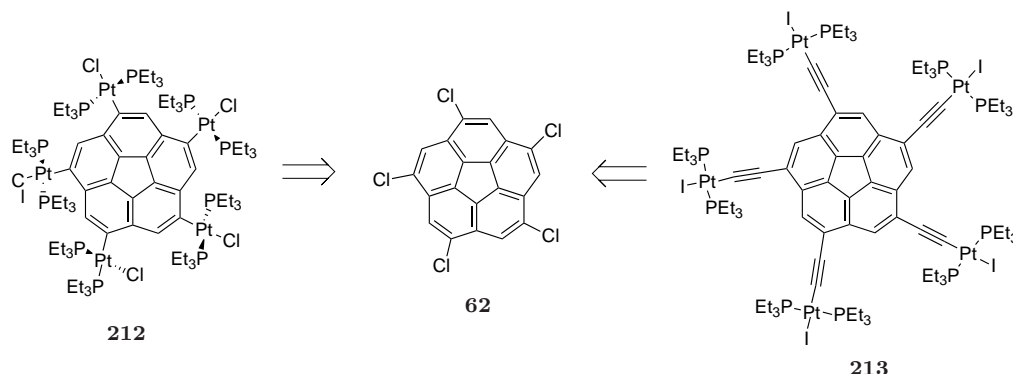
Platonic solids have served as targets for total chemical synthesis in covalent¹⁷⁶ as well as supramolecular variants.^{177,178} Their designs come from replacement of Platonic graph vertices or edges by an appropriate molecular fragment, for example by CH in the case of cubane¹⁷⁹ and dodecahedrane,¹⁸⁰ or a 4-spoke Holliday junction in cubic DNA nanoconstructs.¹⁸¹ Supramolecular targets often include symmetry and geometry-tailored organic tectons and metal–ligand junctions.^{177,178} Among Platonic symmetries, examples of 5-fold symmetric derivatives capable of participating in such assemblies do not yet appear. Such 5-fold symmetric tectons could provide direct access to icosahedrally symmetric supramolecular structures,¹⁸² that have not been accomplished to date.



7.2 Synthesis

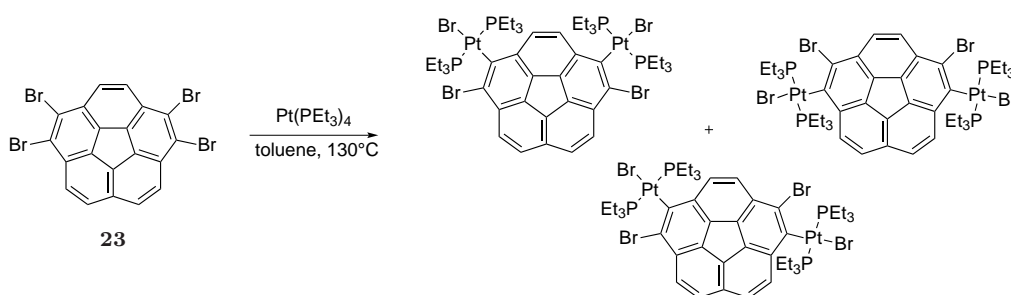
Direct metallation and metalloalkynyl targets **212** and **213**, respectively (Scheme 7.1), based on corannulene, readily spring to mind when 5-fold symmetry is the goal. Given the success with metal mediated 5-fold coupling chemistry⁵⁵ starting from *sym*-pentachloro-

corannulene **62**^{59,81} (see 2.3.1) accessing C_5 -symmetric, directly metallated or ethynyl-platinum derivatives seemed promising.



Scheme 7.1: Retrosynthetic strategy for the formation of pentakis platinum **212** and pentakis ethynyl-platinum **213** corannulene derivatives from *sym*-pentachlorocorannulene (**62**).

Previous work on the tetrabromide **23** reported by Sharp and Lee,¹⁸³ provided additional precedence for dimetallation of corannulene when the halogen is bromine (Scheme 7.2). Even if somewhat hampered by isomeric product formation and limited to disubstitution, this initial platinum insertion work proved the principal.

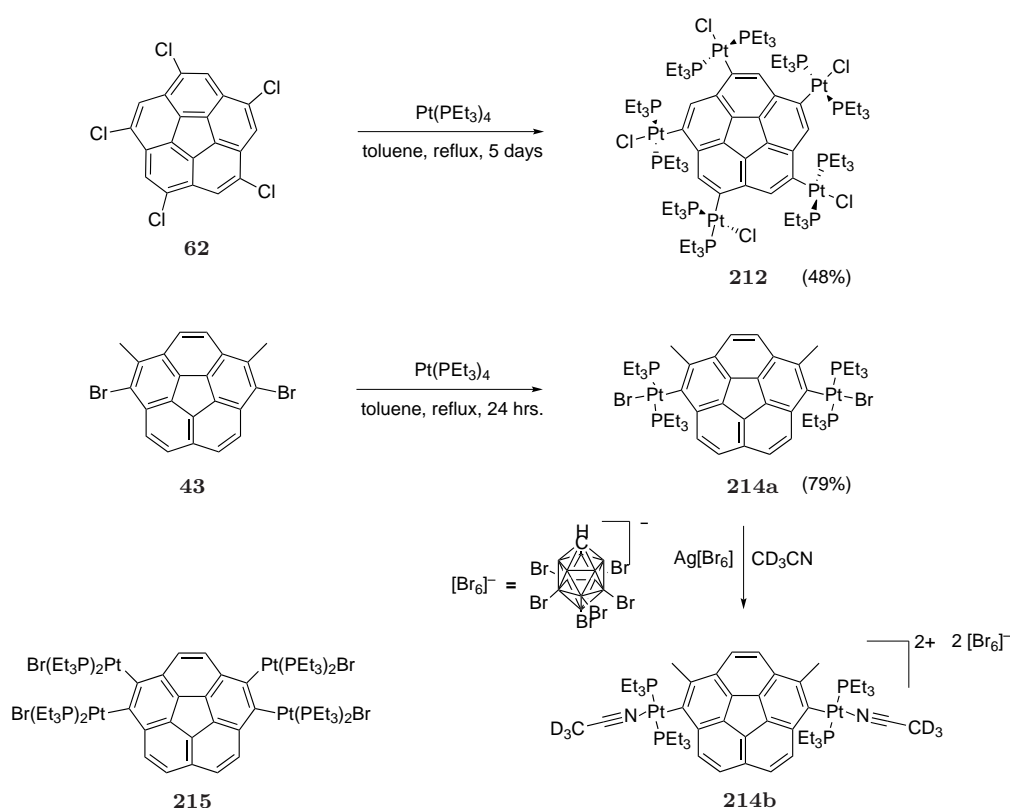


Scheme 7.2: Isomeric mixture of diplatinated tetrabromocorannulenes reported by Sharp and Lee.

7.2.1 Core-platinated Corannulenes

The issue of obtaining an isomeric mixture of diplatinated corannulenes from **23** (Scheme 7.2) could be addressed by employing 1,6-dibromo-2,5-dimethylcorannulene (**43**) which provided a clean dimetallated tecton **214a** with essentially diametrically opposed binding sites on corannulene (Scheme 7.3). Pentakis-Pt(PEt₃)₂Cl corannulene **212** was obtained from a reaction mixture of Pt(PEt₃)₄ and **62** in toluene heated to 95°C over 5 days.

Pt(PEt₃)₄ was prepared from K₂[PtCl₄] with PEt₃ and KOH in EtOH/H₂O (10:1) and was used as the crude after drying. The Pt-insertion product **212** was recrystallized twice from hot MeOH (48 % overall yield). An analogous procedure yielded compound **214a** but the Pt(PEt₃)₄ was recrystallized from *n*-hexane at −30°C and isolated as colorless crystals prior to use. The thus synthesized **214a** was obtained in 79 % yield after trituration with *n*-pentane. For better crystallization and leaving group properties for the future construction of supramolecular assemblies, the bromine atoms in compound **214a** were exchanged with MeCN using a silver(I) salt with the weakly coordinating hexabromocarborane anion.¹⁸⁴ Thus, the corresponding metathesis product **214b** was synthesized.

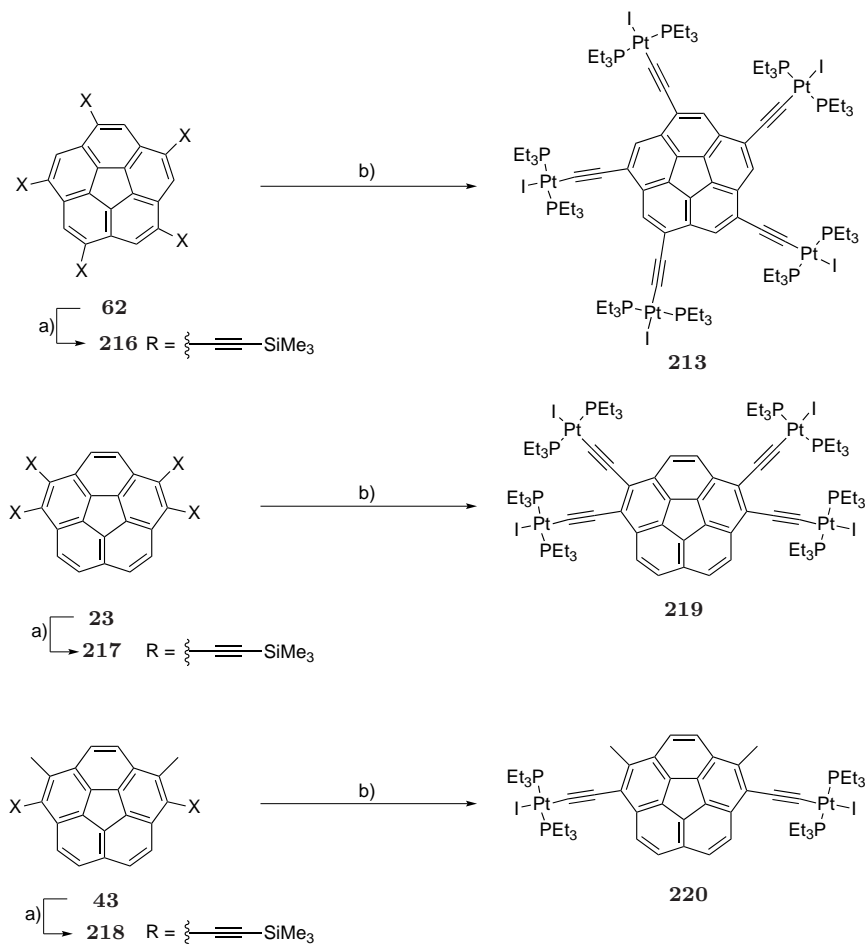


Scheme 7.3: Synthetic procedure for the direct metallation of halocorannulenes **62** and **43**.

7.2.2 Ethynyl-platinum Corannulenes

Hypothetical compound **215** (Scheme 7.3) seems too sterically crowded to form; however, extending the site of metallation with alkyne spacers could alleviate steric problems associated with metallation of vicinal sites. Methods to convert the halide family **62**, **23**, **43** and into their respective TMS-alkyne derivatives **216**, **217** and **218** are established.⁵⁵

Likewise, the conversion of terminal acetylenes to the corresponding ethynyl-platinum complexes is known. However, the base-mediated deprotection of the TMS-alkynes was problematic for **216** and **217**, resulting in low yields. To circumvent an additional de-



Scheme 7.4: Conversion of halocorannulenes **62**, **23**, and **43** to the TMS-acetylenes **216**, **217** and **218** and subsequent *in situ* desilylation/platination leading to ethynyl-platinum corannulenes **213**, **219** and **220**. a) TMS-acetylenes were synthesized according to known procedures.⁵⁵ b) 1. CsF, 2. CuI, 3. Pt(PEt₃)₂ in CH₂Cl₂/DMF/H₂O.

protection step to the free alkynes, a one-pot method for converting TMS-alkynes to Pt-alkyne derivatives was found using CsF, CuI and Pt(PEt₃)₂I₂ in a solvent mixture of DMF/CH₂Cl₂/H₂O (Scheme 7.4). Typically, a solution of the TMS-alkyne was prepared in DMF/CH₂Cl₂ and treated with aqueous CsF to initiate desilylation. Addition of CuI lead to red reaction mixtures, indicative of the formation of Cu(I) acetylides. Quenching with Pt(PEt₃)₂I₂ in CH₂Cl₂ lead to the corresponding yellow ethynyl platinum complexes **213**, **219** and **220**. DMF seems to be an important solvent in this reaction, it is believed to be crucial for the stabilization of the intermediate copper acetylides. Without DMF,

the reaction mixture does not exhibit the red color. Pentakis-ethynyl, tetrakis-ethynyl, and bis-ethynyl platinum derivatives **213**, **219** and **220** were prepared in 35 %, 89 %, and 85 % yield, respectively, from TMS-alkynes **216**, **217** and **218**. The *in situ* platination of the corresponding TMSA-corannulenes proceeds in high yields and is especially attractive for derivatives with adjacent TMSA substituents because the isolation of the free alkynes, which may undergo Bergman cyclizations,¹⁸⁵ can be avoided. Furthermore, subsequent alkyynylation reactions on the platinum center do not occur.

7.3 Characterization

7.3.1 Pentakis-Pt(PEt₃)₂Cl corannulene **212**

X-Ray quality single crystals were obtained for compounds **212**, **214b**, and **220**. The bowl depth from hub centroid to rim plane is 0.764(12) Å in **212**, slightly shallower than the 0.87 Å of the parent corannulene.⁴ The flattening could occur through a relief of steric crowding either around the rim or transannularly. Notable is the stereochemistry at the five platina in **212**, four of which bear phosphines in a *trans* stereochemistry and one *cis*. This novel relationship could support the idea that transannular strain causes the bowl to flatten, but in any case raises the question of whether this stereochemistry persists in solution.

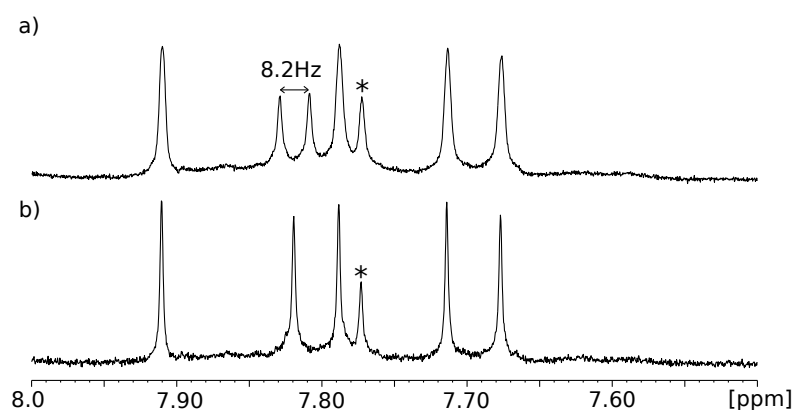


Figure 7.1: ¹H (a) and ¹H{³¹P} NMR (b) of pentakis-Pt(PEt₃)₂Cl corannulene **212**.

High-resolution 700 MHz ¹H spectra of **212** display five distinct rim proton resonances. Four appear as singlets consistent with only *cis* aryl–Pt–Cl relationships; one is a doublet (8.2 Hz), consistent with coupling to a *trans* phosphine.

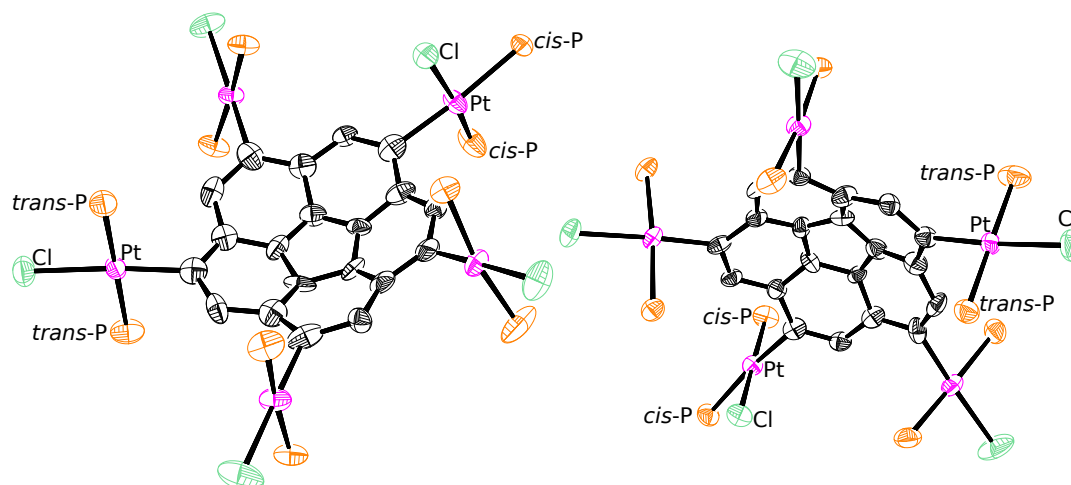


Figure 7.2: Asymmetric unit of the X-ray structure of pentakis-Pt(PEt₃)₂Cl corannulene **212**. Thermal ellipsoids drawn at the 50 % probability level. Hydrogens and ethyl substituents on the phosphines are omitted for clarity.

The ³¹P NMR reveals a cluster of eight PEt₃ groups oriented *trans* about Pt between 13–16 ppm and two PEt₃ groups oriented *cis* about Pt at 11 and 5 ppm. A ³¹P EXSY experiment displays fast exchange among all eight P signals from the *trans* oriented Pt complexes, which accounts for the loss in the ²*J*_{31P–31P} coupling for these signals. In contrast, the EXSY shows no exchange between the ³¹P signals of the *cis*-Pt complex, and ³¹P COSY confirms the 14.7 Hz ²*J*_{31P–31P} coupling. Satellite signals due to the ¹*J*_{31P–195Pt} coupling are also evident in the spectrum. Interestingly, increased CSA-mediated relaxation of ¹⁹⁵Pt leads to considerable broadening of these signals on the 400 MHz spectrometer. The satellites have the appropriate integral according to the 33 % abundance of ¹⁹⁵Pt and the direct ³¹P–¹⁹⁵Pt coupling constant of 2834 Hz corresponds well to P–Pt bond length of 2.296 Å found in the X-ray diffraction analysis as well as a *cis* P–Pt–Cl geometry.¹⁸⁶ Satellite signals are additionally observed for the signals corresponding to the *cis* aryl–Pt–Cl geometry displaying coupling constants of 4200 and 2800 Hz, reflecting one *trans*¹⁸⁷ and one *cis*^{186,188} P–Pt–Cl relation. All together this makes a compelling case for equivalence of the solution and solid structure of **212**. The single *cis* stereochemistry likely results from steric crowding on the *endo* side of the bowl.

7.3.2 Bis-Pt(PEt₃)₂MeCN hexabromocarboranate corannulene **214b**

The structure of **214b** was crystallized as the acetonitrile adduct with two non bound carborane anions. It is not anticipated that this will cause any great structural distortions,

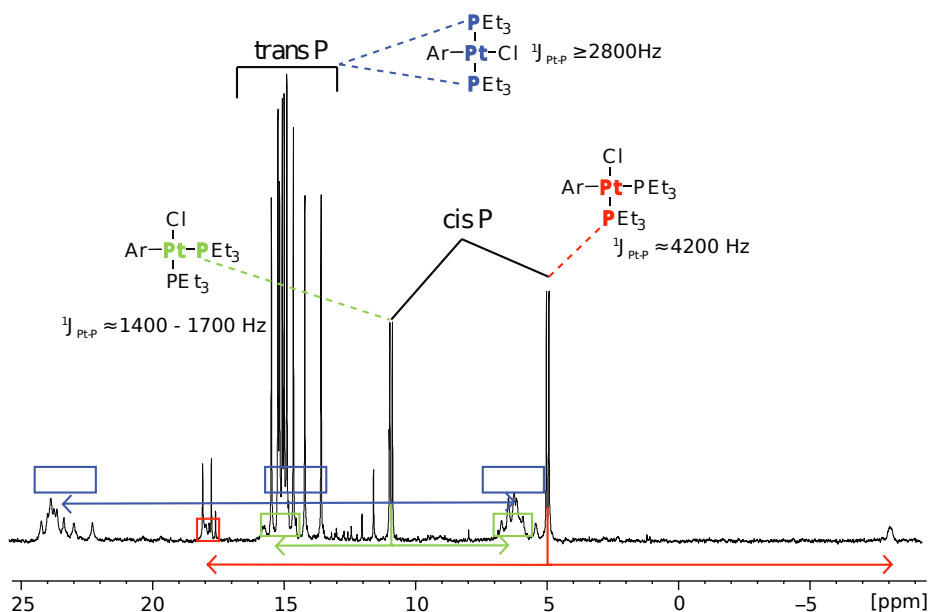


Figure 7.3: ^{31}P NMR of **212** in CD_2Cl_2 showing eight singlets for the *trans*-oriented and two doublets for the *cis*-oriented phosphines, with their respective $^1J_{\text{Pt}-\text{P}}$ -couplings.

but such complexes may have a benefit in complexation chemistry as the nitriles should be very labile ligands.¹⁸⁹

The bowl depth of **214b** is $0.893(13)\text{\AA}$, slightly shallower than its reaction precursor **43** (0.92\AA),⁵⁵ but slightly deeper than the parent corannulene (0.87\AA). The proximity of the ethyl groups on the endo phosphine, reminds one of the attractive van der Waals interactions seen in *sym*-pentamaneisylcorannulene. Variable temperature ^{31}P NMR experiments on **214b** revealed an inversion barrier of 10.7 ± 0.2 kcal/mol, on a par with the ca. 11 kcal/mol expected for corannulene.⁵³

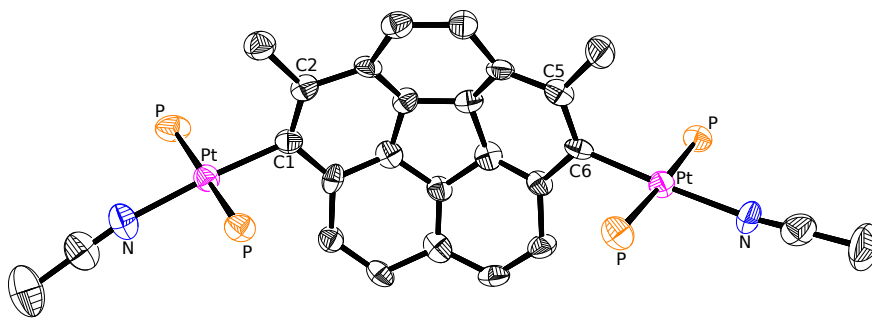


Figure 7.4: X-ray crystal structure of $[\text{bis-Pt}(\text{PEt}_3)_2\text{MeCN corannulene}]^{2+}$ drawn at the 50% probability level. Hydrogens, ethyl substituents on the phosphines and the hexabromocarborane anions are omitted for clarity.

7.3.3 Bisethynyl-platinum corannulene **220**

The structure of **220** revealed a bowl depth of 0.872(9) Å, essentially that of corannulene. Both Pt centers have a *trans* orientation of the PEt₃ ligands and all bond lengths are within normal parameters. The angle between the vectors emanating from roughly diametrically opposing positions on the rim is 140–150° with substantial flexibility due to the low-energy mode of bowl inversion.

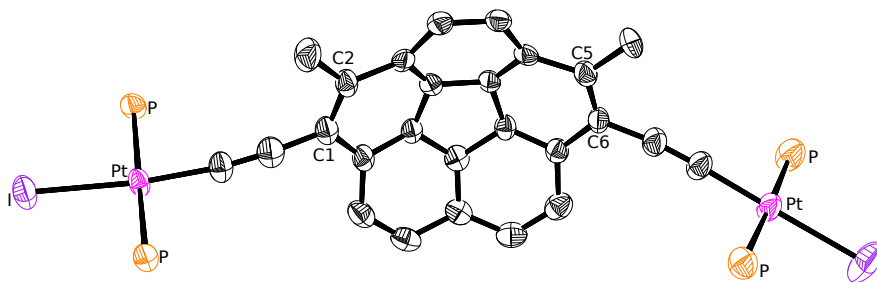


Figure 7.5: X-ray crystal structure of Bisethynyl-platinum corannulene **220** drawn at the 50 % probability level. Hydrogens and the ethyl substituents on the phosphines are omitted for clarity.

7.3.4 Conclusion

In conclusion, the efficient synthesis of core platinated and ethynyl-platinum corannulenes was accomplished. For the synthesis of the ethynyl-platinum corannulenes a one-pot platinadesilylation of TMS-acetylenes was found. The compounds were characterized by NMR-spectroscopy, and if successful by X-ray crystallography. The geometry of tetrakis- and bisethynyl-platinum corannulenes are promising for the incorporation in supramolecular constructs; especially the fivefold symmetry of the *sym*-pentasubstituted platinum corannulenes bode well for the assembly of these supramolecular tectons into higher-order coordination Platonic polyhedra.¹⁹⁰

8 Experimental Section

8.1 General Data

8.1.1 Abbreviations

Ac ₂ O	acetic anhydride
aq.	aqueous
DMF	<i>N,N</i> -dimethylformamide
Et ₂ O	diethyl ether
EtOAc	ethyl acetate
EtOH	ethanol
equiv.	equivalent
hrs.	hours
MeCN	acetonitrile
MeOH	methanol
m.p.	melting point
org.	organic
prep.	preparative
rt	room temperature
THF	tetrahydrofuran

8.1.2 Chromatography and Acquisition of Spectra

Thin-layer chromatography was performed on plastic-backed 0.2 mm UV₂₅₄ silica gel plates from Macherey-Nagel. **Preparative thin-layer chromatography** was performed on glass-supported 1 mm UV₂₅₄ silica gel plates from Merck. Visualization with 254 nm UV light.

Infrared spectra were recorded on a JASCO FT/IR-4100 spectrometer. Absorption

bands are given in wave numbers (cm^{-1}), and the intensities are characterized as follows: *s* = strong (0–33 % transmission), *m* = medium (34–66 % transmission), *w* = weak (67–100 % transmission).

NMR spectra were recorded on Bruker AV-700 (^1H , ^{31}P), DRX-500 (^1H , ^{13}C , ^{31}P), Bruker AV-500 (^1H , ^{13}C , ^{31}P) and Bruker AV-400 NMR Spectrometers. Chemical shifts are given relative to tetramethylsilane ($\delta(\text{Si}(\text{CH}_3)_4) \equiv 0$ ppm for ^1H and ^{13}C and relative to an external sample of 85 % H_3PO_4 unless otherwise indicated. Data are reported as follows: chemical shift in ppm, multiplicity (*s* = singlet, *d* = doublet, *t* = triplet, *q* = quadruplet, *m* = multiplet, *dd* = doublet of doublet, *dt* = doublet of triplet, etc.), coupling constant nJ in Hz, integration, and interpretation. Multiplicities in ^{13}C NMR spectra were determined using DEPT (Distortionless Enhancement by Polarization Transfer) experiments.

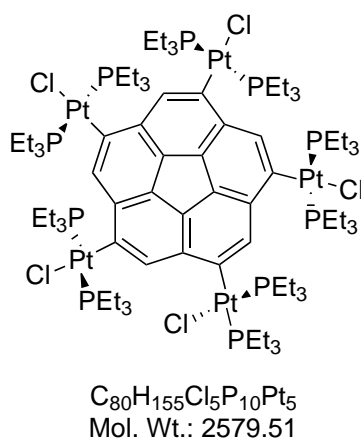
Mass spectra were performed by the MS Laboratory of the Organisch-chemisches Institut of the University of Zurich (ESI, EI and high-resolution mass spectra). Data are reported as follows: *m/z*, % relative intensity and possible fragment.

X-ray structure analyses were carried out by the Laboratorium für Computerchemie und Röntgenstrukturanalyse of the Organisch-chemisches Institut of the University of Zurich. A Nonius KappaCCD diffractometer with $\text{MoK}\alpha$ radiation ($\lambda = 0.71037 \text{ \AA}$) was used.

8.2 Experimental Details

Materials and Methods: compounds **62**, **43**, and **23** were prepared according to literature procedures^{29,55,60} Reactions were conducted under nitrogen atmospheres unless noted. Dry toluene was used from an MBraun solvent purification system. CH₂Cl₂ and *n*-hexane were used after simple distillation. K₂PtCl₄ and PEt₃ (10 % in hexanes, Pressure Chemical Co., Strem Chemicals) were used as purchased, Pt(PEt₃)₄ and Pt(PEt₃)₂I₂ were prepared by known procedures.¹⁹¹

1,3,5,7,9-Pentakis[chlorobis(triethylphosphine)platinum]corannulene (**212**)



In a 100 mL Schlenk flask was placed KOH (1.1 g, 19.3 mmol) under inert atmosphere, followed by degassed EtOH (10 mL) of and degassed H₂O (1mL). The flask was stirred at room temperature until homogeneous. Upon homogeneity, PEt₃ (2.5 g, 21.2 mmol) was added via syringe. In a separate 50 mL Schlenk flask was placed K₂[PtCl₄] (1.6 g, 3.85 mmol) under inert atmosphere, followed by degassed H₂O (5 mL). The aqueous K₂[PtCl₄] was then transferred to the KOH/PEt₃ flask via cannula. The reaction mixture was allowed to stir at room temperature for 1 h and then at 60°C for 3 h. The reaction was then allowed to cool and the solvent was evaporated under high vacuum. The crude Pt(PEt₃)₄ product was taken up in freshly distilled toluene (10 mL) and transferred via cannula through a syringe containing glass wool (to filter particulates) into a Schlenk flask containing **62** (110 mg, 0.25 mmol) under inert atmosphere. The reaction mixture was then closed and allowed to stir at 90–95°C for 5 days. After 5 days the solvent was evaporated under reduced pressure and the product was recrystallized twice from MeOH. Yield: 318 mg (48 %).

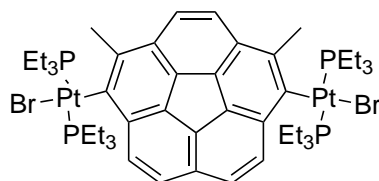
$^1\text{H}\{^{31}\text{P}\}$ NMR (700 MHz, CD_2Cl_2): 7.91 (*s*, 1H); 7.82 (*s*, 1H); 7.79 (*s*, 1H); 7.71 (*s*, 1H); 7.68 (*s*, 1H); 2.1–1.3 (*m*, 60H, CH_2); 1.25–0.85 (*m*, 72H, *trans*- CH_3); 0.71 (*t*, 9H, *cis*- CH_3); 0.45 (*t*, 9H, *cis*- CH_3).

$^{13}\text{C}\{^1\text{H}\}$ NMR (150 MHz, CDCl_3): 138–128 (Ar-C) 16.5–12.7 (CH_2); 7.7–6.6 (CH_3).

$^{31}\text{P}\{^1\text{H}\}$ NMR (175 MHz): 15.51, 15.23, 15.10, 14.98, 14.92, 14.72, 14.15, 13.62 (8 *trans*-P), 10.89 (*d*, $^2J_{\text{P-P}} = 14.7$, *cis*-P), 5.11 (*d*, $^2J_{\text{P-P}} = 14.7$, *cis*-P).

HRMS (ESI-TOF): $[\text{M}^+]$ calculated for $\text{C}_{80}\text{H}_{155}\text{Cl}_5\text{P}_{10}\text{Pt}_5$: 2578.61448; found 2578.61485. $[\text{M}-\text{Cl}]^+$ calculated for $\text{C}_{80}\text{H}_{155}\text{Cl}_4\text{P}_{10}\text{Pt}_5$: 2543.64686; found 2543.64588 (main intensity).

2,5-Dimethyl-1,6-bis[trans-bromobis(triethylphosphine)platinum]corannulene (214a)



Chemical Formula: $\text{C}_{46}\text{H}_{72}\text{Br}_2\text{P}_4\text{Pt}_2$
Molecular Weight: 1298.93

Schlenk conditions: To a degassed solution of 1,6-dibromo-2,5-dimethylcorannulene (**43**, 50 mg, 0.115 mmol) in toluene (20 ml) was added via syringe a solution of $\text{Pt}(\text{PEt}_3)_4$ (176 mg, 0.264 mmol) in toluene (20 ml). The reaction mixture turned red and stirring was continued at room temperature for 24 hrs. The now yellow solution was heated to reflux another 24 hrs. After cooling to room temperature, the solution was filtered through a pad of celite (open to air) and the filtrate was evaporated to give a reddish, oily residue. The residue was covered with *n*-pentane and cooled to -78°C . After supersonication, the supernatant was removed and the procedure is repeated until a yellow powder was obtained (117 mg, 79%).

IR (film): 2964*m*, 2932*m*, 2906*m*, 2876*m*, 2360*w*, 2334*w*, 1610*w*, 1455*m*, 1411*m*, 1375*w*, 1331*w*, 1287*w*, 1256*w*, 1144*w*, 1034*s*, 1009*w*, 986*w*, 926*w*, 828*w*, 793*w*, 764*s*, 729*m*, 688*m*.

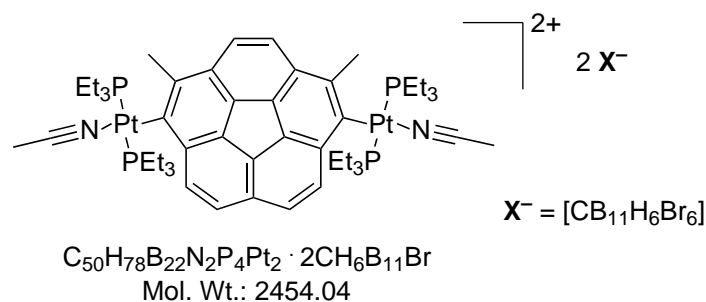
^1H NMR (400 MHz, C_6D_6): 8.45 (*d*, $^3J_{\text{H-H}} = 8.7$ Hz, 2H); 7.90 (*s*, 2H); 7.72 (*d*, $^3J_{\text{H-H}} = 8.7$, 2H); 3.17 (*s*, CH_3 , 3H); 1.70-1.40 (*m*, CH_2 , 24H); 0.72 (*dt*, $^3J_{\text{H-H}} = 7.7$, $^3J_{\text{H-P}} = 15.9$, CH_3 , 36H).

$^{13}\text{C}\{^1\text{H}\}$ NMR (150 MHz, CDCl_3): 139.59 (*t*, $^1J_{\text{C-Pt}} = 490$, $^2J_{\text{C-P}} = 9$), 138.08, 135.37, 133.79, 133.54, 133.08, 131.45, 130.93, 128.63, 124.68, 123.90, 24.25 (Ar-CH_3), 15.31 (virtual *quint*, $^1J_{\text{C-P}} = 16.8$), 8.13 (virtual *t*, $^2J_{\text{C-P}} = 2.7$).

$^{31}\text{P}\{^1\text{H}\}$ NMR (162 MHz, CDCl_3): 10.92 (*s*, $^1J_{\text{Pt-P}} = 2725$).

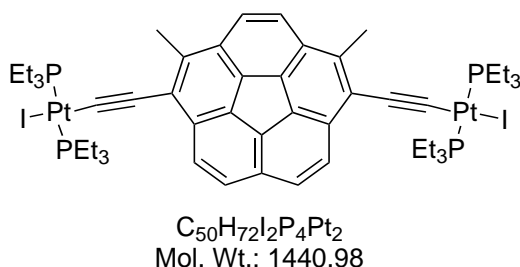
HRMS (ESI-TOF): $[\text{M}^+]$ calculated for $\text{C}_{46}\text{H}_{72}\text{Br}_2\text{P}_4\text{Pt}_2$: 1299.22970; found 1299.22965. $[\text{M-Br}]^+$ calculated for $\text{C}_{46}\text{H}_{72}\text{BrP}_4\text{Pt}_2$: 1219.30250; found 1219.30579 (main intensity).

2,5-Dimethyl-1,6-bis[trans-acetonitrilobis(triethylphosphine)platinum]corannulene hexabromocarboranate (**214b**)



Glovebox: 2,5-dimethyl-1,6-bis[Pt(PEt_3) $_2$ Br]corannulene (**214a**, 7.1 mg, 5.47 mmol) and silver(I) hexabromocarboranate (8 mg, 11 mmol) were placed in a 2 ml-vial and suspended in D_3CCN (1 ml). The yellow suspension became clearer, prior to the precipitation of AgBr. The vial was covered in aluminium foil and the reaction mixture was stirred for 20 hrs. at room temperature. The clear supernatant solution was analyzed by NMR spectroscopy; single crystals were grown by slow diffusion of *n*-hexane into a solution of **214b** in acetone.

1,6-Bis{[trans-iodobis(triethylphosphine)platinum]ethynyl}-2,5-dimethylcorannulene (220)



A solution of 1,6-bis[2-(trimethylsilyl)ethynyl]-2,5-dimethylcorannulene (**218**, 50.7 mg, 0.108 mmol) in DMF (5 ml) and CH_2Cl_2 (7.5 ml) was prepared in a 50 ml Schlenk flask, equipped with stir bar. CsF (35 mg, 0.226 mmol) in H_2O (0.5 ml) was added and the mixture gets slightly darker and turbid. After 5 min. CuI (43 mg 0.226 mmol) was added in one step and the mixture was stirred for 10 min. at room temperature, resulting in a red suspension. A solution of $\text{Pt}(\text{PEt}_3)_2\text{I}_2$ (156 mg, 0.228 mmol) in CH_2Cl_2 (2ml) was added, followed by another addition of DMF (2 mL). The mixture was stirred for 2 days and became a clear yellow solution (except insoluble copper salts). The solvents were removed under reduced pressure and the residue was taken up with CH_2Cl_2 and filtered through a pad of celite. EtOH was added, and the solvents were removed giving a yellow solid. Column chromatography on silica gel with *n*-hexane/ CH_2Cl_2 gave **220** as a yellow solid (132 mg, 85 %).

IR (film): 2963 m , 2932 m , 2908 w , 2875 w , 2364 w , 2098 m , 1454 m , 1411 m , 1378 m , 1348 w , 1324 w , 1254 w , 1034 s , 1007 w , 822 w , 797 w , 766 s , 731 s , 702 m .

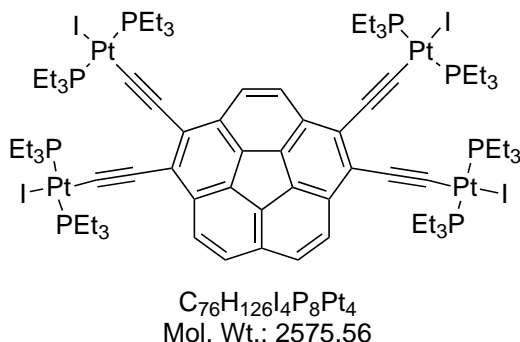
^1H NMR (600 MHz, CDCl_3): 8.01 (d , $^3J_{\text{H-H}} = 8.7$ Hz, 2H); 7.85 (s , 2H); 7.75 (d , $^3J_{\text{H-H}} = 8.8$, 2H); 2.89 (s , CH_3 , 3H); 2.29–2.12 (m , CH_2 , 24H); 1.19 (dt , $^3J_{\text{H-H}} = 7.7$, $^3J_{\text{H-P}} = 16.6$, CH_3 , 36H).

$^{13}\text{C}\{^1\text{H}\}$ NMR (150 MHz, CDCl_3): 135.98, 135.79, 134.26, 133.20, 132.42, 130.72, 130.22, 127.02, 126.64, 124.98, 124.54, 100.54 (t , $^1J_{\text{C-Pt}} = 1452$, $^2J_{\text{C-P}} = 14.6$), 98.25 (t , $^3J_{\text{C-P}} = 2.7$, $^2J_{\text{C-Pt}} = 400$), 16.9 (virtual t , $^1J_{\text{C-P}} = 17.6$), 16.88, 8.54 (t , $^2J_{\text{C-P}} = 10.7$).

$^{31}\text{P}\{^1\text{H}\}$ NMR (162 MHz, CDCl_3): 6.77 (s , $^1J_{\text{Pt-P}} = 2326$).

HRMS (ESI-TOF): $[M^+]$ calculated for $C_{50}H_{72}I_2P_4Pt_2$: 1441.20352; found 1441.20491. $[M-I+MeCN]^+$ calculated for $C_{50}H_{72}IP_4Pt_2(MeCN)$: 1354.31803; found: 1354.31780 (main intensity).

1,2,5,6-Tetrakis{[trans-iodobis(triethylphosphine)platinum]ethynyl}corannulene (**219**)



A solution of 1,2,5,7-tetrakis(2-[trimethylsilyl]ethynyl)corannulene (**217**, 100 mg, 0.158 mmol) in DMF (5 ml) and CH_2Cl_2 (4 mL) was prepared in a 50 ml Schlenk flask, equipped with stir bar, and cooled in an ice-bath. CsF (106 mg, 0.698 mmol) in H_2O (2 mL) was added and the mixture gets slightly darker and turbid. After 5 min. CuI (132 mg, 0.693 mmol) was added in one step and the mixture was stirred for 10 min. at room temperature, resulting in a red suspension. A solution of $Pt(PEt_3)_2I_2$ (475 mg) in CH_2Cl_2 (4 mL) was added, followed by another addition of DMF (5 mL). The mixture was stirred for 2 days and became a clear yellow solution (except insoluble copper salts). CH_2Cl_2 was removed under reduced pressure and a mixture of MeOH/ H_2O was added, resulting in a bright yellow precipitate. The precipitate was washed with H_2O and MeOH and dissolved in CH_2Cl_2 and filtered through a pad of celite. EtOH was added; CH_2Cl_2 was removed giving **219** as a bright yellow precipitate, which was filtered again and washed with EtOH and Et_2O (362 mg, 89 %).

IR (film): 2962 m , 2930 m , 2911 m , 2875 m , 2362 w , 2088 w , 1989 s , 1608 w , 1452 m , 1413 m , 1379 m , 1344 m , 1322 w , 1254 m , 1033 s , 1006 m , 763 s , 730 s , 712 s .

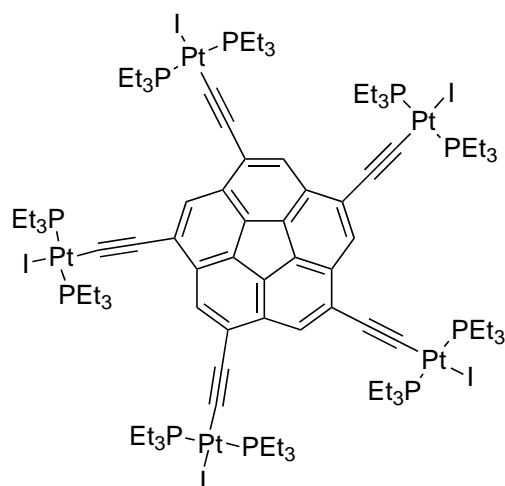
1H NMR (500 MHz, $CDCl_3$): 7.94 (d , $^3J_{H-H} = 8.8$ Hz, 2H); 7.93 (s); 7.83 (d , $^3J_{H-H} = 8.8$, 2H); 2.39–2.18 (m , CH_2 , 48H); 1.28–1.13 (m , CH_3 , 72H).

$^{13}\text{C}\{^1\text{H}\}$ NMR (150 MHz, CDCl_3): 135.42, 134.25, 133.73, 131.39, 130.74, 130.19, 128.07, 127.92, 127.43, 126.12, 125.61, 108.00 (t , $^1J_{\text{C-Pt}} = 1481$, $^2J_{\text{C-P}} = 12.5$), 106.87 (t , $^2J_{\text{C-P}} = 12.5$), 97.99 (t , $^3J_{\text{C-P}} = 2.6$), 97.66 (t , $^3J_{\text{C-P}} = 2.6$, $^2J_{\text{C-Pt}} = 405$), 16.67 (t , $^1J_{\text{C-P}} = 16.6$, CH_2) 16.59 (t , $^1J_{\text{C-P}} = 16.6$, CH_2), 8.66 (s , CH_3), 8.64 (s , CH_3).

$^3\text{P}\{^1\text{H}\}$ NMR (162 MHz, CDCl_3): 1.93 (s , $^1J_{\text{Pt-P}} = 2354$); 1.81 (s , $^1J_{\text{Pt-P}} = 2359$).

HRMS (ESI-TOF): $[\text{M-I}+\text{MeCN}]^+$ calculated for $\text{C}_{76}\text{H}_{126}\text{I}_3\text{P}_8\text{Pt}_4(\text{MeCN})$: 2489.37316; found 2489.37573. $[\text{M}-2\text{I}+2\text{MeCN}]^{2+}$ calculated for $\text{C}_{76}\text{H}_{126}\text{I}_2\text{P}_8\text{Pt}_4(\text{MeCN})_2$: 1201.74851; found: 1201.74765 (main intensity).

1,3,5,7,9-Pentakis{[trans-iodobis(triethylphosphine)platinum]ethynyl}corannulene (213)



$\text{C}_{90}\text{H}_{155}\text{I}_5\text{P}_{10}\text{Pt}_5$
Mol. Wt.: 3156.87

A suspension of 1,3,5,7,9-pentakis(2-[trimethylsilyl]ethynyl)corannulene (**216**, 100 mg, 0.137 mmol) in DMF (15 ml) and CH_2Cl_2 (15 mL) and THF (10 mL) was prepared in a 50 ml Schlenk flask, equipped with stir bar. CsF (108 mg, 0.711 mmol) in H_2O (2 ml) was added and the mixture gets slightly darker. After 5 min. CuI (136 mg, 0.711 mmol) was added in one step and the mixture was stirred for 20 min. at room temperature, resulting in a red suspension. A solution of $\text{Pt}(\text{PEt}_3)_2\text{I}_2$ (488 mg, 0.711 mmol) in CH_2Cl_2 (5 mL) was added, followed by another addition of DMF (5 mL). The mixture was stirred for 2 days and became a clear yellow solution (except insoluble copper salts). The solvents were removed

under reduced pressure and the residue was taken up in CH_2Cl_2 and filtered through a pad of celite. EtOH was added, CH_2Cl_2 was removed and the brownish yellow precipitate was filtered and washed with EtOH (crude yield: 397 mg). Column chromatography on silica gel with *n*-hexane/EtOAc gave **213** as a yellow solid (139 mg, 35 %).

IR (film): 2963 m , 2931 m , 2911 m , 2875 m , 2098 m , 1605 w , 1453 m , 1421 s , 1377 m , 1350 w , 1302 w , 1253 m , 1195 m , 1076 w , 1033 s , 1005 m , 878 w , 764 s , 730 s , 702 m , 633 m)

^1H NMR (500 MHz, CDCl_3): 7.88 (s , 5H); 2.35–2.12 (m , CH_2 , 60H); 1.19 (dt , $^3J_{\text{H-H}} = 7.7$, $^3J_{\text{H-P}} = 16.6$, CH_3 , 90H).

$^{13}\text{C}\{^1\text{H}\}$ NMR (150 MHz, CDCl_3): 133.31, 131.45, 126.74, 126.36, 99.37 (t , $^3J_{\text{C-P}} = 2.7$, $^2J_{\text{C-Pt}} = 400$), 95.10 (t , $^2J_{\text{C-P}} = 14.5$, $^1J_{\text{C-Pt}} = 1450$), 16.76 (t , $^1J_{\text{C-P}} = 17.5$), 8.35 (t , $^2J_{\text{C-P}} = 7.6$).

$^3\text{P}\{^1\text{H}\}$ NMR (200 MHz, CDCl_3): 7.23 (s , $^1J_{\text{Pt-P}} = 2329$).

HRMS (ESI-TOF): $[\text{M-I+MeCN}]^+$ calculated for $\text{C}_{90}\text{H}_{155}\text{I}_4\text{P}_{10}\text{Pt}_5(\text{MeCN})$: 3070.41867; found 3070.41640. $[\text{M-2I+2MeCN}]^{2+}$ calculated for $\text{C}_{90}\text{H}_{155}\text{I}_3\text{P}_{10}\text{Pt}_5(\text{MeCN})_2$: 1492.27005; found: 1492.26967 (main intensity).

8.2.1 X-ray Crystallographic Structure Information

Table 8.1: Crystallographic data for **212**.

Crystallized from	MeOH
Empirical formula	$\text{C}_{80}\text{H}_{155}\text{Cl}_5\text{P}_{10}\text{Pt}_5$
Formula weight [g mol^{-1}]	2579.11
Crystal color, habit	colorless, prism
Crystal dimensions [mm^3]	$0.13 \times 0.15 \times 0.50$
Temperature [K]	160(1)
Crystal system	monoclinic
Space group	$P2_1/n$ (#61)
Z	8
Reflections for cell determination	59131
2θ range for cell determination [$^\circ$]	2–25
Unit cell parameters	
a [\AA]	38.9473(4)
b [\AA]	14.4159(1)
c [\AA]	39.1396(4)
α [$^\circ$]	90
β [$^\circ$]	110.8408(3)
γ [$^\circ$]	90
V [\AA^3]	20537.5(3)
$F(000)$	10080
D_x [g cm^{-3}]	1.668
$\mu(\text{Mo } K\alpha)$ [mm^{-1}]	7.079
Scan type	ϕ and ω
$2\theta_{\text{max}}$ [$^\circ$]	25
Transmission factors (min; max)	0.195; 0.448
Total reflections measured	238902
Symmetry-independent reflections	35803
R_{int}	0.104
Reflections with $I > 2\sigma(I)$	26731
Reflections used in refinement	5556
Parameters refined; restraints	2361;6428
Final $R(F)$ [$I > 2\sigma(I)$ reflections]	0.0658
$wR(F^2)$ (all data)	0.1334
Weights:	$w = [\sigma^2(F_0^2) + (0.12P)^2 + 134.3579P]^{-1}$ where $P = (F_0^2 + 2F_c^2)/3$
Goodness of fit	1.138
Final $\Delta_{\text{max}}/\sigma$	0.001
$\Delta\rho$ (max; min) [e \AA^{-3}]	5.469; -3.999

Table 8.2: Crystallographic data for **214b**.

Crystallized from	acetone/ <i>n</i> -hexane
Empirical formula	C ₅₂ H ₈₀ B ₂₂ Br ₁₂ N ₂ Pt ₂
Formula weight [g mol ⁻¹]	2443.78
Crystal color, habit	yellow, prism
Crystal dimensions [mm ³]	0.17 × 0.20 × 0.28
Temperature [K]	160(1)
Crystal system	orthorhombic
Space group	<i>P</i> 2 ₁ 2 ₁ 2/n (#18)
<i>Z</i>	4
Reflections for cell determination	180941
2 θ range for cell determination [°]	4–50
Unit cell parameters	
<i>a</i> [Å]	31.0338(2)
<i>b</i> [Å]	33.4144(2)
<i>c</i> [Å]	8.0692(1)
α [°]	90
β [°]	90
γ [°]	90
<i>V</i> [Å ³]	8367.6(1)
<i>F</i> (000)	4608
<i>D_x</i> [g cm ⁻³]	1.940
μ (Mo <i>K</i> α) [mm ⁻¹]	9.184
Scan type	ϕ and ω
2 θ_{\max} [°]	50
Transmission factors (min; max)	0.099; 0.230
Total reflections measured	65724
Symmetry-independent reflections	14693
<i>R</i> _{int}	0.090
Reflections with <i>I</i> > 2 σ (<i>I</i>)	12856
Reflections used in refinement	14691
Parameters refined; restraints	959; 396
Final <i>R</i> (<i>F</i>) [<i>I</i> > 2 σ (<i>I</i>) reflections]	0.0685
<i>wR</i> (<i>F</i> ²) (all data)	0.1875
Weights:	$w = [\sigma^2(F_0^2) + (0.12P)^2 + 134.3579P]^{-1}$ where $P = (F_0^2 + 2F_c^2)/3$
Goodness of fit	1.025
Final Δ_{\max}/σ	0.001
$\Delta\rho$ (max; min) [e Å ⁻³]	3.44; -1.84
$\sigma(d_{C-C})$ [Å]	0.002–0.003

Table 8.3: Crystallographic data for **220**.

Crystallized from	<i>n</i> -hexane/ CDCl_3
Empirical formula	$\text{C}_{51.50}\text{H}_{73.50}\text{Cl}_{4.5}\text{I}_2\text{P}_4\text{Pt}_2$
Formula weight $[\text{g mol}^{-1}]$	1619.89
Crystal color, habit	red, prism
Crystal dimensions $[\text{mm}^3]$	$0.12 \times 0.20 \times 0.28$
Temperature $[\text{K}]$	160(1)
Crystal system	orthorhombic
Space group	$P2_1/n$ (#14)
Z	4
Reflections for cell determination	120279
2θ range for cell determination $[\circ]$	4–55
Unit cell parameters	
a $[\text{\AA}]$	20.7278(2)
b $[\text{\AA}]$	14.8192(1)
c $[\text{\AA}]$	22.0662(2)
α $[\circ]$	90
β $[\circ]$	115.2373(6)
γ $[\circ]$	90
V $[\text{\AA}^3]$	6131.09(9)
$F(000)$	3124
D_x $[\text{g cm}^{-3}]$	1.755
$\mu(\text{Mo } K\alpha)$ $[\text{mm}^{-1}]$	5.877
Scan type	ϕ and ω
$2\theta_{\text{max}}$ $[\circ]$	55
Transmission factors (min; max)	0.260; 0.511
Total reflections measured	141083
Symmetry-independent reflections	14009
R_{int}	0.077
Reflections with $I > 2\sigma(I)$	11811
Reflections used in refinement	14009
Parameters refined; restraints	557; 126
Final $R(F)$ $[I > 2\sigma(I)$ reflections]	0.0782
$wR(F^2)$ (all data)	0.2250
Weights:	$w = [\sigma^2(F_0^2) + (0.12P)^2 + 134.3579P]^{-1}$ where $P = (F_0^2 + 2F_c^2)/3$
Goodness of fit	1.059
Final $\Delta_{\text{max}}/\sigma$	0.003
$\Delta\rho$ (max; min) $[\text{e \AA}^{-3}]$	12.49; -4.10
$\sigma(d_{\text{C-C}})$ $[\text{\AA}]$	0.01–0.02

References

- [1] Barth, W. E.; Lawton, R. G. *J. Am. Chem. Soc.* **1966**, *88*, 380–381.
- [2] Barth, W. E.; Lawton, R. G. *J. Am. Chem. Soc.* **1971**, *93*, 1730–1745.
- [3] Gleicher, G. J. *Tetrahedron* **1967**, *23*, 4257–4263.
- [4] Hanson, J. C.; Nordman, C. E. *Acta Cryst.* **1976**, *B32*, 1147–1153.
- [5] Scott, L. T.; Hashemi, M. M.; Meyer, D. T.; Bratcher, M. S. *J. Am. Chem. Soc.* **1992**, *114*, 1920–1921.
- [6] Seiders, T. J.; Elliot, E. L.; Grube, G. H.; Siegel, J. S. *J. Am. Chem. Soc.* **1999**, *121*, 7804–7813.
- [7] Borchardt, A.; Fuchicello, A.; Kilway, K. V.; Baldrige, K. K.; Siegel, J. S. *J. Am. Chem. Soc.* **1992**, *114*, 1921–1923.
- [8] Scott, L. T.; Hashemi, M. M.; Meyer, D. T.; Warren, H. B. *J. Am. Chem. Soc.* **1991**, *113*, 7082–7084.
- [9] Grabowskya, S.; Weber, M.; Chen, Y.-S.; Lentz, D.; Schmidt, B. M.; Hesse, M.; Luger, P. *Z. Naturforsch.* **2010**, *65b*, 452–460.
- [10] Craig, J. T.; Robins, M. D. W. *Aust. J. Chem.* **1968**, *21*, 2237–2245.
- [11] Davy, J. R.; Iskander, M. N.; Reiss, J. A. *Tet. Lett.* **1978**, *42*, 4085–4088.
- [12] Davy, J. R.; Iskander, M. N.; Reiss, J. A. *Aust. J. Chem.* **1979**, *32*, 1067–1078.
- [13] Davy, J. R.; Reiss, J. A. *Aust. J. Chem.* **1976**, *29*, 163–171.
- [14] Mitchell, R. H.; Boekelheide, V. *J. Am. Chem. Soc.* **1970**, *92*, 3510–3512.
- [15] Jessup, P. J.; Reiss, J. A. *Aust. J. Chem.* **1976**, *29*, 173–178.

- [16] Kroto, H. W.; Heath, J.R.; O'Brien, S. C.; Curl, R. F.; Smalley, R. E. *Nature* **1985**, *318*, 162–163.
- [17] Brown, R. F. C.; Eastwood, F. W.; Jackman, G. P. *Aust. J. Chem.* **1977**, *30*, 1757–1767.
- [18] Brown, R. F. C.; Eastwood, F. W.; Harrington, K. J.; McMullen, G. L. *Aust. J. Chem.* **1974**, *27*, 2393–2402.
- [19] Knölker, H.-J.; Braier, A.; Bröcher, D. J.; Jones, P. G.; Piotrowsky, H. *Tet. Lett.* **1999**, *40*, 8075–8078.
- [20] Scott, L. T.; Peng P.-C.; Hashemi, M. M.; Bratcher, M. S.; Meyer, D. T.; Warren, H. B. *J. Am. Chem. Soc.* **1997**, *119*, 10963–10968.
- [21] Liu, Z. C.; Rabideau, P. W. *Tet. Lett.* **1996**, *37*, 3437–3440.
- [22] Borchardt, A.; Hardcastle, K.; Gantzel, P.; Siegel, J. S. *Tet. Lett.* **1993**, *34*, 273–276.
- [23] Zimmermann, G.; Nuechter, U.; Hagen, S.; Nuechter, M. *Tet. Lett.* **1994**, *35*, 4747–4750.
- [24] Mehta, G.; Panda, G. *Tet. Lett.* **1997**, *38*, 2145–2148.
- [25] Seiders, T. J.; Baldrige, K. K.; Siegel, J. S. *J. Am. Chem. Soc.* **1996**, *118*, 2754–2755.
- [26] Olah, G. A.; Prakash, G. K. S. *Synthesis* **1976**, 607–609.
- [27] Ho, T.-L.; Olah, G. A. *Synthesis* **1977**, 170–171.
- [28] Sygula, A.; Rabideau, P. W. *J. Am. Chem. Soc.* **1998**, *120*, 12666–12667.
- [29] Sygula, A.; Rabideau, P. W. *J. Am. Chem. Soc.* **2000**, *122*, 6323–6324.
- [30] Sygula, A.; Xu, G.; Marcinow, Z.; Rabideau, P. W. *Tetrahedron* **2001**, *57*, 3637–3644.
- [31] Stanger, A.; Ashkenazi, N.; Shachter, A.; Blser, D.; Stellberg, P.; Boese, R. *J. Org. Chem.* **1996**, *61*, 2549–2552.
- [32] Stanger, A.; Shachter, A.; Boese, R. *Tetrahedron* **1998**, *54*, 1207–1220.

- [33] Xu, G.; Sygula, A.; Marcinow, Z.; Rabideau, P. W. *Tet. Lett.* **2000**, *41*, 9931–9934.
- [34] Allen, C. F. H.; Bell, A. C.; Bell, A.; Van Allen, J. *J. Am. Chem. Soc.* **1940**, *62*, 656.
- [35] Allen, C. F. H.; Van Allan, J. A. *J. Org. Chem.* **1952**, *17*, 845–854.
- [36] Mackenzie, K. *J. Chem. Soc.* **1960**, 473–483.
- [37] Wolinska-Mocydlarz, J.; Cannone, P.; Leitch, L. C. *Synthesis* **1974**, 566–568.
- [38] Jones, C. S.; Elliott, E.; Siegel, J. S. *Synlett* **2004**, *1*, 187–191.
- [39] Elliott, E. L. PhD thesis, University of California, San Diego, **2003**.
- [40] Maag, R. M. diploma thesis, University of Zurich, **2006**.
- [41] Butterfield, A. M. master thesis, University of Zurich, **2008**.
- [42] Butterfield, A. M.; Gilomen, B.; Siegel, J. S. *Org. Process Res. Dev.* **2012**, *16*, 664–676.
- [43] Girard, A.; Sandulesco, G. *Helv. Chim. Acta* **1936**, *19*, 1095.
- [44] Wheeler, O. H. *Chem. Rev.* **1962**, *62*, 205.
- [45] Buu-Hoi, Ng. Ph.; Cagniant, P. *Rev. Sci.* **1942**, *80*, 130–133.
- [46] Marcinow, Z.; Sygula, A.; Ellern, A.; Rabideau, P. W. *Org. Lett* **2001**, *3*, 3527–3529.
- [47] Wu, Y.-T.; Siegel, J. S. *Chem. Rev.* **2006**, *106*, 4843–4867.
- [48] Sygula, A.; Sygula, R.; Rabideau, P. W. *Org. Lett* **2006**, *8*, 5909–5911.
- [49] Wu, Y.-T.; Hayama, T.; Baldridge, K. K.; Linden, A.; Siegel, J. S. *J. Am. Chem. Soc.* **2006**, *128*, 6870–6884.
- [50] Jackson, E. A.; Steinberg, B. D.; Bancu, M.; Wakamiya, A.; Scott, L. T. *J. Am. Chem. Soc.* **2007**, *129*, 484–485.
- [51] Steinberg, B. D.; Jackson, E. A.; Filatov, A. S.; Wakamiya, A.; Petrukhina, M. A.; Scott, L. T. *J. Am. Chem. Soc.* **2009**, *131*, 10537–10545.

- [52] Abdourazak, A. H.; Sygula, A.; Rabideau, P. W. *J. Am. Chem. Soc.* **1993**, *115*, 3010–3011.
- [53] Seiders, T. J.; Baldrige, K. K.; Grube, G. H.; Siegel, J. S. *J. Am. Chem. Soc.* **2001**, *123*, 517–525.
- [54] Sygula, A.; Karlen, S. D.; Sygula, R.; Rabideau, P. W. *Org. Lett* **2002**, *4*, 3135–3137.
- [55] Wu, Y.-T.; Bandera, D.; Maag, R.; Linden, A.; Baldrige, K. K.; Siegel, J. S. *J. Am. Chem. Soc.* **2008**, *130*, 10729–10739.
- [56] Cellier, P. P.; Spindler, J.-F.; Taillafer, M.; Cristeau, H.-J. *Tet. Lett.* **2003**, *44*, 7191–7195.
- [57] Alonso, F.; Beletskaya, I. P.; Yus, M. *Chem. Rev.* **2002**, *102*, 4009–4091.
- [58] Miyamoto, H.; Yui, K.; Aso, Y.; Otsubo, T.; Ogura, F. *Tet. Lett.* **1986**, *27*, 2011–2014.
- [59] Scott, L.T. *Pure Appl. Chem.* **1996**, *68*, 291–300.
- [60] Mizyed, S.; Georgiou, P. E.; Bancu, M.; Cuadra, B.; Rai, A. K.; Cheng, P.; Scott, L. T. *J. Am. Chem. Soc.* **2001**, *123*, 12770–12774.
- [61] Sevryugina, Y.; Rogachev, A. Y.; Jackson, E. A.; Scott, L. T.; Petrukhina, M. A. *J. Org. Chem.* **2006**, *71*, 6615–6618.
- [62] Georgiou, P. E.; Tran, A. H.; Mizyed, S.; Bancu, M.; Scott, L. T. *J. Org. Chem.* **2005**, *70*, 6158–6163.
- [63] Scott, L. T.; Bronstein, H. E.; Preda, D. V.; Ansems, R. B. M.; Bratcher, M. S.; Hagen, S. *Pure Appl. Chem.* **1999**, *71*, 209–219.
- [64] Steinberg, B. D. PhD thesis, Boston College, **2009**.
- [65] Seiders, T. J.; Baldrige, K. K.; Elliot, E. L.; Grube, G. H.; Siegel, J. S. *J. Am. Chem. Soc.* **1999**, *121*, 7439–7440.
- [66] Mattarella, M. unpublished results, University of Zurich, **2011**.
- [67] Grube, G. H.; Elliott, E. L.; Steffens, R. J.; Jones, C. S.; Baldrige, K. K.; Siegel, J. S. *Org. Lett.* **2003**, *5*, 713–716.

- [68] Hayama, T.; Baldrige, K. K.; Wu, Y.-T.; Linden, A.; Siegel, J. S. *J. Am. Chem. Soc.* **2008**, *130*, 1583–1591.
- [69] Hayama, T. PhD thesis, University of Zurich, **2008**.
- [70] Biscoe, M. R.; Fors, B. B.; Buchwald, S. L. *J. Am. Chem. Soc.* **2008**, *130*, 6686–6687.
- [71] Scott, L. T.; Jackson, E. A.; Zhang, Q.; Steinberg, B. D.; Bancu, M.; Li, B. *J. Am. Chem. Soc.* **2012**, *134*, 107–110.
- [72] Littke, A. F.; Fu, G. F. *Angew. Chem. Int. Ed.* **1998**, *37*, 3387–3388.
- [73] Littke, A. F.; Dai, C.; Fu, G. F. *J. Am. Chem. Soc.* **2000**, *122*, 4020–4028.
- [74] Pappo, D.; Mejuch, T.; Reany, O.; Solel, E.; Gurram, M.; Keinan, E. *Org. Lett* **2009**, *11*, 1063–1066.
- [75] Eberhard, M. R.; Wang, Z.; Jensen, C. M. *Chem. Commun.* **2002**, *8*, 818–819.
- [76] Gershoni-Poranne, R.; Pappo, D.; Solel, E.; Keinan, E. *Org. Lett* **2009**, *11*, 5146–5149.
- [77] Bancu, M.; Rai, A. K.; Cheng, P.; Gilardi, R. D.; Scott, L. T. *Synlett* **2004**, *1*, 173–176.
- [78] Ballester, M.; Molinet, C.; Castañer, J. *J. Am. Chem. Soc.* **1960**, *82*, 4254–4258.
- [79] Hayama, T.; Wu, Y.-T.; Linden, A.; Baldrige, K. K.; Siegel, J. S. *J. Am. Chem. Soc.* **2007**, *129*, 12612–12613.
- [80] Baldrige, K. K.; Siegel, J. S. *Org. Biomol. Chem.* **2010**, *8*, 53–55.
- [81] Cheng, P.-C. PhD thesis, Boston College, **1996**.
- [82] Mack, J.; Vogel, P.; Jones, D.; Kavala, N.; Suttona, A. *Org. Biomol. Chem.* **2007**, *5*, 2448–2452.
- [83] Boedigheimer, H.; Ferrence, G. M.; Lash T. D. *J. Org. Chem.* **2010**, *75*, 2518–2527.
- [84] Sygula, A.; Sygula, R.; Fronczek, F. R.; Rabideau, P. W. *J. Org. Chem.* **2002**, *4*, 6487–6492.
- [85] Sygula, A.; Sygula, R.; Rabideau, P. W. *Org. Lett* **2005**, *7*, 4999–5001.

- [86] Sygula, A.; Sygula, R.; Kobrin, L. *Org. Lett* **2008**, *10*, 3927–3929.
- [87] Hargittai, I. *Fivefold Symmetry*; World Scientific Publishing Co. Inc., 1992; pp 11–20.
- [88] Hasenknopf, B.; Lehn, J.-M.; Kneisel, B. O.; Baum, G.; Fenske, D. *Angew. Chem. Int. Ed.* **1996**, *35*, 1838–1840.
- [89] Day, V. W.; Marks, T. J.; Wachter, W. A. *J. Am. Chem. Soc.* **1975**, *97*, 4519–4527.
- [90] Poonia, N. S.; Bajaj, A. V. *Chem. Rev.* **1979**, *79*, 389–445.
- [91] Silvestru, C.; Breunig, H. J.; Althaus, H. *Chem. Rev.* **1999**, *99*, 3277–3327.
- [92] Voet, D.; Voet, J. G. *Biochemie*; VCH Verlagsgesellschaft mbH, Weinheim, 1992; pp 181–182.
- [93] Pornillos, O.; Ganser-Pornillos, B. K.; Yeager, M. *Nature* **2011**, *469*, 424–428.
- [94] Cardone, G.; Purdy, J. G.; Cheng, N.; Craven, R. C.; Steven, A. C. *Nature* **2009**, *457*, 694–699.
- [95] Ganser, B. K.; Li, S.; Klishko, V. Y.; Finch, J. T.; Sundquist, W. I. *Science* **1999**, *283*, 80–83.
- [96] He, Y.; Ye, T.; Su, M.; Zhang, C.; Ribbe, A. E.; Jiang, W.; Mao, C. *Nature* **2008**, *452*, 198–202.
- [97] Rothmund, P. W. K. *Nature* **2006**, *440*, 297–302.
- [98] Zhang, C.; Su, M.; He, Y.; Zhao, X.; Fang, P.; Ribbe, A. E.; Jiang, W.; Mao, C. *Proc. Natl. Acad. Sci* **2008**, *105*, 10665–10669.
- [99] Kim, J. M.; Lee, Y.-H.; Ku, C. R.; Lee, E. J. *Endocrinology* **201**, *152*, 536–544.
- [100] Fan, E.; Zhang, Z.; Minke, W. E.; Hou, Z.; Verlinde, Ch. L. M. J.; Hol, W. G. J. *J. Am. Chem. Soc.* **2000**, *122*, 2663–2664.
- [101] Zhang, Z.; Liu, J.; Verlinde, Ch. L. M. V.; Hol, W. G. J.; Fan, E. *J. Org. Chem.* **2004**, *69*, 7737–7740.
- [102] Mendoza-Espinosa, D.; Hanna, T. A. *Dalton Trans.* **2009**, 5211–5225.

- [103] Gargiulli C.; Gattuso, G.; Liotta, C.; Notti, A.; Parisi, M. F.; Pisagatti, I.; Pappalardo, S. *J. Org. Chem.* **2009**, *74*, 4350–4353.
- [104] Gallagher, J. F.; Ferguson, G. *Acta Cryst.* **1974**, *C50*, 73–77.
- [105] Dedek, P.; Janout, V.; Regen, S. L. *J. Org. Chem.* **1993**, *58*, 6553–6555.
- [106] Cafeo, G.; Kohnke, F. H.; Parisi, M. F.; Nascone, R. P.; La Torre, G. L.; Williams, D. J. *Org. Lett.* **2002**, *4*, 2695–2697.
- [107] Bardelang, D.; Udachin, K. A.; Anedda, R.; Moudrakovski, I.; Leek, D. M.; Ripmeester, J. A.; Ratcliffea, Ch. I. *Chem. Commun.* **2008**, 4927–4929.
- [108] Qin, B.; Chen, X.; Fang, X.; Shu, Y.; Yip, Y. K.; Yan, Y.; Pan, S.; Ong, W. Q.; Ren, C.; Su, H.; Zeng, H. *Org. Lett.* **2008**, *10*, 5127–5130.
- [109] Qin, B.; Ong, W. Q.; Ye, R.; Du, Z.; Chen, X.; Yan, Y.; Zhang, K.; Suc, H.; Zeng, H. *Chem. Commun.* **2011**, *47*, 5419–5421.
- [110] Bandera, D.; Baldrige, K. K.; Linden, A.; Dorta, R.; Siegel, J. S. *Angew. Chem. Int. Ed.* **2011**, *50*, 865–867.
- [111] Bandera, D. PhD thesis, University of Zurich, **2009**.
- [112] Bergmann, E.; Orchin, M. *J. Am. Chem. Soc.* **1949**, *71*, 1917–1918.
- [113] Bergmann, E. *Nature* **1948**, *161*, 889–890.
- [114] Rice, J. E.; LaVoie, E.; Hoffmann, D. *J. Org. Chem.* **1983**, *48*, 2360–2363.
- [115] Enchavarren, A. M.; Gómez-Lor, B.; Gonzáles, J. J.; de Frutos, Ó. *Synlett* **2003**, *69*, 585–597.
- [116] Tucker, H. S. *J. Chem. Soc.* **1958**, 1462–1465.
- [117] Wehmeier, M.; Wagner, M. Müllen, K. *Chem. Eur. J.* **2001**, *7*, 2197–2205.
- [118] Viala, C.; Secchi, A.; Gourdon, A. *Eur. J. Org. Chem* **2002**, 4185–4189.
- [119] Raasch, M. S. *J. Org. Chem.* **1980**, *45*, 856–867.
- [120] Fabrizio, E. F.; Payne, A.; Westlund, N. E.; Bard, A. J.; Magnus, P. P. *J. Phys. Chem.* **2002**, *106*, 1961–1968.

- [121] Campbell, N.; Gow, R. S.; Wang, H. *Nature* **1948**, 857.
- [122] Campbell, N.; Gow, R. S. *J. Chem. Soc.* **1949**, 1555–1559.
- [123] Gonz  les, J. J.; Francesch, A.; C  rdenas, D. J.; Enchavarren, A. M. *Synlett* **2003**, 69, 585–597.
- [124] Pascual, S.; Bour, Ch.; de Mendoza, P.; Enchavarren, A. M. *Beilstein J. Org. Chem.* **2011**, 7, 1520–1525.
- [125] Wegner, H. A.; Scott, L. T.; de Meijere, A. *J. Org. Chem.* **2003**, 68, 883–887.
- [126] Wu, Y.-T.; Linden, A.; Siegel, J. S. *Org. Lett.* **2005**, 7, 4353–4355.
- [127] Goel, A.; Kumar, V.; Chaurasia, S.; Rawat, M.; Prasad, R.; Anand, R. S. *J. Org. Chem.* **2010**, 75, 3656–3662.
- [128] Panda, K.; Venkatesh, C.; Ila, H.; Junjappa, H. *Eur. J. Org. Chem.* **2005**, 2045–2055.
- [129] Jones, R. L.; Pearson, D. E.; Gordon, M. *J. Org. Chem.* **1972**, 37, 3369–3370.
- [130] Cason, J. *Chem. Rev.* **1947**, 40, 15–32.
- [131] Cason, J.; Prout, F. S. *J. Am. Chem. Soc.* **1944**, 66, 46–50.
- [132] Lee, J. J. *Name Reactions. A Collection of Detailed Reaction Mechanisms*; Springer-Verlag, Berlin Heidelberg, 2003; pp 81.
- [133] Bradsher, C. K. *J. Am. Chem. Soc.* **1940**, 62, 486–488.
- [134] Suzuki, Y.; Takeuchi, K.; Kodomari, M. *J. Chem. Res.* **1947**, 426–427.
- [135] Visweswariah, S.; Prakash, G.; Bhushan, V.; Chandrasekaran, S. *Synthesis* **1982**, 309–310, .
- [136] Mak, T. C. W.; Trotter, J. *Acta Cryst.* **1963**, 811–815, .
- [137] Smith, M. B.; March, J. *March’s Advanced Organic Chemistry–5th ed.*; Wiley inter-science: New York, 2001; pp 362–364.
- [138] Molander, G. A.; Cameron, K. O. *J. Am. Chem. Soc.* **1993**, 115, 830–846.
- [139] Mukaiyama, T.; Sato, T.; Hanna, J. *Chem. Lett.* **1973**, 1041–1044.

- [140] Langer, P.; Köhler, V. *Org. Lett.* **2000**, *2*, 1597–1599.
- [141] Becker, H.-D.; Hansen, L.; Andersson, K. *J. Org. Chem.* **1985**, *50*, 277–279.
- [142] Smith, M. B.; March, J. *March's Advanced Organic Chemistry–5th ed.*; Wiley inter-science: New York, 2001; pp 401–404.
- [143] Maeda, S.; Obora, Y.; Ishii, Y. *Eur. J. Org. Chem.* **2009**, 4067–4072.
- [144] Pirkle, W. H.; Dines, M. B. *J. Org. Chem.* **1969**, *34*, 2239–2244.
- [145] Cho, C.-G.; Park, J.-S.; Lee, H. *Tet. Lett.* **2001**, *42*, 1065–1067.
- [146] Marrison, L. R.; Dickinson, J. M.; Fairlamb, I. J. S. *Bioorg. Med. Chem. Lett.* **2003**, *13*, 2667–2671.
- [147] Mezheritskii, V. V.; Olekhovich, E. P.; Dorofeenko, G. N. *Russ. Chem. Rev.* **1973**, *42*, 392–412.
- [148] Deno, N. C. *J. Am. Chem. Soc.* **1947**, *69*, 2233–2234.
- [149] Bouhadir, K. H.; Zhou, J.-L.; Shevlin, P. B. *Synth. Commun.* **2005**, *69*, 1003–1010.
- [150] Krasnokutskaja, E.A.; D'jakova, A.S.; Ki-Whan Chi *Science and Technology, 2000. KORUS 2000. Proceedings. The 4th Korea-Russia International Symposium on 2000*, *1*, 182–185.
- [151] Tatsugi, J.; Okumara, S.; Izawa, Y. *Bull. Chem. Soc. Jpn.* **1986**, *59*, 3311–3313.
- [152] Pu, S.; Liu, G.; Li, G.; Wang, R.; Yang, T. *J. Mol. Struct.* **2007**, *833*, 23–29.
- [153] Polyakova, S. M.; Belov, V. N.; Bossi, M. L.; Hell, S. W. *Eur. J. Org. Chem.* **2011**, 3301–3312.
- [154] Rozen, S.; Bareket, Y. *J. Chem. Soz., Chem. Commun.* **1994**, 1959.
- [155] Shefer, N.; Harel, T.; Rozen, S. *J. Org. Chem.* **2009**, 6993–6998.
- [156] Becherbauer, R.; Smart, B.; Bareket, Y.; Rozen, S. *J. Org. Chem.* **1995**, *60*, 6186–6187.
- [157] Miyahara, Y.; Inazu, T. *Tet. Lett.* **1990**, *31*, 5955–5958.

- [158] Nenajdenko, V. G.; Gavryushin, A. E.; Balenkova, E. S. *Tet. Lett.* **2001**, *42*, 4397–4399.
- [159] Nenajdenko, V. G.; Moiseev, A. M.; Balenkova, E. S. *Russ. Chem. Bull., Int. Ed.* **2004**, *53*, 2144–2150.
- [160] Bahrami, K. *Tet. Lett.* **2006**, *47*, 2009–2012.
- [161] Antonow, D.; Marrafa, T.; Dawood, I.; Ahmed, T.; Haque, M. R.; Thurston, D. E.; Zinzalla, G. *Chem. Commun.* **2010**, *46*, 2289–2291.
- [162] For review see: Afarinkia, K.; Vinader, V.; Nelson, T. D.; Posner, G. H. *Tetrahedron* **1992**, *48*, 9111–9171.
- [163] Gingrich, H. L.; Roush, D. M.; Van Saun, W. A. *J. Org. Chem.* **1983**, *48*, 4869–4873.
- [164] Jung, M. E.; Hagenah, J. A. *Heterocycles* **1987**, *25*, 117–121.
- [165] Ziegeler, t.; Effenberger, F. *Chem. Ber.* **1987**, *120*, 1339–1346.
- [166] Chen, Ch.-H.; Liao, Ch.-Ch. *Org. Lett.* **2000**, *2*, 2049–2052.
- [167] Boger, D. L.; Mullican, M. D. *J. Org. Chem.* **1984**, *49*, 4033–4044.
- [168] Gutowsky, H. S.; Saika, A. *J. Chem. Phys.* **1953**, *21*, 1688.
- [169] Gutowsky, H. S.; Holm, C. H. *J. Chem. Phys.* **1956**, *25*, 1228.
- [170] Sandstrom, J. *Dynamic NMR Spectroscopy*; Academic press: NY, 1982; 97.
- [171] McMurry, J. E. *Chem. Rev.* **1989**, *7*, 1513–1524.
- [172] Sabelle, S.; Hydrio, J.; Leclerc, E.; Mioskowski, C.; Renard, P.-Y. *Tet. Lett.* **2002**, *43*, 3645–3648.
- [173] Ma, J.; Chan, T.-H. *Tet. Lett.* **1998**, *39*, 2499–2502.
- [174] Miyaura, N.; Suzuki, A. *Chem. Rev.* **1995**, *95*, 2457–2483.
- [175] Rahanyan, N.; Linden, A.; Baldrige, K. K.; Siegel, J. S. *Org. Biomol. Chem.* **2009**, *7*, 2082–2092.
- [176] Hopf, H. *Classics in Hydrocarbon Chemistry: Synthesis, Concepts, Perspectives*; Wiley-VCH, 2000; chapter 3.

- [177] a) Stang, P. J.; Olenyuk, B. *Acc. Chem. Res.* **1997**, *30*, 502. b) Leiniger, S.; Olenyuk, B.; Stang, P. J. *Chem. Rev.*, **2000**, *100*, 853. c) Fujita, M.; Umemoto, K.; Yoshizawa, M.; Fujita, M.; Kusakawa, T.; Biradha, K. *Chem. Commun.*, **2001**, 509. d) Seidel, S. R.; Stang, P. J. *Acc. Chem. Res.* **2002**, *35*, 972. e) Northrop, B. H.; Yang, H.-B.; Stang, P. J. *Chem. Commun.*, **2008**, 5896.
- [178] a) Caulder, D. L.; Raymond, K. N. *Acc. Chem. Res.* **1999**, *32*, 975. b) Holliday, B. J.; Mirkin, C. A. *Angew. Chem. Int. Ed.*, **2001**, *40*, 2022. c) Fujita, M.; Tominaga, M.; Hori, A.; Therrien, B. *Acc. Chem. Res.*, **2005**, *38*, 369. d) Lee, S. J.; Hupp, J. T., *Coord. Chem. Rev.* **2006**, *250*, 1710.
- [179] a) Eaton, P. E.; Cole, T. W. *J. Am. Chem. Soc.* **1964**, *86*, 3157–3158. b) Barborak, J.C.; Watts, L.; Pettit, R. *J. Am. Chem. Soc.*, **1966**, *88*, 1328. c) Griffin, G. W.; Marchand, A. P. *Chem. Rev.*, **1989**, *89*, 997.
- [180] a) Ternasky, R. J.; Balogh, D. W.; Paquette, L. A. *J. Am. Chem. Soc.* **1982**, *104*, 4503–4506. b) Paquette, L. A.; Weber, J. C.; Kobayashi, T.; Miuhara, Y. *J. Am. Chem. Soc.*, **1988**, *110*, 8591–8599. c) Paquette, L. A. *Chem. Rev.*, **1989**, *89*, 1051.
- [181] a) Holliday, R. *Genet. Res.* **1964**, *5*, 282. b) Murchie, A. I. H.; Clegg, R. M.; von Kitzing, E. Duckett, D. R.; Diekman, S.; Lilley, D. M. J. *Nature*, **1989**, *341*, 763. c) Seeman, N. C. *Nature*, **2003**, *421*, 427.
- [182] Olson, A. J.; Hu, Y. H. E.; Keinan, E. *Proc. Natl. Acad. Sci. U.S.A.* **2007**, *104*, 20731.
- [183] Lee, H. B.; Sharp, P. R. *Organometallics* **2005**, *24*, 4875.
- [184] Liston, D. J.; Lee, Y. J.; Scheidt, W. R.; Reed, C. A. *J. Am. Chem. Soc.* **1989**, *111*, 6643.
- [185] Bergman, R. G. *Acc. Chem. Res.* **1973**, *6*, 25.
- [186] Blau, R. J.; Espenson, J. H. *Inorg. Chem.* **1986**, *25*, 878.
- [187] Anderson, G. K.; Lumetta, G. J. *Organometallics* **1985**, *4*, 1542.
- [188] Blau, R. J.; Espenson, J. H.; Kim, S.; Jacobson, R. A. *Inorg. Chem.* **1986**, *25*, 757.
- [189] Davies, J. A.; Hartley, F. R. *Chem. Rev.* **1981**, *81*, 79–90.

- [190] For related Pt-insertion chemistry, see: Choi, H.; Kim, C.; Park, K.-H. Kim, J.; Kang, Y.; Ko, J. *J. Organomet. Chem.* **2009**, *694*, 3529–3532.
- [191] a) Yoshida, T.; Matsuda, T.; Otsuka, S. *Inorg. Synth.* **1990**, *28*, 122–123. b) Jensen, K. A. *Z. Anorg. Allg. Chem.*, **1936**, *229*, 225–232.

A Curriculum Vitae

Roman Marcel Maag

Sex: male
Date of Birth: August 9th, 1980 in Bangkok, Thailand
Nationality: Swiss
Languages: German (mother tongue), English (fluent), French (School education).

Education

December 2006 – present **University of Zurich, Switzerland**
PhD thesis: “Synthesis of an Unsymmetrically Penta-functionalized Corannulene Derivative” and “Synthesis of Platinum and Ethynyl-Platinum Corannulenes”. Research advisor: Prof. Dr. Jay S. Siegel.

October 2000 – October 2006 **University of Zurich, Switzerland**
Diploma thesis: “Synthesis of Corannulene Derivatives with Metal Complexing Substituents: Corannulene–Phenanthroline Hybrids”. Research advisor: Prof. Dr. Jay S. Siegel.

August 1994 – August 1999 **Gymnasium Immensee, Immensee**
Matura Type E (Economics).

Work Experience

December 2006 – present **University of Zurich, Switzerland**
PhD Student in the group of Prof. Dr. Jay S. Siegel. Laboratory advisor for exchange students and apprentices. Teaching assistant in Laboratory Courses in General Chemistry, Organic Chemistry I, and for Secondary School Teachers.

- February 2005 – July 2006* **University of Zurich, Switzerland**
Undergraduate Student in the group of Prof Jay S. Siegel, Organic Chemistry Institute, Zurich, Switzerland.
- Juli 2003 – September 2003* **University of Zurich, Switzerland**
Internship at the Organic Chemistry Institute under the supervision of Dr. Christophe Weymuth: Synthesis of (\pm)-Chokol G.

Oral Presentations

- October 2010* Final COST meeting, Florence, Italy.
- June 2010* DokTag, PhD Students Day of the Organic Chemistry Institute, UZH.
- February 2009* WISPOC, Winter School on Physical Organic Chemistry, Bressanone, Italy.

Poster Presentations

- August 2010* EuChMS Chemistry Congress, Nuremberg, Germany.
- August 2010* Gordon Research Conference, Newport, RI, USA.
- July 2009* ISNA-13 International Symposium on Novel Aromatic Compounds, Luxembourg, Luxembourg.
- May 2008* 3rd Dorothy Cowfoot Hodgkin Symposium, Zurich, Switzerland
- September 2008* EuCheMS Chemistry Congress, Torino, Italy.
- June 2007* 2nd Dorothy Cowfoot Hodgkin Symposium, Zurich, Switzerland

Publications

“Multiethynyl Corannulenes: Synthesis, Structure, and Properties”

Yao-Ting Wu, Davide Bandera, Roman Maag, Anthony Linden, Kim K. Baldrige, and Jay S. Siegel, *J. Am. Chem. Soc.*, **2008**, *130*, 10729–10739.

“Synthesis and X-ray structural analysis of platinum and ethynyl-platinum corannulenes: supramolecular tectons”

Roman Maag, Brian H. Northrop, Anna Butterfield, Anthony Linden, Oliver Zerbe, Young Min Lee, Ki-Whan Chi, Peter J. Stang, Jay S. Siegel, *Org. Biomol. Chem.*, **2009**, *7*, 4881–4885.